Ontario

Ontario Geological Survey
Open File Report 6073

Geochemistry and Metallogenesis of Komatiitic Rocks in the Abitibi Greenstone Belt, Ontario

2003

103-04819/

Ontario

ONTARIO GEOLOGICAL SURVEY

Open File Report 6073

Geochemistry and Metallogenesis of Komatiitic Rocks in the Abitibi Greenstone Belt, Ontario

by

R.A. Sproule, C.M. Lesher, J.A. Ayer and P.C. Thurston

2003

Parts of this publication may be quoted if credit is given. It is recommended that reference to this publication be made in the following form:

Sproule, R.A., Lesher, C.M., Ayer, J.A. and Thurston, P.C. 2003. Geochemistry and metallogenesis of komatiitic rocks in the Abitibi greenstone belt, Ontario; Ontario Geological Survey, Open File Report 6073, 119p.

© Queen's Printer for Ontario, 2003

© Queen's Printer for Ontario, 2003.

Open File Reports of the Ontario Geological Survey are available for viewing at the Mines Library in Sudbury, at the Mines and Minerals Information Centre in Toronto, and at the regional Mines and Minerals office whose district includes the area covered by the report (see below).

Copies can be purchased at Publication Sales and the office whose district includes the area covered by the report. Although a particular report may not be in stock at locations other than the Publication Sales office in Sudbury, they can generally be obtained within 3 working days. All telephone, fax, mail and e-mail orders should be directed to the Publication Sales office in Sudbury. Use of VISA or MasterCard ensures the fastest possible service. Cheques or money orders should be made payable to the *Minister of Finance.*

Mines and Minerals Information Centre (MMIC) Tel: (416) 314-3800
Macdonald Block, Room M2-17
900 Bay St.
Toronto, Ontario M7A 1C3

Mines Library Tel: (705) 670-5615
933 Ramsey Lake Road, Level A3
Sudbury, Ontario P3E 6B5

Publication Sales Tel: (705) 670-5691(local)
933 Ramsey Lake Rd., Level A3 1-888-415-9845(toll-free)
Sudbury, Ontario P3E 6B5 Fax: (705) 670-5770
E-mail: pubsales@ndm.gov.on.ca

Regional Mines and Minerals Offices:

Kenora - Suite 104, 810 Robertson St., Kenora P9N 4J2

Kirkland Lake - 10 Government Rd. E., Kirkland Lake P2N 1A8

Red Lake - Box 324, Ontario Government Building, Red Lake P0V 2M0

Sault Ste. Marie - 70 Foster Dr., Ste. 200, Sault Ste. Marie P6A 6V8

Southern Ontario - P.O. Bag Service 43, 126 Old Troy Rd., Tweed K0K 3J0

Sudbury - Level B3, 933 Ramsey Lake Rd., Sudbury P3E 6B5

Thunder Bay - Suite B002, 435 James St. S., Thunder Bay P7E 6S7

Timmins - Ontario Government Complex, P.O. Bag 3060, Hwy. 101 East, South Porcupine P0N 1H0

Toronto - MMIC, Macdonald Block, Room M2-17, 900 Bay St., Toronto M7A 1C3

This report has not received a technical edit. Discrepancies may occur for which the Ontario Ministry of Northern Development and Mines does not assume any liability. Source references are included in the report and users are urged to verify critical information. Recommendations and statements of opinions expressed are those of the author or authors and are not to be construed as statements of government policy.

If you wish to reproduce any of the text, tables or illustrations in this report, please write for permission to the Team Leader, Publication Services, Ministry of Northern Development and Mines, 933 Ramsey Lake Road, Level B4, Sudbury, Ontario P3E 6B5.

Cette publication est disponible en anglais seulement.

Parts of this report may be quoted if credit is given. It is recommended that reference be made in the following form:

Sproule, R.A., Lesher, C.M., Ayer, J.A. and Thurston, P.C. 2003. Geochemistry and metallogenesis of komatiitic rocks in the Abitibi greenstone belt, Ontario; Ontario Geological Survey, Open File Report 6073, 119p.

Contents

Abstract xv

1 Introduction 1
  1.1 Background 1
  1.2 Aims 1
  1.3 Methodology 2
  1.4 Terminology and Abbreviations 3
  1.5 Abitibi Greenstone Belt 3
    1.5.1 Geological Background 3
    1.5.2 Komatiites as Stratigraphic Markers and Tectonic Indicators 7
  1.6 Komatiites 7
    1.6.1 Background and Nomenclature 7
    1.6.2 Geochemical Classification 9
    1.6.3 Review of the Origin of Komatiites 13
      1.6.3.1 Introduction to Plumes 13
      1.6.3.2 Summary of the Petrogenesis of Komatiites 15

2 Petrography 17

3 Geochemistry 18
  3.1 Introduction 18
  3.2 Alteration 19
    3.2.1 Literature Review 19
    3.2.2 Petrographic Screening 19
    3.2.3 Geochemical Criteria 20
    3.2.4 Alteration Filters 25
  3.3 Major Elements 25
  3.4 Minor Elements 29
    3.4.1 Chromium 29
    3.4.2 Nickel 34
    3.4.3 Copper 34
    3.4.4 Cobalt 34
    3.4.5 Scandium 35
    3.4.6 Vanadium 35
    3.4.7 Zinc 35
  3.5 Trace Elements 35
    3.5.1 Lithophile Elements 35
      3.5.1.1 High Field-Strength Elements 35
      3.5.1.2 Large-Ion Lithophile Elements 39
    3.5.2 Platinum Group Elements 39
      3.5.2.1 Iridium 39
      3.5.2.2 Ruthenium 39
      3.5.2.3 Rhodium 39
      3.5.2.4 Platinum 39
      3.5.2.5 Palladium 44
  3.6 Isotopic Data 44
    3.6.1 Nd Isotopes 44

3.6.2 Os Isotopes 46
3.7 Summary of Geochemical Observations 47
3.8 Petrogenetic Discussion 52
3.8.1 Source Composition and Depth of Melting 52
3.8.2 Petrogenesis of Ferropicrites in the Abitibi Greenstone Belt 55
3.8.3 Crustal Contamination 56

4 Spatial Variations in the Geochemistry of Komatiites in the Abitibi Greenstone Belt 59
4.1 Shining Tree Area 59
4.2 Round Lake Dome 60
4.3 Kidd-Munro Trend 61
4.3.1 Kidd-Munro Trend - Eastern Section 61
4.3.2 Kidd-Munro Trend - Central Section 62
4.3.3 Kidd-Munro Trend - Western Section 63
4.4 Reaume-McCart Trend 63
4.5 Lake Abitibi 63
4.6 Shaw Dome 64
4.7 Bartlett Dome 64
4.8 Halliday Dome 65
4.9 Swayze Belt 65
4.10 Porcupine Destor Fault Zone - Timmins Region 66
4.11 Porcupine Destor Fault Zone - Eastern Matheson to Quebec Border 67
4.12 West of Timmins 68
4.13 Regional Summary and Implications 68

5 Spatial and Temporal Variations in the Geochemistry of Komatiites in the Abitibi Greenstone Belt 70
5.1 Results 70
5.2 Models for the Evolution of Plume-Derived Melts in the Abitibi Greenstone Belt 76

6 Tectonic Implications for the Abitibi Greenstone Belt 79

7 Comparisons with Other Greenstone Belts 79
7.1 Superior Province 79
7.2 Other Greenstone Belts 81

8 Metallogeny 82
8.1 Komatiite-Associated Ni-Cu-(PGE) Deposits 82
8.1.1 Type I Basal Ni-Cu-(PGE) Mineralization 82
8.1.2 Type II Strata-Bound Internal Ni-Cu-(PGE) Mineralization 83
8.1.3 Type III Stratiform "Reef-Style" PGE-(Cu)-(Ni) Mineralization 83
8.1.4 Type IV Hydrothermal-Metamorphic-Metasomatic Ni-Cu-(PGE) Mineralization 84
8.1.5 Type V Tectonically-Mobilized Ni-Cu-(PGE) Mineralization 85
8.2 Summary of Exploration Criteria 85
8.2.1 Types I and II Ni-Cu-(PGE) Mineralization 85
8.2.2 Type III PGE-(Cu)-(Ni) Mineralization 86
8.3 Komatiite-Associated Ni-Cu-(PGE) Deposits in the Abitibi Greenstone Belt 87
8.3.1 Type I Mineralization in the AGB 87
8.3.1.1 Areas Recommended for Further Exploration 88
8.3.2 Type II Mineralization in the AGB 88
8.3.2.1 Areas Recommended for Further Exploration 88

8.3.3 Type III Mineralization in the AGB 89
8.3.3.1 Areas Recommended for Further Exploration 89
8.3.4 Type IV Mineralization in the AGB 89
8.3.5 Type V Mineralization in the AGB 89
8.4 Chalcophile Element Geochemistry of Komatiites in the Abitibi Greenstone Belt 90

9 Future Work 96

Acknowledgments 97

Appendix A*. Sample Preparation and Analytical Methods 98

Bibliography and References 102

Metric Conversion Table 119

* Appendix B (sample descriptions, locations and lithogeochemical analyses) is compiled in Miscellaneous Release–Data 120 (MRD 120), available separately from this report.

FIGURES

1.1. Terrane map of the Superior Province 5

1.2. Assemblage map of the Abitibi greenstone belt 6

1.3. Summary of compositional facies of komatiites 10

1.4. Volcanic facies model for komatiites. 11

1.5. Model of the morphology and anatomy of a mantle plume. 14

3.1. Al_2O_3 vs. SiO_2 (wt.% volatile-free) for komatiitic rocks in the Abitibi greenstone belt and comparisons to komatiitic rocks in other greenstone belts 21

3.2. MgO (wt.% uncorrected) vs. MgO (wt.% volatile-free) for komatiitic rocks in the Abitibi greenstone belt 22

3.3. Loss-on-ignition (LOI) (wt.%) vs. MgO (wt.% uncorrected) for all komatiites 23

3.4. R mode factor analysis for komatiitic rocks in the Abitibi greenstone belt 24

3.5. SiO_2, TiO_2, Al_2O_3, and MnO vs. MgO (wt.% volatile-free) for komatiitic rocks in the Abitibi greenstone belt 26

3.6. Fe_2O_3, CaO, Na_2O, and K_2O vs. MgO (wt.% volatile-free) for komatiitic rocks in the Abitibi greenstone belt 27

3.7. Pearce element ratio plots for komatiitic rocks in the Abitibi greenstone belt 28

3.8. Cr and Ni (ppm) vs. MgO (wt.% volatile-free) for komatiitic rocks in the Abitibi greenstone belt 30

3.9. Cu and Co (ppm) vs. MgO (wt.% volatile-free) for komatiitic rocks in the Abitibi greenstone belt 31

3.10. Sc (ppm) vs. MgO (wt.% volatile-free) for komatiitic rocks in the Abitibi greenstone belt 32

3.11. V and Zn (ppm) vs. MgO (wt.% volatile-free) for komatiitic rocks in the Abitibi greenstone belt 33

3.12a. Th, Nb, Zr, and Y (ppm) vs. MgO (wt.% volatile-free) for komatiitic rocks in the Abitibi greenstone belt 36

3.12b. Gd, Yb, La, and Ce (ppm) vs. MgO (wt.% volatile-free) for komatiitic rocks in the Abitibi greenstone belt 37

3.12c. Nd, and Sm (ppm) vs. MgO (wt.% volatile-free) for komatiitic rocks in the Abitibi greenstone belt 38

3.13a. Cs, and Ba (ppm) vs. MgO (wt.% volatile-free) for komatiitic rocks in the Abitibi greenstone belt 40

3.13b. Rb, Sr, and Eu (ppm) vs. MgO (wt.% volatile-free) for komatiitic rocks in the Abitibi greenstone belt 41

3.14a. Ir, Ru, Rh, and Pt (ppb) vs. MgO (wt.% volatile-free) for komatiitic rocks in the Abitibi greenstone belt 42

3.14b. Pd (ppb) vs. MgO (wt.% volatile-free) for komatiitic rocks in the Abitibi greenstone belt 43

3.15. Summary of Nd isotopic data for komatiitic rocks in the Abitibi greenstone belt and comparisons with sedimentary rocks in the Pontiac metasedimentary belt and Abitibi greenstone belt 45

3.16. Primitive mantle-normalized multi-element diagram for representative analyses of komatiitic rocks in the Abitibi greenstone belt 48

3.17. $[Th/Sm]_{MN}$ vs. $[Nb/Th]_{MN}$ and $[Th/Sm]_{MN}$ vs. $[Gd/Yb]_{MN}$ for komatiites in the Abitibi greenstone belt 49

3.18. Al_2O_3/TiO_2 vs. MgO (wt.% volatile-free) for komatiites in the Abitibi greenstone belt and Al_2O_3/TiO_2 vs. MgO bar chart 50

3.19. Al_2O_3/TiO_2 vs. chondrite-normalized $[Gd/Yb]_{MN}$ for komatiites in the Abitibi greenstone belt compared to komatiites in the Kambalda area (Western Australia), the Steep Rock and Lumby Lake belts (Superior Province), Kola Schist belt (Russia), and the Barberton greenstone belt (South Africa) 51

3.20a. $[TiO_2]_{molar}$ vs. $[Al_2O_3]_{molar}$ olivine projection for komatiites in the Abitibi greenstone belt with comparative data for komatiites at Barberton, Kambalda, Belingwe, Finland, and for komatiites and picrites at Gorgona 53

3.20b. $[Al_2O_3]_{molar}$ vs. $[Gd/Yb]_{MN}$ and $[TiO_2]_{molar}$ vs. $[Gd/Yb]_{MN}$ diagrams for komatiites in the Abitibi greenstone belt with comparative data for komatiites at Barberton, Kambalda, Belingwe, Finland, and for komatiites and picrites at Gorgona 54

3.21. $[La/Sm]_{MN}$, $[Th/Nb]_{MN}$, and $[Th/Sm]_{MN}$ vs. MgO (wt.% volatile-free) for komatiitic rocks in the Abitibi greenstone belt 58

5.1. Pie charts showing lithological components of komatiite-bearing assemblages in the Abitibi greenstone belt 74

5.2. Histograms showing Al_2O_3/TiO_2 ratios of komatiite-bearing assemblages in the Abitibi greenstone belt. 74

5.3a. Models for temporal variations in komatiitic geochemistry in the Abitibi greenstone belt 77

5.3b. Models for temporal variations in komatiitic geochemistry in the Abitibi greenstone belt (cont'd.) 78

8.1. Ni/Pd and Pd/Ir vs. MgO (wt.% volatile-free) for komatiites in the Abitibi greenstone belt 91

8.2. Pd/Ir vs. Ni/Cu for komatiites in the Abitibi greenstone belt 92

8.3. Pd (ppb) vs. Cu (ppm) for komatiites in the Abitibi greenstone belt 93

8.4. Mantle-normalized PGE diagrams for komatiites in the Abitibi greenstone belt 94

TABLES

1.1. Chemical classification of komatiitic rocks 12

1.2. Summary of the geochemical characteristics of ADK–TEK, AUK, and TDKB and interpreted source regions 15

1.3. Geochemical characteristics of each of the magma series from this study 17

3.1. Nd isotopic data for Abitibi greenstone belt komatiitic rocks (after alteration filtering) and other lithologies 44

4.1. Summary of lithological and geochemical features of the regions of the Abitibi greenstone belt 69

5.1. Summary of geochemical characteristics of stratigraphically assigned komatiites in the Abitibi greenstone belt 70

5.2. Representative analyses of komatiites and komatiitic basalts from the Abitibi greenstone belt 70

5.3. Subdivision of komatiites in the Tisdale assemblage 75

7.1. Summary of geochemistry of komatiites in the Superior Province 80

7.2. Summary of geochemical affinities of Archean komatiites worldwide 82

8.1 Calculated R-factors for Abitibi greenstone belt Ni-Cu-PGE deposits/showings 95

Abstract

The ~2.7 Ga Abitibi greenstone belt is one of the largest and best-preserved greenstone belts in the world. It occurs within the Superior Province of the Canadian Shield and contains nine lithotectonic assemblages, four of which contain komatiites: the *Pacaud* (2750-2735 Ma), *Stoughton-Roquemaure* (2725-2720 Ma), *Kidd-Munro* (2718-2710 Ma), and *Tisdale* (2710-2703 Ma) assemblages. Thus, komatiitic magmatism spans a range of ~47 My in the Abitibi greenstone belt.

There are important lithological differences between the komatiites in the different komatiite-bearing assemblages. The Pacaud assemblage contains both non-cumulate and cumulate komatiites. The Stoughton-Roquemaure assemblage contains primarily non-cumulate komatiites. The Kidd-Munro and Tisdale assemblages contain a much greater abundance of cumulate komatiites than the other assemblages, which are interpreted to represent lava channels or lava channel facies of channelized sheet flows. Komatiite-associated Ni-Cu-(PGE) deposits have only been identified within the Kidd-Munro (e.g., Alexo, Dundonald, Mickel, and Marbridge deposits/showings) and Tisdale (e.g., Hart, Langmuir, Redstone, Texmont, and Sothman deposits/showings) assemblages. This is consistent with the interpretation that komatiite-associated Ni-Cu-(PGE) deposits form within lava channels or channelized sheet flows, but not within sheet flows or lava lobes.

Komatiites in the Abitibi greenstone belt exhibit systematic variations in major and trace element geochemistry through the stratigraphic sequence, suggesting multiple melt extraction, magma mixing, and/or contamination events. Those in the Pacaud assemblage are Ti-depleted komatiites (TDKB: Al_2O_3/TiO_2 25-35 and $[Gd/Yb]_{MN}$ ~0.6), suggesting derivation from a garnet-rich source by prior removal of aluminum-depleted komatiite (ADK) or dynamic melting. Those in the Stoughton-Roquemaure assemblage are Al-depleted and Ti-enriched komatiites (ADK–TEK: Al_2O_3/TiO_2 6-15 and $[Gd/Yb]_{MN}$ ~1.2-1.4), suggesting retention of garnet in the source and therefore higher pressures and greater depths for melt extraction, and lesser Al-undepleted komatiites (AUK: Al_2O_3/TiO_2 15-25 and $[Gd/Yb]_{MN}$ ~1), suggesting generation at lower pressures and shallower depths. Those in the Kidd-Munro assemblage are AUK with lesser ADK–TEK, suggesting extraction at relatively shallow (garnet-absent) and relatively great (garnet-present) depths, respectively. Those in the Tisdale assemblage are AUK, suggesting extraction at a relatively shallow (garnet-absent) depths. Thus, there appears to be an overall trend of decreasing influence of garnet in the mantle residues and therefore decreasing depth of melt extraction with time. There are several possible mechanisms to account for these variations: 1) a decrease in the depth of melt extraction as the plume(s) ascended; 2) a decrease in the amount of magma derived from deeper levels in the plume relative to that derived from shallower levels in the plume, possibly representing a change in plume morphology with time, for example as it flattened and was dragged by the overlying plate; 3) a decrease in the rate of plume ascent by interaction with a subducting slab; and 4) a decrease in the thickness of the lithosphere during plume ascent, perhaps related to lithospheric thinning by the rising plume(s). The variations in komatiite geochemistry transgress several previously proposed terrane boundaries, supporting autochthonous models for the Abitibi greenstone belt.

Relatively low $[Nb/Th]_{MN}$ and $[Th/Sm]_{MN}$ of komatiites in the Pacaud and Stoughton-Roquemaure assemblages, similar to normal depleted mantle, suggest that these lavas were not significantly contaminated by crustal rocks. However, $[Nb/Th]_{MN}$ and $[Th/Sm]_{MN}$ of komatiites in the Kidd-Munro and Tisdale assemblages vary between values accepted for depleted upper mantle and upper Archean continental crust, suggesting a continuous range of contamination up to ~35%.

Type I (stratiform contact) Ni-Cu-(PGE) mineralization in the Abitibi greenstone belt has been found thus far only in Al-undepleted cumulate komatiites in the Kidd-Munro (e.g., Alexo-Dundonald, Mickel, Marbridge) and Tisdale (e.g., Hart-Langmuir-Redstone, Texmont, Sothman) assemblages. Although many komatiite-associated Ni-Cu-(PGE) deposits worldwide (e.g., Kambalda, Mt. Keith, Perseverance, Thompson) are hosted by AUK, some (e.g., Boa Vista, Forrestania, Ruth Well) are hosted by ADK, so the depth of melt extraction does not appear to be an important parameter in the genesis of these deposits. The occurrence of komatiite-associated Ni-Cu-(PGE) mineralization in the Kidd-Munro and Tisdale assemblages is attributed to them containing both lava channels (heat and metal sources) and sulfide-facies iron formations, sulfidic slates, or exhalative sulfide lenses (sulfur sources). *Type II* (stratabound disseminated) mineralization has been found in only one locality in the Kidd-Munro assemblage (Dumont). Subeconomic *Type III* (stratiform "reef-style") PGE-(Cu)-(Ni) mineralization has been identified in many locations within the Abitibi greenstone belt, including the Stoughton-Roquemaure (e.g., Boston Creek ferropicrite) and Kidd-Munro (e.g., Fred's Flow) assemblages, and in associated tholeiitic complexes (e.g., Centre Hill Complex). It requires no lava channelization or external S source, so it may be expected to occur in any mafic-ultramafic unit that achieved sulfide saturation through normal fractional crystallization processes.

Geochemistry and Metallogenesis of Komatiitic Rocks in the Abitibi Greenstone Belt, Ontario

R.A. Sproule[1], C.M. Lesher[1], J.A. Ayer[2] and P.C. Thurston[1]

Ontario Geological Survey
Open File Report 6073
2003

---

[1]Mineral Exploration Research Centre, Department of Earth Sciences,
Laurentian University, Sudbury, Ontario, Canada, P3E 6B5

[2]Precambrian Geoscience Section, Ontario Geological Survey
Ministry of Northern Development and Mines, Sudbury, Ontario, Canada, P3E 6B5

1 Introduction

1.1 BACKGROUND

Komatiites are ultramafic volcanic rocks that occur mainly in Archean greenstone belts (Arndt and Nisbet, 1982). They form a wide range of volcanic facies (e.g., lava channels, channelized sheet flows, sheet flows, lava ponds, lava lobes, pillow lavas) and locally host magmatic Ni-Cu-(PGE) sulfide deposits (e.g., Kambalda, Alexo, Raglan) (Lesher, 1989; Barnes et al., 1999). As they have been interpreted to have formed by high degree partial melting of mantle plumes (Campbell and Griffiths, 1990) and to have erupted as voluminous, highly mobile flows capable of traveling very long distances if channelized (Lesher et al., 1984; Lesher, 1989; Hill et al., 1990, 1995), they provide important constraints on the composition and structure of the Archean mantle, the nature of heat flow in, and volcanism on, the early Earth, the stratigraphy and structure of Archean greenstone belts, and the metallogenesis of Ni-Cu-(PGE) deposits.

A large body of work exists on the geochemistry and petrology of komatiitic rocks (e.g., Tomlinson et al., 1999a; Hollings et al., 1999; Hollings and Kerrich, 1999; Polat et al., 1999; Polat and Kerrich, 2000, 2001; Tomlinson and Condie, 2001), particularly in the Abitibi greenstone belt (e.g., Eakins, 1972; Fleet and McRae, 1975; Arndt, 1975, 1986; Coad, 1979; Nesbitt and Sun, 1976; Arndt et al., 1977; Gélinas et al., 1977; Arndt and Nesbitt, 1982; Ludden and Gélinas, 1982; Barnes et al., 1983; Cattell and Arndt, 1987; Davis, 1997, 1999; Xie et al., 1993; Dostal and Mueller, 1997; Fan and Kerrich, 1997; Barrie, 1999; Stone and Stone, 2000) and associated basalts (Hollings and Wyman, 1999; Wyman and Hollings, 1998; Kerrich et al., 1999a, 1999b; Wyman, 1999; Hollings and Kerrich, 2000; Wyman et al., 2000, 2002, 1999a, 1999b; Hollings, 2002; Kerrich and Xie, 2002) in the Superior Province.

Xie et al. (1993) evaluated the depths of melting for different types of komatiites in the Abitibi greenstone belt. Several studies have examined the relationship between mantle plumes, tectonic setting, and komatiitic magmatism in the Abitibi greenstone belt (e.g., Xie et al., 1993; Barrie, 1999; Dostal and Mueller, 1997) and in other parts of the Superior Province (e.g., Tomlinson et al., 1999a; Hollings and Kerrich, 1999; Polat and Kerrich, 2000, 2001), making comparisons between modern day tectonic processes and those operating in the Archean. Naldrett and Gasparini (1971), Coad (1979), Green and Naldrett (1981), Davis (1997, 1999), Barrie (1999), Barrie et al. (1999), and Stone and Stone (2000) examined the link between komatiites and Ni-Cu-(PGE) mineralization in the Tisdale Assemblage in the Shaw Dome. Barrie (1999) provided critical age constraints on the Kidd-Munro assemblage, especially in less well-studied regions, and compiled a large database of unpublished industry-generated geochemical data, parts of which were utilized in this study.

1.2 AIMS

The major aims of this project were to examine spatial and stratigraphic variations in komatiite geochemistry in the Abitibi greenstone belt in order to provide constraints on the petrogenesis of komatiites, to aid in the interpretation of stratigraphic architecture and assembly of the Abitibi greenstone belt, and to aid in the exploration for komatiite-associated Ni-Cu-(PGE) sulfide deposits. Specific goals of the project were to:

1) Establish the geochemistry and petrogenesis of komatiites and komatiitic basalts in the Abitibi greenstone belt.

2) Examine the variations in komatiite geochemistry within the stratigraphic framework of Ayer et al. (2002) to determine whether that framework is valid and whether komatiite geochemical trends vary systematically with geographic and stratigraphic location.

3) Examine the relative importance of primary (e.g., partial melting, fractional crystallization, and crustal contamination) and secondary (e.g., seafloor weathering, hydrothermal alteration, and regional metamorphism) processes on the geochemistry of the komatiites and characterize the mantle source region for the komatiites.

4) Consider the implications of spatial variations in komatiite geochemistry on the tectonic development of the Abitibi greenstone belt (i.e., allochthonous vs. autochthonous models) and the nature of any underlying basement lithologies.

5) Establish the sulfide saturation histories of the komatiites to determine whether certain portions of the komatiitic stratigraphy are more prospective than others for komatiite hosted Ni-Cu-(PGE) mineralization.

6) Compare the geochemistry and petrogenesis of the komatiites in the Abitibi greenstone belt with those in other greenstone belts in the Superior Province and elsewhere.

1.3 METHODOLOGY

The geochemistry and petrology of komatiites in the Abitibi greenstone belt have been studied by Eakins (1972), Fleet and McRae (1975), Coad (1979), Nesbitt and Sun (1976), Arndt et al. (1977), Gélinas et al. (1977), Arndt and Nesbitt (1982), Ludden and Gélinas (1982), Barnes et al. (1983), Arndt (1986), Cattell and Arndt (1987), Xie et al. (1993), Dostal and Mueller (1997), Fan and Kerrich (1997), and Barrie (1999). Our research differs from these studies in several ways:

1) We have studied variations in komatiite geochemistry over a much larger area of the Abitibi greenstone belt, with a focus on the Ontario side.

2) We have sampled within a much better characterized stratigraphic framework, allowing for examination of temporal variations in geochemistry[1].

3) Recent improvements in sample preparation and analytical methods have permitted us (and other workers since the mid-1990s) to measure a much greater number of minor and trace elements with lower detection limits and greater precision.

We have compiled a database of geochemical data for more than 2400 komatiites and komatiitic basalts from both Ontario and Québec that includes data contributed by Outokumpu Ltd. (Stone and Lesher, 1995), the Ontario Geological Survey (OGS), and the Geological Survey of Canada (GSC), and data from the literature (Eakins, 1972; Fleet and McRae, 1975; Coad, 1979; Nesbitt and Sun, 1976; Gélinas et al., 1977; Barnes et al., 1981; Arndt and Nesbitt, 1982; Arndt, 1986; Cattell and Arndt, 1987; Xie et al., 1993; Dostal and Mueller, 1997; Fan and Kerrich, 1997; Ludden and Gélinas, 1982; Barrie, 1999). The database is included in Appendix B (MRD 120), available separately from this report.

---

[1] Because they contain such low abundances of datable radiogenic elements or minerals, komatiites are difficult to date directly. The stratigraphic assignments in this project were made using the geochronological database for associated felsic metavolcanic rocks compiled by Ayer et al. (2002). Additional geochronological data may result in some changes to the assignments.

1.4 TERMINOLOGY AND ABBREVIATIONS

We have adopted the following geochemical terminology and abbreviations in this report:

Alkali metals (alkalis): Cs, Rb, K, Na

Alkaline earth metals (calc-alkalis): Ba, Sr, Ca, Mg

Base metals: Co, Ni, Cu, Zn, Pb

Chalcophile elements (CE): Co, Ni, Cu, Au, Pt, Pd, Rh, Ru, Ir, Os

First period transition metals (FPTM): Sc, Ti, V, Cr, Mn, Fe, Co, Ni, Cu, Zn

High-field strength elements (HFSE, high charge and small ionic radius): Zr, Hf, Nb, Ta, Th, U

Highly incompatible lithophile elements (HILE): Cs, Rb, Ba, Th, U, Nb, Ta, K, La, Ce, Pb, Pr, Nd, Sr

Large-ion lithophile elements (LILE, low charge and large ionic radius): Cs, Rb, Tl, K, Ba

Major elements (in komatiites): Si, Al, Fe, Mg, Ca

Minor elements (in komatiites): Ni, Cr, Ti, Mn, Na, K, P

Moderately incompatible lithophile elements (MILE): Sm, Eu, Gd, Tb, Dy, Eu, Ho, Ti, Er, Tm, Yb, Lu

Platinum-group elements (PGE): Pt, Pd, Rh, Ru, Ir, Os
    Platinum-group PGE (PPGE): Pt, Pd, Rh
    Iridium-group PGE (IPGE): Ru, Ir, Os

Precious metals (PM): Au, Pt, Pd, Rh, Ru, Ir, Os

Rare-earth elements (REE): La, Ce, Pr, Nd, Sm, Eu, Gd, Tb, Dy, Ho, Er, Tm, Yb, Lu
    Light REE (LREE): La, Ce, Pr, Nd, (Pm)
    Heavy REE (HREE): Ho, Er, Tm, Yb, Lu
    Middle REE (MREE): Sm, Eu, Gd, Tb, Dy

Ti-depleted komatiitic basalts (TDKB): characterized by $25 < Al_2O_3/TiO_2 < 35$ and $0.6 < [Gd/Yb]_{MN} < 0.8$

Ti-enriched komatiites (TEK, similar to some komatiites in Finland): characterized by $Al_2O_3/TiO_2 < 15$ and $[Gd/Yb]_{MN} > 1.2$

Al-depleted komatiites (ADK, also referred to as Barberton-type komatiites): characterized by $Al_2O_3/TiO_2 < 15$ and $[Gd/Yb]_{MN} > 1.2$

Al-undepleted komatiites (AUK, also referred to as Munro-type komatiites): characterized by $15 < Al_2O_3/TiO_2 < 25$ and $[Gd/Yb]_{MN} \sim 1$

1.5 ABITIBI GREENSTONE BELT

1.5.1 Geological Background

The Abitibi greenstone belt is part of the Superior Province, one of the largest Archean cratons in the world (Figure 1.1). Because of locally superb exposure, generally excellent preservation, and generally low metamorphic grade, the Abitibi greenstone belt is an excellent place to evaluate volcanic, petrogenetic, and tectonic processes in the Archean.

The Abitibi belt developed between 2.8 to 2.6 Ga (Jackson and Fyon, 1991). It is bounded by the Kapuskasing Structural Zone to the west, the Palaeoproterozoic Huronian Supergroup and the Neoarchaean Pontiac Subprovince and high-grade gneisses and granitoids to the south and east, and the Neoarchean Opatica Subprovince to the North (Figure 1.1).

The Abitibi belt has been subdivided into Northern and Southern regions/zones, although different authors have proposed different boundaries. In the subdivision proposed by Dimroth et al. (1982), the Northern region contains abundant tonalite-trondhjemite-granodiorite (TTG)-type intrusions, large anorthosite complexes, and many ultramafic intrusive complexes of dominantly tholeiitic affinity, but no komatiites. The rocks in the Northern region vary from greenschist- to amphibolite-facies. In contrast, the Southern region contains few TTG suites, abundant metavolcanic and metasedimentary units, abundant syn-volcanic peridotitic to granodioritic intrusions, and abundant komatiite flows/sills. The rocks in the Southern region vary from predominantly sub-greenschist to greenschist facies, but rise to amphibolite facies at the margins of intrusive complexes. Ludden et al. (1986) subdivided the Northern and Southern regions of Dimroth et al. (1982) into 1) a Northern Volcanic Zone, 2) a Central Granite-Gneiss Zone, 3) a Southern Volcanic Zone, and 4) a Southern Granite-Gneiss Zone.

Older rocks (~2.8 Ga) are observed only in the Northern zone/region of the Abitibi belt. In the Southern zone/region, metavolcanic rocks and associated metasedimentary and syn-volcanic peridotite to granodiorite intrusions formed between 2.75 and 2.70 Ga. Extensive volumes of TTG suites and lesser syenites were emplaced between 2.70 and 2.68 Ga (Jackson and Fyon, 1991). Clastic sedimentary rocks and alkalic volcanic rocks of the Timiskaming assemblage were deposited in close spatial association with regional-scale, steeply-dipping shear zones (e.g., Porcupine-Destor and Larder-Cadillac Fault Zones) during and after the main magmatic episode.

The ~2.7 Ga Abitibi greenstone belt contains several lithologically-distinct and possibly structurally-repeated volcano-sedimentary assemblages[2], which have been subdivided into several stratigraphically- and structurally-distinct terranes[3]. The relationships between terranes are ambiguous and the belt may represent: 1) a collage of allochthonous terranes, each a single lithotectonic assemblage formed in a different tectonic setting; 2) a single autochthonous terrane representing a series of assemblages formed along a stratigraphically and tectonically-complex and structurally-deformed convergent margin, or 3) a combination of the above. Ultramafic and mafic volcanic rocks, including komatiites, komatiitic basalts, picrites, ferropicrites, and tholeiites outcrop throughout the Abitibi greenstone belt, predominantly in the Southern Volcanic Zone (Ludden and Gélinas, 1982). Although Jensen (1985) provided compelling stratigraphic evidence for regional scale correlations across large parts of the Abitibi greenstone belt, allochthonous models have been favoured since then (e.g., Jackson and Fyon, 1991; Jackson et al., 1994). Recently, however, Heather (1998) and Ayer et al. (1999) recognized that the Swayze area of the Abitibi greenstone belt consists of distinct volcanic cycles and suggested that this stratigraphy might be applicable to other parts of the Abitibi greenstone belt. Based on ~200 high-precision U-Pb zircon dates, Ayer et al. (1999) subdivided the Abitibi greenstone belt into nine stratigraphic assemblages that locally cross some of the terrane boundaries proposed by Jackson and Fyon (1991). At this stage, the geochronologic and stratigraphic evidence appears to favour an autochthonous model for at least parts of the Abitibi greenstone belt (Ayer et al., 2002). Figure 1.2 shows an interpretative map of the Western Abitibi greenstone belt showing the lithotectonic assemblages.

---

[2] A sequence of stratified volcanic/sedimentary units deposited during a discrete interval of time in a common depositional or volcanic setting (Thurston, 1991).

[3] A fault-bounded area containing tectonic assemblages (lithostratigraphic units representing a specific depositional or volcanic setting responding to a tectonic event) that differ from those of adjacent terranes.

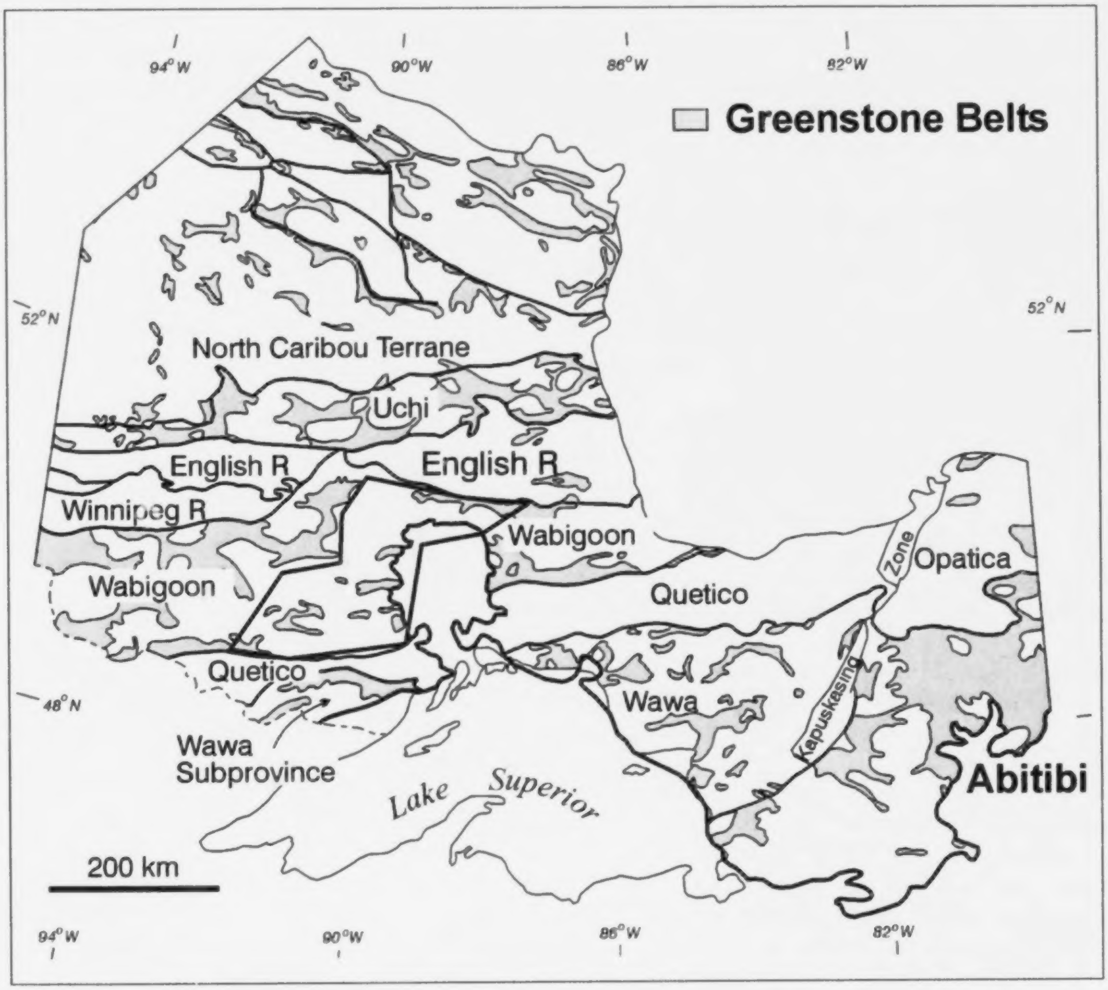
94°W
90°W
86°W
82°W
Greenstone Belts
52°N
52°N
North Caribou Terrane
Uchi
English R
English R
Winnipeg R
Wabigoon
Wabigoon
Quetico
Zone
Opatica
Quetico
Kapuskasing
Wawa
48°N
Wawa
Subprovince
Lake Superior
Abitibi
200 km
94°W
90°W
86°W
82°W

Figure 1.1. Terrane map of the Superior Province.

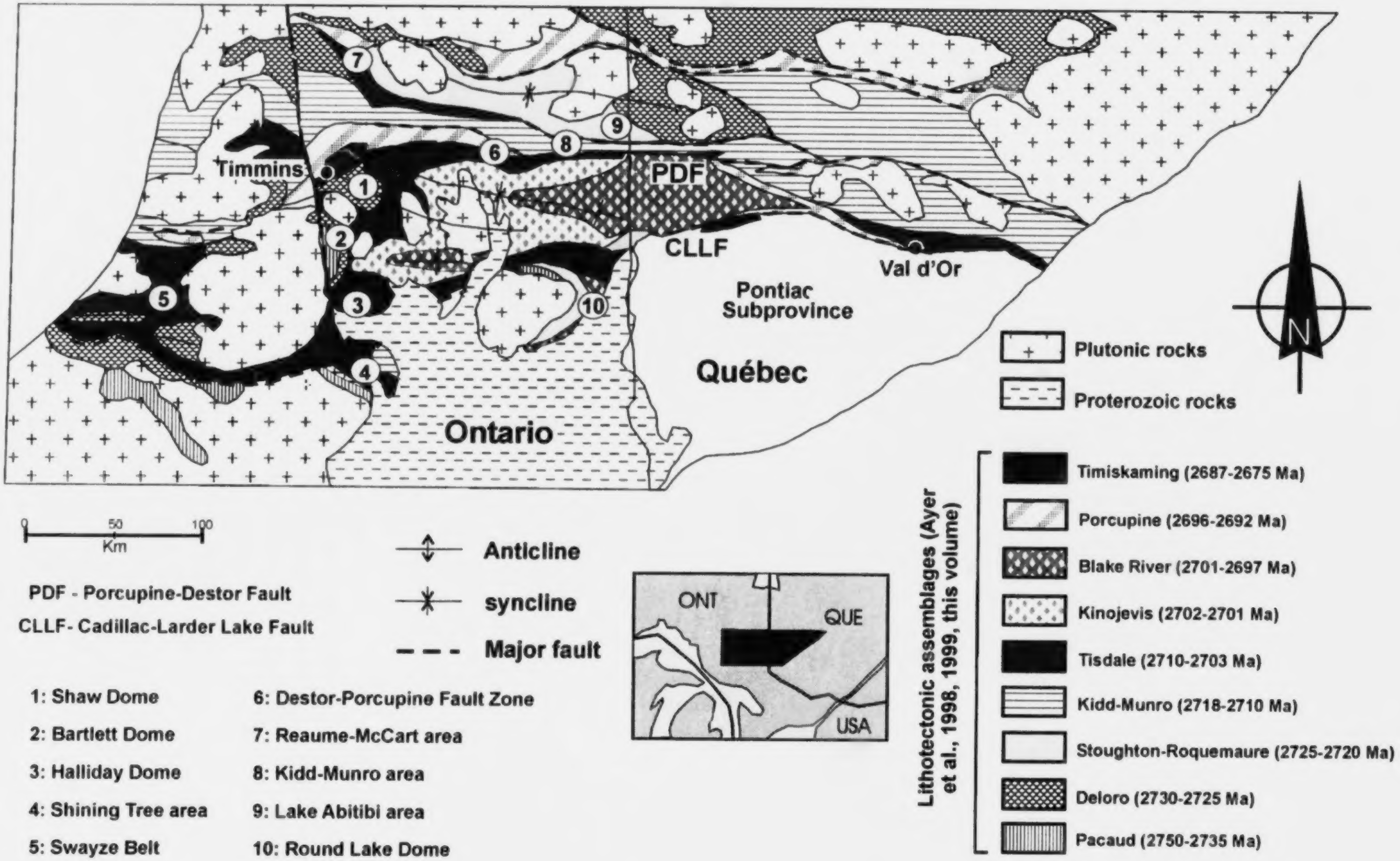

Timmins
PDF
CLLF
Val d'Or
Pontiac Subprovince
Québec
Ontario
1
2
3
4
5
6
7
8
9
10
N
0
50
100
Km
ONT
QUE
USA
Anticline
syncline
Major fault
Plutonic rocks
Proterozoic rocks
Lithotectonic assemblages (Ayer et al., 1998, 1999, this volume)
Timiskaming (2687-2675 Ma)
Porcupine (2696-2692 Ma)
Blake River (2701-2697 Ma)
Kinojevis (2702-2701 Ma)
Tisdale (2710-2703 Ma)
Kidd-Munro (2718-2710 Ma)
Stoughton-Roquemaure (2725-2720 Ma)
Deloro (2730-2725 Ma)
Pacaud (2750-2735 Ma)
PDF - Porcupine-Destor Fault
CLLF- Cadillac-Larder Lake Fault
1: Shaw Dome
2: Bartlett Dome
3: Halliday Dome
4: Shining Tree area
5: Swayze Belt
6: Destor-Porcupine Fault Zone
7: Reaume-McCart area
8: Kidd-Munro area
9: Lake Abitibi area
10: Round Lake Dome

Figure 1.2. Assemblage map of the Abitibi greenstone belt (*after* Ayer et al., 1998, 1999, 2002).

1.5.2 Komatiites as Stratigraphic Markers and Tectonic Indicators

Komatiites are present within four of the assemblages in the Abitibi greenstone belt: 1) *Pacaud* (2745-2735 Ma), 2) *Stoughton-Roquemaure* (2722-2720 Ma), 3) *Kidd-Munro* (2717-2712 Ma), and 4) *Tisdale* (2708-2703 Ma). Komatiites represent only a minor proportion of the lithologies present within each assemblage. There is much less than 1% by volume of komatiitic rocks in the Pacaud assemblage, ~2% in the Stoughton-Roquemaure assemblage, ~5% in the Kidd-Munro assemblage, and ~5% in the Tisdale assemblage. However, komatiites are interpreted to have had very low viscosities and, unlike more viscous felsic and mafic lavas, are interpreted to have formed very voluminous, highly mobile flows (Viljoen and Viljoen, 1969) that if channelized may have flowed great distances (Huppert et al., 1984; Lesher et al., 1984; Hill et al., 1990, 1995). Because komatiites exhibit a wide range of geochemical characteristics (e.g., Nesbitt et al., 1979; Arndt and Nisbet, 1982; Lesher and Stone, 1996; Herzberg and O'Hara, 1998; Sproule et al., 2002), komatiite geochemistry and geochronology may provide critical information on the continuity of assemblages, which in turn has ramifications for development of tectonic models and exploration strategies. Furthermore, as products of mantle-derived plume magmatism, komatiites may help elucidate the relationship between plumes and tectonic processes. For example, in a potentially hotter Archean mantle, heat may have been dissipated via plumes producing extensive amounts of oceanic plateaux (Thurston, 1994).

1.6 KOMATIITES

1.6.1 Background and Nomenclature

Arndt and Nisbet (1982) defined *komatiites* as ultramafic volcanic rocks with 18 to 32% MgO (volatile-free). Petrogenetically-related basalts with 12-18% MgO (volatile-free) were identified with the prefix *komatiitic*, but no recommendations were made for any of the associated cumulate rocks or intrusive rocks. The IUGS terminology for mafic and ultramafic igneous units defines all coarse-grained cumulate rocks (e.g., *gabbro*, *pyroxenite*, *peridotite*, and *dunite*) as plutonic, and fine-grained equivalents (e.g., *basalt*, *komatiite*) as volcanic; no terminology is provided for fine-grained intrusive rocks or coarse-grained extrusive rocks.

However, the mineralogy and textures of mafic and ultramafic igneous rocks are determined by their compositions and cooling histories, which are only indirectly related to volcanic or subvolcanic setting (Lesher and Keays, 2002). Consequently, rapidly cooled intrusive and slowly cooled extrusive varieties of these rocks may have identical textures (e.g., fine-grained chilled margins on lava flows and sills; coarse-grained spinifex-textured rocks in lava flows and veins; coarse-grained olivine cumulate rocks in lava channels and sub-volcanic sills) and are distinguishable only where geological relationships provide unequivocal information regarding the mode of emplacement. However, unequivocal field relationships are rare and interpretations change with additional information, new insights, and new fashions. For example, most of the "peridotites" in the Kambalda area of the Norseman-Wiluna Greenstone Belt were initially interpreted as intrusives (Woodall and Travis, 1969) and then as ponds overlying feeding fissures (Gresham and Loftus-Hills, 1981), but have subsequently been reinterpreted as distal lava channels (Lesher et al., 1984; Hill et al., 1990, 1995). Similarly, most of the "dunites" in the Perseverance-Mt. Keith area of the Archean Norseman-Wiluna Greenstone belt of Australia were originally interpreted as intrusions (Naldrett and Turner, 1977), but have since been reinterpreted as lava channels (Donaldson et al., 1986; Barnes et al., 1988; Hill et al., 1990, 1995). Some of the "komatiitic basalts" intersected in diamond-drill holes in the Dundonald Beach area in Dundonald Township of the Abitibi greenstone belt that were interpreted to be extrusive and intercalated with graphitic sediments (Muir and Comba, 1979) have since been reinterpreted as intrusive and invasive into the sediments based on mapping of stripped outcrops (Davis, 1997, 1999; Houlé et al., 2002; see also Beresford and Cas, 2001). Intrusive "komatiite" dikes with coarse olivine spinifex textures occur in the Dundonald (Davis, 1997, 1999) and Bartlett Dome (Houlé et al., 2001) areas of the Abitibi greenstone belt. Therefore, in this report the terms gabbro, pyroxenite, wehrlite, peridotite, and dunite will be used to refer to rocks with appropriate mineralogy and textures, without any genetic implications regarding volcanic or subvolcanic setting.

High-Mg komatiites derived from magmas with 25-32% MgO occur almost exclusively within Archean greenstone belts, including Paleoarchean (e.g., Barberton, South Africa; Selukwe, Zimbabwe), Mesoarchean (e.g., Ruth Well, Western Australia: Krapez and Eisenlohr, 1998; M. Barley and B. Krapez, pers. comm., 2002), and Neoarchean terranes (e.g., Abitibi, Canada; Belingwe, Zimbabwe; Baltic Shield, Finland and Russia; Yilgarn Craton, Western Australia). Low-Mg komatiites, komatiitic basalts, and ferropicrites derived from magmas with 18-25% MgO are abundant in the Paleoproterozoic (e.g., Cape Smith Belt, New Québec; Thompson Nickel Belt, Manitoba) and are only rarely present in the Phanerozoic (e.g., Gorgona: Echeverria, 1982; Echeverria and Aitken, 1986; Arndt et al., 1997b). Xenocrysts of Mg-rich olivine (up to Fo_{93}) are present in many Phanerozoic volcanic rocks (e.g., West Greenland: Larsen and Pedersen, 2000; Etendeka: Thompson and Gibson, 2000), indicating the presence of low-Mg komatiitic magmas in the Phanerozoic. However, there is no evidence for the presence of high-Mg komatiitic magmas in the Proterozoic or Phanerozoic and no evidence for a *systematic* decline in MgO content through time (cf. Abbott et al., 1994). It appears that Archean plume source regions were hotter, possibly indicating that Archean plumes may have initiated at the core-mantle boundary, whereas Proterozoic and Phanerozoic plumes may have initiated at the 650 km discontinuity (Campbell and Griffiths, 1990; Herzberg and O'Hara, 1998).

Most komatiites were erupted into subaqueous environments and all of those in the Abitibi greenstone belt are presently interpreted as subaqueous. However, subaerial komatiites have been described in the Baltic Shield (Saverikko, 1983, 1985), on Gorgona Island (Echeverria, 1986), and in the Barberton Greenstone Belt (Lowe, 2000).

Komatiites exhibit important physical and thermal characteristics that are critical in controlling their emplacement and crystallization (Nisbet, 1982; Huppert et al., 1984; Lesher et al., 1984):

1) very high degree partial melts of the mantle (10-15%, even if a sequential melting process is involved, but up to 50% for batch melting)

2) very high liquidus temperatures (1640-1360°C)

3) very large interval between the liquidus and solidus (460-180°C)

4) extremely low viscosities (0.1-2 Pa s)

5) high specific heats (1800-1700 J kg^{-1} $^{o}C^{-1}$)

6) high densities (2800-2700 g m^{-3})

Because of the large volumes of melt produced and because the eruption rates of magmas and the flow rates of lavas vary inversely with viscosity, komatiites should erupt and flow rapidly, forming voluminous, highly mobile flows (Viljoen and Viljoen, 1969), which, unless ponded, should travel great distances (Huppert et al., 1984; Lesher et al., 1984; Williams et al., 1998). The flows should fill depressions or flow down pre-existing valleys and flowage is likely to become channelized, with most lava transport confined to central conduits or lava tubes between more stagnant areas (Lesher et al., 1984). Because of the high specific heats and large interval between the liquidus and solidus (Arndt, 1976; Bickle, 1978a; Kinzler and Grove, 1985), komatiite lava will take a relatively long time to cool and solidify and will crystallize and accumulate olivine over a very wide temperature interval, forming a wide range of lava facies depending on the amount of olivine accumulation and differentiation (Lesher et al., 1984). Komatiite volcanism is likely, therefore, to have involved the eruption of very hot, highly fluid lava that flowed rapidly, for long periods, through conduits that probably followed depressions, grabens, or valleys in the pre-existing volcanic topography. During this flowage, the rocks that underlie the lava conduit are likely to suffer at least some degree of erosion (Huppert et al., 1984; Lesher et al., 1984; Williams et al., 1998).

The textural and compositional variations observed in komatiites resulting from variations in the relative degrees of olivine accumulation (flow-through) and *in situ* differentiation (timing of ponding) is summarized in Figure 1.3 and within a schematic lava flow field in Figure 1.4. The most economically important section of the flows are lava channels and channelized sheet flows, as these high-energy and more erosive regions are interpreted to preferentially host magmatic Ni-Cu-(PGE) deposits (Lesher et al., 1984; Lesher, 1989; Barnes et al., 1999; Lesher and Keays, 2002). A more detailed discussion of the physical volcanology and textural development of the komatiitic lavas and intrusions in the Abitibi greenstone belt is beyond the scope of this report, but is presently being studied by M. Houlé as part of a PhD dissertation based at Laurentian University and the University of Ottawa (Houlé et al., 2000, 2001, 2002).

1.6.2 Geochemical Classification

The major element compositions of komatiites vary as a function of the composition of the erupted lava and the degree of olivine fractionation and/or accumulation, resulting in compositional overlaps between aphyric, olivine-phyric, orthocumulate, mesocumulate, and adcumulate rocks derived from different parental magma compositions (Table 1.1). However, rocks derived by accumulation of olivine into a high-Mg komatiite will have higher Mg contents, higher Mg/Fe ratios, and will contain more magnesian olivines than those derived by accumulation of identical amounts of olivine into a low-Mg komatiite (Lesher and Groves, 1984; Lesher, 1989). All of the major element data in Table 1.1 and Appendix B (MRD 120) have been recalculated on a volatile-free basis and classified according to MgO content.

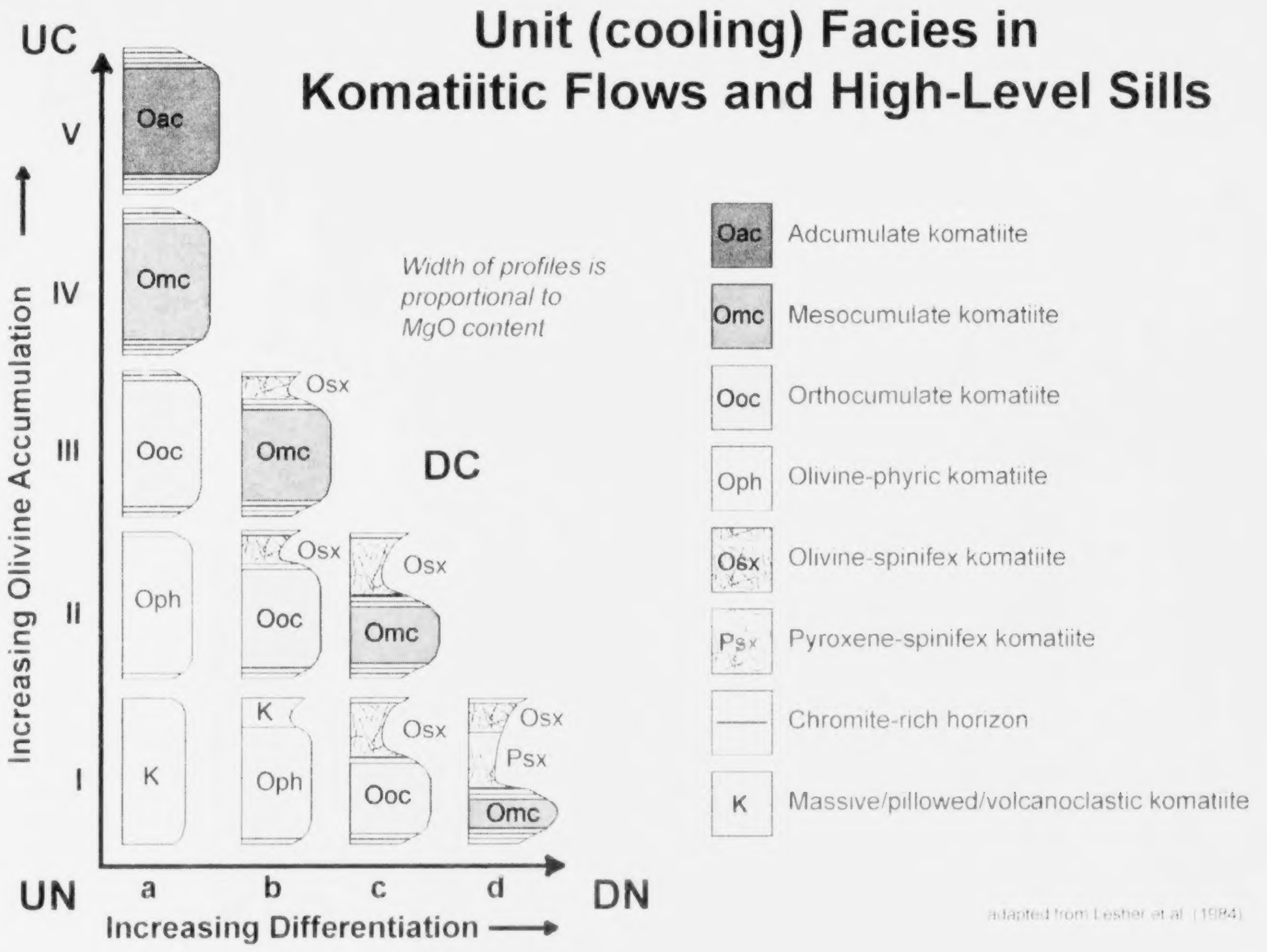

Unit (cooling) Facies in
Komatiitic Flows and High-Level Sills
UC
V
IV
III
II
I
UN
Increasing Olivine Accumulation
a
b
c
d
DN
Increasing Differentiation
DC
Oac
Omc
Ooc
Oph
K
Osx
Psx
Width of profiles is proportional to MgO content
Oac Adcumulate komatiite
Omc Mesocumulate komatiite
Ooc Orthocumulate komatiite
Oph Olivine-phyric komatiite
Osx Olivine-spinifex komatiite
Psx Pyroxene-spinifex komatiite
Chromite-rich horizon
K Massive/pillowed/volcanoclastic komatiite
adapted from Lesher et al. (1984)

Figure 1.3. Summary of compositional facies of komatiites (*modified after* Lesher et al., 1984). UC = undifferentiated cumulate; UN = undifferentiated non-cumulate; DC = differentiated cumulate; DN = differentiated non-cumulate.

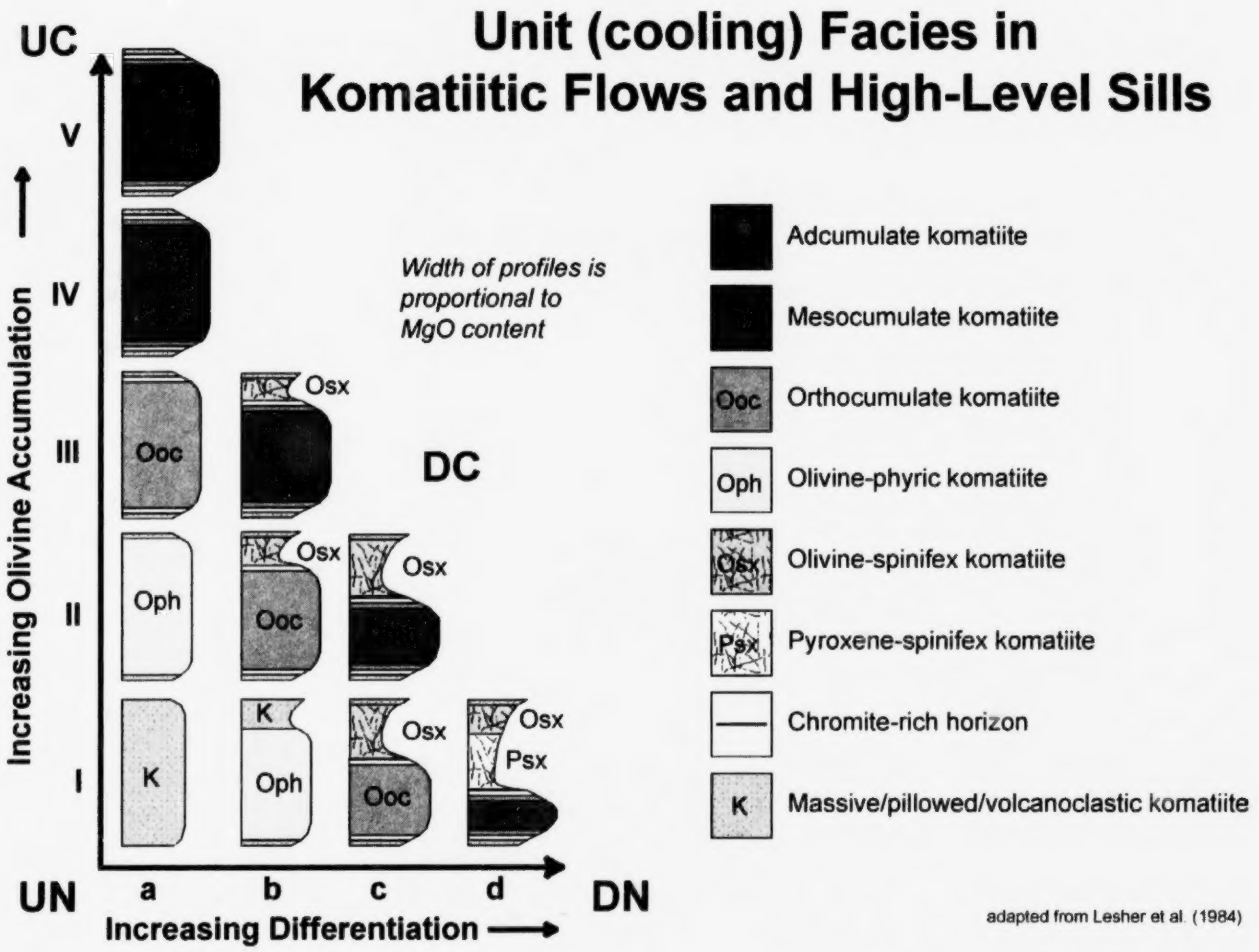

Unit (cooling) Facies in Komatiitic Flows and High-Level Sills

UC
V
IV
III
II
I
UN
Increasing Olivine Accumulation
a
b
c
d
DN
Increasing Differentiation
DC
Ooc
Oph
K
Osx
Psx
Width of profiles is proportional to MgO content
Adcumulate komatiite
Mesocumulate komatiite
Ooc Orthocumulate komatiite
Oph Olivine-phyric komatiite
Osx Olivine-spinifex komatiite
Psx Pyroxene-spinifex komatiite
Chromite-rich horizon
K Massive/pillowed/volcanoclastic komatiite

adapted from Lesher et al. (1984)

Figure 1.3. Summary of compositional facies of komatiites (*modified after* Lesher et al., 1984). UC = undifferentiated cumulate; UN = undifferentiated non-cumulate; DC = differentiated cumulate; DN = differentiated non-cumulate.

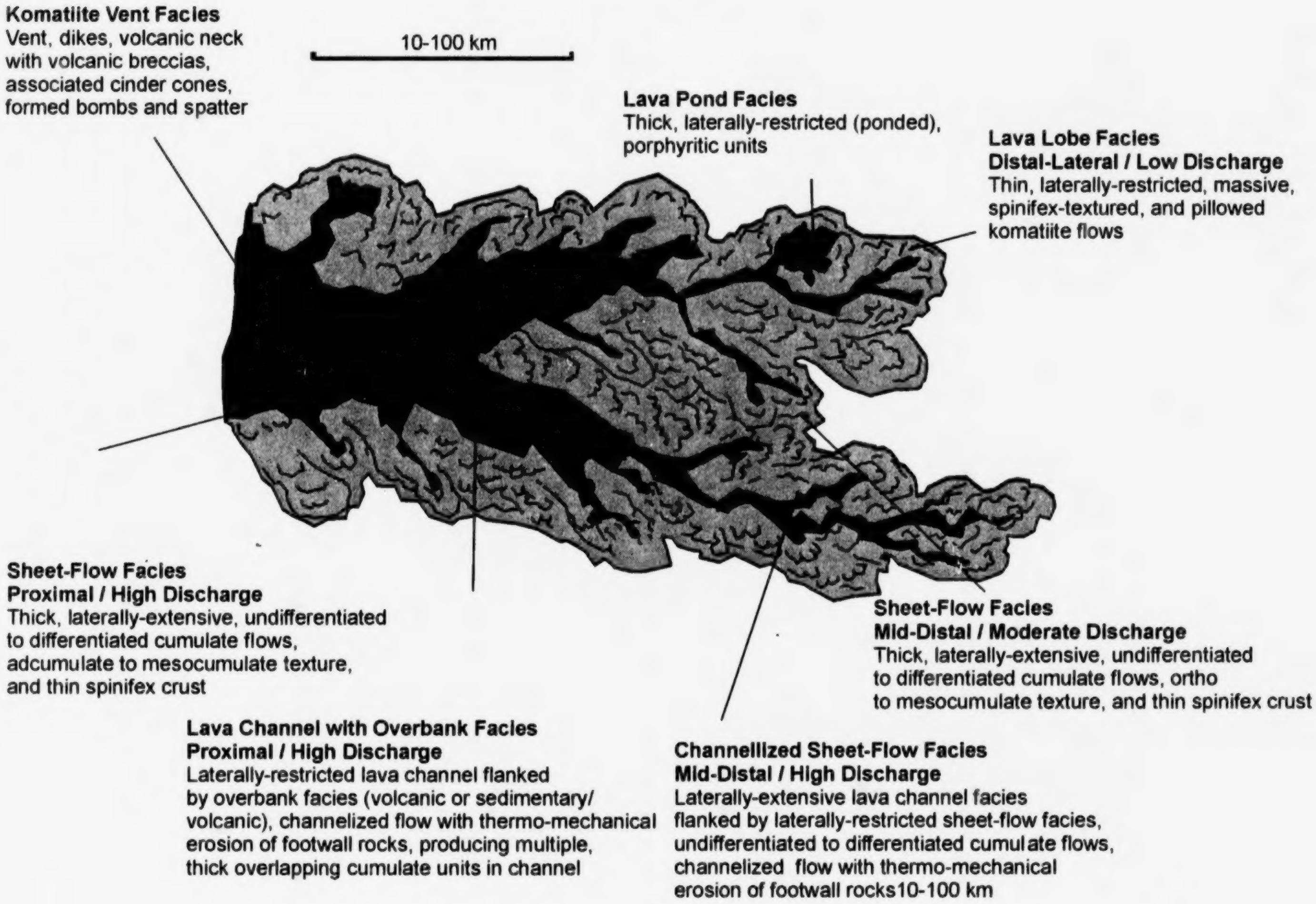
Komatiite Vent Facies
Vent, dikes, volcanic neck with volcanic breccias, associated cinder cones, formed bombs and spatter
10-100 km
Lava Pond Facies
Thick, laterally-restricted (ponded), porphyritic units
Lava Lobe Facies
Distal-Lateral / Low Discharge
Thin, laterally-restricted, massive, spinifex-textured, and pillowed komatiite flows
Sheet-Flow Facies
Proximal / High Discharge
Thick, laterally-extensive, undifferentiated to differentiated cumulate flows, adcumulate to mesocumulate texture, and thin spinifex crust
Sheet-Flow Facies
Mid-Distal / Moderate Discharge
Thick, laterally-extensive, undifferentiated to differentiated cumulate flows, ortho to mesocumulate texture, and thin spinifex crust
Lava Channel with Overbank Facies
Proximal / High Discharge
Laterally-restricted lava channel flanked by overbank facies (volcanic or sedimentary/ volcanic), channelized flow with thermo-mechanical erosion of footwall rocks, producing multiple, thick overlapping cumulate units in channel
Channellized Sheet-Flow Facies
Mid-Distal / High Discharge
Laterally-extensive lava channel facies flanked by laterally-restricted sheet-flow facies, undifferentiated to differentiated cumulate flows, channelized flow with thermo-mechanical erosion of footwall rocks10-100 km

Figure 1.4. Volcanic facies model for komatiites (*after* Hill et al., 1995).

Table 1.1. Chemical classification of komatiitic rocks (*adapted from* Donaldson et al., 1986).

Rock	Parental Magma	MgO (wt.%)	FeO (wt.%)	Cr (ppm)
Ferropicrite	Ferropicrite	12-18	14-20	~500
Komatiitic basalt	Komatiitic basalt	12-18	8-12	~500-2500
Low-Mg komatiite	Low-Mg komatiite	18-24	8-13	~2000-4000
High-Mg komatiite	High-Mg komatiite	24-30	8-12	~4000-3000
Porphyritic komatiite	Komatiitic basalt	18-32	14-16	~3000-5000
	Transitional*	22-34	8-14	~1500-4000
	Komatiite	24-36	8-11	~1800-2500
Komatiitic peridotite (orthocumulate-mesocumulate)	Komatiitic basalt	32-44	16-18	~4000-7000
	Transitional*	34-46	6-12	~1500-5000
	Komatiite	36-48	6-10	~800-1500
Komatiitic dunite (mesocumulate-adcumulate)	Komatiitic basalt	44-48	14-20	~7000-9000
	Transitional*	46-50	6-9	~500-6000
	Komatiite	48-52	5-8	~500

*Transitional: porphyritic or cumulate rocks in which the magma evolved from chromite-undersaturated to chromite-saturated *during* olivine accumulation (see discussion by Lesher and Stone, 1996).

As discussed by Donaldson et al. (1986), Lesher and Stone (1996), Baird (1999), and Barnes and Brand (1999), one of the most useful discriminants between cumulate rocks derived from komatiites and komatiitic basalts is the abundance of Cr: magmas with greater than ~20% MgO are undersaturated in chromite and accumulate only olivine, whereas magmas with less than ~20% MgO are chromite-saturated and accumulate cotectic proportions (~50:1) of olivine and chromite (Murck and Campbell, 1986). Thus, the abundance of Cr in a cumulate komatiite can be used to determine the affinity of the magma from which it crystallized. However, because cumulate rocks can form from lavas that fractionated and became saturated in chromite *during* crystallization, some komatiites contain a component of olivine derived from early high-Mg (chromite-undersaturated) magmas and a component of olivine-chromite derived from late low-Mg (chromite-saturated magmas). These komatiites will have intermediate Cr contents (Donaldson et al., 1986; Lesher and Stone, 1996; Baird, 1999). The point at which the lavas become saturated in chromite varies from area to area (e.g., Alexo vs. Barberton vs. Belingwe vs. Cape Smith vs. Kambalda vs. Mt. Clifford vs. Shaw Dome) and from flow to flow within an area (e.g., Tripod Hill vs. Silver Lake members at Kambalda), suggesting that variations in fO_2 and the timing of chromite saturation varied from location to location (Lesher and Stone, 1996; Barnes and Brand, 1999).

Importantly, however, the rocks with the highest Mg or Ni and lowest Cr contents are not necessarily the ones that are most mineralized (Muir, 1979; Larson, 1996; Baird, 1999). The differences in Cr/Mg and Cr/Ni simply reflect differences in the degree of replenishment and fractionation between channel-flow and sheet-flow facies (Lesher and Groves, 1984; Lesher and Arndt, 1995; Lesher and Stone, 1996; Lesher et al., 2001). Thus, Cr contents can be used to distinguish lava channels and magma conduits (olivine cumulates) from sheet flows and sills (olivine + chromite cumulates) in komatiites, but they cannot distinguish different facies in komatiitic basalts.

1.6.3 Review of the Origin of Komatiites

1.6.3.1 INTRODUCTION TO PLUMES

The high Mg contents of aphyric and spinifex-textured komatiites, which range up to ~32% MgO, imply eruption temperatures up to 1640°C and mantle potential temperatures up to 440° hotter than the present day mantle. Magma generation by decompression melting, for example at an Archean mid-ocean ridge or beneath an Archean continental rift, would require extreme geothermal gradients in the Archean, inconsistent with those recorded in Archean metamorphic assemblages (Bickle, 1978b; Campbell et al., 1989). Thus, the higher temperatures of komatiites are better explained by generation in anomalously hot regions, of which mantle plumes represent the best candidate (Campbell et al., 1989).

Mantle plumes are hot upwellings produced by thermal instabilities that are interpreted to form in boundary layers generated by heat conduction across the core-mantle boundary (Campbell et al., 1989; Boehler et al., 1995). The material in the thermal boundary layer rises because it is hotter, less dense, and less viscous than the overlying mantle. Starting plumes are hypothesized to consist of a plume head and a plume tail. The more rapidly flowing material in the plume tail feeds the plume head and heated material from the surrounding mantle is entrained into the plume head as it rises. Starting plumes are believed to reach diameters up to 2500 km as they approach the base of the lithosphere (Campbell and Griffiths, 1990), however, the size of Archean plumes may have been smaller by a factor of about 2 owing to the higher temperature and lower viscosity of the Archean mantle (Davies, 1999). Melting is interpreted to occur in the plume head and tail owing to adiabatic decompression (Campbell and Griffiths, 1990). The depth range of melting is temperature dependent and only slightly influenced by the composition of the source and the adiabatic gradient, but experimental data suggest that most komatiite melts formed in upper mantle within the range 2-9 GPa (~200-900 km: Herzberg and O'Hara, 1998). Although most Phanerozoic plumes appear to be derived from enriched sources and are interpreted to contain a component of subducted oceanic lithosphere (Richards et al., 1989; White and McKenzie, 1989), some are derived from depleted mantle (Gorgona Island: Arndt et al., 1997b). Most Archean plumes appear to be derived from depleted mantle (Campbell et al., 1989; Storey et al., 1991; Anderson, 1994; Lesher and Arndt, 1995; this study), suggesting a relatively long time scale for recycling oceanic lithosphere (see discussion by Campbell, 2000). The different Archean komatiite types are best explained by partial melting of different parts of plumes at various depths (Figure 1.5 and Table 1.2). Temperature variations within a plume determine the MgO content of the magmas produced (Campbell and Griffiths, 1990).

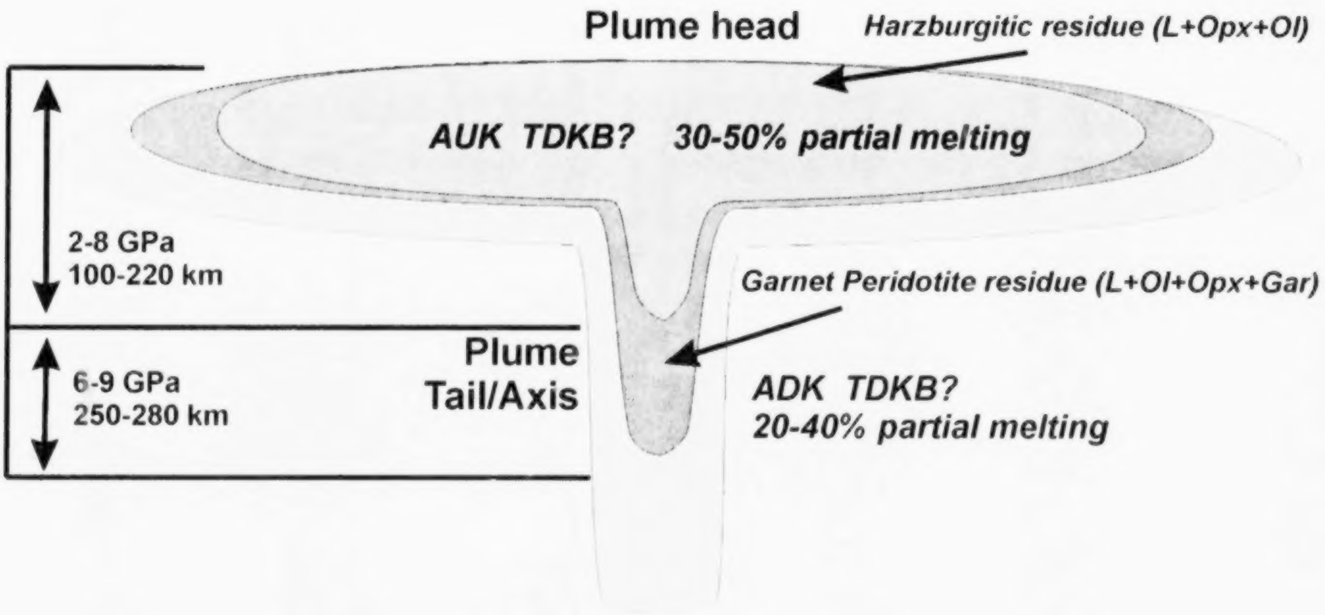
Plume head
Harzburgitic residue (L+Opx+Ol)
AUK TDKB? 30-50% partial melting
2-8 GPa
100-220 km
Garnet Peridotite residue (L+Ol+Opx+Gar)
Plume
Tail/Axis
6-9 GPa
250-280 km
ADK TDKB?
20-40% partial melting

Figure 1.5. Model of the morphology and anatomy of a mantle plume. L = liquid; Ol = olivine; Opx = orthopyroxene; Gar = garnet.

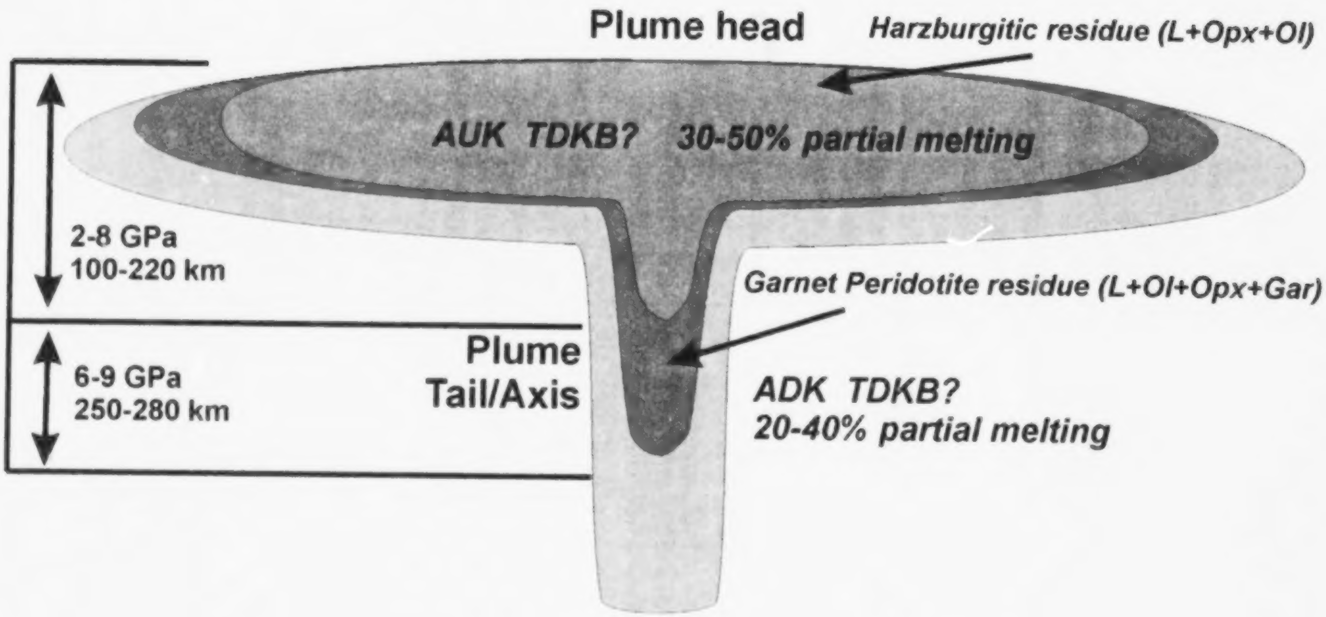
Plume head
Harzburgitic residue (L+Opx+Ol)
AUK TDKB? 30-50% partial melting
2-8 GPa
100-220 km
Garnet Peridotite residue (L+Ol+Opx+Gar)
Plume
Tail/Axis
6-9 GPa
250-280 km
ADK TDKB?
20-40% partial melting

Figure 1.5. Model of the morphology and anatomy of a mantle plume. L = liquid; Ol = olivine; Opx = orthopyroxene; Gar = garnet.

Table 1.2. Summary of the geochemical characteristics of ADK–TEK, AUK, and TDKB and interpreted source regions (Sproule et al., 2002). L = liquid; Ol = olivine; Opx = orthopyroxene; Cpx = clinopyroxene; Gar = garnet.

Magma Type **Type Area**	**Al-undepleted** **Munro**	**Al-depleted** **Barberton**	**Ti-enriched** **Finland**	**Ti-depleted** **Shining Tree**	
Al_2O_3/TiO_2	15-25	<15	<15	25-35	
$[Gd/Yb]_{MN}$	~1.0	1.2-2.8	>1.2	0.6-0.8	
Source	Garnet lherzolite [L+Ol+Opx+Cpx+Gar]	Garnet lherzolite [L+Ol+Opx+Cpx+Gar]	Garnet lherzolite [L+Ol+Opx+Cpx+Gar]	Garnet lherzolite [L+Ol+Opx+Cpx+Gar]	Garnet lherzolite [L+Ol+Opx+Cpx+Gar]
Type of melting	Single-stage	Single-stage	Single-stage	Single-stage dynamic	Two-stage
Degree of melting	30-50%	20-40%	>20%	30-50%	20-40%
Residuum	Dunite [L+Ol]	Garnet lherzolite [L+Ol+Opx+Cpx+Gar]	Dunite [L+Ol]	Dunite [L+Ol]	Dunite [L+Ol]
Depth of separation	2-8 GPa	6-9 GPa	4-9 GPa	2-8 GPa	6-9 GPa
Hypothetical source region	Plume head	Plume tail	Plume head	Plume head	Plume tail

1.6.3.2 SUMMARY OF THE PETROGENESIS OF KOMATIITES

The geochemistry of komatiites is controlled by: 1) the compositions of the source and residue, 2) the pressure, temperature, and degree of partial melting, 3) the nature of the melting process (e.g., equilibrium vs. fractional vs. dynamic), 4) the nature and degree of crustal contamination, 5) the degree of fractional crystallization and/or accumulation, and 6) the degree of remobilization of elements via hydrothermal alteration, regional metamorphism, and/or metasomatism (Figure 1.6; Nesbitt et al., 1979; Beswick, 1982; Arndt and Nisbet, 1982; Lesher and Stone, 1996; Arndt et al., 1997a).

The high MgO contents (up to 32% MgO) of aphyric and random spinifex-textured komatiites and the high forsterite contents (up to Fo_{94}) of relict igneous olivines require derivation from a mantle source leaving a dunitic (Ol) or harzburgitic (Ol-Opx) residue (Herzberg and O'Hara, 1998). Very low abundances of moderately incompatible lithophile elements (MILE: Y, Zr, MREE, HREE, Ti) suggest moderate to high degrees of partial melting (30-60%), depending on the composition of the source and the degree of prior melt extraction (Lesher and Stone, 1996).

Sources that have experienced prior melting are depleted in highly incompatible lithophile elements (HILE: Cs, U, Th, LREE) relative to MILE. This yields sources with $[Th/Sm]_{MN} < 1$ and $[La/Sm]_{MN} < 1$, where the degree of depletion is proportional to the degree of partial melting. Conversely, sources that have been enriched by the incorporation of a subducted sedimentary component are enriched in HILE relative to MILE. This yields sources with $[Th/Sm]_{MN} > 1$ and $[La/Sm]_{MN} > 1$, with the degree of enrichment proportional to the degree of source enrichment.

In addition, the major and trace element geochemistry of komatiites is strongly controlled by the retention and/or melting of minerals in the source, which vary with the composition of the source and the degree and depth of partial melting. For example, komatiitic magmas derived from sources in which majorite garnet is retained in the residue will be depleted in Al, Sc, Y, and HREE relative to Ti, MREE, LREE, and LILE (e.g., Nesbitt et al., 1979; Ohtani, 1990). Melts derived from sources in which clinopyroxene, orthopyroxene, and/or olivine are retained do not have significantly distinctive trace element signatures (e.g., Arth, 1976; Fujimaki et al., 1984). Melts derived from sources in which clinopyroxene or orthopyroxene are retained have different Si and Ca contents relative to melts derived from sources where only olivine is retained (Herzberg and O'Hara, 1998), but they are often difficult to resolve, as those elements are commonly mobile during serpentinization, talc-carbonatization, and chloritization (Lesher and Stone, 1996; this study).

Several types of komatiite and komatiitic basalt are present in the geologic record (e.g., Sun and Nesbitt, 1976; Nesbitt et al., 1979) and in the Abitibi greenstone belt (Xie et al., 1993; this study), including: *Al-undepleted komatiites*, *Al-depleted komatiites*, *Ti-enriched komatiites*, and *Ti-depleted komatiitic basalts*[4]. The petrogenesis of each of the komatiite types is summarized in Table 1.2, and the geochemical characteristics of each of these series is summarized in Table 1.3.

Komatiites contaminated by continental crust or clastic sediments will be enriched in HILE relative to MILE, but less enriched in Nb, Ta, and Ti relative to elements of similar compatibility (e.g., Jochum et al., 1991), leading to negative $[Nb/Th]_{MN}$, $[Ta/La]_{MN}$, and $[Ti/Y]_{MN}$ anomalies. The nature of the contamination can be further restricted by its distribution (Lesher and Arndt, 1995; Lesher and Stone, 1996; Lesher et al., 2001):

1) If all of the lavas in a particular sequence are contaminated, then contamination probably occurred in the source.
2) If contamination varies systematically through the sequence, then contamination probably occurred during ascent through the crust.
3) If contamination is restricted to specific lava flows or specific parts of individual lava flows, then contamination probably occurred during emplacement.

Allègre (1982), Ghomshei et al. (1990), Inoue (1994), and Parman et al. (1997) have proposed that wet melting could generate komatiites. Although some komatiites, including several in the Abitibi greenstone belt, contain igneous amphibole (Stone et al., 1997) and vesicles (e.g., Lewis and Williams, 1973; Eckstrand and Williamson, 1985; Arndt, 1986; Beresford et al., 2000; Dann, 2001), a major problem with wet melting is that the high Mg contents, low incompatible element abundances, HILE depletion, and positive ε_{Nd} signatures of most komatiites require derivation by high degree partial melting of a long-term depleted mantle source. Water behaves as an incompatible element during melting, therefore any water present should have been consumed during the depletion event and any water that might have been added should have been accompanied by the addition of HILE. For this and other reasons, most komatiites are interpreted to be generated by anhydrous melting (Arndt et al., 1997a). The presence of *local* vesicles and/or igneous amphibole suggests that the water was derived locally, via a crustal contamination mechanism (Stone et al., 1997).

---

[4] All komatiites of this type appear to be formed from komatiitic basalt liquids.

Table 1.3. Geochemical characteristics of each of the magma series from this study.

	ADK–TEK uncontaminated			ADK–TEK contaminated			Ferropicrites		
	Mean	SD (1σ)	Range	Mean	SD (1σ)	range	Mean	SD (1σ)	range
Al_2O_3/TiO_2	11.5	2.2	2.2-14.6	10.3	3.9	4.4-14.3	7.7	0.87	4.3-8.0
$[Y]_{MN}$	3.61	5.24	0.19-5.45	2.83	2.29	0.80-4.41	4.83	1.85	1.85-6.48
$[Yb]_{MN}$	2.48	1.24	0.20-4.10	2.58	2.20	0.94-4.45	4.03	0.63	2.67-5.65
$[Al]_{MN}$	1.65	0.70	0.20-2.68	0.93	0.55	0.44-1.88	1.86	0.11	1.71-1.94
$[Sc]_{MN}$	1.50	0.53	0.61-2.52	1.10	0.90	0.49-2.87	1.81	0.06	1.72-1.85
$[La/Sm]_{MN}$	0.80	0.31	0.32-1.86	1.46	0.78	0.40-2.23	1.09	0.04	1.08-1.13
$[Ti/Y]_{MN}$	0.90	0.57	0.41-1.60	0.77	0.44	0.60-1.60	0.99	0.90	0.48-1.05
$[Th/Sm]_{MN}$	0.51	0.15	0.23-0.91	2.80	1.84	1.02-1.82	0.65	0.12	0.50-0.12
$[Nb/Th]_{MN}$	1.43	0.57	0.97-3.06	0.62	0.36	0.35-1.05	1.31	0.20	0.91-1.57
$[Gd/Yb]_{MN}$	1.29	0.23	0.98-1.73	1.39	0.39	0.99-2.00	1.58	0.21	1.40-2.01

	TDKB			AUK uncontaminated			AUK contaminated		
	Mean	SD (1σ)	Range	Mean	SD (1σ)	Range	Mean	SD (1σ)	range
Al_2O_3/TiO_2	32.6	2.0	28-35	18.9	5.4	14-35	19.8	3.6	14-26
$[Y]_{MN}$	2.12	0.90	0.95-3.6	2.09	0.88	0.27-4.14	2.04	1.11	0.24-5.23
$[Yb]_{MN}$	2.45	1.02	1.0-4.07	2.12	0.89	0.62-4.30	2.03	1.10	0.25-5.23
$[Al]_{MN}$	2.16	0.83	1.16-3.32	1.80	0.69	0.48-3.22	1.66	0.72	0.49-2.49
$[Sc]_{MN}$	1.87	0.04	1.84-1.89	1.61	0.47	0.38-3.02	1.55	0.67	0.55-2.49
$[La/Sm]_{MN}$	0.39	0.06	0.27-0.47	0.64	0.20	0.26-1.33	0.95	0.64	0.7-5.18
$[Ti/Y]_{MN}$	0.41	0.09	0.14-0.44	0.75	0.59	0.30-5.82	0.63	0.22	0.41-1.39
$[Th/Sm]_{MN}$	0.26	0.05	0.18-0.35	0.47	0.18	0.21-0.99	1.10	0.67	1.12-3.80
$[Nb/Th]_{MN}$	1.23	0.20	1.02-1.69	1.34	0.38	0.44-2.27	0.66	0.19	0.14-0.84
$[Gd/Yb]_{MN}$	0.66	0.04	0.59-0.72	1.01	0.09	0.80-1.20	1.02	0.10	0.70-1.30

Data presented as mean, one standard deviation (SD), and range. ADK: aluminum-depleted komatiite, AUK: aluminum-undepleted komatiite, TEK: Ti-enriched komatiites, TDKB: Ti-depleted komatiitic basalt; MN: primitive mantle-normalized (McDonough and Sun, 1995).

2 Petrography

Komatiites and komatiitic basalts in the Abitibi greenstone belt exhibit the same wide range of textures observed in komatiites worldwide, including massive aphyric, random platy olivine spinifex, parallel platy olivine spinifex, random pyroxene spinifex, parallel acicular pyroxene spinifex, hopper and chevron olivine, olivine orthocumulate, olivine mesocumulate, and olivine adcumulate textures. The origins of these textures have been reviewed by Donaldson (1982), Arndt (1986), and Shore and Fowler (1999).

The komatiites in the Abitibi greenstone belt have experienced varying degrees of hydration and carbonatization during seafloor weathering, hydrothermal alteration, and regional metamorphism (e.g., Beswick, 1982; Arndt, 1986, 1994; Arndt et al., 1989; Lahaye et al., 1995; Lahaye and Arndt, 1996). The komatiites are typically metamorphosed to lower to upper greenschist facies, but rarely to lower amphibolite facies along the margins of batholiths. Typical mineral assemblages include chlorite-actinolite-magnetite ± dolomite in komatiitic basalts, serpentine-tremolite-chlorite-magnetite ± talc ± dolomite in komatiites, and serpentine-chlorite-magnetite ± talc ± magnesite in komatiitic peridotites and dunites. The only amphibolite facies komatiites sampled in this study are those at the Marbridge Mine site in La Motte Township in Québec. The mineral assemblage in those samples is serpentine-hornblende-chlorite-talc-tremolite-magnetite.

Relict igneous chromite is commonly preserved as disseminated lobate and interstitial intercumulus grains in cumulate rocks and as dendritic cruciform crystals in the glassy interstitial spaces of spinifex-textured rocks, but is normally partially to completely replaced by Fe-rich chromite (e.g., Baird, 1999; Barnes and Brand, 1999). Relict igneous pyroxene is sometimes preserved as polyhedral crystals in pyroxene cumulate rocks, oikocrysts in "knobby" peridotites, and as acicular crystals in spinifex-textured rocks, but is commonly altered to chlorite (pigeonite cores) and tremolite or actinolite (clinopyroxene rims). Relict igneous olivine is rarely preserved (e.g., Alexo in Dundonald Township, Pyke Hill in Munro Township), but is normally altered to serpentine (lizardite and/or antigorite) and magnetite, progressing inwards along fractures, sometimes leaving cores of re-equilibrated olivine. Chrysotile is rarely present in sheared komatiites in the Porcupine-Destor and Larder-Cadillac Fault Zones. The glassy to microspinifex-textured groundmass is completely altered to fine-grained intergrowths of chlorite ± talc ± tremolite. Identification of these phases is extremely difficult because of their fine grain size.

Carbonates (magnesite, ankerite, and/or dolomite) locally occur in veins, in the groundmass of the rock, or as pseudomorphs after olivine. Silicification is only rarely observed in Abitibi komatiites, typically near shear zones (e.g., Cadillac-Larder Lake fault zone, Porcupine-Destor fault zone, basal shear zones in the Shining Tree area), where is it typically characterized by the generation of fuchsite (Cr-rich muscovite).

Sulfides are normally present only in trace (<1%) amounts in komatiites, typically comprising minor amounts of secondary pyrite, but pyrrhotite, pentlandite, and chalcopyrite is locally abundant (e.g., Alexo, Dumont, Dundonald, Marbridge). Mineralized zones contain massive, net-textured, and disseminated ores and, where mobilized into wall rocks, may form massive veins and veinlets.

3 Geochemistry

3.1 INTRODUCTION

As discussed previously, the major and trace element geochemistry of the komatiites in the Abitibi greenstone belt is controlled by: 1) source composition, 2) degree of partial melting, 3) composition and abundance of residual phases, 4) degree of equilibrium crystallization (EC), fractional crystallization (FC), partial fractional crystallization (PFC), or assimilation-fractional crystallization (AFC)[5], 5) degree of olivine, pyroxene, chromite, and/or sulfide accumulation, and 6) degree of post-magmatic metasomatism. The influence of these factors on the geochemistry of komatiites in the Abitibi greenstone belt will be examined using whole-rock major, minor, and trace element data and whole-rock Sm-Nd and Re-Os isotopic data.

---

[5] *Equilibrium crystallization* (EC), which maintains constant equilibrium between the solid and liquid, results in less pronounced geochemical variations than pure *fractional crystallization* (FC), which involves removal and isolation of the solid during crystallization. *Partial fractional crystallization* (PFC) involves the removal of a component of trapped liquid with the solid, producing geochemical trends intermediate between EC and FC. *Assimilation-fractional crystallization* (AFC) and *assimilation equilibrium crystallization* (AEC) involve the assimilation of a contaminant.

3.2 ALTERATION

All of the komatiites in the Abitibi greenstone belt have experienced some degree of seafloor weathering, hydrothermal alteration, and/or regional metamorphism (e.g., Arndt, 1986, 1994; Arndt et al., 1989; Lahaye and Arndt, 1996). These processes were capable of mobilizing elements and resetting isotopic compositions, therefore, they must be carefully evaluated when studying the geochemistry of komatiites. Several methods were employed to evaluate these processes:

1) An extensive study of the literature was conducted to determine which trace and major elements are mobile under which alteration and/or metamorphic conditions.
2) A large number of thin sections (~500) were examined to document alteration types within the dataset.
3) The behaviour of major and trace elements were studied on MgO variation diagrams and Pearce element ratio plots.
4) Factor analysis (R-mode) was used to constrain which elements and ratios are linked and unaffected by post-magmatic remobilization.

3.2.1 Literature Review

Many studies have shown that seafloor weathering, hydrothermal alteration, and/or regional metamorphism may modify the major and trace element and isotopic compositions of komatiites (e.g., Beswick, 1982; Arndt et al., 1989; Tourpin et al., 1991; Gruau et al., 1992; Lesher and Arndt, 1995; Lahaye and Arndt, 1996; Lesher and Stone, 1996). However, these studies have also shown that many of the magmatic geochemical characteristics of komatiites may be retained. The degree of mobility of the individual elements depends on their geochemical behaviour, where they are housed in the igneous and metamorphic mineral assemblages, and the type and intensity of alteration.

For example, incompatible lithophile elements with small ionic radii and high charges (e.g., REE, Y, Zr, Nb, Hf, Ta, and Th) that are housed in the interstitial glass phase but difficult to complex in metamorphic fluids end up in metamorphic accessory phases and are therefore normally relatively immobile (e.g., Arndt, 1986; Lesher and Stone, 1996). However, these elements may be mobile during intense carbonatization (Lahaye and Arndt, 1996). Transition elements (e.g., Ti, Cr, V, Mn, Fe, Mg, Ni and Co) that are housed in easily hydrated igneous phases but readily accommodated in metamorphic minerals (e.g., serpentine, amphibole, and chlorite) are therefore also normally relatively immobile (Lesher and Stone, 1996).

In contrast, incompatible lithophile elements with large ionic radii and low charges (e.g., Cs, Rb, K, Na, Ba, Sr, Ca, and Eu^{2+}) that were housed primarily in the interstitial glass phase and were easily complexed in hydrothermal and/or metamorphic fluids were typically mobilized during alteration (Lesher and Stone, 1996). Si is mobile during strong serpentinization, rodingitization, and chloritization (O'Hanley, 1997; Lahaye and Arndt, 1996; Lesher and Stone, 1996).

3.2.2 Petrographic Screening

From a geochemical perspective, the most problematic alteration types are clearly pervasive silicification, chloritization, amphibolitization, and carbonatization (Lahaye and Arndt, 1996; Lesher and Stone, 1996). Consequently, any samples showing other than pseudomorphous chloritization or amphibolitization and other than incipient silicification or carbonatization in thin section were eliminated from the database that was used for petrogenetic interpretations.

3.2.3 Geochemical Criteria

Altered samples were screened from the data by plotting major and trace elements on MgO variation diagrams and on Pearce element ratio plots (Sections 3.3-3.5). Coherent geochemical behaviour of Ti, V, Mn, Fe, Mg, Ni, Co, Cr, and Zr suggests that these elements have not been significantly affected by alteration and/or metamorphism (see also Beswick, 1982; Arndt, 1986; Lesher and Stone, 1996). In contrast, significant dispersion of Na, K, Ca, and Sr indicate that these elements were mobilized during seafloor weathering, hydrothermal alteration, and/or regional metamorphism.

Si and Al exhibit some degree of dispersion, typically associated with intense chloritization (loss of Si) or intense amphibolitization (addition of Si). Si and Al abundances are also controlled by the depth at which partial melting occurs (e.g., Herzberg and O'Hara, 1998), with lower Al/Si ratios associated with increasing depth of partial melting. Thus, we compared our data to other global data sets to determine normal Al and Si abundances for a range of pressures (Figure 3.1). Samples plotting outside this range were excluded. However, this filter was only employed on samples with greater than 23 wt.% MgO (anhydrous), as rocks with lower MgO contents have fractionated or accumulated pyroxenes and plot outside this field.

Volatile abundances increase with MgO content (Figure 3.2), consistent with addition of H_2O during serpentinization of olivine. CO_2 analyses were only available for a very small number (less than 5%) of the samples in the database, so CO_2 abundances could not be employed as a filter in this study. However, samples with volatile (loss-on-ignition) contents greater than those that could be accommodated by serpentine and chlorite (Deer et al., 1992; O.M. Burnham, unpublished data, 2001; this study) likely contain CO_2 and were therefore removed from the database (Figure 3.3).

R mode factor analysis was used to examine the relationships between key petrogenetic indicators (MgO, Al_2O_3, TiO_2, Cr_2O_3, Al_2O_3/TiO_2, La/Sm, Gd/Yb) and key alteration indices (e.g., Rb, K, Na, Ba, Sr) (Figure 3.4). The factors that account for the majority of the observed geochemical variations in the database include, in order of increasing proportion of variance explained:

1) olivine fractionation-accumulation
2) crustal contamination
3) fractionation of garnet, presumably by retention in the residue
4) garnet- and incompatible element enrichment of the source
5) post-emplacement LILE mobility

Importantly, the factor analysis indicates that mobility of alkali elements and LILE does not correlate with important petrogenetic indicators such as $[La/Sm]_{MN}$, $[Th/Nb]_{MN}$, or $[Gd/Yb]_{MN}$. This means that these ratios may be used to constrain the petrogenesis of even those komatiites that have experienced mobility of alkali elements and LILE.

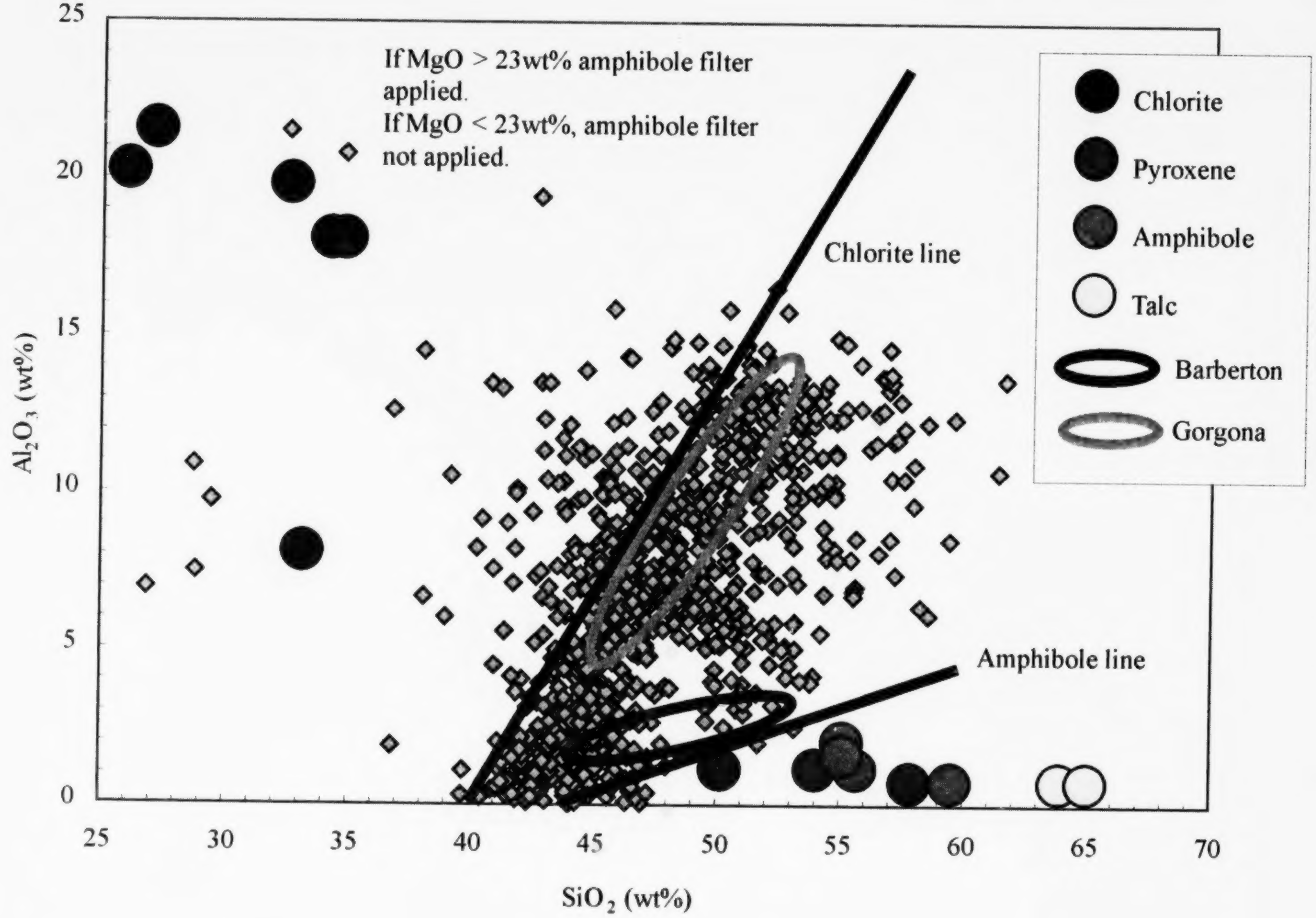

Figure 3.1. Al_2O_3 vs. SiO_2 (wt.% volatile-free) for komatiitic rocks in the Abitibi greenstone belt and comparisons to komatiitic rocks in other greenstone belts.

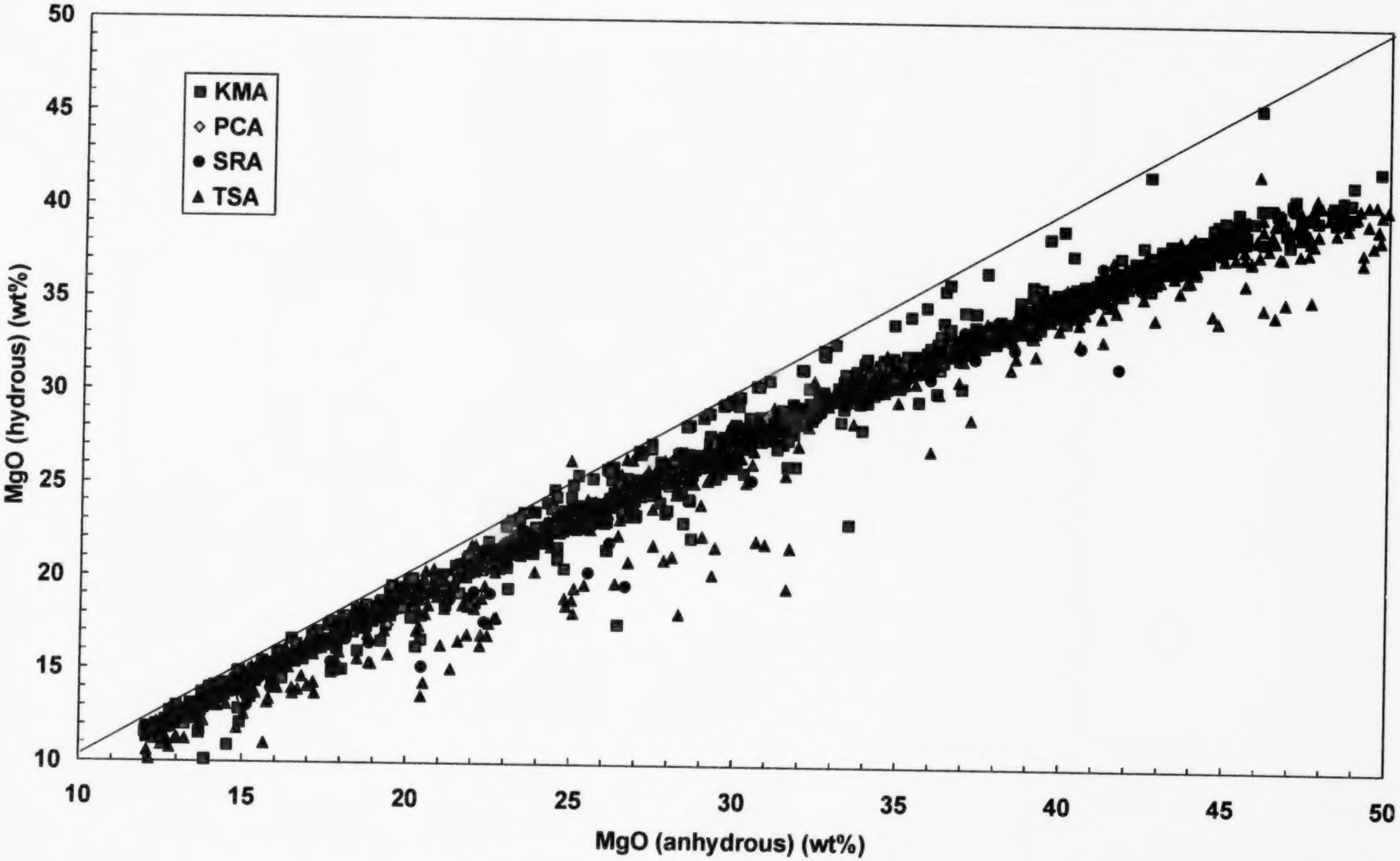

Figure 3.2. MgO (wt.% uncorrected) (hydrous) vs. MgO (wt.% volatile-free) (anhydrous) for komatiitic rocks in the Abitibi greenstone belt. KMA = Kidd-Munro assemblage; PCA = Pacaud assemblage; SRA = Stoughton-Roquemaure assemblage; TSA = Tisdale assemblage.

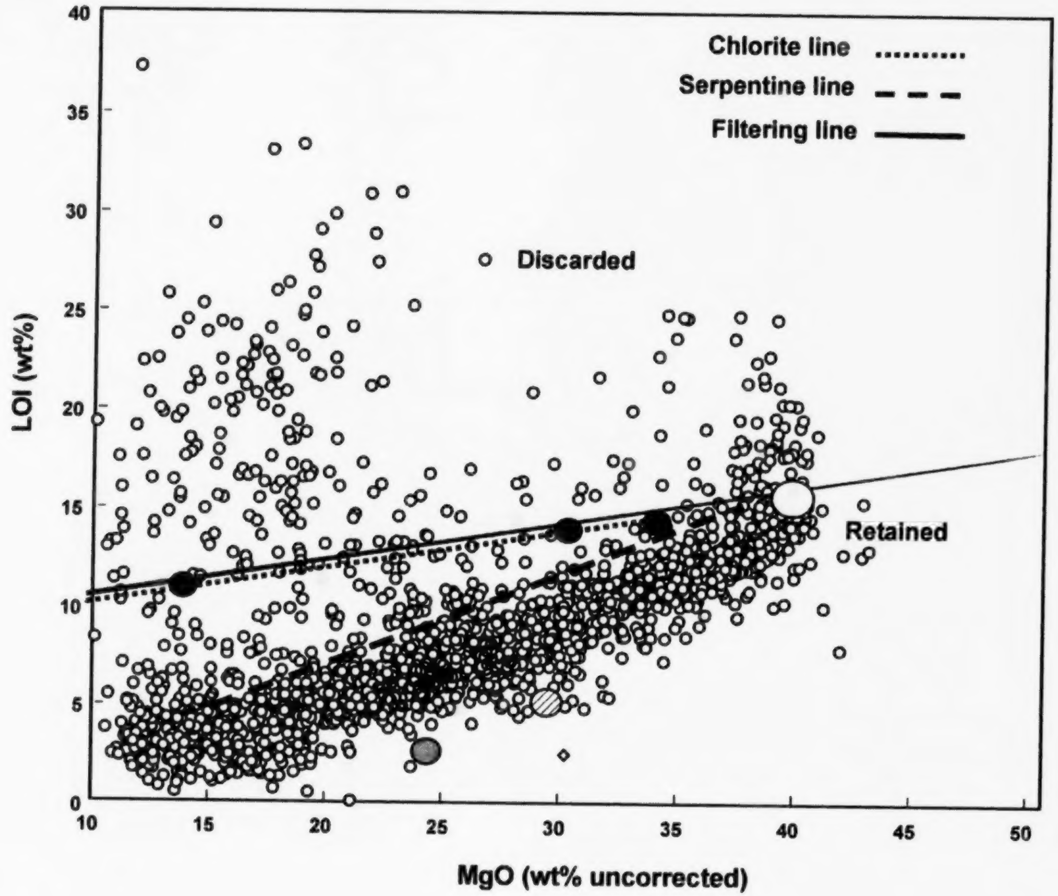

Figure 3.3. Loss-on-ignition (LOI) (wt.%) vs. MgO (wt.% uncorrected) for all komatiites. Stoichiometric Mg-chlorite (black circle), talc (stippled circle), Mg-tremolite (light grey circle), and Mg-serpentine (unfilled circle) compositions (Deer et al., 1992) are shown for reference. The chlorite line represents the tie line between basaltic glass and chlorite; the serpentine line represents the tie line between olivine and serpentine. Only samples for which LOI is less than or equal to that in 100% serpentine ± chlorite ± talc have been included in this study.

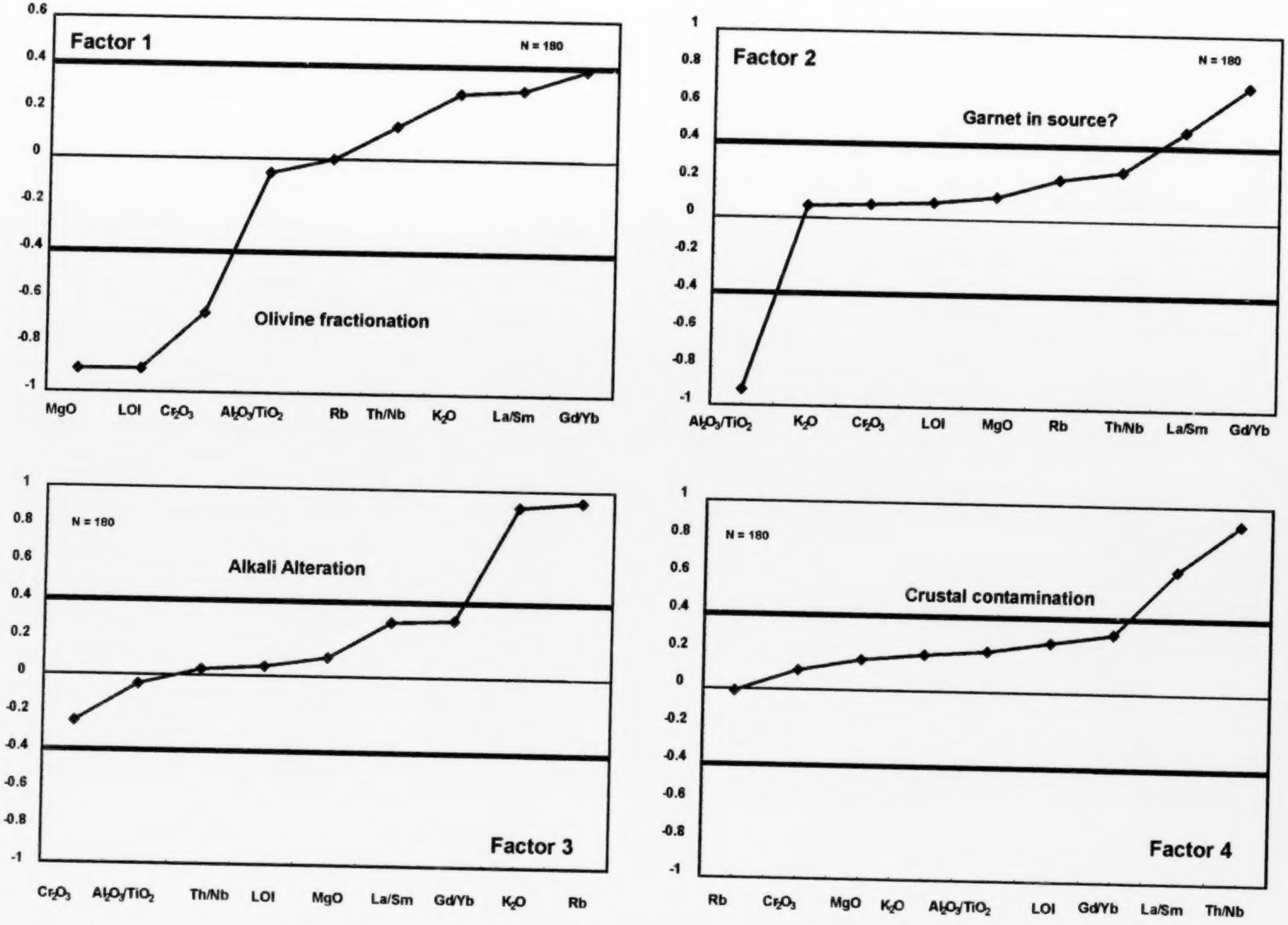

Figure 3.4. R mode factor analysis for komatiitic rocks in the Abitibi greenstone belt.

3.2.4 Alteration Filters

Based on the above analysis, the following alteration filters were employed in this study:

1) petrographic evidence of strong carbonatization, chloritization, or amphibolitization
2) strongly carbonated or hydrated samples with volatile contents greater than can be accounted for by simple hydration (serpentinization ± amphibolitization ± chloritization) of olivine ± pyroxene ± glass:

   $$0.15\mathrm{MgO(raw)} - \mathrm{LOI} + 8 > 0$$

3) chloritized samples with lower Si and higher Al contents than can be accounted for by isochemical metamorphism of pyroxene ± glass:

   $$Al_2O_3 - 1.67*SiO_2 + 66.7 < 0$$

4) amphibolitized samples with higher Si and lower Al contents than can be accounted for by isochemical metamorphism of pyroxene ± glass:

   $$Al_2O_3 - 0.3*SiO_2 + 13 > 0$$

The first filter was applied when thin sections were available (~700 samples) or when detailed petrography was provided by the original author.

The second filter was applied to all samples, but for those few samples for which CO_2 analyses were available, samples with more than 2 wt.% CO_2 were excluded.

The third and fourth filters were applied only to samples containing >23 wt.% MgO (anhydrous) and is designed to remove samples that contain extremely high amounts of chlorite and amphibole, but little pyroxene. These filters were calibrated using petrographic criteria and a database of Al and Si abundances in rocks for which chlorite and amphibole contents are known (Lesher, 1983).

The alteration filtering reduced the database to ~2050 komatiite analyses. Only data that passed the alteration filtering has been used to constrain the petrogenesis of the komatiites in this report.

3.3 MAJOR ELEMENTS

All major element analyses have been recalculated to 100% on a volatile-free basis. This is particularly important for komatiites, which may contain up to 22 wt.% H_2O if completely serpentinized. MgO is used as a measure of fractionation because it is a major constituent of olivine, which crystallizes in komatiitic magmas over a very wide temperature interval (e.g., Arndt, 1976; Bickle, 1978a; Kinzler and Grove, 1985). Figures 3.5 and 3.6 show how each of the major elements varies as a function of MgO content (volatile-free, unless stated otherwise). Si, Al, Ti, Mn, and Fe define single, relatively coherent trends between ~18 and ~30% MgO, where olivine is the principal liquidus phase, and between ~30% and ~55% MgO, where olivine in the principal cumulus phase. At lower Mg contents (<18 wt.% MgO), Ca and Al exhibit a wider spread, as pyroxene may also be on the liquidus.

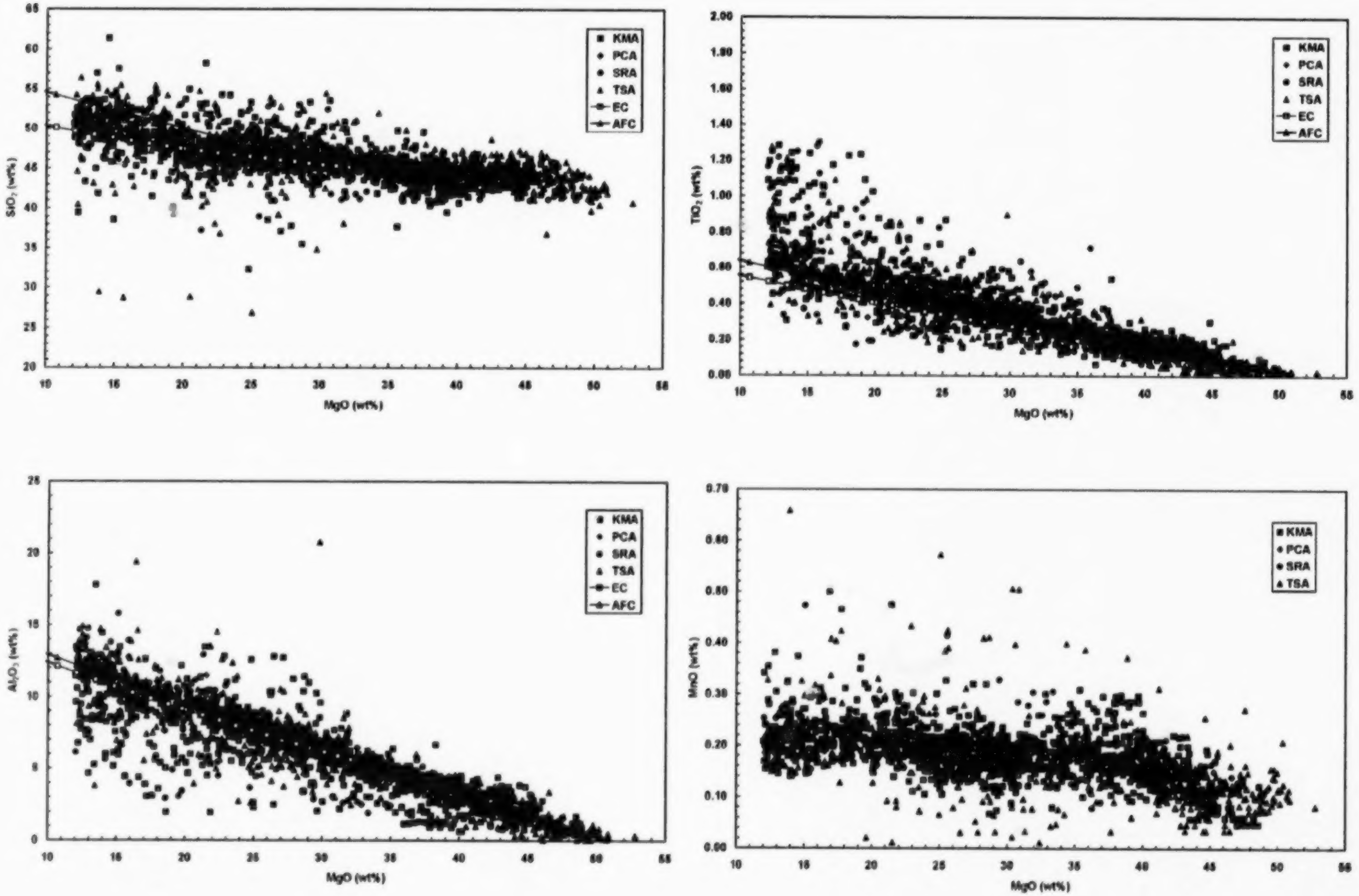

Figure 3.5. SiO$_2$, TiO$_2$, Al$_2$O$_3$, and MnO vs. MgO (wt.% volatile-free) for komatiitic rocks in the Abitibi greenstone belt. KMA = Kidd-Munro assemblage; PCA = Pacaud assemblage; SRA = Stoughton-Roquemaure assemblage; TSA = Tisdale assemblage; EC = equilibrium crystallization; AFC = assimilation-fractional crystallization.

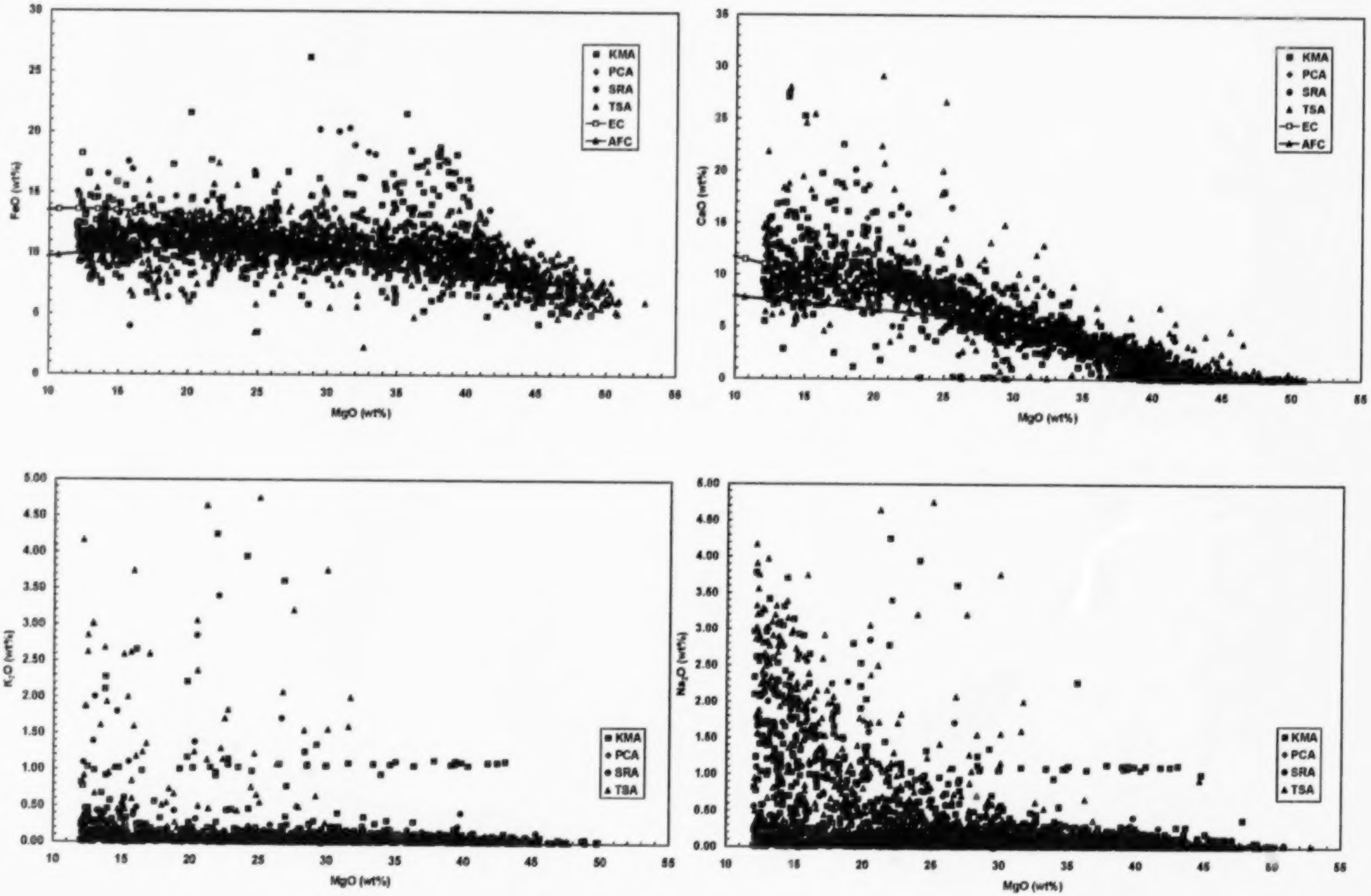

Figure 3.6. FeO, CaO, Na_2O, and K_2O vs. MgO (wt.% volatile-free) for komatiitic rocks in the Abitibi greenstone belt.

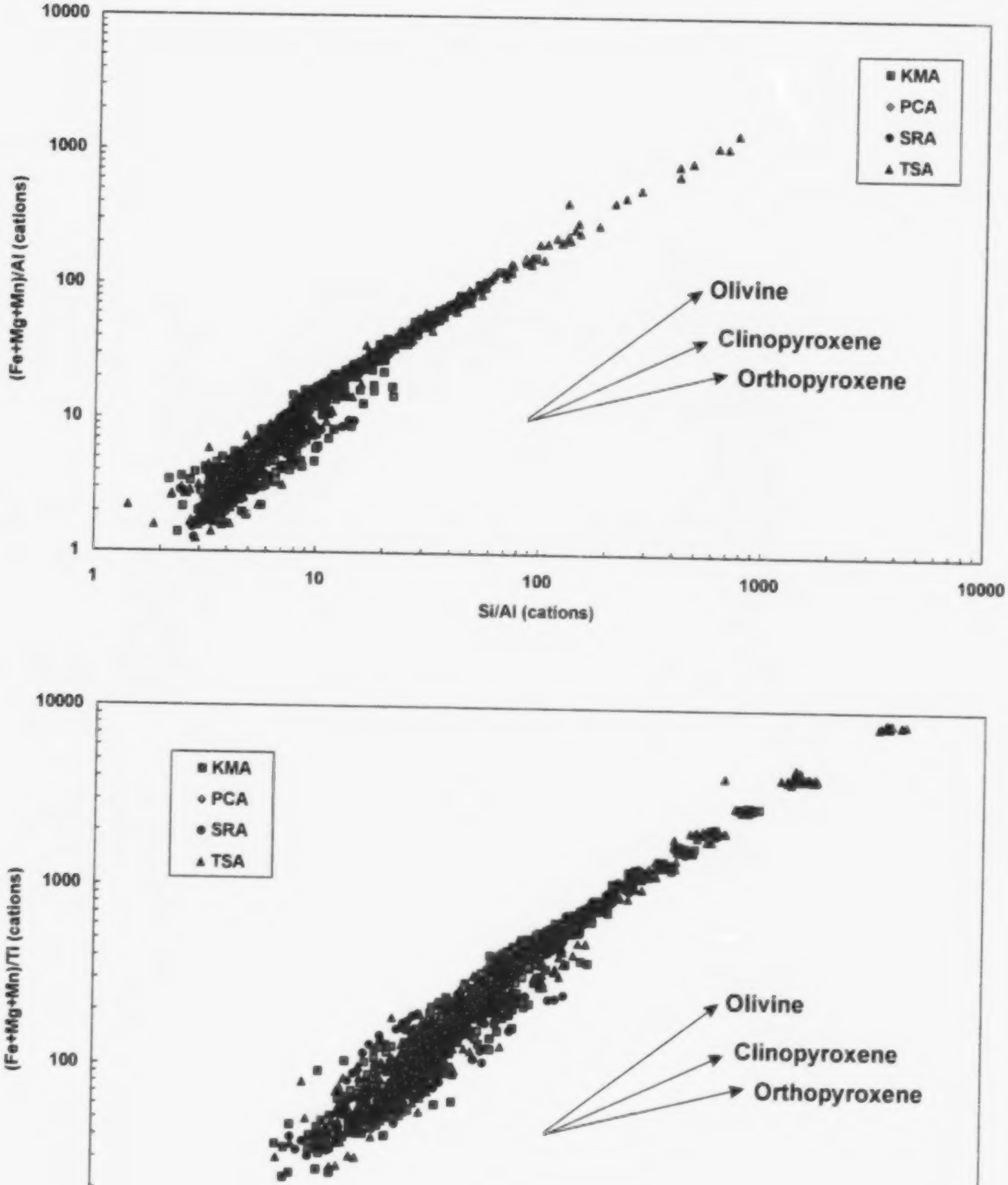

Figure 3.7. Pearce element ratio plots for komatiitic rocks in the Abitibi greenstone belt.

Olivine fractionation/accumulation is confirmed on atomic (Mg+Fe+Mn)/Al vs. Si/Al and (Mg+Fe+Mn)/Ti vs. Si/Ti plots (Figure 3.7), where the majority of samples define a trend with a slope of 2, corresponding to the atomic (Mg+Fe+Mn)/Si ratio in olivine. Minor trends are also observed at slopes of 1 and 0.5, which represent the (Mg+Fe+Mn)/Si ratios in clinopyroxene and orthopyroxene, respectively.

K and Na are present in low abundances (<0.5 wt.% K_2O or Na_2O) between 55 and ~20% MgO, but increase sharply at lower MgO contents (up to 9 wt.% K_2O). Both are incompatible in olivine and pyroxene and there is no evidence for crystallization of any phases containing significant abundances of these elements, so the higher abundances at lower MgO contents are attributable to sequestering of these elements in less magnesian, more aluminous rocks during seafloor weathering, hydrothermal alteration, and/or regional metamorphism.

3.4 MINOR ELEMENTS

All minor element abundances have also been recalculated to 100% on a volatile-free basis and have been plotted against MgO in Figures 3.8 to 3.11.

3.4.1 Chromium

Cr is slightly compatible in olivine and strongly compatible in chromite. The Cr contents of *aphyric* komatiites in the Abitibi greenstone belt increase with decreasing Mg content down to ~20 wt.% MgO (Figure 3.8), reflecting crystallization of olivine, then decrease with decreasing Mg content, reflecting crystallization of olivine and chromite in a proportion of ~50:1. The MgO content at which chromite saturation is achieved depends on the fO_2 (oxygen fugacity) of the magma (Murck and Campbell, 1986). The Cr contents of *cumulate* komatiites are controlled by two factors: 1) the composition of the magma (Cr-undersaturated vs. Cr-saturated) and 2) the degree of olivine ± chromite accumulation (i.e., orthocumulate, mesocumulate, or adcumulate[6]). Komatiites *sensu stricto* accumulate only olivine, which contains only minor amounts of Cr, and therefore define a trend of decreasing Cr with increasing Mg. Komatiitic basalts accumulate olivine and chromite and therefore define a trend of increasing Cr with increasing Mg. Low-Mg komatiites that reach chromite saturation during fractionation may exhibit intermediate Cr contents (Figure 3.8) (see discussion by Lesher and Stone, 1996).

Several komatiites with 15-35 wt.% MgO contain <1000 ppm Cr. These probably do not reflect a Cr-depleted source, as many of the rocks in other parts of the same areas have normal Cr contents. Most are pyroxene cumulate rocks, which formed by accumulation of pyroxene (which has lower Mg and Cr contents than olivine) into a Cr-depleted komatiitic basaltic lava/magma.

A small number of komatiitic basalts with 15-20 wt.% MgO contain ~3000-4500 ppm Cr. They likely represent delayed chromite saturation owing to more reduced conditions. These komatiites appear to occur more commonly, but not exclusively, in the Kidd-Munro assemblage, which coincidently contains reduced graphitic shale horizons.

---

[6] *Orthocumulate* rocks contain ~50-75% cumulus phases and ~50-25% intercumulus liquid. *mesocumulate* rocks contain ~75-95% cumulus phases and ~25-5% intercumulus liquid. and *adcumulate* rocks contain >95% cumulus phases and <5% intercumulus liquid.

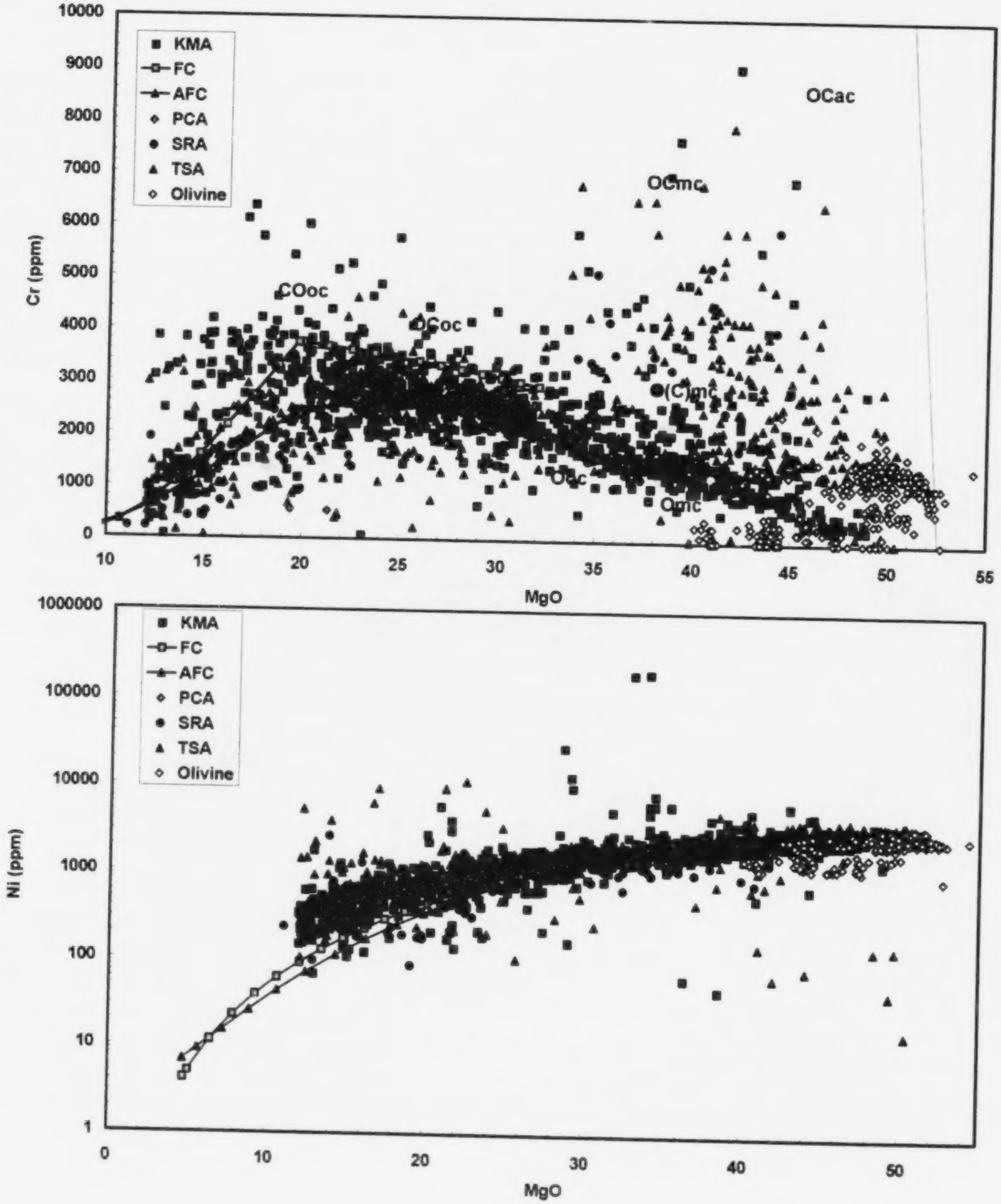

Figure 3.8. Cr and Ni (ppm) vs. MgO (wt.% volatile-free) for komatiitic rocks in the Abitibi greenstone belt. C = chromite; O = olivine; oc = orthocumulate; ac = adcumulate; mc = mesocumulate.

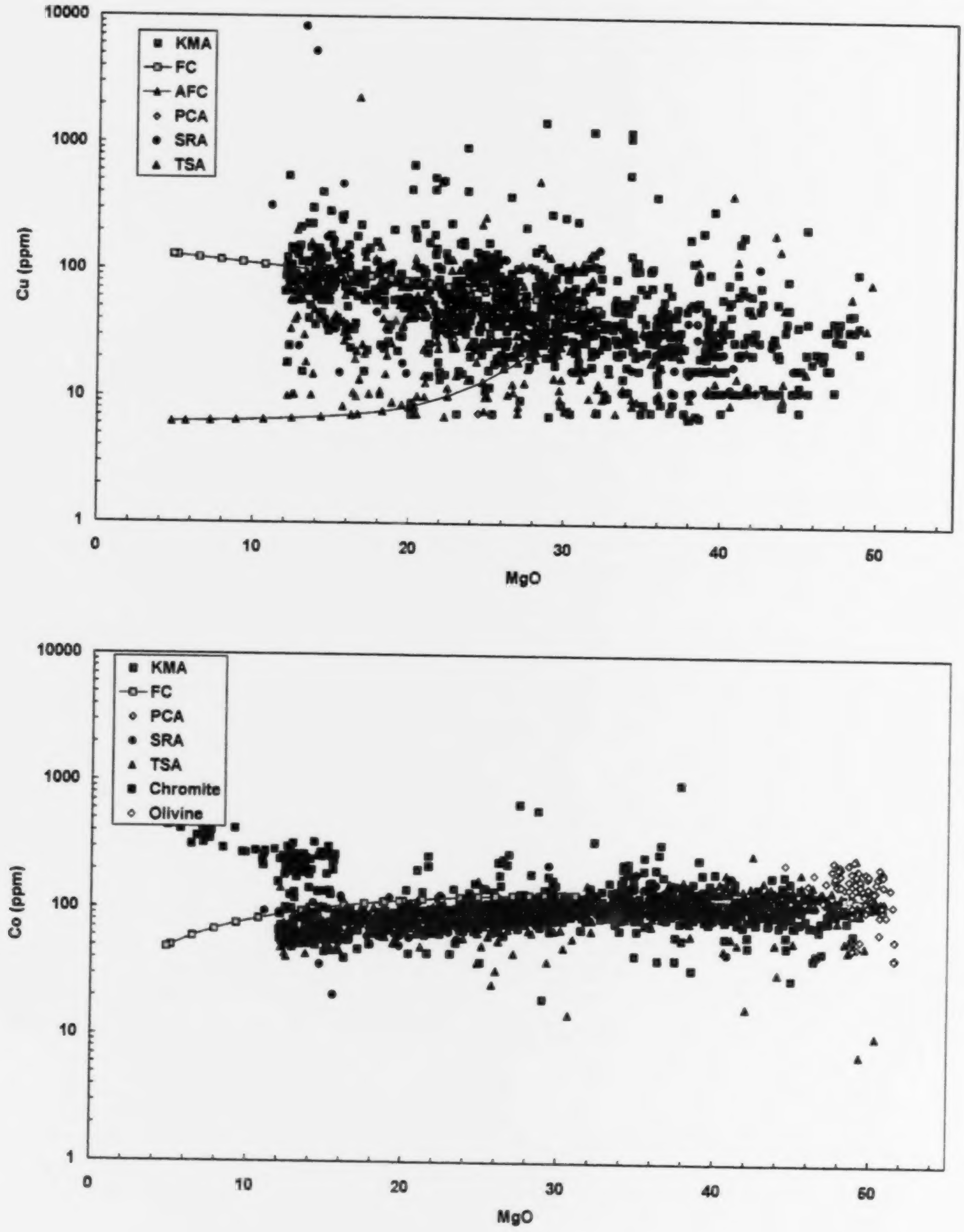

Figure 3.9. Cu and Co (ppm) vs. MgO (wt.% volatile-free) for komatiitic rocks in the Abitibi greenstone belt.

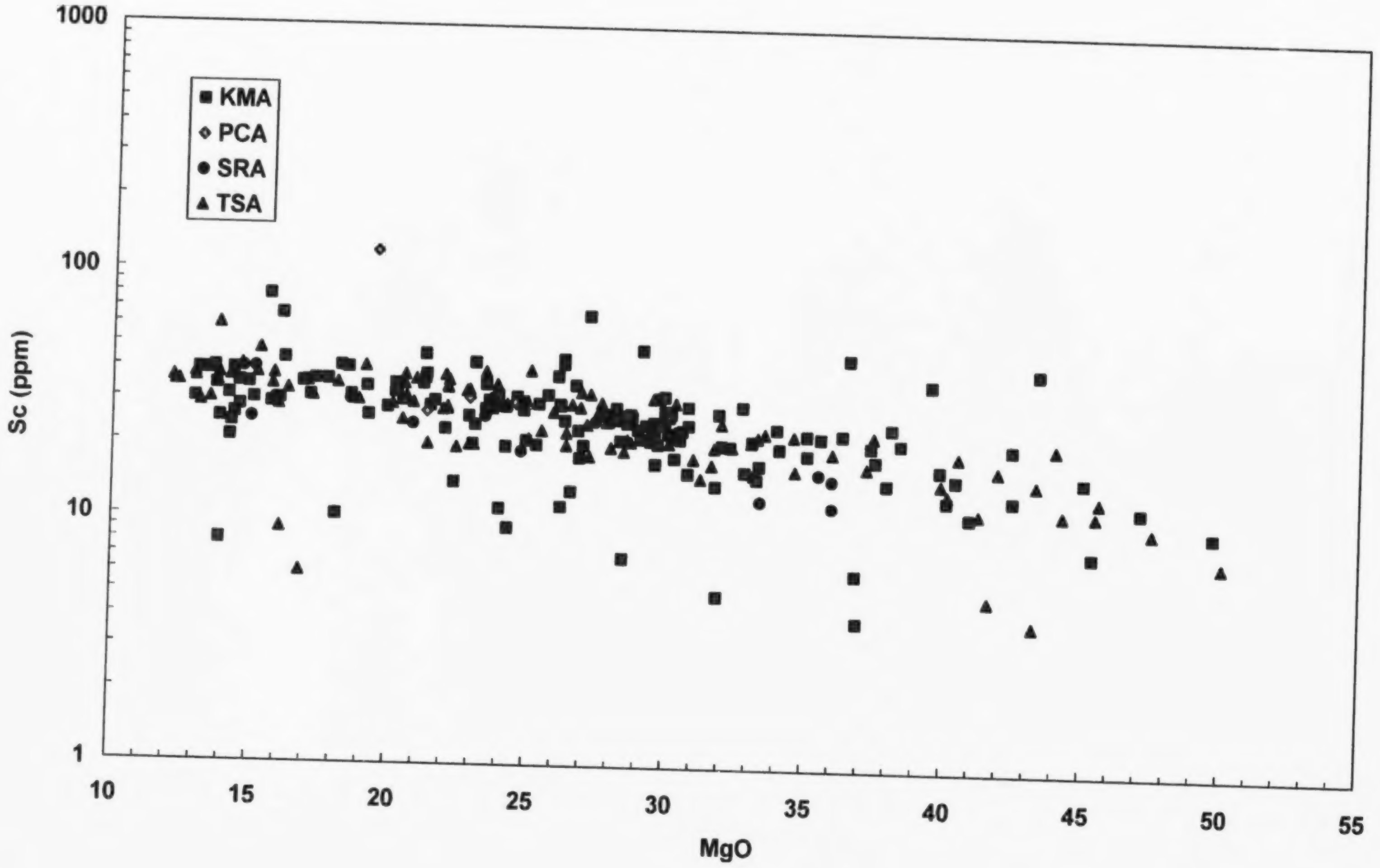

Figure 3.10. Sc (ppm) vs. MgO (wt.% volatile-free) for komatiitic rocks in the Abitibi greenstone belt.

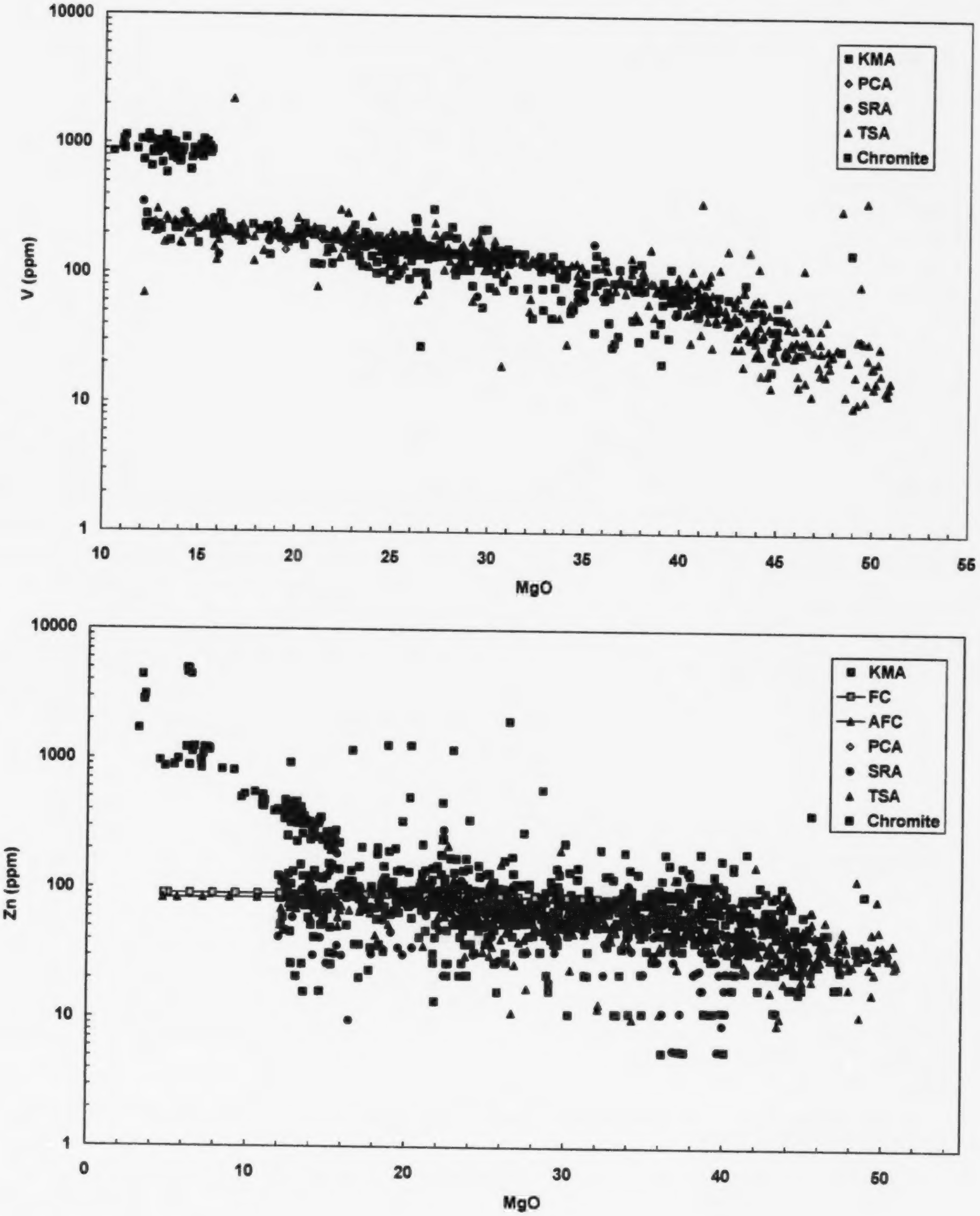

Figure 3.11. V and Zn (ppm) vs. MgO (wt.% volatile-free) for komatiitic rocks in the Abitibi greenstone belt.

3.4.2 Nickel

Ni is moderately compatible in olivine ($D_{Ni}^{olivine/liquid}$ ~2) and strongly compatible in sulfides ($D_{Ni}^{sulfide/liquid}$ ~100-200) in komatiites. The Ni contents of aphyric and cumulate komatiites in the Abitibi greenstone belt increase with increasing Mg content (Figure 3.8) and define trends that are consistent with crystallization and accumulation of olivine, respectively. The abundances of Ni in the aphyric lavas define a trend that is intermediate between those predicted by equilibrium and fractional crystallization of olivine and can probably be attributed to *partial* fractional crystallization (see Lesher and Stone, 1996). The abundances of Ni in cumulate komatiites occupy a field between the trend of evolved liquids and the trends of equilibrium olivines (Figure 3.8), with the Ni (and Mg) contents depending on the degree of olivine accumulation.

A small number of aphyric komatiites with 12-32 w% MgO have Ni >3000 ppm (Figure 3.8). This is unlikely to be attributable to analytical errors, as samples with high Ni contents have been analyzed by both AAS and WD-XRF techniques. A Ni-enriched source is unlikely, as other samples in the same units or sequences have normal Ni contents. Thin sections are not available for all of the samples, but the enrichments in Ni in those samples for which thin sections are available appear to reflect accumulation of olivine and/or rarely sulfides.

Similarly, a small number of porphyritic and cumulate komatiites with >30% MgO have Ni <1000 ppm (Figure 3.8). The lower Ni contents of these samples probably reflect equilibration with sulfides (Duke and Naldrett, 1978; Duke, 1979) and/or accumulation of olivine into liquids that have experienced prior olivine crystallization. These samples occur predominantly in the mineralized Tisdale (Lower Komatiite Horizon of the Shaw Dome in Carman, Deloro, Eldorado, Langmuir, and Shaw Townships: Stone and Stone, 2000) and Kidd-Munro (Dundonald Township: Davis, 1999) assemblages (see Figure 1.2).

3.4.3 Copper

Cu is incompatible in most of the silicate and oxide phases that crystallize from mafic-ultramafic magmas, but strongly compatible in sulfides ($D_{Cu}^{sulfide/liquid}$ ~600) in komatiites. Thus, Cu abundances should increase systematically during fractionation, as it becomes concentrated in the magma/lava during removal of other components in crystallizing phases. The Cu contents of many aphyric and cumulate komatiites in the Abitibi greenstone belt scatter widely when plotted as a function of Mg content (Figure 3.9[7]), suggesting mobility during alteration and/or metamorphism (Lesher and Stone, 1996), but the majority of the data lie between or near the trends predicted by FC and AFC models. The Cu contents of cumulate komatiites are quite variable, depending on the amount of trapped liquid and interstitial sulfide phases, but it is difficult to distinguish depletion attributable to sulfide segregation or enrichment attributable to sulfide accumulation from alteration. As noted below, it is better to use less mobile chalcophile elements and/or elemental ratios (e.g., Pt/Ni or Cu/Ir) to evaluate sulfide segregation and accumulation processes.

3.4.4 Cobalt

Co is incompatible in most of the silicate and oxide phases that crystallize from mafic-ultramafic magmas, but strongly compatible in sulfides ($D_{Co}^{sulfide/liquid}$ ~600) in komatiites. Co contents of aphyric and cumulate komatiites in the Abitibi greenstone belt increase with increasing Mg content (Figure 3.9) and define trends that are consistent with crystallization and accumulation of olivine, respectively. A small number of cumulate rocks with MgO >35 wt.% are depleted in Co (<80 ppm), which may be related to removal of sulfides. It is less likely that this is attributable to prior olivine fractionation, as the high MgO contents of these samples indicate that they contain Fo-rich olivine and crystallized from high-Mg magmas. These samples are the same ones that are depleted in Ni and occur predominantly in the mineralized Tisdale (Lower Komatiite Horizon of the Shaw Dome in Carman, Deloro, Eldorado, Langmuir, and Shaw Townships: Stone and Stone, 2000) and Kidd-Munro (Dundonald Township: Davis, 1999) assemblages (see Figure 1.2).

---

[7] Samples containing <7 ppm Cu have not been plotted in Figure 3.9.

3.4.5 Scandium

Sc is incompatible in most mafic minerals except garnet and clinopyroxene (Rollinson, 1993). Thus, the abundances of Sc in komatiites are strongly determined by whether all of the garnet was consumed during melting or whether it remained as a residual phase in the residue. The abundances of Sc in Abitibi komatiites increase with decreasing Mg content (Figure 3.10), confirming that it is incompatible in olivine. Sc abundances are generally low, as Sc in incompatible in olivine, and abundances are controlled by the trapped melt fraction (partial fractional crystallization).

3.4.6 Vanadium

Vanadium, like Sc, is incompatible in most mafic minerals except garnet and spinel (Rollinson, 1993). The abundances of V in Abitibi komatiites increase with decreasing Mg content (Figure 3.11), confirming that it is incompatible in olivine.

3.4.7 Zinc

Zinc is incompatible in olivine and weakly compatible in sulfides, but is mobile during metamorphism/alteration. This is supported by an overall increase in incompatibility (in agreement with the modeled fractionation curve), but with a large degree of scatter (see Figure 3.11).

3.5 TRACE ELEMENTS

3.5.1 Lithophile Elements

3.5.1.1 HIGH FIELD-STRENGTH ELEMENTS

The abundances of HFSEs (e.g., Th, U, Nb, Ta, Zr) as well as Y and REEs increase with decreasing Mg content (Figure 3.12), consistent with them being incompatible in olivine. La and Sm exhibit only limited amounts of scatter, less than observed for the LILE (see below), however, Nd does not display well-defined fractionation trends. This behaviour is particularly striking at higher Mg contents. The high-Mg samples containing high Nd (>10 ppm) are all from komatiites in the footwall of the giant Kidd Creek

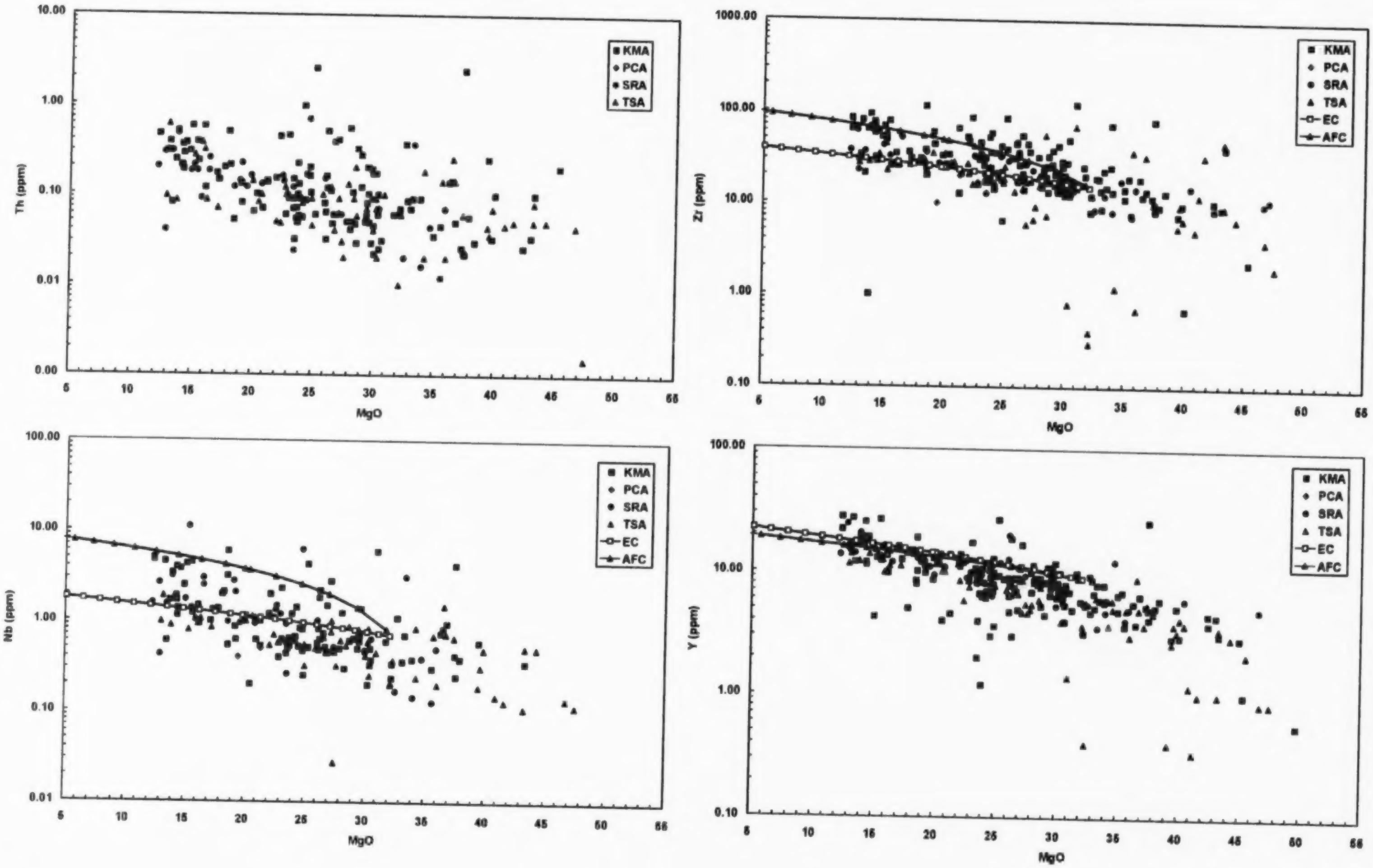

Figure 3.12a. Th, Nb, Zr, and Y (ppm) vs. MgO (wt.% volatile-free) for komatiitic rocks in the Abitibi greenstone belt.

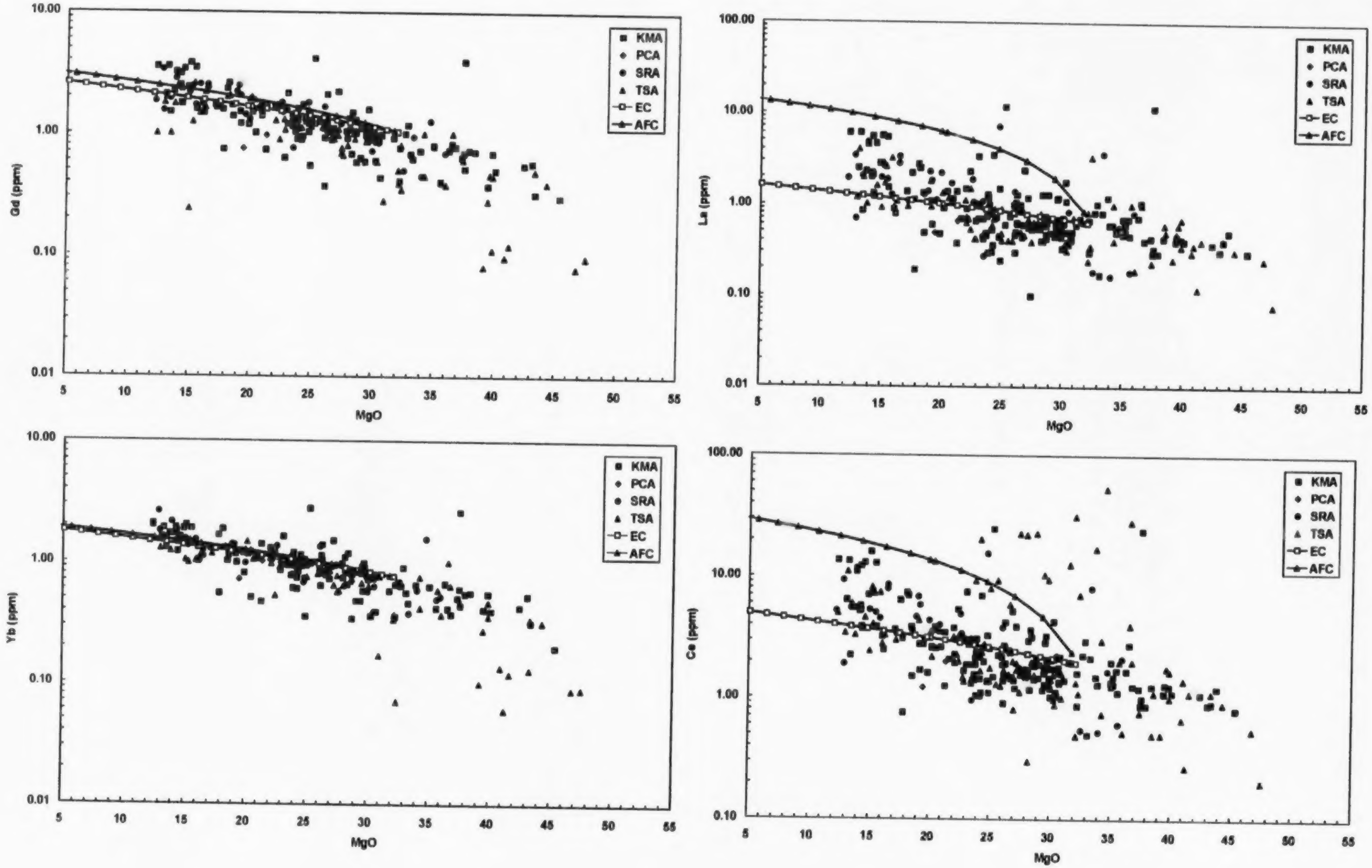

Figure 3.12b. Gd, Yb, La, and Ce (ppm) vs. MgO (wt.% volatile-free) for komatiitic rocks in the Abitibi greenstone belt.

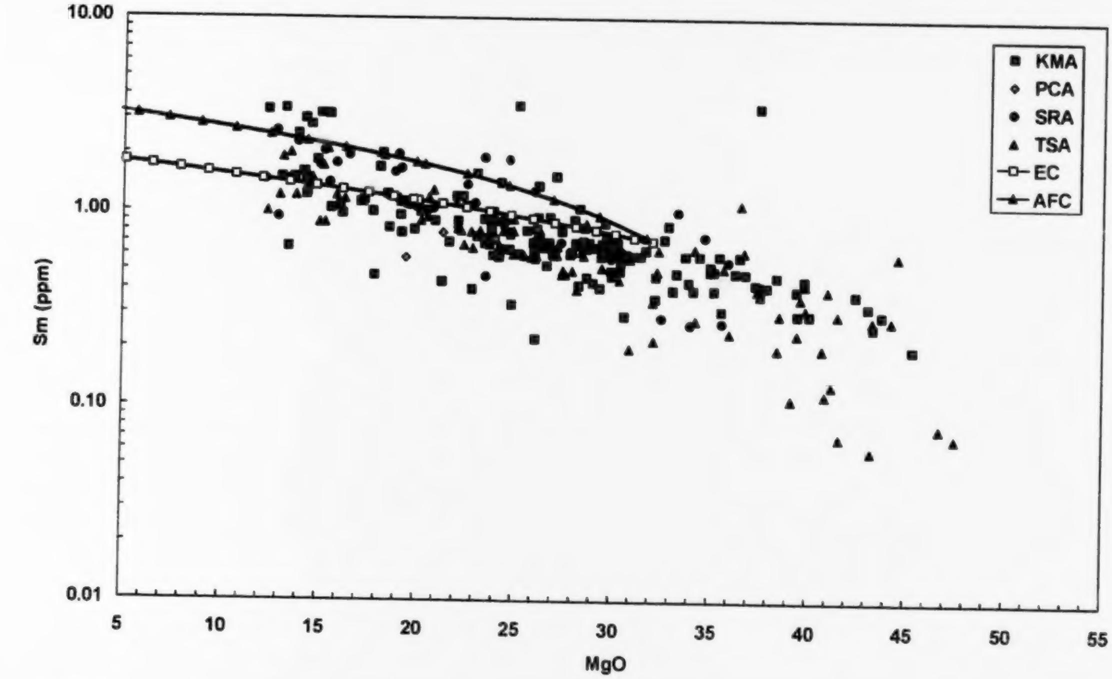

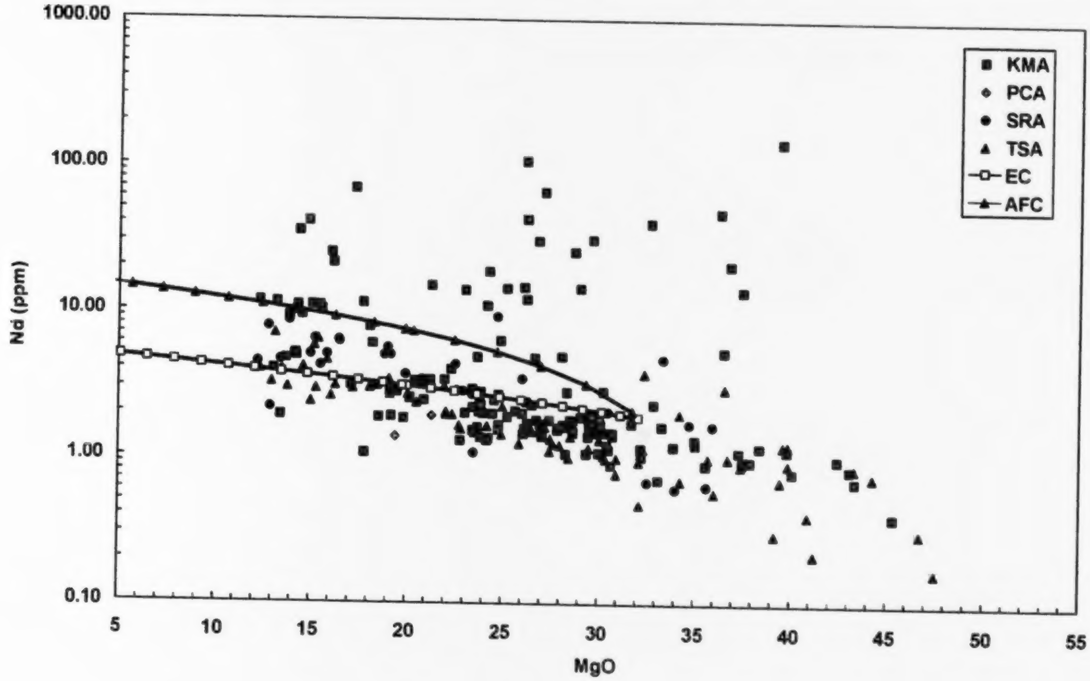

Figure 3.12c. Nd. and Sm (ppm) vs. MgO (wt.% volatile-free) for komatiitic rocks in the Abitibi greenstone belt.

volcanic-associated massive Cu-Zn sulfide deposit (Barrie, 1999), which is located within a large hydrothermal system in which Nd (and other MREE) appear to have been mobilized relative to LREE and HREE (see also Campbell et al., 1984).

3.5.1.2 LARGE-ION LITHOPHILE ELEMENTS

LILEs (e.g., Cs, Rb, K, Ba, Sr, and Eu^{+2}) are easily mobilized in komatiites during seafloor weathering, hydrothermal alteration, and/or regional metamorphism. Cs, Rb, Ba, and Sr all exhibit a considerable amount of scatter (Figure 3.13), indicating that these elements have been mobile. However, Eu displays more coherent fractionation trends (Figure 3.13) and appears to have experienced only limited mobility, suggesting relatively oxidizing conditions (i.e., Eu^{3+} rather than Eu^{2+}) during alteration.

3.5.2 Platinum Group Elements

3.5.2.1 IRIDIUM

Ir is strongly compatible in sulfide ($D^{sulfide/liquid} \sim 1.5 \times 10^4$: Peach et al., 1990), moderately compatible in olivine, and appears to be relatively immobile during seafloor weathering, hydrothermal alteration, and/or regional metamorphism (Keays et al., 1982). The Ir abundances of most Abitibi komatiites decrease with decreasing Mg content (Figure 3.14), consistent with olivine fractionation/accumulation.

3.5.2.2 RUTHENIUM

Ru is strongly compatible in sulfide, slightly to moderately compatible in olivine, and apparently relatively immobile during seafloor weathering and regional metamorphism, but can be mobile during intense hydrothermal alteration. It displays a similar decrease with fractionation as Ir (see Figure 3.14) and the Ru abundances of most Abitibi komatiites decrease with decreasing Mg content (Figure 3.14), consistent with olivine fractionation/accumulation.

3.5.2.3 RHODIUM

Rh is strongly compatible in sulfide ($D^{sulfide/liquid} \sim 1.5 \times 10^4$: Peach et al., 1990), slightly compatible in olivine, and apparently relatively immobile during seafloor weathering and regional metamorphism, but can be mobile during intense hydrothermal alteration. The Rh abundances of most Abitibi komatiites decrease with decreasing Mg content (Figure 3.14), consistent with olivine fractionation/accumulation.

3.5.2.4 PLATINUM

Pt is strongly compatible in sulfide ($D^{sulfide/liquid} \sim 3 \times 10^4$: Peach et al., 1990), incompatible in olivine, and apparently relatively immobile during seafloor weathering and regional metamorphism, but can be mobile during intense hydrothermal alteration. Komatiitic magmas do not typically reach sulfide-saturation until about ~10 w% MgO, unless sulfide-saturation is induced via assimilation of crust or sediment (Lesher and Stone, 1996). The Pt abundances of most Abitibi komatiites increase with decreasing Mg content (Figure 3.14), consistent with olivine fractionation/accumulation. The absence of Pt depletion (cf. AFC trend in Figure 3.14) indicates that the sampled magmas did not equilibrate with sulfides.

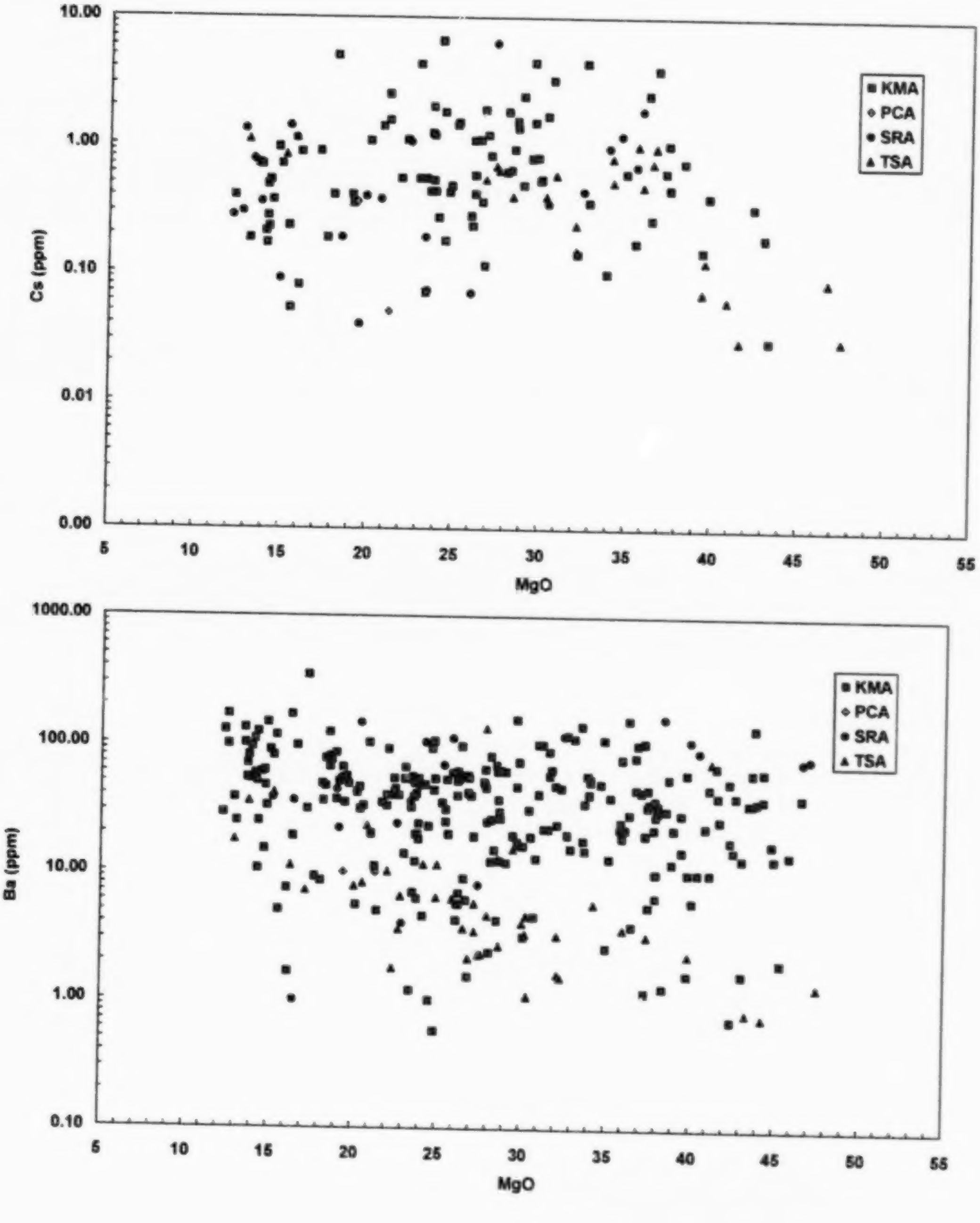

Figure 3.13a. Cs. and Ba (ppm) vs. MgO (wt.% volatile-free) for komatiitic rocks in the Abitibi greenstone belt.

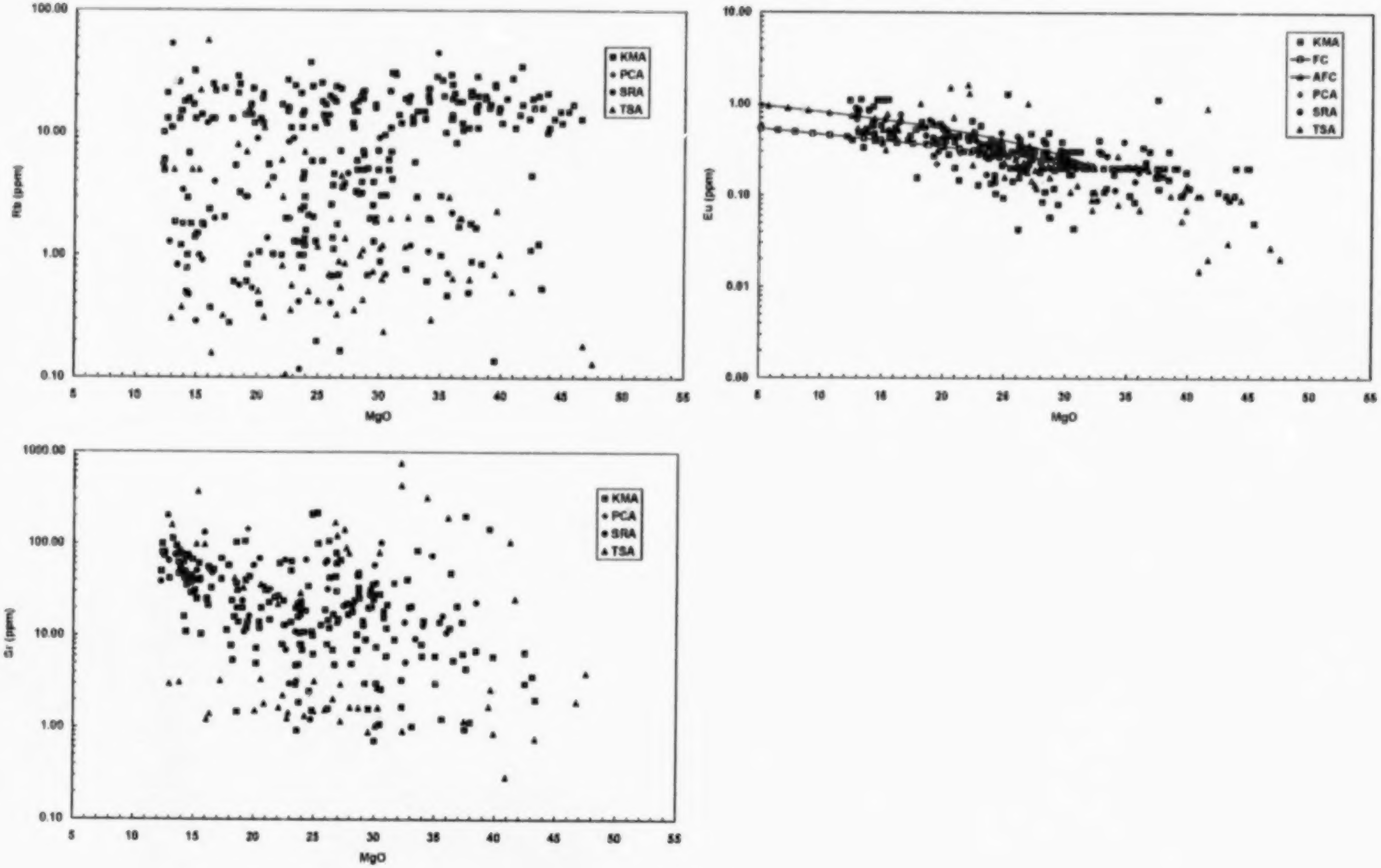

Figure 3.13b. Rb, Sr, and Eu (ppm) vs. MgO (wt.% volatile-free) for komatiitic rocks in the Abitibi greenstone belt.

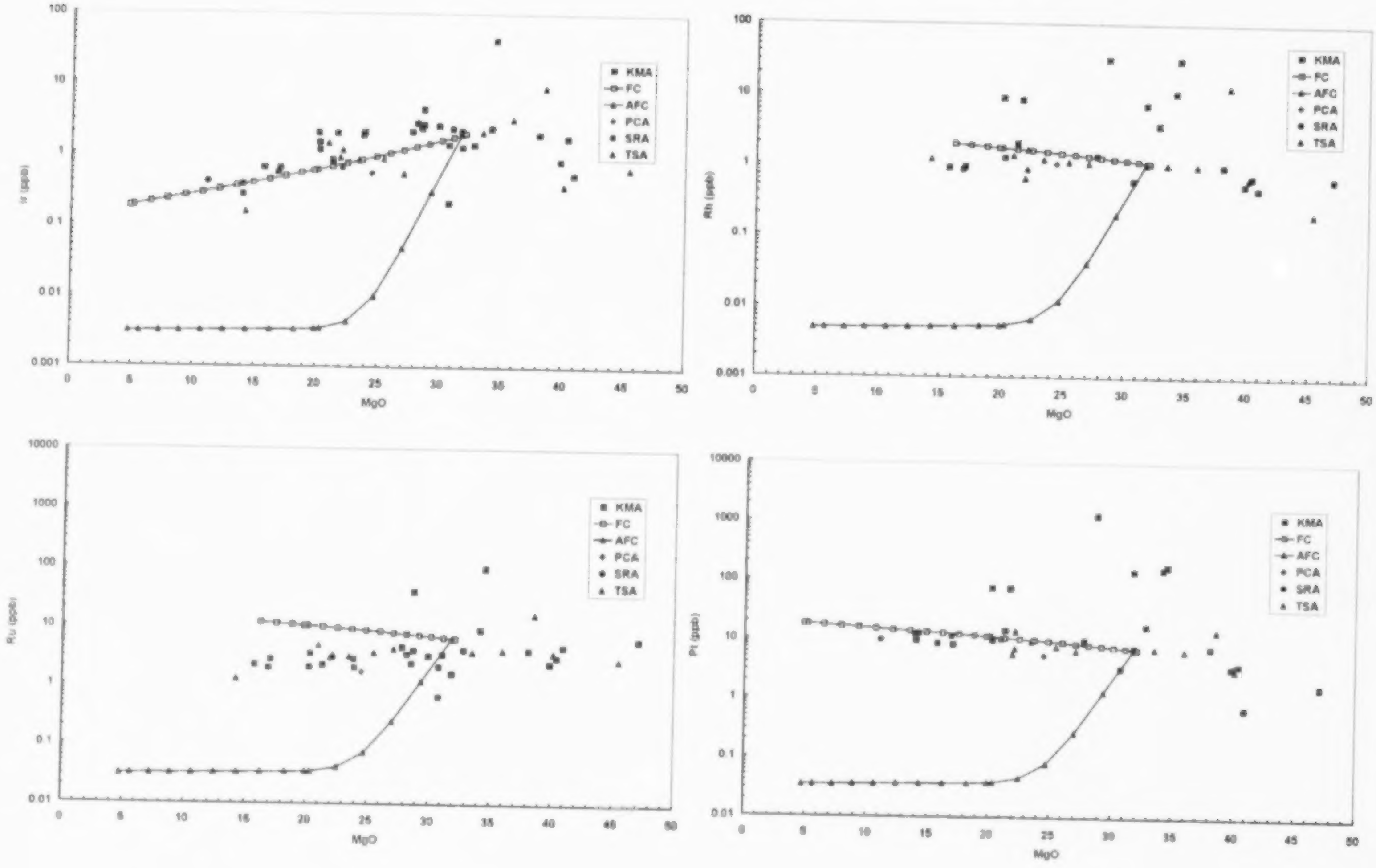

Figure 3.14a. Ir, Ru, Rh, and Pt (ppb) vs. MgO (wt.% volatile-free) for komatiitic rocks in the Abitibi greenstone belt.

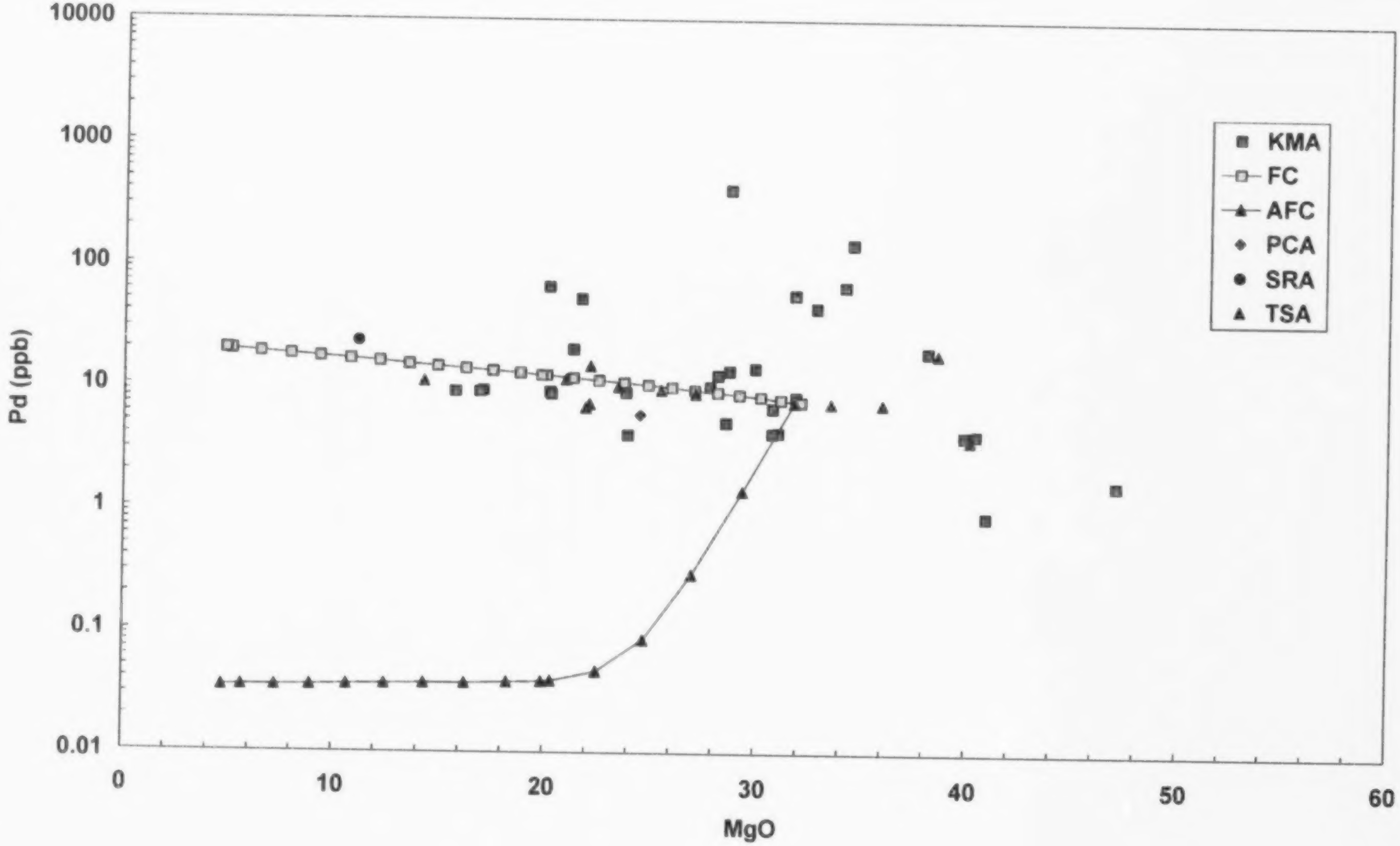

Figure 3.14b. Pd (ppb) vs. MgO (wt.% volatile-free) for komatiitic rocks in the Abitibi greenstone belt.

3.5.2.5 PALLADIUM

Pd is strongly compatible in sulfide ($D^{sulfide/liquid}$ ~3×10^4: Peach et al., 1990) and displays almost identical behaviour to Pt (Figure 3.14), indicating that none of the samples within the dataset have equilibrated with sulfides.

3.6 ISOTOPIC DATA

3.6.1 Nd Isotopes

Nd isotopic ratios in komatiites, particularly high-Mg komatiites that have very low abundances of Nd and Sm, are highly susceptible to modification during seafloor weathering, hydrothermal alteration, and/or regional metamorphism (e.g., Arndt et al., 1989; Gruau et al., 1992; Lahaye et al., 1995; Lesher et al., 1997). Therefore, Nd isotopic data from the komatiites in the Abitibi greenstone belt must be interpreted within that context.

The Nd isotopic deviations of Abitibi komatiites from the chondritic uniform reservoir (CHUR) vary between $\varepsilon_{Nd} = +0.1$ and +5.2. After alteration filtering (see Section 3.2), the range is reduced to between $\varepsilon_{Nd} = +1.2$ and +5.2 (Table 3.1 and Figure 3.15). These data indicate the following:

(1) Komatiites in the Abitibi greenstone belt display a long-term history of LREE-depletion (100-650 Ma).

(2) There is an overlap between the ε_{Nd} compositions for Abitibi greenstone belt komatiitic rocks and other lithologies (see Table 3.1) within the greenstone belt.

(3) There is no systematic variation of ε_{Nd} in komatiites within individual assemblages in the Abitibi greenstone belt.

(4) There is no clear evidence of crustal contamination or source enrichment, which are typically recognized by $\varepsilon_{Nd}<0$, in any of the komatiites, even in komatiites that display trace element evidence of crustal contamination (see Section 3.83).

Table 3.1. Nd isotopic data for Abitibi greenstone belt komatiitic rocks (after alteration filtering) and other lithologies.

Assemblage	Pacaud	Deloro	Stoughton-Roquemaure	Kidd-Munro	Tisdale	Kinojevis
ε_{Nd} (komatiite rocks)	2.6-5.2 n = 4	-	2.4-5.6 n = 7	1.9-3.6 n = 41	1.2-2.8 n = 31	-
ε_{Nd} (komatiitic rocks and other volcanic rocks)	2.6-5.2 n = 4	2.1-3.3 n = 3	2.4-5.6 n = 7	1.0-3.6 n = 44	1.2-3.4 n = 34	2.6-2.9 n = 2
References	a	b	a, b ,d	a, b, c	a, b	a, b

a = this study (including Lesher et al., 1997). b = Ayer et al. (unpublished data). c = Lahaye and Arndt (1996). d = Dostal and Mueller (1997). Those from Lahaye and Arndt (1996) include only non-rodingitized whole-rock samples. Rodingitization is associated with large degrees of trace element mobility, and isotopic closure is more likely in whole rock than in mineral separates (see discussion in text).

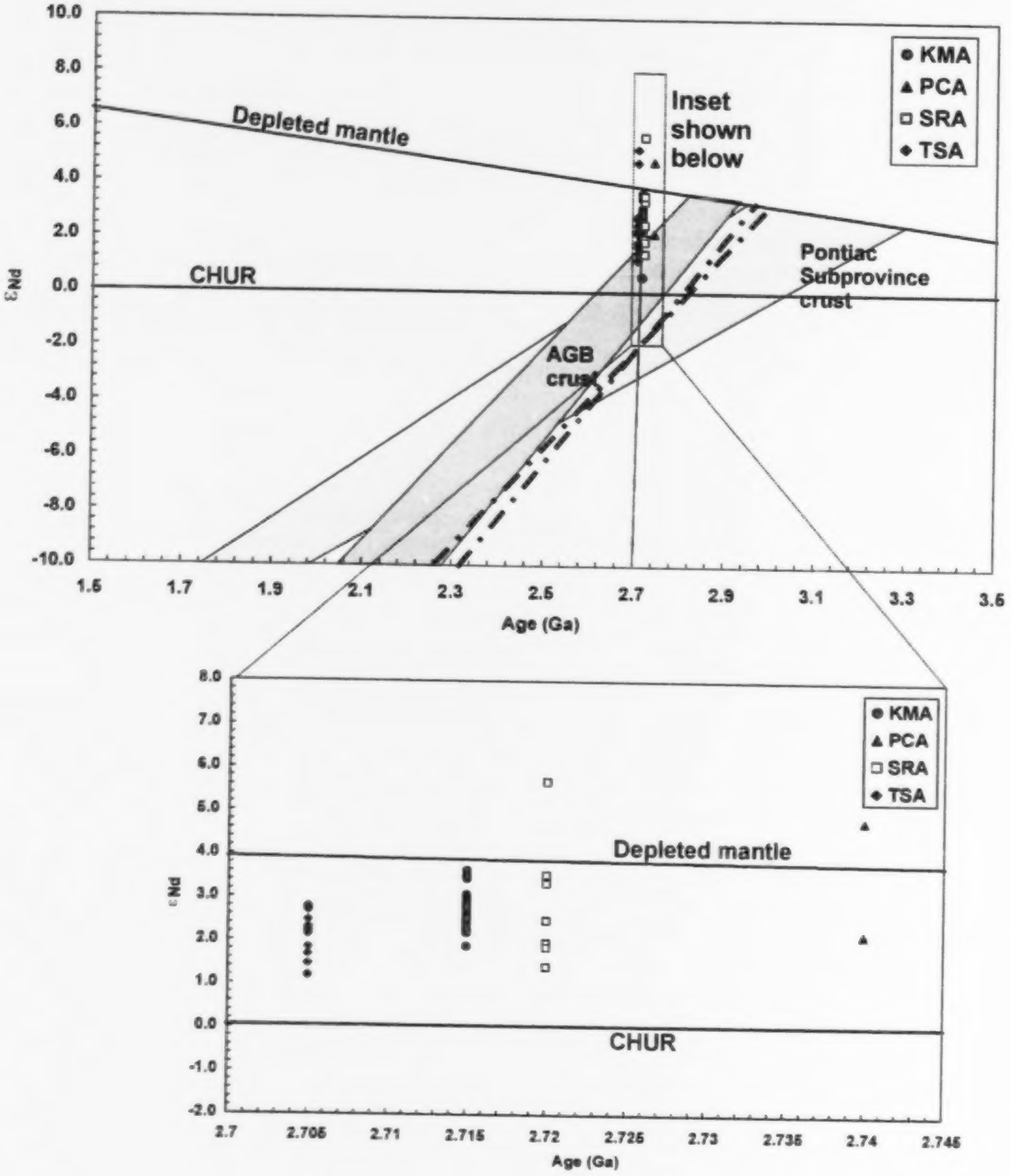

Figure 3.15. Summary of Nd isotopic data for komatiitic rocks in the Abitibi greenstone belt and comparisons with sedimentary rocks in the Pontiac metasedimentary belt (light grey) and the Abitibi greenstone belt (dark grey) (Feng et al., 1993). Crust with a Nd isotopic signature of $\varepsilon_{Nd} = -2$ at 2.7 Ga (developed using ^{147}Sm/^{144}Nd ratios from Abitibi metasediments: ^{147}Sm/^{144}Nd = 0.0967 - 0.1559: Feng et al., 1993) which is sufficiently low to be resolved from that of 2.7 Ga Abitibi komatiites is shown for comparison (heavy stippled lines).

The absence of an enriched source or a crustal Nd isotopic signature does not, by itself, indicate that the komatiites were not derived from an enriched source or contaminated by upper crustal rocks, as the source enrichment or crustal rocks may have been juvenile and may not have had sufficient time to evolve to lower ε_{Nd} compositions. The primitive Nd isotopic signatures of metasediments in the Abitibi greenstone belt, which range between -0.71 and +1.83 ε_{Nd} (Feng et al., 1993) with Nd model ages close to their depositional ages, suggest that the crust was relatively juvenile at the time the komatiites were erupted.

Using $^{147}Sm/^{144}Nd$ ratios from Abitibi greenstone belt metasediments ($^{147}Sm/^{144}Nd = 0.0967$ – 0.1559: Feng et al., 1993), and the most depleted Abitibi komatiite ($^{143}Nd/^{144}Nd = 0.50933$, $^{147}Sm/^{144}Nd =$ 0.2817, 0.42 ppm Sm, 0.92 ppm Nd), the crust would need to be ~250 Ma older than the new magma to develop an isotopic composition resolvable from the primitive magmas (e.g., $\varepsilon_{Nd} = -2$) (Figure 3.15). For typical enriched ocean island basalt (OIB)-like reservoirs, at least 1 Ga would be required to develop ε_{Nd} <0. Thus, crustal contamination or enriched sources are likely not detectable in Abitibi komatiites using Nd isotopes.

3.6.2 Os Isotopes

Komatiites at Pyke Hill have high abundances of Os and relatively low abundances of Re, as expected for a high degree partial melts of the mantle (Walker et al., 1988; Shirey and Walker, 1995). The initial Os isotopic ratios are near chondritic ($\gamma_{Os} = -3$), consistent with a normal depleted source without significant source enrichment or crustal interaction (Walker et al., 1988; Shirey and Walker, 1995).

Lahaye et al. (2001) studied the Re-Os isotope geochemistry of komatiite lavas and associated Ni-Cu-(PGE) mineralization in the Abitibi greenstone belt to evaluate the "ground melting" model for ore genesis and the superimposed effects of seafloor weathering, hydrothermal alteration, and regional metamorphism on ore environments and non-ore environments. He selected the Alexo deposit in the Dundonald area of the Kidd-Munro assemblage, the Hart deposit in the Shaw Dome area of the Tisdale assemblage, and the Texmont deposit in the Bartlett Dome area of the Tisdale assemblage for his study. Although they demonstrated that Re and Os had been mobile on the mineral grain scale, the moderately radiogenic Os isotopic compositions of well-preserved komatiites and olivine mineral separates at Alexo ($\gamma_{Os} = +20$ and +33) and variably radiogenic Os isotopic compositions of sulfides at Texmont ($\gamma_{Os} = 0$ to +3), Alexo ($\gamma_{Os} = +31$ to +141), and Hart ($\gamma_{Os} = +66$ to +135) are consistent with variable degrees of contamination by crustally-derived material under relatively low (Hart and Alexo) and relatively high (Texmont) R factors (see discussion by Lesher and Burnham, 2001). The Abitibi crust is juvenile (Machado et al., 1986; Corfu and Noble, 1992) and has low Os abundances that make it an unlikely source for the radiogenic Os in the Alexo komatiites. Instead the Os isotopic data are consistent with 1-4% contamination by associated Os-rich graphitic, sulfidic shales. Thus, the Os isotopic compositions of the Abitibi sulfides are consistent with assimilation of sulfidic sediments to generate *local* contamination in the komatiites and melting of sulfides to generate the Ni-Cu-(PGE) mineralization (Lahaye et al., 2001).

3.7 SUMMARY OF GEOCHEMICAL OBSERVATIONS

The majority of the major element variations of komatiitic rocks in the Abitibi greenstone belt are consistent with fractional crystallization and/or accumulation of olivine ± chromite ± clinopyroxene.

The komatiitic rocks in the Abitibi greenstone belt can be subdivided into three groups: Ti-depleted komatiitic basalts (TDKB), Al-depleted–Ti-enriched komatiites (ADK–TEK), and Al-undepleted komatiites (AUK) on the basis of:

1) the abundances of lithophile elements that are compatible in garnet (e.g., Al, HREE, Y, Sc) relative to other MILE (see Xie et al., 1993; Fan and Kerrich, 1997), and
2) the abundances of HILE (e.g., Th, U, LREE) relative to the abundance of MILE (e.g., Y, Zr, HREE, Ti) (see Cattell and Arndt, 1987; Xie et al., 1993; Stone and Lesher, 1995; Fan and Kerrich, 1997; Dostal and Mueller, 1997).

ADK–TEK are considered as one group, as the two types could not be completely separated in the database.

The komatiites were further subdivided into those that have been affected by crustal contamination and those that have not (Table 1.3). Importantly, key petrogenetic indicators such as $[Gd/Yb]_{MN}$ (an indicator of fractionation between HREE and MREE) and Al_2O_3/TiO_2 are nearly identical for contaminated and uncontaminated magmas. ADK, regardless of whether crustally contaminated or not, have Al_2O_3/TiO_2 ratios between 14 and 26 (mean ~19-20) and $[Gd/Yb]_{MN}$ ~1.0. ADK–TEK, regardless of whether crustally contaminated or not, have Al_2O_3/TiO_2 ratios between 2 and 15 (mean ~10-11) and $[Gd/Yb]_{MN}$ ~1.4. TDKB, all of which appear to be uncontaminated, have Al_2O_3/TiO_2 ratios between 28 and 35 (mean ~32) and $[Gd/Yb]_{MN}$ ~0.7.

Primitive mantle-normalized multi-element plots for representative examples of each of the principal magma types are shown in Figure 3.16. ADK–TEK exhibit evidence of garnet fractionation, including mild to significant depletion in HREE and minor depletion in Y. ADK have unfractionated HREE abundances. Some ADK–TEK and AUK have negative Nb anomalies and are enriched in LREE, a clear signature of contamination by a crustal component. Komatiites without negative Nb anomalies are depleted in HILE, consistent with derivation from a depleted source.

There is a positive correlation between $[Th/Sm]_{MN}$ and $[Nb/Th]_{MN}$ (Figure 3.17) in Abitibi komatiites that is consistent with 1) contamination by HILE-enriched Archean upper-middle continental crustal rocks (Taylor and McLennan, 1995), 2) contamination by sedimentary materials derived from upper to middle continental crustal rocks, or 3) derivation from a source containing a continentally-derived component of subducted crust (Carlson, 1991). The exceptions are ferropicrites, which are typically mildly depleted in LREE, but have $[Nb/Th]_{MN} > 1$ and $[Th/Sm]_{MN} < 1$. There is no correlation between $[Gd/Yb]_{MN}$ and $[Th/Sm]_{MN}$ (Figure 3.17) in the ferropicrites, suggesting that crustal contamination has not affected the abundances of MILE in those rocks.

Al_2O_3/TiO_2 ratios are commonly used to distinguish different types of komatiites (Nesbitt et al., 1979). TDKB and ADK–TEK typically have lower Mg contents, whereas AUK span the complete range of MgO abundances (Figure 3.18). There is a strong correlation between Al_2O_3/TiO_2 and $[Gd/Yb]_{MN}$ (Figure 3.19) in all komatiites and ferropicrites.

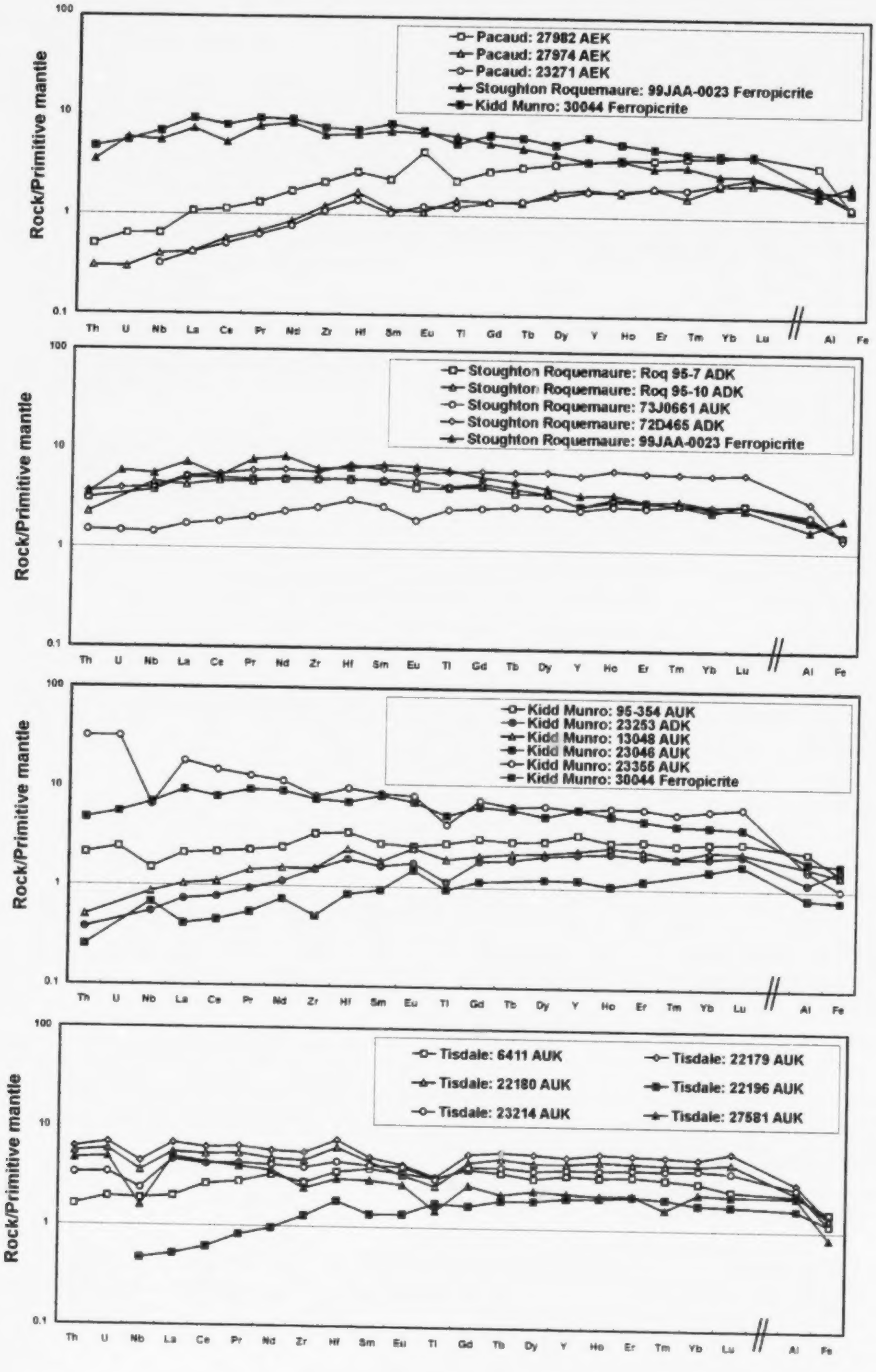

Figure 3.16. Primitive mantle-normalized multi-element diagram for representative analyses of komatiitic rocks in the Abitibi greenstone belt. Normalizing values from McDonough and Sun (1995). TDKB = Ti-depleted komatiitic basalt; TEK = Ti-enriched komatiite; ADK = Al-depleted komatiite; AUK = Al-undepleted komatiite.

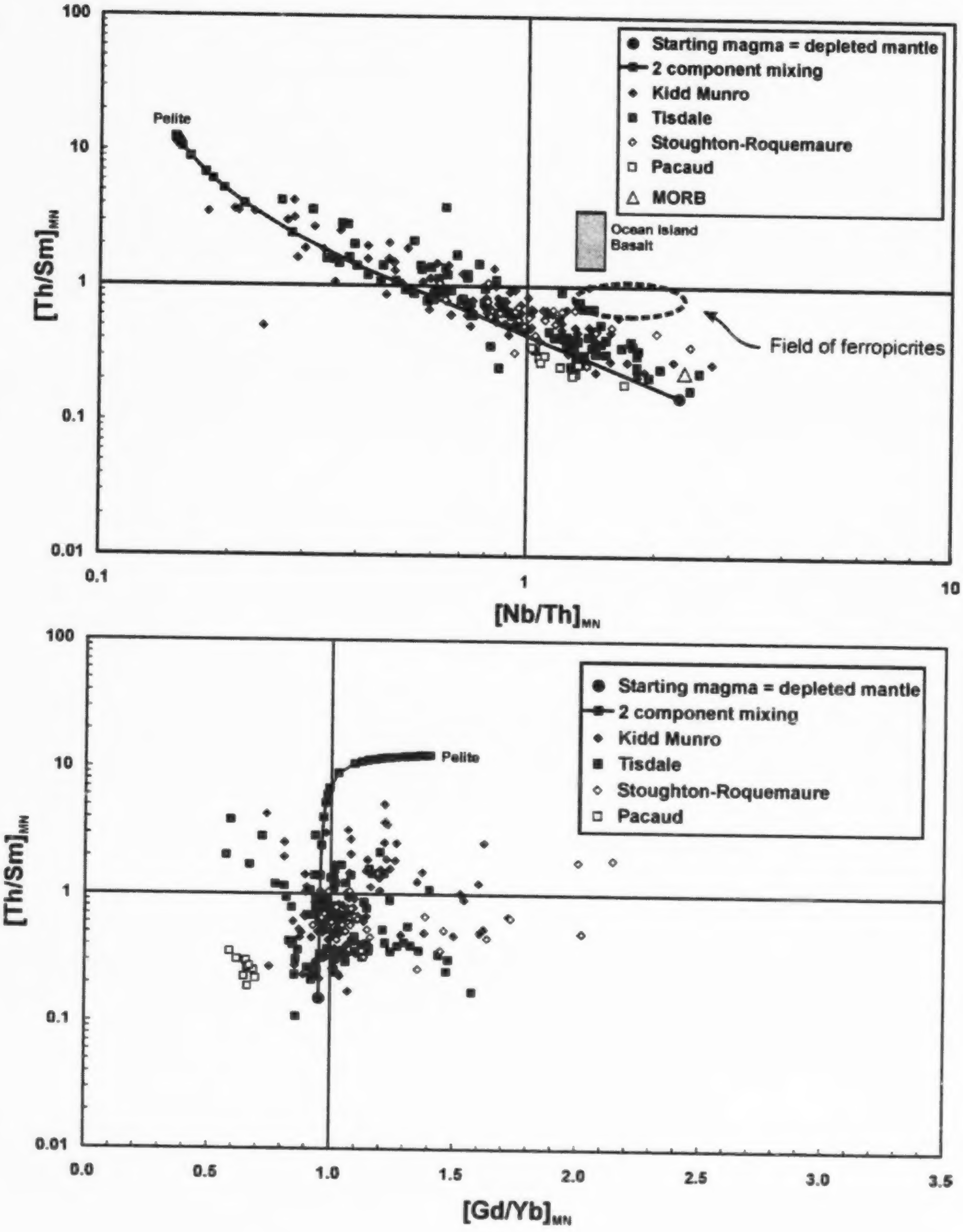

Figure 3.17. [Th/Sm]$_{MN}$ vs. [Nb/Th]$_{MN}$ (top) and [Th/Sm]$_{MN}$ vs. [Gd/Yb]$_{MN}$ (bottom) for komatiites in the Abitibi greenstone belt. A two-component mixing trend representing contamination of a komatiite (MgO ~30 wt.%, Sm = 0.7 ppm, Th = 0.04 ppm, Nb = 1.0 ppm, Gd = 1.4 ppm, Yb = 1.2 ppm) with a pelite (Sm = 6.5 ppm, Th = 18.8 ppm, Nb = 13.8 ppm, Gd = 3.8 ppm, Yb = 2.2 ppm) in 10% increments is shown for comparison. N-MORB and ocean island basalt fields are from Sun (1980) and Saunders and Tarney (1984); primitive mantle normalizing values are from McDonough and Sun (1995); average pelite from Condie (1992) and Taylor and McLennan (1995).

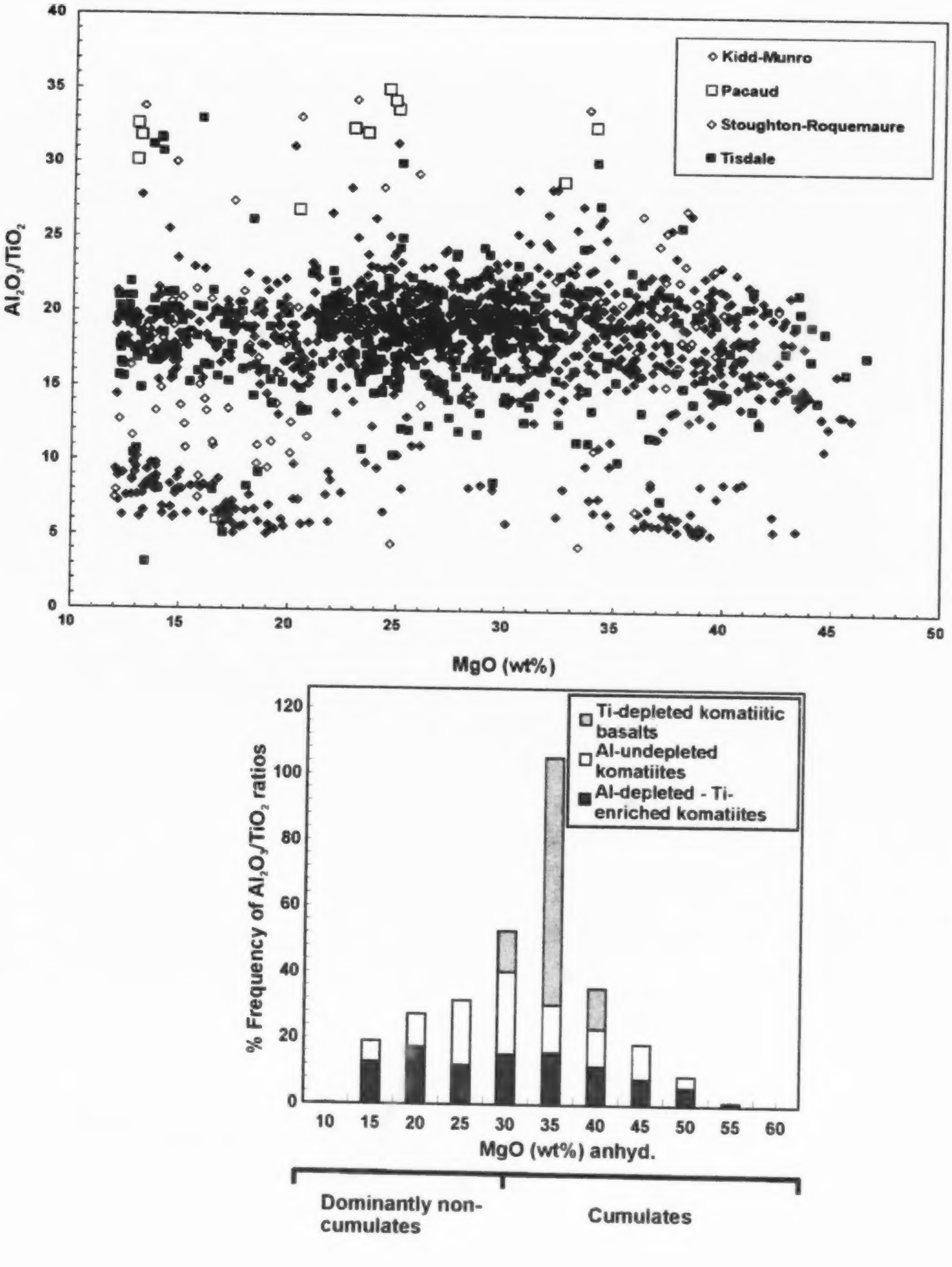

Figure 3.18. Al_2O_3/TiO_2 vs. MgO (wt.% volatile-free) for komatiites in the Abitibi greenstone belt (top). ADK typically have MgO <26 wt.%, excluding cumulate rocks that do not represent magma compositions. Al_2O_3/TiO_2 vs. MgO bar chart (bottom).

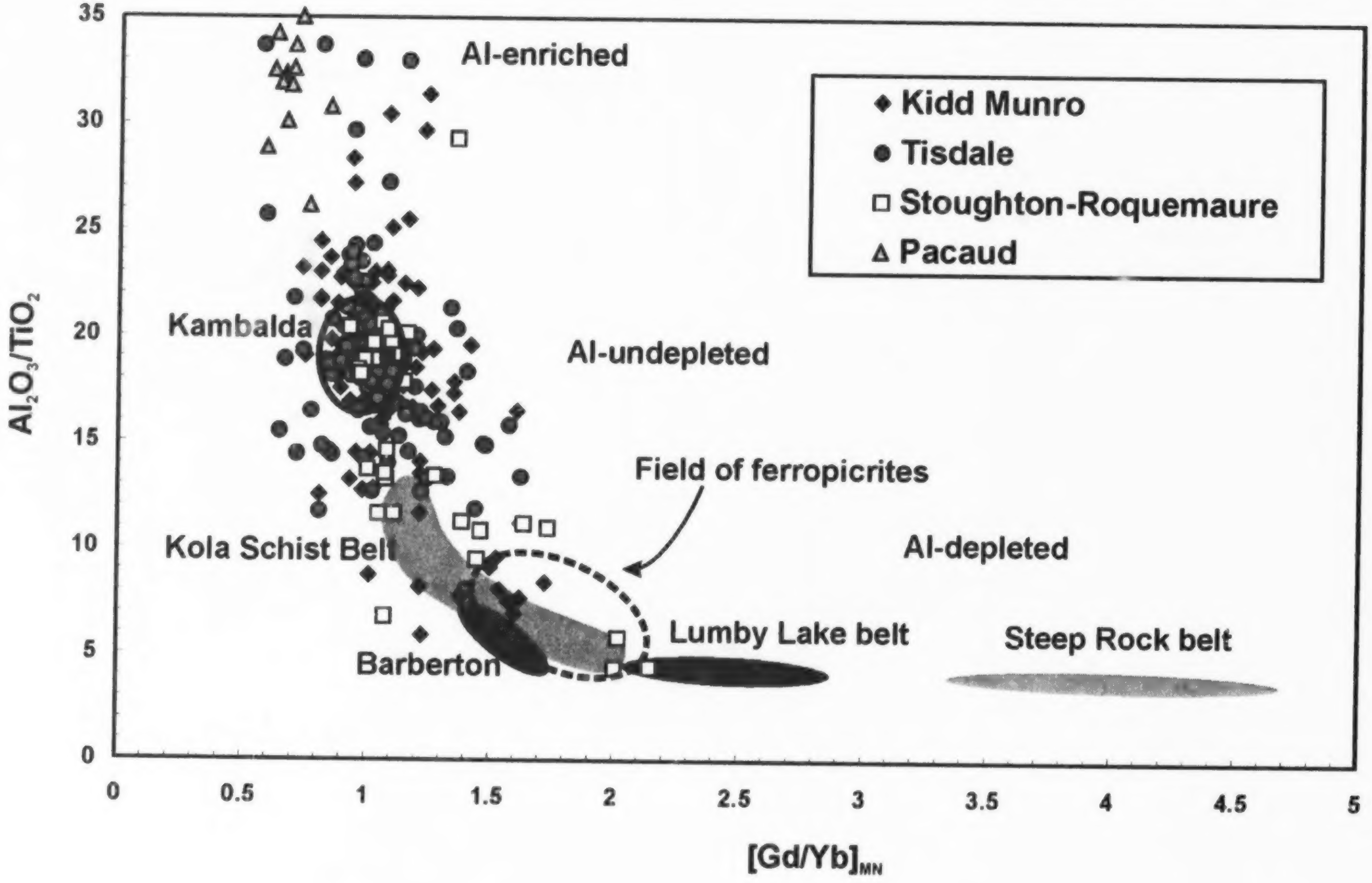

Figure 3.19. Al_2O_3/TiO_2 vs. chondrite-normalized $[Gd/Yb]_{MN}$ for komatiites in the Abitibi greenstone belt compared to komatiites in the Kambalda area, Western Australia (data from Lesher et al., 2001); the Steep Rock and Lumby Lake belts, Superior Province (Tomlinson et al., 1999a); Kola Schist belt, Russia (Puchtel et al., 1997); and the Barberton greenstone belt, South Africa (Byerley, 1999; Jahn et al., 1982; Lahaye et al., 1995). Primitive mantle values from McDonough and Sun (1995).

As the komatiites in this study encompass a wide range of Mg contents, the method of Hanski (1992) was used to calculate molar $[TiO_2]_{Ol}$ and molar $[Al_2O_3]_{Ol}$, where $[TiO_2]_{Ol} = TiO_2/(2/3\text{-}MgO\text{-}FeO)$ and $[Al_2O_3]_{Ol} = Al_2O_3/(2/3\text{-}MgO\text{-}FeO)$. These transformations project the compositions of the rocks into the Al-Ti system from olivine, removing the effects of olivine fractionation and allowing a better comparison of komatiites with differing MgO abundances. TDKB are mildly enriched in Al, strongly depleted in Ti (Figure 3.20), and strongly depleted in HREE ($[Gd/Yb]_{MN}$ = 0.6-0.8), similar to Barberton Al-enriched komatiites (e.g., Jahn et al., 1982) and Gorgona picrites (e.g., Arndt et al., 1997b). AUK form a relatively restricted compositional range on $[TiO_2]_{Ol}$ and $[Al_2O_3]_{Ol}$ vs. $[Gd/Yb]_{MN}$ diagrams (Figure 3.20), comparable to Archean AUK in other regions (e.g., Belingwe, Kambalda). ADK–TEK in the Abitibi greenstone belt show a larger degree of scatter (Figure 3.20) and overlap low-Ti komatiites in the Barberton Greenstone Belt. Some ADK–TEK have higher $[Ti]_{Ol}$ and slightly higher $[Al]_{Ol}$, and trend toward TEK in Finland (Figure 3.20). Thus, the ADK–TEK in the Abitibi greenstone belt span a range between 1) Finnish-type TEK and 2) Barberton-type ADK.

3.8 PETROGENETIC DISCUSSION

3.8.1 Source Composition and Depth of Melting

The petrogenesis of komatiites provides important constraints on the stratigraphic and tectonic architecture of the Abitibi greenstone belt. Similarities and differences in the petrogenesis of komatiites within and between assemblages and within and between various geographic regions of the greenstone belt are critical in understanding whether the assemblages are allochthonous terranes or autochthonous terranes. Understanding the relationships between the different assemblages is critical in understanding the metallogenesis of the komatiites and the continuity of mineralized komatiite units and sequences across the belt.

The high MgO contents (up to 30%), very low highly incompatible lithophile element contents, and uniformly low moderately incompatible lithophile element contents of non-cumulate AUK in the Abitibi greenstone belt suggest that they were generated by high degree partial melting of a depleted mantle source outside the stability field of majorite garnet. Experimental data suggest that komatiites of this type are derived from *dunite* [Liquid + Olivine] residua at 3-7 GPa (see discussion by Sproule et al., 2002).

ADK in other greenstone belts have MgO contents up to 33%, including those in the Barberton type area (Green, 1975). However, the lower MgO contents (max. 26%) of non-cumulate ADK–TEK in the Abitibi greenstone belt (Figure 3.18) are consistent with lower degrees of partial melting or partial melting of a less depleted source than AUK in the Abitibi greenstone belt or with fractional crystallization of olivine from all of the analyzed samples. The generally lower Al, Sc, Y, and HREE contents of ADK–TEK in the Abitibi greenstone belt favour generation within the stability field of majorite garnet. Experimental data suggest that ADK are derived from peridotite sources leaving *garnet peridotite* [Liquid + Olivine + Garnet] residua at 6-9 GPa. (Herzberg and O'Hara, 1998). Blichert-Toft and Arndt (1999) used Lu-Hf isotopes to show that Barberton ADK were not only derived from a garnet-rich residuum, but that the source must have been enriched in garnet. The greater depth of generation of ADK relative to AUK may be quite important. Herzberg et al. (1983) suggested that komatiites are very dense and may ascend only very slowly, such that less magnesian differentiates may preferentially ascend and erupt. However, differences in magma density are quite small ($\Delta\rho$ = 0.1-0.2 g cm^{-3}), differences in magma viscosity are quite large ($\Delta\eta$ = 10-1000 Pa s), and magma ascent rates are controlled more by channel

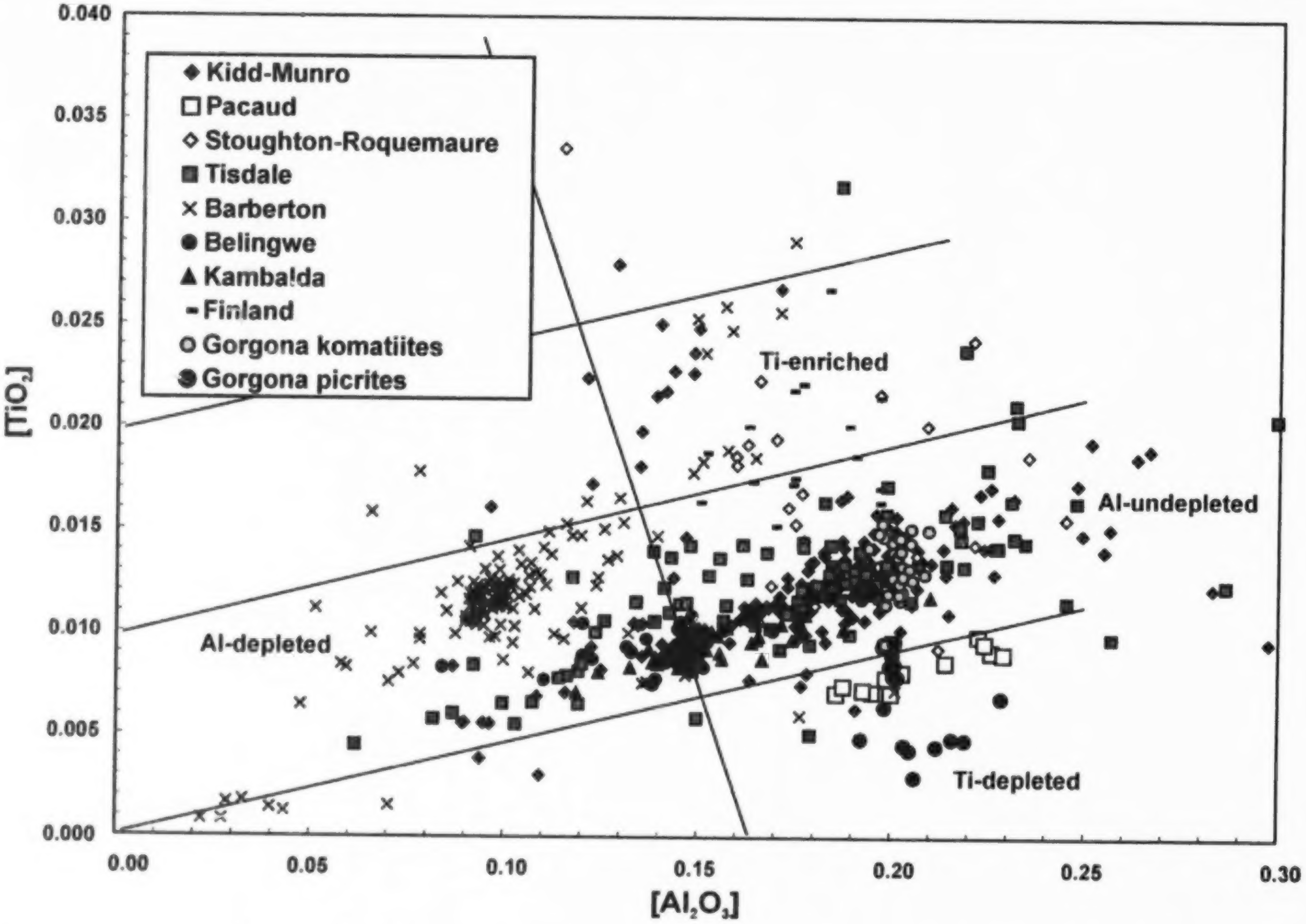

Figure 3.20a. $[TiO_2]_{molar}$ vs. $[Al_2O_3]_{molar}$ olivine projection for komatiites in the Abitibi greenstone belt with comparative data for komatiites at Barberton (Jahn et al., 1982; Lahaye et al., 1995; Byerley, 1999); Kambalda (Lesher and Arndt, 1995); Belingwe (as compiled by Herzberg and O'Hara, 1998); Finland (Hanski et al., 2001); and for komatiites and picrites at Gorgona (Arndt et al., 1997b).

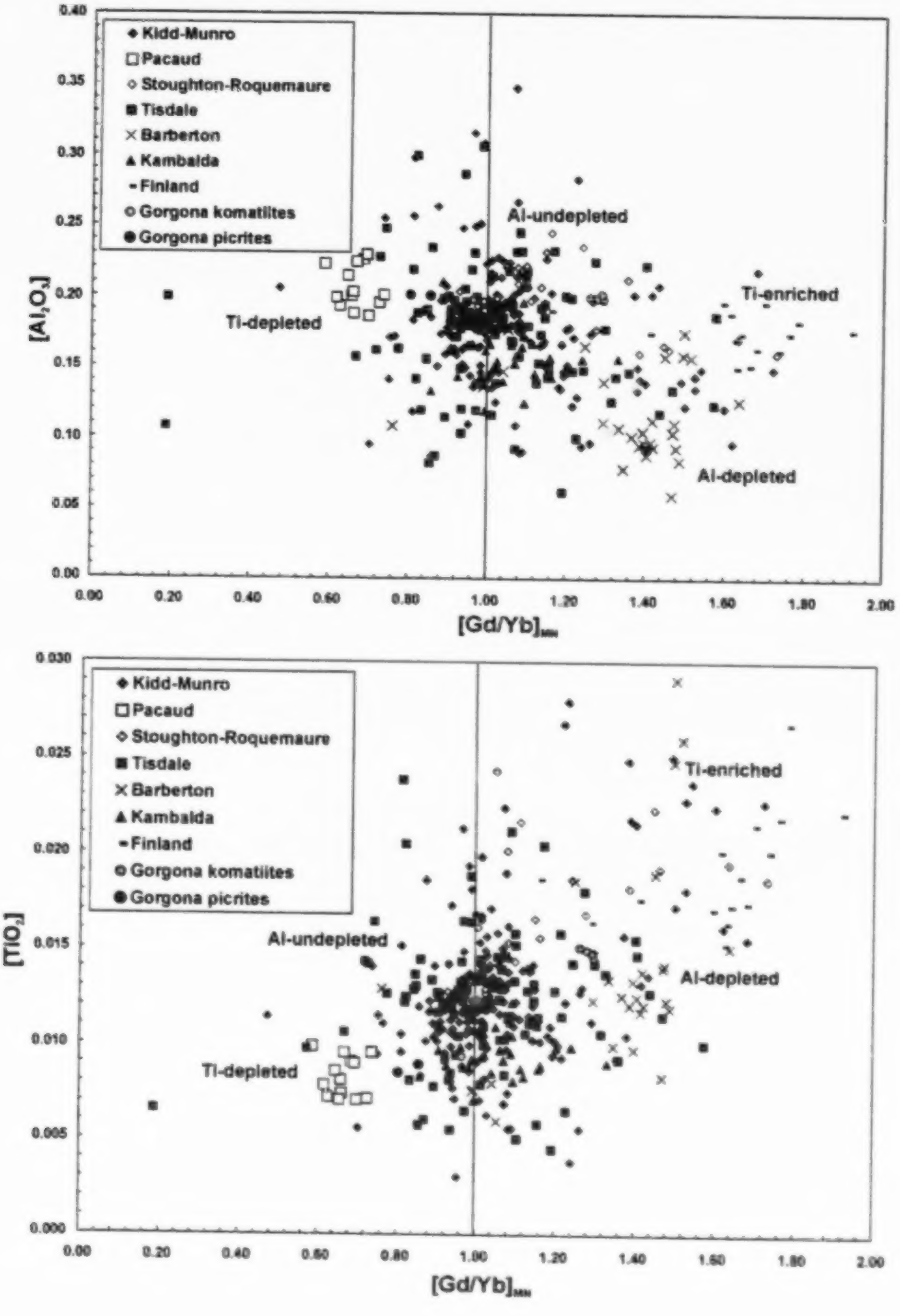

Figure 3.20b. $[Al_2O_3]$ vs. $[GdYb]_{MN}$ and $[TiO_2]_{molar}$ vs. $[GdYb]_{MN}$ diagrams for komatiites in the Abitibi greenstone belt with comparative data for komatiites at Barberton (Jahn et al., 1982; Lahaye et al., 1995; Byerley, 1999); Kambalda (Lesher and Arndt, 1995); Belingwe (as compiled by Herzberg and O'Hara, 1998); Finland (Hanski et al., 2001); and for komatiites and picrites at Gorgona (Arndt et al., 1997b).

width and viscosity than by density ($v = w^2 g \Delta\rho 3\eta^{-1}$, where w = channel width, g = gravitational constant, ρ = density, and η = viscosity). Thus, although the density of the magma relative to the overlying crust is a critical constraint on whether the magma will erupt at all, the *rate* of eruption is controlled more by viscosity than by density.

The origin of TEK is more problematic. Ti-enriched komatiites in Norway (Barnes and Often, 1990) and Finland (Hanski et al., 2001) are enriched in HILE and depleted in HREE, but do not exhibit the same depletion in Al, Sc, and Y that is observed in Barberton-type ADK; thus they are not considered to have formed via retention of garnet in the residue (Barnes and Often, 1990; Hanski et al., 2001). However, the ADK–TEK in the Abitibi greenstone belt are transitional in composition between Scandinavian and Barberton ADK: they are mildly depleted in Y and range from AUK to ADK. Thus, there appears to be some evidence for garnet involvement in the source region of these komatiites. Hanski et al. (2001) proposed that the high $[Gd/Yb]_{MN}$ ratios of Finnish komatiites resulted from preferential enrichment of the source in LREE (and MREE) relative to HREE. Thus, the ADK–TEK in the Abitibi greenstone belt may reflect a petrogenetic process involving retention of majorite garnet in a source that had been previously enriched in LREE (and MREE) relative to HREE.

The lower Ti and higher HREE contents of TDKB in the Abitibi greenstone belt are similar to Gorgona picrites (Arndt et al., 1997b). These komatiites can be produced in two ways: 1) dynamic melting of refractory (previously depleted) mantle, most likely in a plume axis (Arndt et al., 1997b) or 2) moderate degree partial melting (<20%) of a *garnet lherzolite* [Liquid + Ol + Opx + Cpx + Gar] or *garnet harzburgite* [Liquid + Ol + Opx + Gar] source at 8-9 GPa followed by higher degree (>30%) partial melting of the residuum at <8 GPa to consume all of the clinopyroxene and garnet. We presently prefer dynamic melting of a refractory source, as the Al abundances would be expected to be higher at a given MgO content than observed if the komatiitic basalts were derived from a garnet-enriched source (Sproule et al., 2002). Arndt et al. (1997b) produced a degree of HREE depletion similar to that observed in the Abitibi greenstone belt TDKB at ~15% dynamic melting.

After allowance for the effects of contamination, all the komatiites in the Abitibi greenstone belt appear to have been derived from a similar source with $[La/Sm]_{MN}$ ~0.3, $[Nb/Th]_{MN}$ ~2.2, and $[Th/Sm]_{MN}$ ~0.1.

Coupled $[Th/Nb]_{MN} < 1$ and $[La/Sm]_{MN} > 1$, as observed in some continental flood basalts (CFB) and OIB derived from enriched portions of the mantle (e.g., Barling and Goldstein, 1990; Meijer et al., 1990; Carlson, 1991), have not been observed in komatiites in the Abitibi greenstone belt. The origin of the enriched components in Phanerozoic mafic-ultramafic magmas is not clear, however, they are proposed by many workers to be associated with subducted slab components in the mantle, even the lower mantle, which have been returned to the lithosphere by plume magmatism (Barling and Goldstein, 1990; Meijer et al., 1990; Carlson, 1991). The absence of such enriched components in Archean komatiite source regions may indicate that slab-derived enriched components had not yet reached the Archean core-mantle boundary (Campbell, 2000; McCulloch and Bennett, 2000).

3.8.2 Petrogenesis of Ferropicrites in the Abitibi Greenstone Belt

Ferropicrites are high-Fe, high-Mg magmas with 14-20 wt.% FeO and 12-18 wt.% MgO (Hanski, 1992). The ferropicrites in the Abitibi greenstone belt exhibit Al_2O_3/TiO_2 = 4 to 9 and $[Gd/Yb]_{MN} > 1.2$ (Stone et al., 1987), suggesting retention of garnet in the source (Hanski, 1992). However, they exhibit lower Al_2O_3/TiO_2 and higher $[Gd/Yb]_{MN}$ than ADK–TEK, suggesting even more garnet fractionation than most ADK. When examined on a mantle-normalized trace element variation diagram (Figure 3.16), Abitibi ferropicrites are enriched in all HILE (U, Th, Nb, Ta, LREE) relative to MILE (MREE, Ti, HREE, Y), are depleted in Al relative to other MILE, and are enriched in Fe relative to other slightly compatible elements. Thus, the petrogenesis of Abitibi ferropicrites must involve a process that results in depletion in Al and enrichment of highly incompatible lithophile elements and Fe.

The geochemical characteristics of ferropicrites in the Abitibi greenstone belt and other Archean ferropicrites (e.g., Lake of the Enemy: Francis et al., 1999) are broadly similar to Proterozoic to Phanerozoic ferropicrites in Pechenga (Hanski, 1992), Madagascar (Storey et al., 1997), and Parana-Etendeka (Gibson et al., 2000) and trend toward Phanerozoic OIB (Sun, 1980; Barling and Goldstein, 1990) in terms of their trace element compositions. However, the amount of incompatible element enrichment in Abitibi ferropicrites is not as extreme as in OIB. The $[Th/Sm]_{MN}$ and $[Nb/Th]_{MN}$ ratios of Abitibi ferropicrites overlap those of some Abitibi komatiites (Figure 3.17), suggesting that they were derived from a mantle source that was more enriched than the komatiite source, but much less enriched than an OIB source.

The extremely high Fe contents of ferropicrites require high pressure melting of a fertile peridotite source or an Fe-rich peridotite source (e.g., Hanski, 1992; Francis et al., 1999; Gibson et al., 2000). Francis et al. (1999) and Gibson et al. (2000) suggest that Fe enrichment cannot be easily explained by different degrees or pressures of partial melting, but suggest that it requires an Fe-rich source. Francis et al. (1999) point out that the residues resulting from low-moderate degree partial melting of most peridotite sources are enriched in Fe compared to the original source and that many Archean mantle-derived melts are more Fe-rich than their Phanerozoic counterparts. Remelting such a refractory source is apparently difficult in the cooler modern mantle, requiring the addition of water (yielding boninites) or CO_2 (yielding kimberlites), but may have been achievable in the hotter Archean mantle by the addition of any subduction-related enriched component. Thus, it may be possible to produce Archean and Proterozoic ferropicrites by remelting the refractory mantle residue formed by production of normal tholeiitic basalts via addition of an enriched subduction-related component. In any case, if remelting of the refractory Fe-rich source that produced the associated tholeiitic basalts produced the ferropicrites in the Abitibi greenstone belt, it suggests that at least four compositionally distinct sources (ADK–TEK, AUK, TEK, and ferropicrite) have been involved in producing the complete spectrum of ultramafic magmatism present in the Abitibi greenstone belt.

3.8.3 Crustal Contamination

The upper continental crust is enriched in HILE (Cs, U, Th, Nb, Ta, LREE) relative to MILE (MREE, Y, Zr, Hf) and highly compatible elements (Cr, Mg, Ni, Co). However, the upper continental crust is less enriched in Ta and Nb relative to Th and less enriched in Ti relative to MREE, which has been attributed to retention of these elements in oxide phase(s) of eclogite during crustal recycling (e.g., Weaver and Tarney, 1981; Rudnick et al., 1998). As a consequence, komatiites that are contaminated by upper continental crust (or sediments derived from upper continental crust) are normally enriched in HILE relative to MILE (e.g., $[Th/Sm]_{MN} > 1$ and $[La/Sm]_{MN} > 1$) with pronounced negative Ta and Nb anomalies (e.g., $[Th/Nb]_{MN} < 1$) (see discussion by Lesher et al., 2001).

Because of the significant differences in their compositions and modes of formation, the mantle and crustal components of contaminated magmas may also exhibit significant differences in radiogenic and/or stable isotopic compositions. For example, if the crust is substantially older than the magma, it will also be enriched in radiogenic Sr, Os, and Pb and unradiogenic Nd (Faure, 1986; Dickin, 1995). If the contaminant is a sedimentary rock, it may contain significant amounts of anomalously heavy or light S or C, depending on the environment of formation (Ohmoto, 1986). Finally, sulfide-bearing sedimentary rocks normally have significantly higher S/Se ratios than rocks containing only magmatic sulfides (Stanton, 1972). Although crustal contamination should therefore be evident from changes in the geochemical and isotopic compositions of the magmas, the magnitude of these changes will vary with the relative masses of the different components in the system (Lesher and Burnham, 1999, 2001).

Komatiites in the Kidd-Munro and Tisdale assemblages exhibit [Nb/Th]$_{MN}$ and [Th/Sm]$_{MN}$ ratios ranging between those characteristic of depleted upper mantle and those consistent with contamination by up to ~15% upper Archean continental crust (Figure 3.17). ADK–TEK and ADK are both enriched and depleted in LREE. However, relatively low [Nb/Th]$_{MN}$ and [Th/Sm]$_{MN}$ ratios in the Pacaud and Stoughton-Roquemaure assemblages, which are much closer to the ratios inferred for depleted mantle, suggest that these lavas were not contaminated.

The trends of komatiites in the Abitibi greenstone belt define AFC mixing trajectories between the most primitive komatiite magma (depleted mantle) and upper crust (Taylor and McLennan, 1995) or crustally-derived sediment (e.g., North American Shale Composite (NASC)) on [Th/Sm]$_{MN}$ vs. [Th/Nb]$_{MN}$ diagrams (Figure 3.17). This suggests that the variation in [La/Sm]$_{MN}$ ratios is most likely attributable to crustal contamination rather than source enrichment. There is no correlation between [Gd/Yb]$_{MN}$ and [La/Sm]$_{MN}$ (Figure 3.17), suggesting that crustal contamination did not significantly affect HREE ratios and that [Gd/Yb]$_{MN}$ ratios may be used as an indicator of the composition of the mantle source region.

Importantly, crustal contamination in the Kidd-Munro and Tisdale assemblages is very localized, occurring on the scale of individual lava flows (Shaw Dome: Larson, 1996; Munro and Dundonald Townships: Davis, 1997). Therefore, crustal contamination is not a source characteristic and is probably not a consequence of contamination during ascent through the upper crust, both of which would result in contamination over a wider stratigraphic interval (Huppert and Sparks, 1985b; Lesher and Arndt, 1995; Lesher et al., 2001). This suggests that contamination most likely occurred during emplacement.

The restricted range of [Nb/Th]$_{MN}$ and [Th/Sm]$_{MN}$ ratios and apparent absence of contamination in the Pacaud and Stoughton-Roquemaure assemblages relative to the Kidd-Munro and Tisdale assemblages (Figure 3.17) suggests a compositional difference in the nature of the lithosphere through which the older and younger komatiites ascended and/or a difference in magma discharge rates (see discussion by Huppert and Sparks, 1985b; Lesher and Arndt, 1995; Lesher et al., 2001). For example, the Kidd-Munro and Tisdale assemblages may have erupted through sialic crust, whereas the older Pacaud and Stoughton-Roquemaure assemblages may have erupted through more simatic crust. Underlying sialic crust is likely for the Kidd-Munro and Tisdale assemblages, as intercalated intermediate-felsic volcanic rocks contain inherited zircons ranging in age up to 2725 Ma (Ayer et al., 1998, 1999, 2002). Ayer et al. (2002) report that felsic volcanic rocks intercalated with komatiites in the Stoughton-Roquemaure assemblage also contain inherited zircons, suggesting that the absence of geochemical evidence for crustal contamination in those rocks are more likely to be related to low magma discharge rates (which would result in low degrees of contamination) or very high magma discharge rates (which would result in contamination, but also high degrees of dilution: see discussion by Lesher et al., 2001). Low discharge rates are consistent with the dominance of pillowed komatiites (Houlé et al., 2001) in the Stoughton-Roquemaure assemblage. In contrast, komatiites in the Kidd-Munro and Tisdale assemblages include greater proportions of lava channel facies representing higher discharge rates and greater capacities to thermomechanically erode footwall rocks (Huppert and Sparks, 1985a; Williams et al., 1998, 1999). The komatiites in the Pacaud assemblage are also dominated by pillowed komatiites (Houlé et al., 2001), consistent with low discharge rates and eruption through sialic or simatic crust. The sialic crust underlying the Stoughton-Roquemaure, Kidd-Munro and Tisdale assemblages must have been juvenile based on primitive Nd isotopic compositions (Jensen, 1985; Jackson and Sutcliffe, 1990; Dostal and Mueller, 1997; Lesher et al., 1997).

Komatiitic basalts in the Tisdale and Kidd-Munro assemblages are more commonly contaminated than komatiitic basalts in the Pacaud and Stoughton-Roquemaure assemblages (Figure 3.21). This

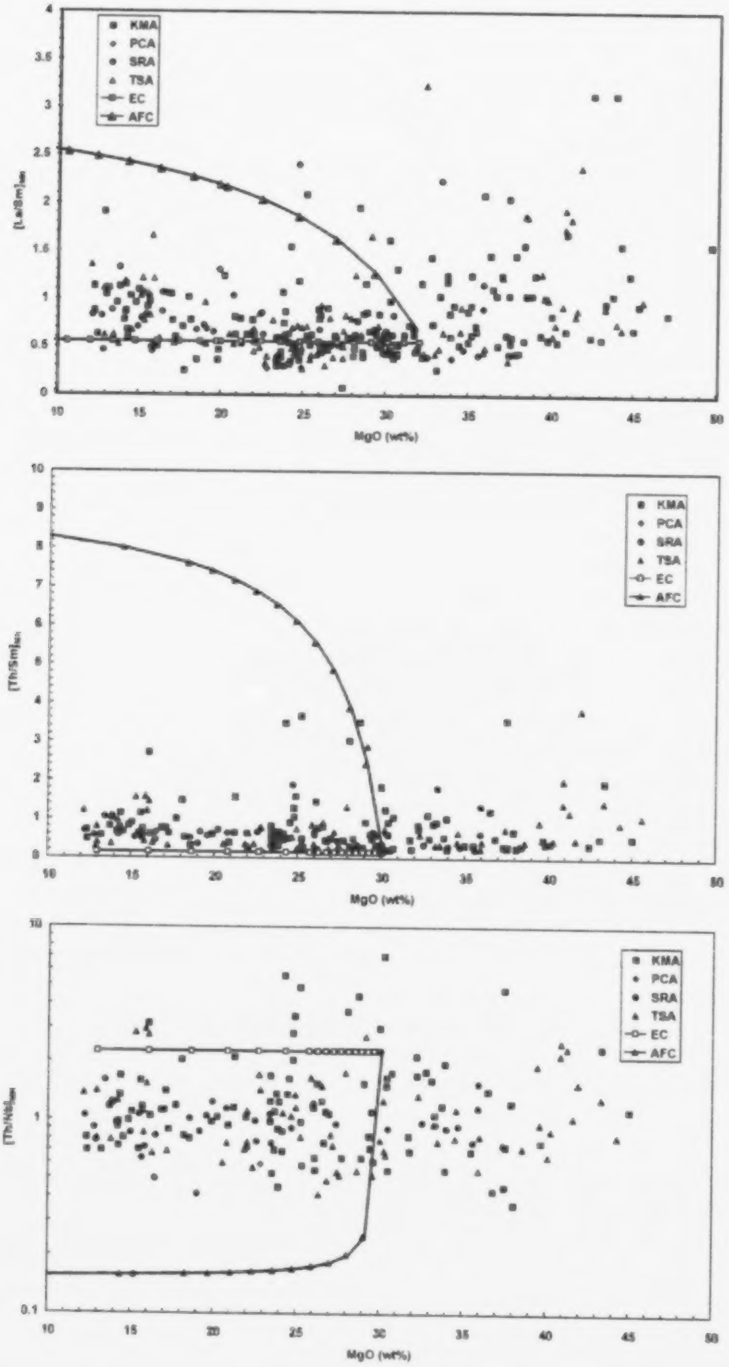

Figure 3.21. $[La/Sm]_{MN}$, $[Th/Nb]_{MN}$, and $[Th/Sm]_{MN}$ vs. MgO (wt.% volatile-free) for komatiitic rocks in the Abitibi greenstone belt. A two-component mixing trend path representing contamination of a komatiite (MgO ~30 wt.%, Th = 0.04 ppm, Nb = 1.0 ppm, Sm = 2.5 ppm, and La = 0.2 ppm) with a pelite (Th = 18.8 ppm, Nb = 13.8 ppm, Sm = 4 ppm, and La = 33 ppm) in 10% increments is shown for comparison.

suggests that some of the komatiitic basalts in the Tisdale and Kidd-Munro assemblages could have been derived from parental komatiitic magmas via assimilation fractional crystallization (AFC) processes, as suggested for komatiitic basalts in the Kambalda area of Western Australia (Arndt and Jenner, 1986; Lesher and Arndt, 1995). The greater apparent variability in the degree of contamination of komatiitic basalts in the Abitibi greenstone belt may be a consequence of the crust in the Abitibi region being more heterogeneous than the crust in the Norseman-Wiluna belt and/or there being a more limited geochemical database for komatiitic basalts in the Norseman-Wiluna belt.

However, not all of the komatiitic basalts in the Abitibi greenstone belt lie on AFC trends derived from the komatiites (Figure 3.21), suggesting that some of the komatiitic basalts were derived by lower degrees of partial melting, possibly from the cooler periphery of the plume head (e.g., Tomlinson et al., 1999a).

4 Spatial Variations in the Geochemistry of Komatiites in the Abitibi Greenstone Belt

Spatial variations in komatiite geochemistry provide constraints on the architecture of komatiite flow fields, the nature of the underlying lithosphere, and information about komatiite source regions. Each of the sampled regions or trends in the Abitibi greenstone belt is discussed below and can be located on Figure 1.2.

4.1 SHINING TREE AREA

Komatiites are present in the Pacaud, Kidd-Munro, and Tisdale assemblages in the Shining Tree area (Oliver et al., 1999, 2000). Their ages are constrained by U-Pb zircon geochronology (Ayer et al., 2002).

The komatiitic rocks in the Pacaud assemblage (Churchill Twp.) form two horizons; the lower horizon has a true thickness <100 m and the upper horizon has a true thickness of ~400 m. The komatiites in each unit are intercalated with basalts. The komatiites in the lower horizon are sheared at the base, contain abundant fuchsite, and grade upwards into talc-bearing pillowed komatiitic basalts. The pillows are typically <30 cm in diameter. The komatiites in the upper horizon are composed of massive aphyric, pillowed, and ortho- to mesocumulate rocks that formed from komatiitic basalt and rare low-Mg and high-Mg komatiite magmas. Alkali abundances are typically low (<1 wt.% total alkalis), but variable, with three samples containing 2-3 wt.% total alkalis. All of the komatiites in the Pacaud assemblage are Shining Tree-type TDKB, which thus far appear to be unique to the Abitibi greenstone belt. They are depleted in LREE relative to MREE ($[La/Sm]_{MN}$ = 0.6-0.8) and are depleted in MREE relative to HREE ($[Gd/Yb]_{MN}$ = 0.5-0.7).

The komatiites in the Kidd-Munro assemblage (Natal Township) are either massive ortho-, meso-, and adcumulate flows or differentiated flows with spinifex-textured upper parts (A zones: Pyke et al. 1973) and ortho- to mesocumulate lower parts (B zones) that formed from komatiitic basalt magmas. Those in the Moon Lake area of Natal Township have $Al_2O_3/TiO_2 < 15$ (excluding one adcumulate sample with low TiO_2) and are enriched in MREE relative to HREE ($[Gd/Yb]_{MN} \sim 1.2$), typical of ADK-TEK and derivation from a garnet-bearing residue. They are enriched in LREE relative to MREE ($[La/Sm]_{MN} \sim 2$) and depleted in Nb relative to Th ($[Th/Nb]_{MN} \sim 4$), suggesting crustal contamination. Those in the Arthur Lake area of Natal Township are AUK, and are depleted in LREE relative to MREE ($[La/Sm]_{MN}$ = 0.5) without any HREE fractionation ($[Gd/Yb]_{MN}$ = 0.95). This suggests derivation by high degree partial melting of a depleted source at relatively shallow depths with no contamination by crust.

There is only a single massive komatiitic basalt sample from the Tisdale assemblage in the Shining Tree area (Kelvin Township). It is enriched in LREE ($[La/Sm]_{MN} = 1.2$), depleted in Nb relative to Th ($[Th/Nb]_{MN} = 3$), and undepleted in HREE relative to MREE ($[Gd/Yb]_{MN} = 1.02$). This suggests that the sample is an AUK that has been contaminated by crust.

Thus, all komatiite types (TDK, ADK–TEK, AUK) are observed within a single geographical district in the Shining Tree area. The >30 Ma time break between the TDKB in the Pacaud assemblage and the AUK and ADK–TEK komatiites in the Kidd-Munro and Tisdale assemblages is marked by strikingly dissimilar komatiite geochemistry. The Pacaud assemblage komatiites were derived from a garnet-enriched source (Sproule et al., 2002) or via dynamic melting (Arndt et al., 1997b; Sproule et al., 2002). The komatiites in the Kidd-Munro assemblage were derived by a combination of moderate-degree partial melting at 8-9 GPa followed by garnet fractionation (ADK) and higher degree partial melting at 2-7 GPa (AUK) (Sproule et al., 2002). The komatiites in the Tisdale assemblage were generated by consistently higher degree partial melting at 2-7 GPa (AUK) (Sproule et al., 2002). Crustal contamination is only a feature of the younger komatiites in the Kidd-Munro and Tisdale assemblages, suggesting differences related to magma flow rate and/or the nature of the lithosphere through which the komatiites were erupted (see Section 3.8.3). The uncontaminated komatiites in the Pacaud assemblage may have been erupted into an oceanic setting. In contrast, the komatiites in the Kidd-Munro and Tisdale assemblages passed through continental crust. There are no Nd isotopic data for Kidd-Munro and Tisdale komatiites in the Shining Tree area, but based on other regions of the Abitibi greenstone belt the lithosphere was likely juvenile.

4.2 ROUND LAKE DOME

Komatiitic and ferropicritic rocks in the Round Lake Dome area occur in the Stoughton-Roquemaure and Tisdale assemblages (Jensen, 1981, 1985; Stone et al., 1987, 1993, 1996, 1997; Xie et al., 1993; Xie, 1996).

The ferropicritic rocks in the Stoughton-Roquemaure assemblage are all part of the Boston Creek sill[8], which has a strike length greater than 30 km, the longest of any known unit in the Abitibi greenstone belt. The northern part of the sill is differentiated, containing (from base to top): olivine cumulate rocks, clinopyroxene cumulate rocks, gabbro, acicular pyroxene spinifex, and random olivine spinifex zones (Stone et al., 1996). The rocks in the Boston Creek sill are ferropicrites (Stone et al., 1987, 1993, 1996, 1997), which have a distinctive geochemistry, with high FeO (14-18 wt.%), high TiO_2 (0.8 to 1.2 wt.%), and intermediate MgO (12 to 20 wt.%) (Hanski, 1992). They are mildly enriched in LREE ($[La/Sm]_{MN} \sim 0.9\text{-}1.1$), but are not depleted in Nb relative to other elements of similar incompatibility (e.g., Th). They appear to be derived from a slightly enriched source, like modern OIB, but do not exhibit as extreme a degree of source enrichment. The HREE are strongly fractionated ($[Gd/Yb]_{MN} \sim 1.5\text{-}2.4$), consistent with retention of garnet in the residue. Jensen (1985) identified potential komatiitic basalts in the overlying and underlying parts of the Stoughton-Roquemaure assemblage with major element compositions similar to ADK–TEK and AUK, but no trace element data are available to verify their petrogenetic affinity.

The komatiites in the Tisdale assemblage have ages covering the entire known range of the Tisdale assemblage (Ayer et al., 2002). They include massive aphyric, pillowed, and differentiated flows with spinifex-textured upper parts (A zones) and lesser orthocumulate to mesocumulate lower parts (B zones), which formed from komatiitic basalt, low-Mg komatiite, and high-Mg komatiite magmas. Adcumulate komatiites are not present. AUK are the most abundant komatiite type in the Tisdale assemblage, with minor occurrences of ADK–TEK. AUK may be depleted or enriched in LREE and are typified by unfractionated chondrite-normalized REE patterns. ADK–TEK are depleted in HREE ($[Gd/Yb]_{MN}$ = 1.1 – 1.4). The predominance of AUK relative to ADK–TEK suggests that most of the magmas were derived by partial melting at 2-7 GPa with only a minor contribution from magmas generated at 8-9 GPa (Sproule et al., 2002). The majority of the rocks are depleted in LREE ($[La/Sm]_{MN} < 1$) and do not exhibit a depletion in Nb relative to Th, suggesting that they have not assimilated crustal materials (Sproule et al., 2002). Komatiitic basalts are also undepleted in Nb relative to Th that suggests they formed by lower degrees of partial melting and not by AFC processes. A single komatiite sample in the Otto Lake area (sample 23214) is enriched in LREE ($[La/Sm]_{MN}$ = 1.2) and depleted in Nb relative to Th ($[Nb/Th]_{MN}$ = 0.7), indicating crustal contamination.

---

[8] This unit has been previously interpreted as a flow (Stone et al., 1987, 1993, 1995, 1996), but has recently been reinterpreted as a sill on the basis of xenoliths of overlying rocks in the upper chilled margin and apophyses of the upper chilled margin in overlying rocks (Houlé et al., 2001). This does not change any of the geochemical interpretations, but has important volcanological implications.

4.3 KIDD-MUNRO TREND

The Kidd-Munro trend forms the majority of the Kidd-Munro assemblage and forms an approximately 80 km-long, northwest-trending belt north of the Porcupine-Destor Fault Zone (PDFZ) in the north-central part of the Ontario portion of the Abitibi greenstone belt (Figure 1.2). This part of the Kidd-Munro assemblage contains the greatest volume of komatiitic rocks of any of the regions in the Abitibi greenstone belt (up to 12 vol.%: C.T. Barrie, pers. comm., 1999). The komatiites in the Kidd-Munro trend are among the best studied in the Abitibi greenstone belt (e.g., Arndt, 1975, 1976, 1986; Arndt and Nesbitt, 1982; Barnes et al., 1983, 1985; Johnstone, 1987; Lahaye and Arndt, 1996; Davis, 1997; Barrie, 1999; Ontario Geological Survey, 2001). This project focuses on the geochemistry of the komatiitic rocks. The reader is referred to Davis (1997) and Barrie et al. (1999) for recent summaries of their volcanology and stratigraphy.

The komatiitic rocks in the Kidd-Munro assemblage typically occur within a wide package of intercalated komatiitic and tholeiitic basalts. The mafic and ultramafic rocks typically overlie calc-alkalic rhyolitic, dacitic, and/or andesitic rocks of the Kidd-Munro assemblage. Davis (1997, 1999) identified a virtually identical stratigraphy for the Kidd-Munro assemblage over >100 km from Munro Township through Dundonald Township to Kidd Township. Barrie (1999) confirmed the correlation between Kidd Creek and Dundonald Townships using U-Pb zircon geochronology. Barrie (1999) also proposed that the komatiites in the eastern parts of the trend (Walker to Munro Townships) were younger than in the western part of the trend (e.g., Kidd Creek Mine).

In this study the Kidd-Munro trend has been subdivided into three sections: the *eastern* Kidd-Munro section (Garrison, Michaud, Munro, McCool, and Warden Townships), the *central* Kidd-Munro section (Clergue, Dundonald, and Stock Townships), and the *western* Kidd-Munro section (SW Little, SW Tully, Prosser, Wark, Carnegie, and Kidd Townships). The volume of komatiitic rocks appears to vary across the trend with thicker sections in Munro, Dundonald, and Kidd-Tully Townships, which have been interpreted as volcanic centres or topographic lows in which the komatiites were ponded (Davis, 1997, 1999).

4.3.1 Kidd-Munro Trend - Eastern Section

Komatiitic flows are particularly abundant in the eastern section of the Kidd-Munro trend. Komatiites occur within a thick package of basalts, overlying intermediate to felsic calc-alkalic rocks of the Kidd-Munro assemblage, similar to other sections of the Kidd-Munro trend. A wide variety of komatiite facies are present in this section, ranging from thin (~1 m) to thick (~40 m) differentiated flows with spinifex-textured upper parts (A zones), and ortho-, meso-, and adcumulate lower parts (B zones), pillowed komatiites, and aphanitic to ortho-, meso-, and rare adcumulate massive flows. The komatiites formed from magmas ranging in composition from komatiitic basalt through low-Mg komatiite to high-Mg komatiite.

Geochemical features of the komatiitic rocks in the eastern section include:

1) AUK are the most abundant komatiite type and occur throughout this section of the trend (e.g., Pyke Hill).
2) ADK–TEK komatiitic basalts are rare and occur in close proximity to Fred's and Theo's Flows in Munro Township in the northern section and in Garrison Township in the eastern part of the section.
3) TDKB are absent (all samples with elevated Al_2O_3/TiO_2 ratios are cumulate rocks with low TiO_2).
4) Ferropicrites are uncommon, but are locally present (e.g., feeder dykes to host rocks at the Potter Mine) and may be distinguished from ADK–TEK based on FeO > 14 wt.% and $[TiO_2] > 0.02$.
5) A single AUK in McCool Township (see sample 23346) is depleted in Nb relative to Th (e.g., $[Nb/Th]_{MN} < 1$) and enriched in LREE ($[La/Sm]_{MN} > 1$), suggesting that the magma was contaminated by crust.

4.3.2 Kidd-Munro Trend - Central Section

Komatiitic rocks do not appear to be as abundant in the central section as in the eastern and western sections of the Kidd-Munro trend. They overlie intermediate to felsic calc-alkalic volcanic sequences (Davis, 1997, 1999; Barrie, 1999), a relationship similar to the lower komatiitic horizon in the eastern section (e.g., host sequence to Dee's Flow: Davis, 1997, 1999). These komatiites formed from magmas ranging in composition from komatiitic basalt to low-Mg and high-Mg komatiite and form a variety of textures including aphanitic, spinifex, and cumulate komatiites ranging from orthocumulate and mesocumulate rocks to rare adcumulate rocks; pillowed komatiites are rare (Davis, 1997, 1999).

Geochemical features of the komatiitic rocks the central section include:

1) AUK is the dominant komatiite type and ranges from depleted to undepleted to mildly enriched in LREE, typically with unfractionated HREE.
2) ADK–TEK are rare, but are typically mildly depleted in LREE and depleted in HREE relative to MREE ($[Gd/Yb]_{MN}$ from 1.0 to 1.6).
3) TDKB are not present.
4) Ferropicrites are rare, but have been tentatively identified in diamond drill core in Dundonald Township by Falconbridge that has not been reanalyzed.
5) Some komatiites are enriched in LREE, enriched in HFSE relative to MREE, and depleted in Nb relative to Th, suggesting localized crustal contamination.
6) Unlike the majority of komatiitic rocks in the Abitibi greenstone belt (Figure 3.8), chromite saturation appears to have been suppressed, producing a continuation of the Cr-undersaturated trend of the komatiites in Dundonald Township to less than 15% MgO. This suppression may be attributed to a lower fO_2 in the magma resulting from interaction with graphitic sediments in the Dundonald South area (Davis, 1997, 1999).

4.3.3 Kidd-Munro Trend - Western Section

The amount of komatiitic rocks in the western section is less than in the eastern section, but greater than in the central section. Many of the rocks in this section are altered (carbonatization, chloritization, and silicification), particularly near the giant Kidd Creek volcanogenic massive Cu-Zn-Ag sulfide deposit. The aphanitic to orthocumulate komatiites that dominate this portion of the Kidd-Munro trend originated from magmas that had low- and high-Mg komatiite compositions.

Geochemical features of the komatiitic rocks in the western section include:

1) AUK are dominant, and are depleted to enriched in LREE ($[La/Sm]_{MN} = 1.6\text{-}0.5$) with unfractionated HREE ($[Gd/Yb]_{MN} = 0.9\text{-}1.2$);
2) ADK–TEK are not present;
3) TDKB are not present;
4) Ferropicrites are not present;
5) Some of the AUK ($n = 11$) in Little and Kidd Townships are enriched in LREE, enriched in HFSE compared to MREE (e.g., $1.1 < [Th/Sm]_{MN} < 3.5$), and are depleted in Nb relative to Th, suggesting that they were locally contaminated by crust.

4.4 REAUME-MCCART TREND

This section refers to rocks of the Stoughton-Roquemaure assemblage in Reaume, Hanna, Mann, Duff, and McCart Townships (Barrie, 1999; see Figure 1.2). Outcrop in this area is sporadic, only limited geochronology has been conducted, and there is no definitive evidence for komatiitic flows (Barrie, 1999). Samples from this region include massive cumulate rocks collected in this study and intersected in INCO, Falconbridge, or Noranda diamond drill core. Barrie (1999) noted an absence of spinifex-textured rocks or flow-top breccias in the INCO, Falconbridge, and Noranda diamond drill logs, suggesting that these komatiites are intrusive in origin. The rocks have compositions ranging from komatiitic basalt to low- and high-Mg komatiite, and range in texture from orthocumulate to adcumulate.

Geochemical data for cumulate rocks indicate that the komatiites in this region are dominated by AUK with unfractionated HREE relative to MREE ($[Gd/Yb]_{MN} = 1.0$). When samples with low TiO_2 are excluded from the database only rare ADK–TEK, with fractionated HREE relative to MREE ($[Gd/Yb]_{MN} = 1.2$), are present. Trace element data are only available for two samples, one ADK–TEK (sample 6315) and one AUK (sample 6484), the former of which is enriched in HILE relative to MILE ($[Th/Sm]_{MN} = 1.4$) and depleted in Nb relative to Th ($[Nb/Th]_{MN} = 0.6$).

4.5 LAKE ABITIBI

The komatiitic rocks in the Lake Abitibi region are part of the Stoughton-Roquemaure assemblage. They are interlayered within a thick (up to 10 km?) sequence of basalts and only represent <1% by volume of the total assemblage. The komatiitic rocks formed from magmas with compositions ranging from komatiitic basalt to rarer low-Mg komatiite. The komatiites exhibit a range of textures and structures including massive aphanitic, spinifex-textured, pillowed, rare orthocumulate, and extremely rare meso- to adcumulate komatiites (Jensen, 1976; 1985; Dostal and Mueller, 1997; Barrie, 1999).

Komatiites and komatiitic basalts in the Lake Abitibi region are dominated by ADK–TEK with lesser AUK. The komatiites display a continuum of Al_2O_3/TiO_2 from ADK–TEK to AUK, suggesting mixing of magmas from a range of depths. Three samples having Al_2O_3/TiO_2 greater than 25 are explained by minor Al or Ti mobility and do not appear to represent a separate magma type. All, except one sample, are depleted in LREE ($[La/Sm]_{MN} = 0.34 – 1.33$). The komatiites and komatiitic basalts have unfractionated to fractionated HREE abundances ($[Gd/Yb]_{MN}$ from 1.0-1.8). The degree of HREE fractionation correlates with Al_2O_3/TiO_2, suggesting variable degrees of retention of garnet in the source.

One sample, a low-Mg komatiite basalt in Agate Township, is enriched in HILE and depleted in Nb relative to Th, suggesting that the sample is contaminated by a crustal component. This suggests that sialic crust may be present beneath the Stoughton-Roquemaure assemblage, but this possibility requires more investigation.

4.6 SHAW DOME

Larson (1996), Baird (1999), and Stone and Stone (2000) have studied the komatiites and komatiitic basalts in the Shaw Dome area (see Figure 1.2). The komatiitic rocks occur in the stratigraphically lower part of the Tisdale assemblage. Felsic volcanic rocks underlying the komatiites have been dated at 2708 Ma (Barrie and Corfu, 1999) and contain 2725 Ma (Deloro assemblage age) inherited zircons. The komatiites in the Shaw Dome have been subdivided into two units, a 500 to 1000 m thick lower komatiitic horizon (LKH) and a 500-3000 m thick upper komatiitic horizon (UKH) (Jensen, 1985). The LKH is composed of differentiated intrusive dunites, wehrlites, and gabbros. The UKH is composed of poorly undifferentiated komatiites and komatiitic basalts, local high-Mg komatiites, komatiitic peridotites, and komatiitic dunites, and less common differentiated spinifex-textured flows (Larson, 1996; Baird, 1999; Stone and Stone, 2000). The komatiites in the UKH have been interpreted to range from distal (spinifex-textured komatiite and komatiitic basalt) to proximal (undifferentiated komatiite) facies (Larson, 1996; Baird, 1999; Stone and Stone, 2000). The Redstone, Langmuir, and Hart Ni-Cu-(PGE) deposits are hosted by the thicker, more olivine-enriched, less differentiated parts of the UKH (Green and Naldrett, 1981). The komatiites formed from magmas with compositions ranging from komatiitic basalt to low-Mg and high-Mg komatiite.

The LKH is composed almost entirely of AUK. Five samples have Al_2O_3/TiO_2 ratios consistent with ADK–TEK or TDK, but are meso- to adcumulate komatiites with low TiO_2 contents (i.e., close to detection limits) and have trace element characteristics (i.e., $[Gd/Yb]_{MN} \sim 1$) more similar to AUK. Many komatiites in the LKH are enriched in HILE and depleted in Nb relative to Th, suggesting that they are contaminated by a crustal component.

All samples from the UKH are AUK. Highly localized crustal contamination (as indicated by enrichment in HILE and depletion in Nb relative to Th) has been detected in the cumulate rocks in the lower part of the sequence, but not in the spinifex-textured rocks in the upper part of the sequence. This suggests that the contamination of the komatiitic magmas in the UKH and LKH occurred during emplacement, rather than during passage through the crust, and that the lava in channels was selectively contaminated (see Lesher et al., 2001).

4.7 BARTLETT DOME

The komatiitic rocks in the Bartlett Dome (see Figure 1.2) are part of the Tisdale assemblage and appear to be stratigraphically equivalent to the UKH in the Shaw Dome. They range in texture and composition from spinifex-textured rocks to ortho-, meso-, and adcumulate rocks. They have MgO and Cr contents suggesting that they formed from magmas that ranged in composition from high-Mg and low-Mg komatiite to komatiitic basalt. Typically, the komatiitic sequences are composed of thick sequences of minor thick massive ad- to mesocumulate flows overlain by more abundant thin differentiated flows (<2 m in thickness) with upper platy and random spinifex-textured upper parts (A zones) and lower meso- to orthocumulate lower parts (B zones).

These komatiites are dominantly AUK and have unfractionated chondrite-normalized HREE abundances. The majority of the komatiites are depleted in LREE ($[La/Sm]_{MN} < 1$), except for a small number of komatiites in Powell and Geike Townships that are enriched in LREE, likely a result of contamination processes.

Tabatabai (1978) identified ADK–TEK in the Bartlett Dome and AUK and ADK–TEK in the Goose Lake and Donut formations in McArthur Township. However, subsequent workers (Barnes, 1985; Lahaye et al., 1995; Pyke, 1978; Xie, 1996; this study) have only reported AUK. Lahaye et al. (1995) showed that many of the komatiites in this area are extensively carbonatized, which may alter their Al and Ti abundances (Lahaye et al., 1995). Thus, it seems likely that the komatiites in this region are variably altered AUK.

4.8 HALLIDAY DOME

The komatiitic rocks in the Halliday Dome (Figure 1.2) occur in the lower part of the Tisdale assemblage and appear to be stratigraphically equivalent to those in the Bartlett and Shaw Domes, although komatiitic rocks are less abundant in the Halliday Dome than the Bartlett and Shaw Domes. The komatiites in Bannockburn Township (on the western margin of the Halliday Dome) are considered to be stratigraphically higher, still part of the Tisdale assemblage. The komatiites in the Halliday Dome exhibit a similar textural and compositional variations as those in the Bartlett Dome.

All of the komatiites in the Halliday Dome are AUK, except for a single sample with $Al_2O_3/TiO_2 = 28$. CO_2 and LOI data are not available, so it cannot be determined whether this sample would pass alteration filtering. There is, however, a population of komatiites in Burrows Township with $Al_2O_3/TiO_2 \sim 15$ and fractionated MREE-HREE abundances ($[Gd/Yb]_{MN} = 1.2$). These geochemical characteristics range between ADK–TEK and AUK. These komatiites may represent a mixed magma that sampled two sources or one magma that experienced a minor degree of garnet fractionation in the source. Trace element data are only available for five komatiites in the Halliday dome: all are depleted in HILE and undepleted in Nb relative to Th. These data suggest that the komatiites in the Halliday Dome have not experienced significant amounts of crustal contamination.

The komatiites in Bannockburn Township, along the western margin of the Halliday dome, are poorly exposed, so the samples for this study were taken from diamond drill cores provided by Outokumpu Mines Ltd. The komatiite flows are 20-40 m thick, composed of primarily olivine- to pyroxene-bearing, ortho- to mesocumulate rocks, some containing disseminated sulfides, and are extensively serpentinized. Flow-top breccias and rare spinifex-textured rocks suggest an extrusive origin. These komatiites are all AUK, similar to those in the Halliday Dome.

4.9 SWAYZE BELT

The Swayze belt (Figure 1.2) contains komatiitic basalts and komatiites (Cattell and Arndt, 1987; Ayer, 1995; Heather and Shore, 1999) located in the Tisdale (south of the Porcupine-Destor Fault Zone) and Kidd-Munro (north of the Ridout High Strain Zone) assemblages. Some spinifex-textured komatiites (in both the Tisdale and Kidd-Munro assemblages) contain up to 23 wt.% MgO, suggesting relatively high MgO contents for the parental magmas.

The komatiites in the Kidd-Munro assemblage in the Swayze belt formed from magmas ranging in composition from komatiitic basalt to low- and high-Mg komatiite. The komatiites include low-Cr olivine adcumulate rocks (dunites), low-Cr olivine orthocumulate rocks (peridotites), and olivine spinifex-textured rocks. The komatiitic basalts range from aphanitic to differentiated flows with pyroxene spinifex-textured upper zones and pyroxene-bearing cumulate rocks. An extremely rare pyroclastic komatiite located in the central-northern part of Keith Township in the Kidd-Munro assemblage contains relict fiamme (flattened pumice).

The komatiites in the Kidd-Munro assemblage in the Swayze belt are dominated by AUK (n = 45) with minor ADK–TEK (n = 8), similar to Kidd-Munro komatiites in other sections of the Abitibi greenstone belt. All ADK–TEK samples, excluding pyroxene cumulate rocks, have low TiO_2 (less than 0.2 wt.%), which can hamper discrimination of komatiite types on the basis Al_2O_3/TiO_2 ratios alone. However, the low Al_2O_3/TiO_2 ratios are accompanied by MREE-HREE fractionation ($[Gd/Yb]_{MN} = 1.2$), consistent with other ADK–TEK.

The AUK in the Swayze belt range from komatiitic basalts to komatiites and include ortho- to adcumulate rocks and spinifex-textured rocks. Cumulate rocks appear to be more common in the Kidd-Munro assemblage than in the Tisdale assemblage in the Swayze belt and the komatiites in the Kidd-Munro assemblage appear to be more primitive than those in the Tisdale assemblage. They are typically depleted in LREE without any MREE-HREE fractionation ($[Gd/Yb]_{MN} \sim 1$). A small number of samples are enriched in HILE and depleted in Nb relative to Th, consistent with crustal contamination.

The komatiites in the Tisdale assemblage in the Swayze belt are stratigraphically equivalent to the youngest sections of the Tisdale assemblage east of the Round Lake Dome. They formed from magmas ranging in composition from komatiitic basalt to low- and high-Mg komatiite. Textures include abundant platy olivine spinifex- and acicular pyroxene spinifex-textured rocks, pyroxene cumulate rocks, and lesser olivine ad- to orthocumulate rocks. Overall, the komatiitic rocks in the Tisdale assemblage in the Swayze belt are less MgO-rich than those in the Kidd-Munro assemblage.

The dominant komatiite type in the Tisdale assemblage in the Swayze belt is AUK (n = 48) with lesser ADK–TEK (n = 7). All of the ADK–TEK occur in Newton Township (Cattell and Arndt, 1987) in an intensely carbonatized zone (Heather and Shore, 1999). As discussed earlier, carbonatization may affect Al_2O_3/TiO_2 and result in fractionation of MREE to HREE (Lahaye and Arndt, 1996). Our sampling of the same ADK–TEK sequences along strike, well away from the carbonatized zone, yielded only AUK. Thus, the komatiites in the Tisdale assemblage of the Swayze belt appear to be predominately AUK. Komatiitic basalts in Dore and Swayze Townships are enriched in HILE and are depleted in Nb relative to Th, suggesting that the magmas were contaminated by continental crust. Detrital zircons in a Tisdale assemblage felsic tuff in Heenan Township range from 2730-2740 Ma in age (Ayer et al., 2002), which are 20-40 Ma older than the 2710-2703 Ma age of the Tisdale assemblage, suggesting the presence of underlying sialic crust in this area.

4.10 PORCUPINE DESTOR FAULT ZONE - TIMMINS REGION

This region includes Tisdale assemblage komatiites in Whitney, Murphy, and Tisdale Townships (Jackson and Fyon, 1991; Xie et al., 1993), in proximity to the Porcupine Destor Fault Zone (Ayer et al., 1999).

Komatiitic rocks in this region have typically experienced higher degrees of carbonatization and chloritization than other sectors of the Abitibi greenstone belt, which is reflected in 9 of 28 samples failing the alteration filtering tests. Komatiitic rocks in this region include massive komatiites with ortho- to mesocumulate textures, differentiated flows with well-developed spinifex-textured upper parts (A zones) and ortho- to mesocumulate lower parts (B zones), and rare pillowed komatiitic basalts. The komatiites formed from magmas ranging in composition from rare komatiitic basalt to low-Mg komatiite.

Komatiites from this area include both AUK (n = 13) and ADK–TEK (n = 5). However, there are some inconsistencies between Al_2O_3/TiO_2 ratios and degree of HREE fractionation. All samples have variably fractionated HREE ($[Gd/Yb]_{MN} > 1.12$), even samples with Al_2O_3/TiO_2 ratios typical of AUK. These inconsistencies are likely a function of the strong carbonate alteration in this region, as most samples from this study contain carbonate veins, even those with relatively low volatile contents (i.e., samples that pass the loss-on-ignition [LOI] alteration filter). Although HFSE (e.g., Th, Nb, Ta, Ti, Zr, Hf, HREE) are normally much less mobile than LILE (e.g., Cs, Rb, Na, K, Ba, Sr, Ca), petrogenetic interpretations based on the geochemistry of these samples must be viewed with caution.

One sample from Whitney Township appears to be crustally contaminated, based on coupled enrichment in HILE relative to MILE and depletion in Nb relative to Th.

4.11 PORCUPINE DESTOR FAULT ZONE - EASTERN MATHESON TO QUEBEC BORDER

Komatiites in Hislop, Guibord, Holloway, Michaud, Garrison, Harker, and Marriot Townships occur in close proximity to the Porcupine Destor Fault Zone (PDFZ). By definition, the komatiites north of the PDFZ are part of the Kidd-Munro assemblage in the Kidd-Munro Trend, whereas those south of the PDFZ are part of the Tisdale assemblage. However, discrimination between the Tisdale and Kidd-Munro assemblages in this area is difficult because of structural complexity. The komatiites in the northern sequence within Harker and Holloway Townships are tentatively assigned to the Kidd-Munro assemblage.

Outcrop in this region is typically poor. The komatiites contain rare hyaloclastites, massive ortho- to meso-textured cumulates, and differentiated flows with well-developed spinifex-textured upper parts (A zones) and thin ortho- to mesocumulate cumulate lower parts (B zones). The komatiites in the Kidd-Munro assemblage formed from magmas with low- and high-Mg komatiite compositions. Komatiites in the Tisdale assemblage formed from magmas ranging in composition from low-Mg komatiite to komatiitic basalt.

Many of the komatiite samples in this region (16 of 57), including samples from both the Tisdale and Kidd-Munro assemblages, fail the alteration filtering tests for carbonatization and chloritization, similar to other komatiitic rocks near the PDFZ. Although HFSE (e.g., Th, Nb, Ta, Ti, Zr, Hf, HREE) are normally less mobile than LILE (e.g., Cs, Rb, Na, K, Ba, Sr, Ca), petrogenetic interpretations based on the geochemistry of these rocks must again be viewed with caution.

The komatiitic rocks of the Tisdale assemblage are predominantly AUK with minor ADK–TEK. The ADK–TEK occur in the eastern extension (eastern part of Garrison Township), where the assignment to the Tisdale or Kidd-Munro is the most tenuous. The komatiites in the southernmost horizon in Michaud and Guibord Townships are all AUK. All komatiitic rocks for which trace element data are available are not depleted in Nb relative to Th, suggesting that the magmas were not contaminated by continental crust.

After alteration filtering and removal of those samples containing less than 0.20 wt.% TiO_2, the komatiitic rocks in the Kidd-Munro assemblage are composed of predominantly AUK and lesser ADK–TEK. Three of the samples are depleted in Nb relative to Th, suggesting that they have been contaminated by continental crust.

4.12 WEST OF TIMMINS

Thornloe and Denton townships contain few komatiitic rocks, but Ayer et al. (1999) assigned them to the Kidd-Munro assemblage. They are interbedded with tholeiitic basalts and have been described as massive, foliated flows to pillowed flows. Many of the samples from these komatiites are cumulate rocks with ortho-, meso-, and adcumulate textures.

The komatiites have high MgO contents and chromite was not yet a liquidus phase, suggesting that the magmas had high Mg contents. Based on their Al_2O_3/TiO_2 ratios (15-17), all are AUK. No komatiitic basalts have been identified, suggesting that only magmas from the hottest parts of the source were extracted and erupted, that the magmas/lavas did not experience significant amounts of assimilation fractional crystallization (AFC), and/or that they are very distal lavas that because of their lower viscosities flowed further than any associated komatiitic basalts.

4.13 REGIONAL SUMMARY AND IMPLICATIONS

Table 4.1 summarizes the spatial distribution of komatiite types through the Ontario part of the Abitibi greenstone belt. AUK are the most common type in the Abitibi greenstone belt, occurring in all regions of the belt. ADK–TEK also occur in all of the subregions of the Abitibi greenstone belt, except in the Shaw Dome and western Kidd-Munro regions. However, ADK–TEK with positively fractionated MREE-HREE ($[Gd/Yb]_{MN} > 1.2$) are less common and are restricted to the Round Lake Dome, Halliday Dome, Shining Tree belt, Kidd-Munro belt, Shaw Dome, Lake Abitibi region, and Swayze belt. TDKB with negatively fractionated MREE-HREE ($[Gd/Yb]_{MN} < 0.8$) appear to only occur in the ~2.75 Ga Pacaud assemblage in the Shining Tree area. Ferropicrites are restricted to the Stoughton-Roquemaure and Kidd-Munro assemblages.

The widespread distribution of AUK and ADK–TEK throughout the Abitibi greenstone belt requires either extraction from multiple plumes or extraction of different komatiite types from a single plume at varying depths (Sproule et al., 2002). The inferred low viscosities of komatiitic magmas (Viljoen and Viljoen, 1969; Nisbet, 1982) implies that they are capable of flowing great distances (600 km or more), depending on factors such as discharge rate, slope, topography, and thermal conductivity (Huppert et al., 1984; Williams et al., 1999). Therefore, these factors do not allow distinction between one and several plumes. The scale of komatiitic volcanism in the Abitibi greenstone belt is comparable to that in other Archean greenstone belts (e.g., Norseman-Wiluna belt: Lesher et al., 1984; Lesher, 1989; Hill et al., 1995) and in Phanerozoic flood basalt provinces (e.g., Siberian Traps, Deccan Traps, Columbia River Basalts: see Hill, 1993), and is consistent with the large sizes calculated for mantle plumes (Campbell and Griffiths, 1990). The time interval over which individual komatiite sequences have erupted in the Abitibi greenstone belt (<5-10 m.y.) is within the duration of modern plume-related *volcanism* (1-10 m.y.: Coffin and Eldholm 1994). The time interval over which all four assemblages erupted in the Abitibi greenstone belt (~45 m.y.) is within the duration of Archean and Phanerozoic plume-related *magmatism* (10-50 m.y.: Isley and Abbott 1999). The duration of plume magmatism can be extended through continued ascent of less viscous material into a plume long after the head has flattened against the base of the lithosphere, subsequently protracting magmatism (Campbell, 2000). Thus, it not possible to distinguish between models involving multiple plumes or models involving single plumes.

Table 4.1. Summary of lithological and geochemical features of the regions of the Abitibi greenstone belt.

Area		Assemblage	Parental magmas	Meso-Adcumulate Rocks	Magma Type(s) *	Crustal contamination
Shining Tree		PCA	kb, lk, hk	no	TDKB	No
		KMA	kb	yes	AUK, ADK–TEK	Yes
		TSA	kb	no	AUK	Yes
Round Lake Dome		SRA	FP	no	FP, ADK–TEK?, AUK?	No
		TSA	kb, lk, hk	yes	AUK, ADK–TEK	Yes
Kidd-Munro	East	KMA	kb, lk, hk	yes	AUK, FP, ADK–TEK	Yes
	Central	KMA	kb, lk, hk	yes	AUK, FP, ADK	Yes
	West	KMA	lk, hk,	yes	AUK	Yes
Reaume-McCart		SRA	kb, lk, hk	yes?	AUK, ADK–TEK	Yes
Lake Abitibi		SRA	kb, lk	no?	ADK, AUK, FP	Yes
Shaw Dome		TSA	kb, lk, hk	yes	AUK	Yes
Bartlett Dome		TSA	kb, lk, hk	yes	AUK, ADK–TEK??	Yes
Halliday Dome		TSA	kb, lk, hk	yes	AUK, ADK–TEK	No
Swayze Belt		KMA	kb, lk, hk	yes	AUK, ADK-TK, FP?	Yes
		TSA	kb, lk, hk	yes	AUK, ADK?	Yes
PDFZ	Timmins	TSA	kb, lk	no	AUK, ADK–TEK	Yes
	Matheson	KMA	kb, lk	yes	AUK, ADK–TEK	Yes
	Québec	TSA	kb, lk	no	AUK, ADK–TEK	No
West Timmins		KMA	lk, hk	yes	AUK	No

PCA = Pacaud assemblage; SRA = Stoughton-Roquemaure assemblage; KMA = Kidd-Munro assemblage; TSA = Tisdale assemblage; kb = komatiitic basalt; lk = low-Mg komatiite; hk = high-Mg komatiite; kd = komatiitic dunite; AUK = Al-undepleted komatiite; TEK = Ti-enriched komatiites; ADK = Al-depleted komatiite; TDKB = Ti-depleted komatiite; FP = ferropicrite.

Excluding the older 2750-2735 Pacaud assemblage (Ayer et al., 2002), there is a general trend of decreasing age of komatiite magmatism from northeast to southwest across the Abitibi greenstone belt: the 2725-2720 Ma Stoughton-Roquemaure komatiitic magmatism occurs in the eastern part of the belt, the 2718-2710 Ma Kidd-Munro komatiitic magmatism occurs in the central part, and the 2710-2703 Ma Tisdale komatiitic magmatism occurs predominantly in the western part. Although komatiite magmas may flow for extremely long distances, this trend is consistent with a broadly westward migration of the eruptive centre(s) during plume or lithospheric movement.

Another important feature is the close spatial proximity of ADK–TEK and AUK, which were possibly extracted from the same plume but which are interpreted to have been extracted at different depths (Herzberg and O'Hara, 1998; Sproule et al., 2002). This relationship is widespread in the Abitibi greenstone belt (i.e., everywhere except the Bartlett Dome, Porcupine-Destor Fault Zone, and Reaume-McCart Trend, which appear to contain only AUK). The alternations in geochemical type occur on a flow-by-flow scale (e.g., Newton Township in the Swayze belt: Cattell and Arndt, 1987) and on a regional scale (e.g., Kidd-Munro Trend). In some cases, apparent variations in geochemical type may be attributed to carbonatization (Lahaye and Arndt, 1996; Heather, 1998), however, the majority of the variations appear to be real. The intercalation of magmas derived from deep and shallow mantle sources can be explained by variations in: 1) mantle source heterogeneity, 2) depth of melt extraction, 3) residual phase chemistry and/or degree of melting, 4) multiple melt extraction and enrichment processes, and/or

5) rate of magma ascent (see Sproule et al., 2002). The lithosphere beneath the Abitibi greenstone belt has been interpreted to have been thinner and hotter than other greenstone belts, given the greater volume of arc-related rocks (Dostal and Mueller, 1997). This hotter lithosphere would also have had a lower density compared to, for example, the Yilgarn craton, Western Australia, where the komatiites are underlain by a much thicker sequence of older granitic crust and tholeiitic basalts (Gresham and Loftus-Hills, 1981; Chauvel et al., 1985; Myers and Swager, 1997). A lower density lithosphere may have reduced the ascent velocity of komatiite magmas and may have promoted the development of crustal magma chambers and/or the emplacement of sills (see discussion by Lesher and Keays, 2002). Slower ascent of magmas through the lithosphere may have also permitted magmas derived from different parts of the plume to intermingle during ascent. Thus, the lower density of the Abitibi lithosphere may have facilitated the development of a wider range of magma products (AUK, ADK–TEK, and TDKB) from one or more plumes than would have been possible in greenstone belts underlain by denser lithosphere.

5 Spatial and Temporal Variations in the Geochemistry of Komatiites in the Abitibi Greenstone Belt

5.1 RESULTS

The geochemical features of the komatiitic magmas that are inferred to have produced the komatiitic rocks in each assemblage of the Abitibi greenstone belt are summarized in Table 5.1. Representative whole rock geochemical analyses from each of the komatiite types from each assemblage are listed in Table 5.2.

Table 5.1. Summary of geochemical characteristics of stratigraphically assigned komatiites in the Abitibi greenstone belt.

	Pacaud Assemblage	**Stoughton-Roquemaure Assemblage**	**Kidd-Munro Assemblage**	**Tisdale Assemblage**
n	13	141	1108	444
Al_2O_3/TiO_2	TDKB	AUK ~ ADK–TEK > TDKB?	AUK > ADK–TEK	AUK >> ADK–TEK
$[Gd/Yb]_{MN}$	~0.6	>1	0.7-1.7, ave. 1.0	0.4-1.5, ave. 1.1
$[La/Sm]_{MN}$	<1	<1	>1<	>1<
$[Th/Nb]_{MN}$	<1	<1	>1<	>1<

Table 5.2 (facing page). Representative analyses of komatiites and komatiitic basalts from the Abitibi greenstone belt. Major elements are recalculated to 100% on an anhydrous basis.

Source notations: * this study; ** Dostal and Mueller (1997); † from OGS archives and reanalysed in this study; ‡ from B. Berger (OGS, unpublished data).

Abbreviations: KB = komatiitic basalt; KP = komatiite peridotite; PK = peridotitic basalt; RS = random spinifex; OC = orthocumulate; Low-Mg K = low-Mg komatiite; High-Mg K = high-Mg komatiite; KM = Kidd-Munro assemblage; SR = Stoughton-Roquemaure assemblage; TDKB = Ti-depleted komatiitic basalt; TEK = Ti-enriched komatiite; ADK = Al-depleted komatiite; AUK = Al-undepleted komatiite.

Tag#	27982	27974	23271	Roq95-10	Roq95-7	23252	23341	22179	23214
Source	*	*	*	**	**	*	*	*	*
Area	Shining Tree	Shining Tree	Shining Tree	Lake Abitibi	Lake Abitibi	Kidd-Munro	Shining Tree	Shaw Dome	Round Lake Dome
Strat. unit	Pacaud	Pacaud	Pacaud	SR	SR	KM	KM	Tisdale	Tisdale
UTM N	5270125	5270350	5270360	5374000	5374000	5377720	5281266	5360755	5324512
UTM E	481584.5	481450	481480	618000	618000	567920	493967	496500	568075
Rock Type	KB	KB	KP	KB	KB	PK	PK	KB	KB
Texture	RS	RS	OC	Aphanitic	Aphanitic	OC	OC	RS	RS
SiO_2	51.11	47.97	47.81	49.40	50.58	49.55	41.76	54.30	52.08
TiO_2	0.45	0.29	0.25	0.87	0.84	0.54	0.19	0.65	0.62
Al_2O_3	14.75	9.31	8.43	9.71	9.18	3.17	1.50	13.27	11.94
Cr_2O_3	0.07	0.46	0.51	0.26	0.23	0.42	0.57	0.13	0.21
FeO	10.03	10.36	10.39	11.99	11.80	7.81	14.70	9.43	10.94
MnO	0.25	0.19	0.17	0.20	0.19	0.13	0.29	0.16	0.18
MgO	12.91	23.50	24.75	16.47	16.49	37.49	39.70	12.17	12.95
NiO	0.01	0.09	0.44	0.08	0.07	0.26	0.26	0.02	0.05
CaO	7.56	7.76	7.26	9.79	9.03	0.62	1.03	6.45	8.42
Na_2O	1.42	0.01	0.00	1.17	1.51	0.00	0.00	3.32	2.61
K_2O	1.39	0.02	0.00	0.02	0.01	0.00	0.00	0.01	0.01
P_2O_5	0.04	0.03	0.00	0.05	0.06	0.01	0.00	0.09	n/a
Al_2O_3/TiO_2	33	32	34	11	11	6	8	20	19
Type	TDK	TDK	TDK	ADK-TEK	ADK-TEK	ADK-TEK	ADK-TEK	AUK	AUK
LOI	3.29	5.88	5.99	4.00	1.90	12.50	11.35	2.87	2.69
Co	56.9	57.4	103			157	159	54.6	73.0
Cr	513	3170	3430	1758	1560	3210	4000	884	1390
Cu	24.8	57.4	5.32			5.62	5.65	103	68.9
Ni	95.2	691	945	650	567	2220	2040	193	357
V	229	167	147	218	214	44.9	63.3	220	227
Zn	59	116	84	9.5	95	42.7	110	69.0	72.0
Cs	1.33	0.07	0.28			1.02	0.03	0.01	0.14
Rb	53.4	0.12	0.48	4.00	2.00	20.6	0.38	0.38	0.33
Th	0.04	0.02		0.18	0.25	2.43	0.04	0.49	0.27
U	0.01	0.01				0.62		0.14	0.07
Nb	0.42	0.26	0.21	3.00	2.50	4.23	0.43	2.94	1.58
La	0.70	0.27	0.27	2.80	3.32	11.4	0.67	4.44	3.03
Ce	1.91	0.96	0.85	7.94	8.56	24.1	1.78	10.4	7.10
Pr	0.34	0.17	0.16	1.20	1.25	3.21	0.27	1.63	1.10
Sr	65.0	3.22	5.9	50.0	48.0	199	3.30	54.8	66.3
Nd	2.17	1.07	0.97	6.32	6.19	14.0	1.47	7.29	5.22
Sm	0.94	0.47	0.43	2.02	1.95	3.48	0.41	2.05	1.70
Zr	22.6	12.8	11.5	53.0	52.0	80.9	8.61	58.9	41.6
Hf	0.77	0.48	0.40	1.41	1.43	2.65	0.27	2.13	1.29
Eu	0.67	0.17	0.19	0.76	0.64	1.12	0.09	0.66	0.63
Gd	1.54	0.76	0.75	2.52	2.37	3.95	0.46	3.02	2.23
Tb	0.31	0.14	0.14	0.41	0.37			0.58	0.41
Dy	2.26	1.19	1.08	2.50	2.48	4.33	0.51	3.80	2.60
Y	15.5	8.15	7.75	12.0	12.0	26.0	2.88	22.9	17.1
Ho	0.56	0.26	0.27	0.50	0.47	0.95	0.10	0.86	0.59
Er	1.65	0.86	0.86	1.37	1.36	2.76	0.28	2.44	1.77
Tm	0.27	0.11	0.13	0.22	0.20			0.37	0.27
Yb	1.80	0.93	0.97	1.25	1.11	2.61	0.27	2.31	1.79
Lu	0.29	0.15	0.17	0.20	0.20	0.44	0.04	0.41	0.26
Sc								36.3	37.9
$[La/Sm]_{MN}$	0.47	0.37	0.39	0.87	1.07	2.05	1.02	1.36	1.12
$[Th/Sm]_{MN}$	0.22	0.26		0.46	0.65	3.57	0.50	1.22	0.81
$[Nb/Th]_{MN}$	1.28	1.32		2.01	1.21	0.21	1.30	0.72	0.71
$[Gd/Yb]_{MN}$	0.7	0.7	0.6	1.6	1.7	1.23	1.38	1.1	1.0

Table 5.2 (cont'd).

Tag#	6411	27581	22180	95-354	73J0661	22196	23355	23352
Source	*	*	*	‡	†	*	*	*
Area	Halliday Dome	Shaw Dome	Shaw Dome	Kidd-Munro	Lake Abitibi	Shaw Dome	Kidd-Munro	Kidd-Munro
Strat. unit	Tisdale	Tisdale	Tisdale	KM	SR	Tisdale	KM	KM
UTM N	5292700	5351650	5360760	5396532	5389348	5357899	5382285	5382280
UTM E	473720	494538	496500	488650	595989.1	496990	559670	559680
Rock Type	KB	KB	KB	Low-Mg K	Low-Mg K	High Mg K	High-Mg K	Peridotite
Texture	RS	Pyroxenite	OC	RS	Aphanitic	Flow top	RS	OC
SiO_2	51.50	54.06	53.00	48.93	47.10	46.04	44.21	45.09
TiO_2	0.64	0.30	0.53	0.56	0.51	0.36	0.23	0.16
Al_2O_3	10.18	9.89	10.69	10.68	10.35	7.32	5.23	3.73
Cr_2O_3	0.21	0.24	0.21	n/a	0.34	0.42	0.46	0.27
FeO	12.36	6.84	9.35	11.85	11.63	10.90	13.17	8.28
MnO	0.18	0.19	0.17	0.21	0.23	0.19	0.20	0.10
MgO	15.78	15.86	15.96	17.10	19.58	27.45	31.83	39.84
NiO	0.04	0.03	0.06	8.11	1.10	0.18	0.19	0.31
CaO	7.08	10.33	7.94	2.50	8.17	6.80	4.20	2.19
Na_2O	1.97	0.61	2.01	0.05	0.86	0.22	0.20	0.00
K_2O	0.01	1.60	0.01	0.00	0.13	0.08	0.07	0.02
P_2O_5	0.05	0.05	0.06	0.00	0.00	0.04	0.03	0.00
Al_2O_3/TiO_2	16	33	20	19	20	20	23	23
Type	AUK	AUK	AUK	AUK	AUK	AUK	AUK	AUK
LOI	3.58	2.28	3.17	6.19	4.00	6.60	5.08	11.30
Co	72.6	47.1	69.2	76.8		104	106	106
Cr	1480	1670	1490	1510	2250	2960	3140	1910
Cu	32.2	5.12	69.2	57.6		34.3	46.5	5.6
Ni	333	262	484	498	8550	1430	1420	2430
V	233	124	177	221		169	144	77.9
Zn	73.7	67.6	72.3	82.2		62.1	69.7	47.4
Cs	0.34	1.14			0.04	1.52	0.51	0.23
Rb	0.68	56.9	0.23		0.54	4.98	3.81	1.09
Th	0.13	0.38	0.44	0.17	0.12		0.03	
U	0.04	0.10	0.12	0.05	0.03			
Nb	1.25	1.05	2.37	1.00	0.95	0.31	0.36	0.17
La	1.30	3.21	3.58	1.39	1.13	0.34	0.48	0.26
Ce	4.48	7.40	8.91	3.70	3.10	1.04	1.32	0.71
Pr	0.72	1.02	1.38	0.59	0.52	0.21	0.24	0.14
Sr	25.1	97.8	32.0		16.3	34.2	39.6	7.2
Nd	4.18	4.61	6.07	3.11	2.94	1.21	1.41	0.74
Sm	1.58	1.21	1.85	1.12	1.08	0.55	0.66	0.28
Zr	29.4	25.8	49.0	36.0	27.2	13.6	15.7	7.51
Hf	1.02	0.87	1.79	1.00	0.87	0.52	0.54	0.25
Eu	0.54	0.42	0.52	0.40	0.30	0.21	0.27	0.11
Gd	2.13	1.47	2.49	1.70	1.42	0.92	1.01	0.45
Tb	0.36	0.22	0.50	0.29	0.27	0.19	0.19	0.09
Dy	2.16	1.63	3.09	2.01	1.82	1.29	1.43	0.68
Y	15.0	9.91	19.7	15.0	11.0	8.90	9.58	4.27
Ho	0.50	0.33	0.72	0.44	0.42	0.31	0.34	0.16
Er	1.50	0.98	2.04	1.32	1.20	0.95	0.93	0.43
Tm	0.22	0.11	0.31	0.19	0.20	0.14	0.14	0.06
Yb	1.33	1.03	1.98	1.29	1.24	0.80	0.92	0.39
Lu	0.17	0.15	0.32	0.20	0.20	0.12	0.15	0.06
Sc	37.9		28.4	31.0		26.7	27.4	16.7
$[La/Sm]_{MN}$	0.52	1.66	1.21	0.78	0.66	0.39	0.46	0.58
$[Th/Sm]_{MN}$	0.42	1.58	1.21	0.77	0.57		0.23	
$[Nb/Th]_{MN}$	1.16	0.34	0.65	0.71	0.96		1.45	
$[Gd/Yb]_{MN}$	1.3	1.2	1.0	1.1	0.9	0.9	0.9	0.9

The komatiitic rocks in the Abitibi greenstone belt can be categorized as *non-cumulate* (aphyric and fine-grained spinifex-textured rocks) or *cumulate* (coarse-grained spinifex[9], porphyritic, crescumulate, orthocumulate, mesocumulate, or adcumulate) based on petrographic criteria and/or MgO abundances and trends on FeO and Cr vs. MgO diagrams (see Figures 3.8 and 5.1). The oldest komatiite-bearing assemblage (Pacaud: 2750-2735 Ma) contains both non-cumulate and orthocumulate rocks, the 2725-2720 Ma Stoughton-Roquemaure assemblage contains mainly non-cumulate rocks, and the 2718-2710 Ma Kidd-Munro and 2710-2703 Ma Tisdale assemblages contain a large proportion of cumulate rocks (dominated by ortho- and mesocumulate with lesser adcumulates) and a smaller proportion of non-cumulate rocks. This means that the komatiitic rocks in the Kidd-Munro and Tisdale assemblages have higher maximum MgO contents than those in the Pacaud and Stoughton-Roquemaure assemblages.

Al_2O_3/TiO_2 ratios of the komatiitic rocks (excluding ferropicrites) vary systematically between assemblages (Figure 5.2). Only TDKB ($Al_2O_3/TiO_2 > 25$) have been identified in the Pacaud assemblage. The Stoughton-Roquemaure assemblage comprises a continuum from ADK–TEK to AUK. The Kidd-Munro assemblage contains a broad, but bimodal Al_2O_3/TiO_2 population, with one minor peak at $Al_2O_3/TiO_2 \approx 10$ (ADK–TEK) and a major peak at $Al_2O_3/TiO_2 \approx 22$ (AUK). Importantly, the ADK–TEK and AUK in the Kidd-Munro assemblage overlap spatially. In contrast, the Tisdale assemblage comprises a single population of AUK.

There is a distinct correlation between Al_2O_3/TiO_2 ratios and degree of MREE-HREE fractionation (expressed by $[Gd/Yb]_{MN}$ ratios; Figure 3.20) in all komatiites. Komatiites in the Pacaud assemblage are TDKB with low Al_2O_3/TiO_2 (25-35) and negative MREE-HREE fractionation ($[Gd/Yb]_{MN} < 0.7$). Komatiites in the Stoughton-Roquemaure assemblage range from ADK–TEK to AUK with low-intermediate Al_2O_3/TiO_2 (4-25) and unfractionated to positively fractionated MREE-HREE ($[Gd/Yb]_{MN} =$ 1.0-2.4). The komatiites in the Kidd-Munro assemblage range are predominantly AUK and minor ADK–TEK with low-intermediate Al_2O_3/TiO_2 (10-25) and unfractionated to positively fractionated MREE-HREE ($[Gd/Yb]_{MN} =$ 1.0-1.4). The komatiites in the Tisdale assemblage are predominantly AUK and rare ADK–TEK with low-intermediate Al_2O_3/TiO_2 (10-25) and unfractionated to mildly positively fractionated MREE-HREE ($[Gd/Yb]_{MN} =$ 0.9-1.2).

Komatiitic rocks of the Tisdale assemblage exhibit a trend of decreasing MgO content with increasing stratigraphic height (Table 5.3) with more komatiitic basalts in the younger sequences.

Ratios of $[Nb/Th]_{MN}$ and $[Th/Sm]_{MN}$ in the Kidd-Munro and Tisdale assemblages span the complete range between those characteristic of depleted upper mantle ($[Nb/Th]_{MN} \sim 1$ and $[Th/Sm]_{MN} \sim 1$) and ratios similar to upper Archean continental crust ($[Nb/Th]_{MN} \sim 12$ and $[Th/Sm]_{MN} \sim 4.5$) (Figure 3.17), suggesting a relatively continuous range of contamination by upper continental crust up to ~10%. The relatively low $[Nb/Th]_{MN}$ and $[Th/Sm]_{MN}$ ratios in the Pacaud and Stoughton-Roquemaure assemblages, much closer to those of depleted mantle, indicates that these lavas were not significantly contaminated. Importantly, crustal contamination in the Kidd-Munro and Tisdale assemblages is very localized, occurring on the scale of individual lava flows (e.g., Shaw Dome, Dundonald Township), indicating that it occurred during emplacement, not during ascent (see discussion by Lesher and Arndt, 1995; Lesher et al., 2001). Crustal contamination in the Tisdale assemblage occurs within komatiitic rocks of all ages (Table 5.3).

---

[9] As noted by Lesher et al. (1981) and Bickle (1982), coarse-grained platy spinifex-textured rocks contain a significant component of accumulated olivine. Only aphyric and fine random spinifex-textured rocks are representative of magmatic liquids.

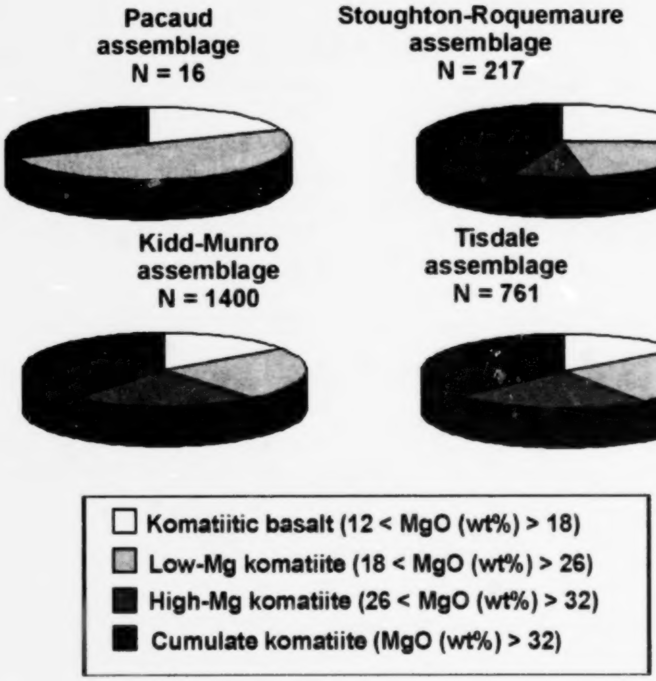

Figure 5.1. Pie charts showing lithological components of komatiite-bearing assemblages in the Abitibi greenstone belt.

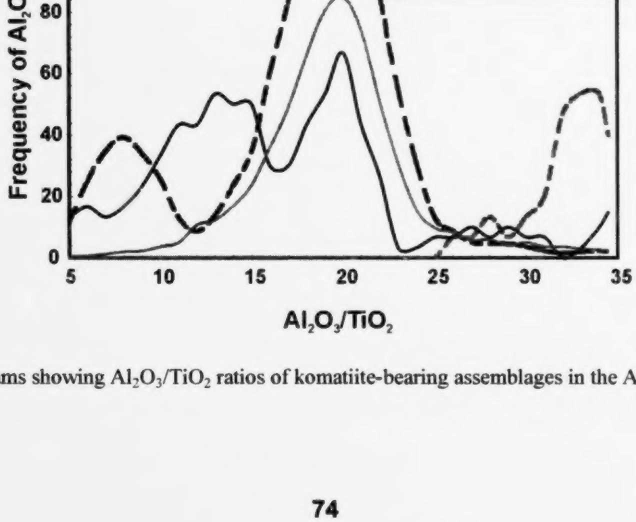

Figure 5.2. Histograms showing Al_2O_3/TiO_2 ratios of komatiite-bearing assemblages in the Abitibi greenstone belt.

Table 5.3. Subdivision of komatiites in the Tisdale assemblage.

Region	Upper or Lower Tisdale	Parental magmas	Komatiite types	Crustal contamination
Round Lake Dome	Upper	kb > lk = hk	AUK>>ADK–TEK	No
	Lower	kb ~ lk ~ hk	AUK>>ADK–TEK	Yes
Shaw Dome	Lower	kb ~ lk ~ hk	AUK	Yes
Bartlett Dome	Lower	kb < lk ~ hk	AUK	Yes
Halliday Dome	Lower	kb ~ lk ~ hk	AUK >>ADK–TEK	No
Shining Tree	?	Insufficient data	AUK	Yes
Swayze Belt	Upper	kb > lk = hk	AUK	Yes

TDKB in the Pacaud assemblage erupted between 2750 and 2735 Ma (Ayer et al., 2002). They show a restricted degree of negative MREE-HREE fractionation (i.e., $[Gd/Yb]_{MN}<1$: Figure 3.19), which may have been derived by dynamic melting of a refractory component in a plume similar to that proposed for Gorgona picrites (Arndt et al., 1997b). If so, it appears that the higher MgO components of such a plume were not erupted or sampled in the Pacaud assemblage. Alternatively, the TDKB may have been derived by melting a more garnet-rich source than other komatiite-bearing assemblages in the Abitibi greenstone belt. If so, the 2750-2735 Ma age of the Pacaud assemblage (Ayer et al., 2002) requires this to have occurred 8-23 Ma earlier than the production of ADK–TEK and AUK in the Stoughton-Roquemaure assemblage.

ADK–TEK and AUK in the Stoughton-Roquemaure assemblage erupted between 2725 and 2720 Ma (Ayer et al., 2002). AUK show unfractionated MREE-HREE abundances, suggesting derivation by high-degree partial melting of "normal" depleted garnet-harzburgite or garnet-peridotite sources leaving a dunitic residue at 3-7 GPa. The ADK-TEK show MREE-HREE fractionation (i.e., $[Gd/Yb]_{MN}>1$: Figure 3.19) and were derived by melting a source the same as the AUK, but appear to have left garnet peridotite residues at 6-9 GPa. Mixing or pooling of magmas derived from different depths may explain the continuous variation in Al_2O_3/TiO_2 ratios (Figure 5.2).

AUK and ADK-TEK in the Kidd-Munro assemblage erupted between 2718 and 2710 Ma (Ayer et al., 2002). AUK show unfractionated MREE-HREE abundances, suggesting derivation by high-degree partial melting of "normal" depleted garnet-harzburgite or garnet-peridotite sources leaving a dunitic residue at 3-7 GPa. The ADK-TEK show MREE-HREE fractionation (i.e., $[Gd/Yb]_{MN}>1$: Figure 3.19) and were derived by melting a source the same as the AUK, but appear to have left garnet peridotite residues at 6-9 GPa. Although this assemblage exhibits a distinctly bimodal distribution of Al_2O_3/TiO_2 ratios (Figures 3.19 and 5.2), the two geochemical types overlap spatially. It therefore appears that different parts of the plume(s) containing different residual assemblages were tapped almost simultaneously.

AUK in the Tisdale assemblage erupted between 2710 and 2703 Ma (Ayer et al., 2002). They do not show MREE-HREE fractionation (i.e., $[Gd/Yb]_{MN}\sim1$: Figure 3.19) suggesting that they were derived by high-degree partial melting of a "normal" depleted garnet-peridotite source leaving a dunitic residue at 3-7 GPa (Herzberg and O'Hara, 1998).

Thus, there appears to be a decreasing degree of influence by garnet in the mantle source region(s) with time.

5.2 MODELS FOR THE EVOLUTION OF PLUME-DERIVED MELTS IN THE ABITIBI GREENSTONE BELT

This section summarizes some of the models for the genesis of Abitibi komatiites in mantle plumes that have been discussed in more detail by Sproule et al. (2002).

The temporal variations in komatiite geochemistry in the Abitibi greenstone belt are consistent with successively shallower levels of melt extraction during the ~47 My duration of komatiitic magmatism. The geochemical variations imply progressively shallower depths of magma-source equilibration, possibly representing incremental extraction of magmas from a plume ascending through and out of the garnet stability field. If a single plume were involved in producing all of the komatiitic volcanism in the Abitibi greenstone belt, then the ~50 Ma duration of *volcanism* would be comparable to that proposed for Finnish komatiites (Hanski et al., 2001) and comparable to the duration of Phanerozoic plume *magmatism* (10-50 m.y.: Isley and Abbott, 1999). If three plumes were involved (Pacaud assemblage, Stoughton-Roquemaure assemblage, and Kidd-Munro and Tisdale assemblages), the duration of *volcanism* from the individual plumes would be comparable to Phanerozoic plume *volcanism* (less than 5-10 m.y.: White and McKenzie, 1989).

The decreasing depth of melt extraction producing the stratigraphic progression from ADK–TEK to AUK may be attributed to: 1) plume(s) ascent, 2) a decrease in the amount of magma derived from depth relative to that derived from shallower levels in the plume head as the plume is dragged by the overlying plate (e.g., Mueller et al., 1999), 3) interaction of plumes with descending slabs (Dalziel et al., 2001), and/or 4) stalling of the plume by an initially thick lithosphere, which thinned over time allowing the plume to rise (Figure 5.3). Models 1, 3 and 4 are applicable to either single or multiple plume models, whereas, Model 2 is only applicable to single plume models.

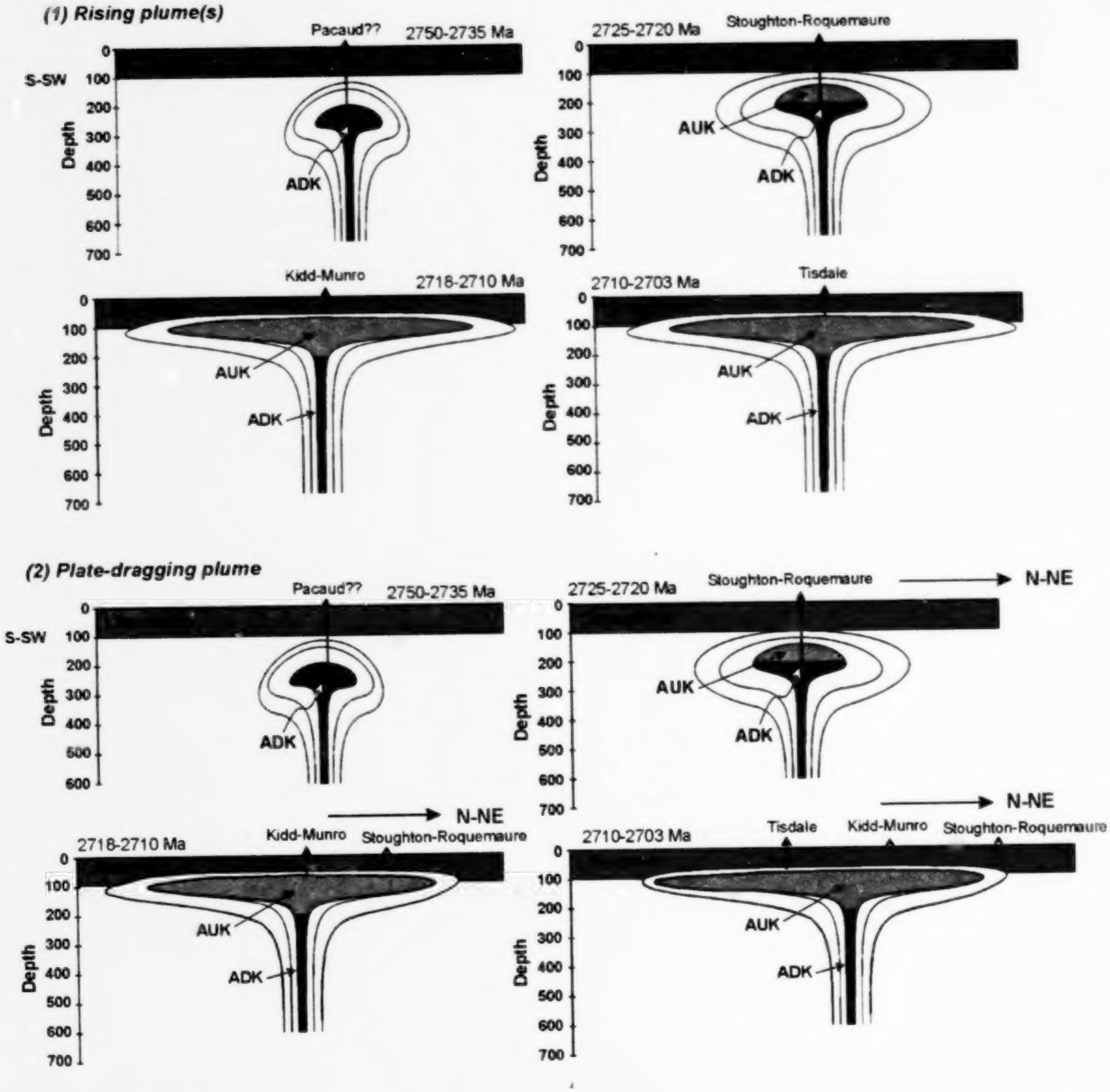
(1) Rising plume(s)
Pacaud??
2750-2735 Ma
S-SW
Depth
0
100
200
300
400
500
600
700
ADK
2725-2720 Ma
Stoughton-Roquemaure
AUK
ADK
Kidd-Munro
2718-2710 Ma
AUK
ADK
2710-2703 Ma
Tisdale
AUK
ADK
(2) Plate-dragging plume
Pacaud??
2750-2735 Ma
S-SW
ADK
2725-2720 Ma
Stoughton-Roquemaure
N-NE
AUK
ADK
N-NE
2718-2710 Ma
Kidd-Munro
Stoughton-Roquemaure
AUK
ADK
N-NE
2710-2703 Ma
Tisdale
Kidd-Munro
Stoughton-Roquemaure
AUK
ADK

Figure 5.3a. Models for temporal variations in komatiitc geochemistry in the Abitibi greenstone belt: 1) ascending plume(s) and 2) plate-dragging plume.

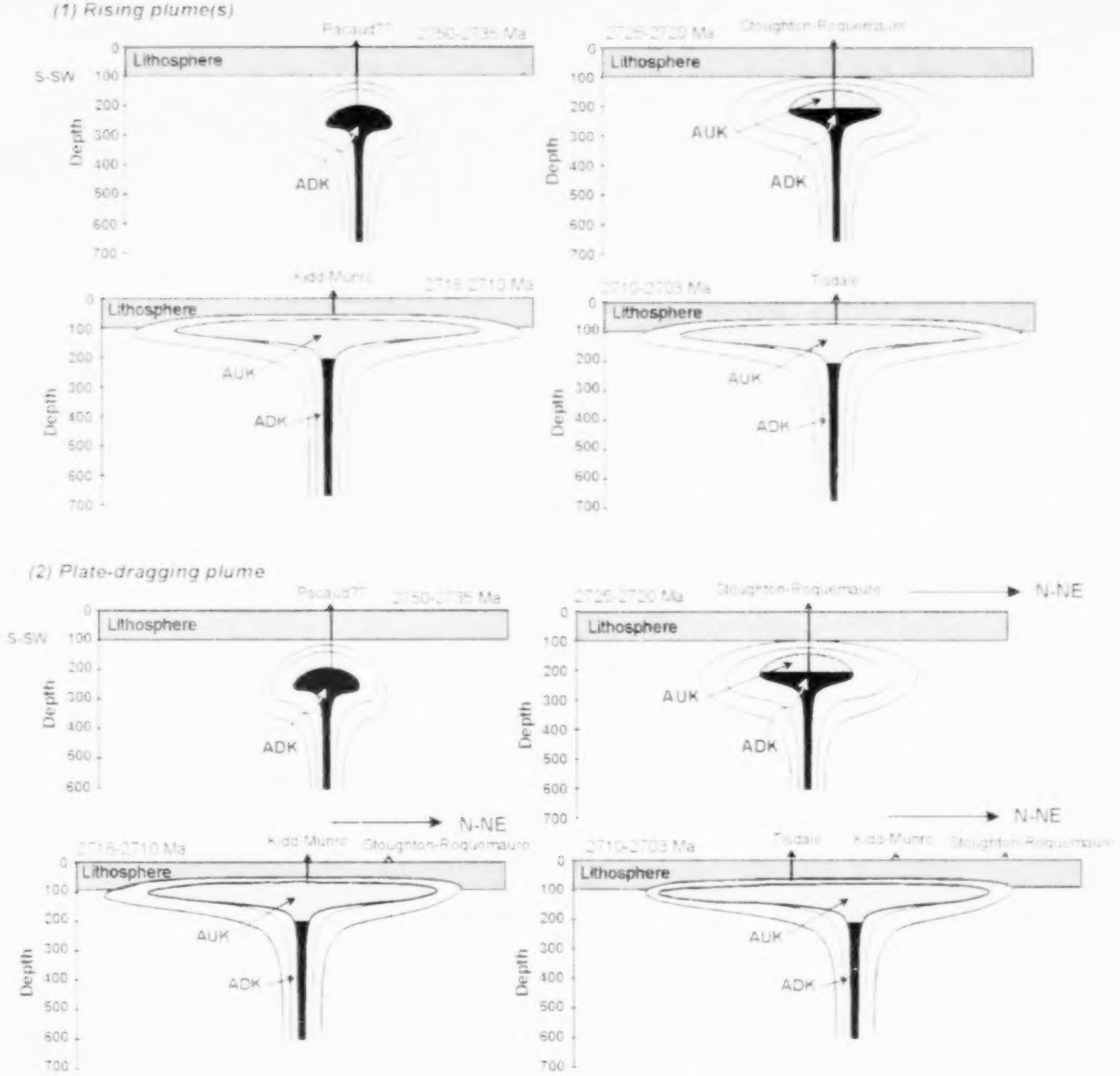
(1) Rising plume(s)
Pacaud??
2750-2735 Ma
S-SW
Lithosphere
Depth
0
100
200
300
400
500
600
700
ADK
2725-2720 Ma
Stoughton-Roquemaure
AUK
Kidd-Munro
2716-2710 Ma
2710-2703 Ma
Tisdale
(2) Plate-dragging plume
N-NE

Figure 5.3a. Models for temporal variations in komatiite geochemistry in the Abitibi greenstone belt: 1) ascending plume(s) and 2) plate-dragging plume.

(3) Stalling of plume ascent by interaction with downgoing slabs

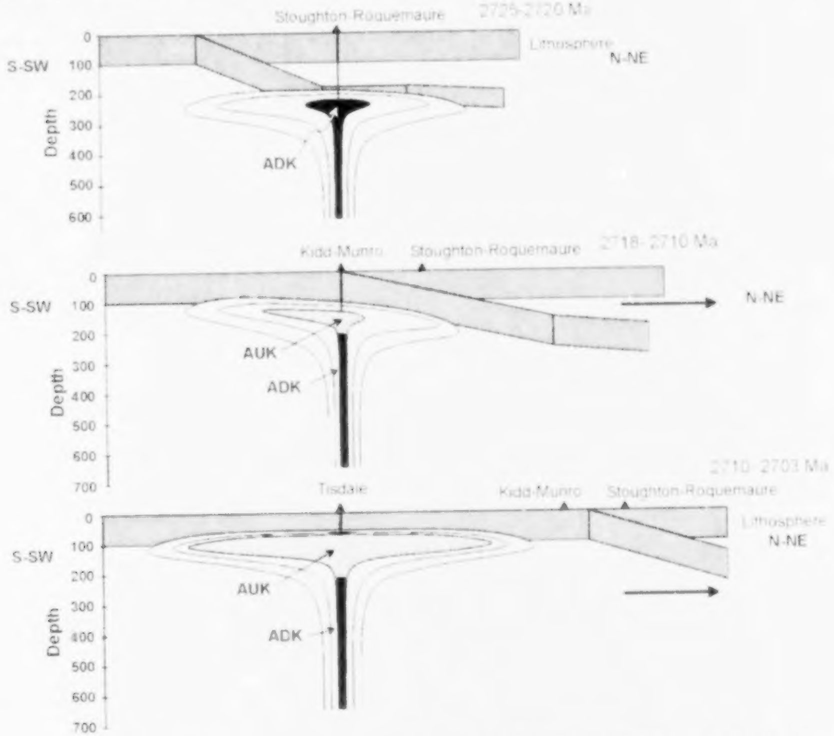
Stoughton-Roquemaure
2725-2720 Ma
Lithosphere
S-SW
N-NE
Depth
0
100
200
300
400
500
600
ADK
Kidd-Munro
Stoughton-Roquemaure
2718-2710 Ma
S-SW
N-NE
Depth
0
100
200
300
400
500
600
700
AUK
ADK
2710-2703 Ma
Tisdale
Kidd-Munro
Stoughton-Roquemaure
Lithosphere
S-SW
N-NE
Depth
0
100
200
300
400
500
600
700
AUK
ADK

(4) Stalling of plume ascent by thick lithosphere, followed by lithospheric thinning and subsequent plume ascent

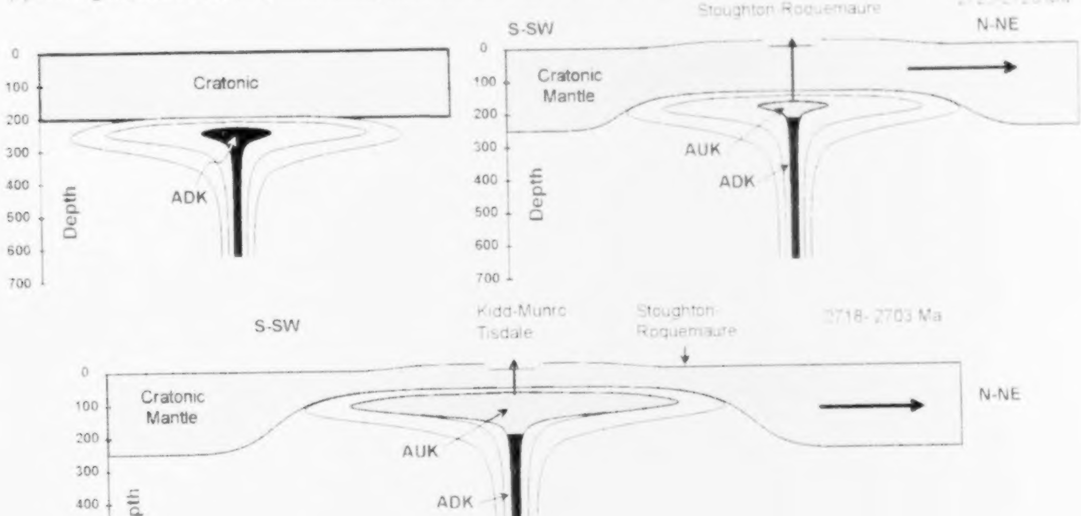
0
100
200
300
400
500
600
700
Depth
Cratonic
ADK
Stoughton-Roquemaure
2725-2720 Ma
S-SW
N-NE
0
100
200
300
400
500
600
700
Depth
Cratonic
Mantle
AUK
ADK
S-SW
Kidd-Munro
Tisdale
Stoughton-Roquemaure
2718-2703 Ma
N-NE
0
100
200
300
400
500
600
700
Depth
Cratonic
Mantle
AUK
ADK

Figure 5.3b. Models for temporal variations in komatiitic geochemistry in the Abitibi greenstone belt (cont'd.): 3) stalling of ascending plume(s) by interaction with downgoing delaminated slabs and 4) thick lithosphere stalling ascending plume(s) then lithospheric thinning, with subsequent plume ascent. The transition from ADK to AUK occurs at ~200 km depth.

(3) Stalling of plume ascent by interaction with downgoing slabs

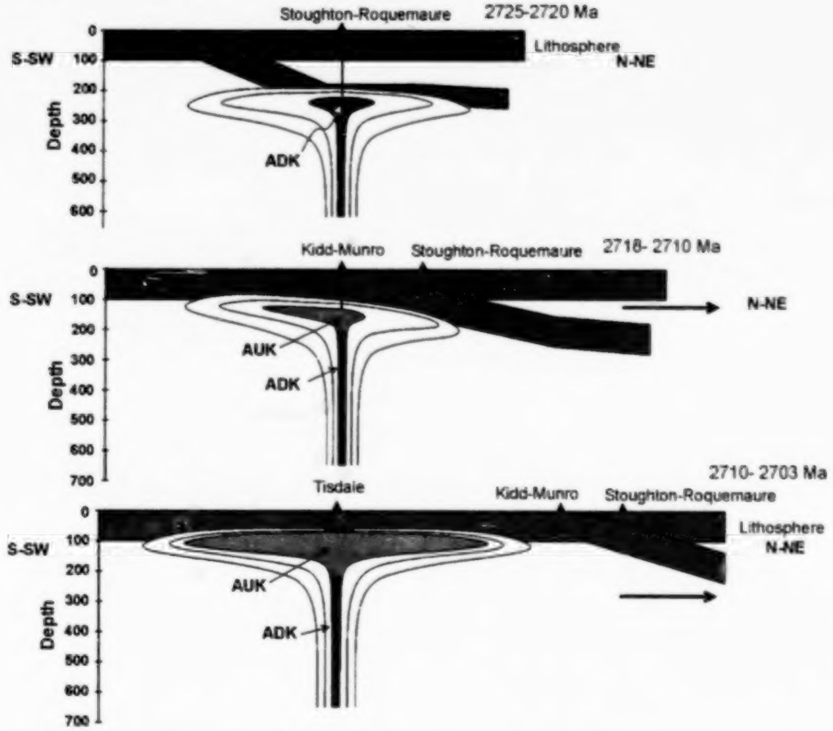
Stoughton-Roquemaure
2725-2720 Ma
Lithosphere
S-SW
N-NE
Depth
0
100
200
300
400
500
600
ADK
Kidd-Munro
Stoughton-Roquemaure
2718- 2710 Ma
S-SW
N-NE
AUK
ADK
Depth
0
100
200
300
400
500
600
700
2710- 2703 Ma
Tisdale
Kidd-Munro
Stoughton-Roquemaure
Lithosphere
N-NE
S-SW
AUK
ADK
Depth
0
100
200
300
400
500
600
700

(4) Stalling of plume ascent by thick lithosphere, followed by lithospheric thinning and subsequent plume ascent

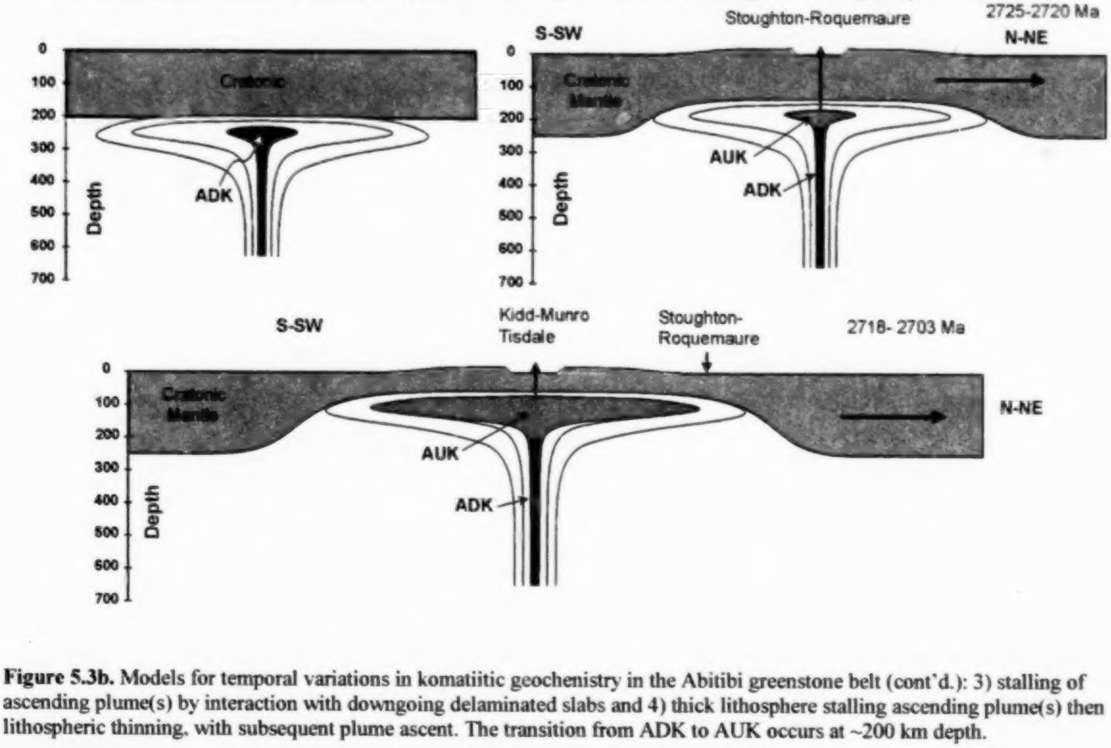
Cratonic
ADK
Depth
0
100
200
300
400
500
600
700
Stoughton-Roquemaure
2725-2720 Ma
S-SW
N-NE
Cratonic Mantle
AUK
ADK
Depth
0
100
200
300
400
500
600
700
S-SW
Kidd-Munro
Tisdale
Stoughton-Roquemaure
2718- 2703 Ma
Cratonic Mantle
N-NE
AUK
ADK
Depth
0
100
200
300
400
500
600
700

Figure 5.3b. Models for temporal variations in komatiitic geochemistry in the Abitibi greenstone belt (cont'd.): 3) stalling of ascending plume(s) by interaction with downgoing delaminated slabs and 4) thick lithosphere stalling ascending plume(s) then lithospheric thinning, with subsequent plume ascent. The transition from ADK to AUK occurs at ~200 km depth.

6 Tectonic Implications for the Abitibi Greenstone Belt

The 75 x 300 km extent of komatiites in the Abitibi greenstone belt is comparable to that observed for Phanerozoic plume-related magmas (Hill, 1993) and spatially separated komatiite sequences of similar ages are geochemically similar, suggesting derivation from similar sources and possibly a single plume.

The Abitibi greenstone belt has been previously subdivided into a series of ~50 assemblages, many of which were thought to have been allochthonous and assembled by plate-tectonic processes (e.g., Jackson and Fyon, 1991; Jackson et al., 1994). However, Ayer et al. (1998, 1999, 2002) and Heather (1999) have proposed that the Abitibi greenstone belt formed via autochthonous processes with much of the current complexity being structurally superimposed by later regional deformation. Much of the evidence for the latter interpretation is based on the rocks in the younger assemblages containing xenocrystic zircons derived from underlying older assemblages (Heather, 1999; Ayer et al., 2002).

Jackson and Fyon (1991) drew their assemblage boundaries conservatively. In areas where they observed a shear zone or a stratigraphic discontinuity, they postulated an assemblage boundary. However, the Ayer et al. (2002) model of the assemblage concept produced regional-scale units incorporating several of the old assemblages, based on continuity of stratigraphic trends and equivalence of age ranges for those larger units, (by U-Pb zircon ages) using a much larger geochronologic database. There are instances in which Jackson and Fyon (1991) assemblages contain komatiite units with similar geochemistry and volcanology. For example, the lower Tisdale assemblage, which is composed of geochemically similar komatiites of similar age, occurs within several of the assemblages previously interpreted as terranes by Jackson and Fyon (1991) (e.g., lower Tisdale in the Shaw, Halliday and Bartlett domes). Similarly, the upper Tisdale assemblage occurs in both the Halcrow-Swayze (Swayze belt) and the Larder Lake (Round Lake Dome) Jackson and Fyon (1991) terranes. Furthermore, ferropicrites occur on both sides of major structural discontinuities previously interpreted as terrane boundaries (e.g., Porcupine-Destor Fault Zone), requiring the presence of an unusual Fe-rich source beneath both assemblages. As ferropicrites are so rare, it is more likely that both regions shared the same source and formed close to each other. This provides an additional basis for the erection of larger scale assemblages. The temporal variations observed in komatiite geochemistry in the Abitibi greenstone belt are NOT, by themselves proof of autochthonous development, as komatiites with similar geochemistry may have erupted in different terranes, however, in conjunction with the more compelling inherited old zircon ages observed by Ayer et al. (2002), they provide additional evidence for an autochthonous model for the Abitibi greenstone belt.

7 Comparisons with Other Greenstone Belts

7.1 SUPERIOR PROVINCE

Komatiitic rocks in the Superior Province are found within the central Wabigoon Terrane (CWT: 2.96-2.90 Ga) and the North Caribou Terrane (NCT: 2.93 Ga) to the west, the Abitibi greenstone belt, and rare komatiites have recently been identified in greenstone belts in northern Québec, including the Lac Guyer (2.749 Ga), Hamelin (2.82 Ga), Trempe (2.86-2.2 Ga), Lac Buet-Nagvaraaluk (not dated), Gayot (2.82 Ga), and Venus (2.875 Ga) belts (Maurice and Francis, 2000; Lafrance, 2001; Stamatelopoulou-Seymour et al., 1983; Stamatelopoulou-Seymour and Francis, 1988; Madore and Larbi, 2000).

The komatiite-tholeiite sequences within the CWT and NCT are geochemically diverse (Table 7.1). They range from: 1) pyroclastic ADK in the CWT; 2) spinifex-textured AUK, komatiitic basalts, and basalts in the CWT and NCT; and 3) basalts (similar to modern oceanic plateau basalts) in the CWT and NCT. Nb-depletion and Th-enrichment in many of the komatiitic and tholeiitic rocks in the CWT and NCT provide evidence for crustal contamination (e.g., Hollings and Kerrich, 1999; Tomlinson et al., 1999a, 1999b; Tomlinson and Sasseville, 2000), suggesting a partly ensialic setting for the belts. At present, there is insufficient geochronology to accurately examine the temporal variation in komatiite chemistry through the Mesoarchean assemblages in the Western Superior Province.

Table 7.1. Summary of geochemistry of komatiites in the Superior Province.

Greenstone Belt	Age (Ga)	Magmas present	Arc-rocks present
North Caribou Terrane	2.93	AUK	Yes
Central Wabigoon	2.96- 2.90	AUK, ADK	No
Northern Quebec	2.86-2.82		
Venus	2.875	AUK	No
Trempe	2.86-2.82	AUK	No?
Lac Guyer	2.749	AUK, ADK?	No
Abitibi greenstone belt	2.75-2.701	AUK, ADK–TEK, TDKB, FP	Yes
Pacaud	2.745-7.735	TDKB	Yes
Stoughton-Roquemaure	2.725-2.725	ADK, AUK	Yes
Kidd-Munro	2718-2710	AUK, ADK–TEK	Yes
Tisdale	2708-2703	AUK	Yes

Compiled from: Maurice and Francis (2000); Tomlinson et al. (1999a, 1999b); Hollings and Kerrich (1999), I. Lafrance (personal communication, 2001); Stamatelopoulou-Seymour and Francis (1988).

The komatiites in northern Québec have not been studied in detail and little geochemical data are available. However, AUK have been identified in the Lac Trempe (Maurice and Francis, 2000) and Venus (Lafrance, 2001) belts.

Although there is a decrease in the abundance of ADK and increase in AUK globally between 3.3 and 2.7 Ga (Arndt, 1994), there is no clear relationship between the types of komatiitic magmas (e.g., AUK and/or ADK) and age of magmatism in the Superior Province as a whole. However, there appears to be an overall decrease in the abundance of ADK relative to AUK during the ~50 Ma duration of komatiitic volcanism in the Abitibi greenstone belt. The global trend suggests that the Mesoarchean (3.3-2.9 Ga) mantle may have been hotter than the Neoarchean (2.9-2.5 Ga) mantle, permitting melts to separate from their residues at greater depths in the Mesoarchean than in the Neoarchean, but the Abitibi trend indicates that such variations can also occur within individual plume events.

AUK are present throughout the Superior Province, whereas ADK are more restricted in their occurrence. However, there is no clear relationship between the presence or absence of ADK and arc tectonics in the Superior Province, which suggests there is minimal interaction between the plumes and the downgoing slabs. The plumes were probably generated at the core-mantle boundary (Campbell and

Griffiths, 1990) and would not have been influenced to any significant degree by the overlying plate tectonic setting until the final stages of plume impingement on the base of the lithosphere. Similarly, the plate tectonic regime is driven by global-scale processes and is not significantly influenced by plume-related processes in the mantle until the final stages of plume impingement on the base of the lithosphere. On the other hand, TDKB are only observed in regions where an arc is present. This suggests that their petrogenesis may be related to interaction with the downgoing slab (e.g., Dalziel et al., 2001), however, geochemical evidence of interaction with slab derived eclogitic components is not observed (e.g., positive Nb and/or Ti anomalies: Rudnick et al., 1998).

The geochronologic resolution available in the Abitibi greenstone belt is far greater than that generally available elsewhere. Thus, the secular variation we observe in the Abitibi greenstone belt may exist in other greenstone belts. However, the duration of the Abitibi greenstone belt plume may be longer than some other greenstone belts, in which case the entire magmatic progression observed in the Abitibi greenstone belt may be abbreviated elsewhere.

7.2 OTHER GREENSTONE BELTS

Komatiite types in various locations worldwide are summarized in Table 7.2, categorized by magma type and association with arc rocks. As noted above and as is evident in this compilation, the amount of ADK relative to AUK decreases with age (Arndt, 1994). Mesoarchean (3.3-2.9 Ga) greenstone belts contain primarily ADK, whereas Neoarchean (2.9-2.5 Ga) greenstone belts contain primarily AUK. The Abitibi greenstone belt, which is Neoarchean and contains predominantly AUK, fits broadly into this apparent trend, but contains more ADK than many other Neoarchean greenstone belts (e.g., Norseman-Wiluna belt in Western Australia).

Most greenstone belts contain arc-like rocks, but some do not, including the Neoarchean Norseman-Wiluna and Mesoarchean Forrestania belts in the Yilgarn Craton and the Neoarchean Belingwe Belt in the Zimbabwe craton. There is some correlation between the presence of ADK and arc rocks, but this does not apply to all greenstone belts or to the Abitibi greenstone belt. TDKB and AEK appear to be only present in greenstone belts associated with arcs. More work is required to validate these relationships and to explore their explanations.

Dalziel et al. (2001) suggested that plume-slab interaction occurred during the Gondwanide orogeny of South American, Antarctica, and southern Africa around the time of eruption of the ~180 Ma Karoo and Ferrar Large Igneous Provinces (LIPs). However, there is no direct evidence that rising plumes have interacted geochemically with downgoing slabs (Dalziel et al., 2001). Nevertheless, the compositions of mantle plumes may have been affected by introduction of subducted oceanic crustal components beneath the greenstone belts, which may have been incorporated during plume ascent. Indirectly, an arc may slow the ascent of plume, allowing for decompression over a wider range of intervals and production of a wider range of komatiite magma types (ADK and AUK) and a greater volume of lavas.

Table 7.2. Summary of geochemical affinities of Archean komatiites.

Craton/Province	Greenstone Belt/ Subprovince/Terrane	Age (Ga)	Magmas present	Arc-rocks present
Kaapvaal	Barberton	3.5-3.0	ADK, AUK, AEK	Yes
	Nonwendi	3.5-3.3	ADK	Yes
Pilbara		3.6-3.3	ADK	Yes
Western Superior	North Caribou	2.93	AUK	No
	Central Wabigoon	2.96-2.90	AUK, ADK	No
India		3.5-2.7	AUK	Yes
São Francisco		3.0-2.7	AUK, ADK	?
Amazonian		3.0-2.8	AUK	Yes
Tocantins	Crixás	2.9	ADK	?
Baltic-Fennoscandia	Karelia	2.8-2.7	AUK, ADK	Yes
	Kola Schist Belt	2.9-2.7	AUK, ADK	Yes
Eastern Superior	Québec	2.84-2.76	AUK	?
	Abitibi	2.7	AUK, ADK–TEK, TDKB	Yes
Zimbabwe	Belingwe	2.7	AUK	No
Yilgarn	Norseman-Wiluna	2.7	AUK	No
	Forrestania	2.7	ADK	No

References: Attoh and Ekwueme (1997), Baars (1997), Blenkinsop et al., (1997), Borg and Shackleton (1997), Brandt and de Wit (1997); **Crixás**: Ferreira-Filho et al. (submitted), Grove et al. (1997), Kushev (1997), Kushev and Kornilov, (1997), Myers et al. (1997); **Forrestania**: Perring et al. (1995), Puchtel et al. (1997), Rogers and Giral (1997), Stott (1997), Tassinari (1997); **Caribou and Wabigoon**: Tomlinson et al. (1999a, 1999b); **Abitibi**: Hollings and Kerrich (1999), Maurice and Francis (2000), Jahn et al., (1982); **Kola**: Puchtel et al. (1998).

8 Metallogeny

8.1 KOMATIITE-ASSOCIATED NI-CU-(PGE) DEPOSITS

The ores in komatiite-associated Ni-Cu-(PGE) deposits may be subdivided into several types on the basis of their distribution within the host rocks. The following descriptions are summarized from a review of these deposits by Lesher and Keays (2002) and are intended to provide perspective for classifying the deposits in the Abitibi greenstone belt.

8.1.1 Type I Basal Ni-Cu-(PGE) Mineralization

Type Ia stratiform basal Ni-Cu-(PGE) mineralization occurs as layers at or near the bases of individual host sequences. Where it occurs at the base of the sequence it is referred to as contact ore and where it occurs at the base of overlying flow units it is referred to as hanging wall ore. A typical ore profile comprises a thinner and less continuous layer of massive sulfides (<20% gangue), sometimes inclusion-bearing, overlain successively by a thicker and generally more continuous layer of net-textured (matrix) sulfides (20-60% gangue), disseminated sulfides (60-90% gangue), and non-mineralized host rocks. Some profiles are very simple, but some exhibit complex repetitions indicating multiple episodes of ore emplacement. The proportion of massive ore appears to increase with shoot size, but the thicknesses of massive ores, which are very ductile during deformation, are influenced to a very large degree by deformation (see section 8.1.5). Some Type I deposits contain very thick (10s of m) zones of low-grade disseminated mineralization that overlie and are contiguous with the contact mineralization and represent a transition into Type IIb mineralization. Many Type I deposits also contain spatially separate Type IIa or IIb mineralization. Type I ore shoots vary considerably in size and grade both within and between major districts. Individual shoots or zones are generally less than 5 x 10^6 tonnes, and contain between 2 and 4% Ni. The shoots are often ribbon-like in form with dimensions varying from 100 m to 2.5 km, or more, in length, and from 50 to 250 m in width, although some are composed of multiple pods. Thicknesses vary from 1 to 5 m in those containing more than 2% Ni to 5 to 20 m or more in lower grade shoots.

Type Ib footwall vein mineralization occurs as magmatic veins and veinlets in massive footwall rocks and may also fill interstitial spaces in underlying pillow basalts, breccias, and spinifex-textured komatiites. Because most komatiite-associated Ni-Cu-(PGE) deposits appeared to have cooled quickly, the sulfide melts did not fractionally crystallize and segregate Cu-poor monosulfide solid solution (*Mss*) from Cu-PPGE-rich sulfide melt as efficiently as in slowly cooled deposits. Nevertheless, most Type I deposits contain Cu-PPGE-rich footwall stringers and there are rare Cu-rich net-textured ores that appear to represent fractionated sulfide melts.

8.1.2 Type II Strata-Bound Internal Ni-Cu-(PGE) Mineralization

Type IIa strata-bound internal Ni-Cu-(PGE) mineralization is strata-bound and normally occurs in the central parts of individual cooling units, although it sometimes occurs in basal chilled margins and rarely in minor to trace amounts in upper chilled margins. Where sulfides occur as coarsely disseminated spheroidal patches it is referred to as blebby mineralization (Type IIa), where it occurs as fine interstitial to lobate disseminations between cumulus olivine crystals it is referred to as interstitial mineralization (Type IIb), and where it occurs as extremely fine (almost invisible) zones of interstitial disseminations it is referred to as cloud mineralization (Type IIc). In many areas, mineralized rocks grade into sulfide-free rocks, so ore boundaries are arbitrarily defined by cut-off grades. Much of the Ni in the lower grade deposits has been derived by serpentinization of olivine and the cloud sulfide mineralization in some deposits has been shown to form by sulfidation of magnetite, produced during serpentinization of olivine. Type IIb ores are typically low grade (<1% Ni), but large tonnage (up to 250 x 10^6 tonnes). Type IIa ores may have higher grades, but are typically smaller. Type IIb deposits are typically 100-300 m wide and 1-2 km long, several of which have been drilled to over 1 km depth. Only a few of the large Type II deposits have Type I deposits associated with them.

8.1.3 Type III Stratiform "Reef-Style" PGE-(Cu)-(Ni) Mineralization

Type III stratiform "reef-style" mineralization typically occurs in orthocumulate to pegmatoidal zones at the top of the cumulate zones in thick, strongly differentiated flows or sills. The host units typically contain olivine ± pyroxene cumulate rocks in their lower parts and gabbroic rocks in their upper parts; the PGE mineralization occurs at or near the point at which plagioclase appears as a cumulus phase (~10% MgO). This suggests that the magma attained sulfide saturation as a consequence of fractionation crystallization and that the PGE were preferentially concentrated into a sulfide phase that settled to form discrete PGE-enriched horizons. Grades are typically anomalous, but subeconomic, usually less than 1 g/t total PGE+Au.

Although most mafic-ultramafic magmas, including komatiitic and ferropicritic magmas, have the potential to form stratiform (reef-style) PGE mineralization if they differentiate enough to reach sulfide saturation (see Lesher and Stone, 1996), thus far no *economic* deposits have been found associated with komatiitic lavas or sills, which do not appear to have formed the thick, periodically-replenished, dynamic systems that favour the same style of PGE concentration that occurred in PGE deposits (e.g., Campbell et al., 1983) hosted by tholeiitic and boninitic mafic-ultramafic layered intrusions (e.g., Bushveld, Great Dyke, Stillwater).

8.1.4 Type IV Hydrothermal-Metamorphic-Metasomatic Ni-Cu-(PGE) Mineralization

Type IVa Ni-enriched metasediment mineralization occurs in sulfidic metasediments associated with Type I mineralization. Ore-sediment relationships vary considerably, even between deposits in the same district; ores may i) grade laterally into metasedimentary rocks, ii) directly overlie or lap onto metasedimentary rocks which may be altered, thinned, or discontinuous beneath the ore zone, or iii) occur along strike from barren metasedimentary rocks, separated by a zone of barren contact. Type IVa mineralization is only found *adjacent* to Type I or Type V mineralization and may occur in a wide range of metamorphic environments, ranging from middle greenschist through lower amphibolite to upper amphibolite.

Type IVb hydrothermal vein mineralization is sometimes associated with Type I mineralization. The veins normally occur in the more brittle footwall rocks rather than in the more ductile ultramafic host rocks. They are distinguished from the other types of mineralization by a close association with hydrothermal quartz and/or carbonate, depletion in Ir relative to Ni, and depletion in Cr relative to Fe. Although they may locally contain high abundances of Ni, most occurrences of hydrothermal Ni sulfide mineralization are only a scientific curiosity.

Elevated PGE contents have also been suggested to be associated with late stage exsolution of volatiles. For example, Stone et al. (1987) suggested that sulfides in the amygdaloidal top of Fred's Flow formed by degassing of S during emplacement, diffusion of metals into rising S-rich vapour bubbles, and subsequent crystallization of sulfides. They rejected an origin as immiscible sulfide droplets because of the association with amygdules, the high metal tenors of the blebs, and because of their high density relative to the silicate lava. However, as discussed by Lesher and Keays (2002), the metal tenors of the blebs (10-19% Ni) are *not* higher than could be achieved by transport during emplacement (Lesher and Campbell, 1993) and sulfide blebs are commonly trapped in the margins of MORB flows (Mathez, 1999). Importantly, the amygdaloidal sulfides in Fred's Flow (see Lesher and Keays, 2002: figure 5K) are compositionally similar to many Type I ores, except for minor enrichment in Pd. An alternative explanation, proposed for a similar occurrence at Dundonald (Eckstrand and Williamson, 1985), is that they are immiscible sulfide droplets that floated upwards attached to vapour bubbles. The presence of a thin layer of chromites along the margins of the blebs (Stone et al., 1987) is more consistent with an origin as magmatic sulfide droplets than with crystallization from a vapour. In any case, such a process is not a very efficient PGE collection mechanism, as vesiculation was confined to the upper portion of the magmatic system and metals from lower portions of the unit (below the vesiculation front) could not be partitioned into the vesicles. The PGE grades in the flow top at Fred's Flow are extremely low (~0.3 g/t total PGE+Au), consistent with the inefficiency of this concentration mechanism.

8.1.5 Type V Tectonically-Mobilized Ni-Cu-(PGE) Mineralization

Type V tectonic offset mineralization occurs in fault and shear zones associated with Type I mineralization. Because massive sulfides are much more ductile than disseminated sulfides, they are more easily mobilized into fault and shear zones. Thus, Type V mineralization is more closely-associated with Type I mineralization than with Type II or Type III mineralization. A distinction is made between Type I ores that are merely deformed, but may contain fragments of adjacent wall rocks, reaction zones, and veins, and Type V ores that have been *mobilized* into wall rocks and are no longer physically contiguous with the original host rocks.

8.2 SUMMARY OF EXPLORATION CRITERIA

8.2.1 Types I and II Ni-Cu-(PGE) Mineralization

The following exploration criteria for komatiite-associated Ni-Cu-(PGE) deposits have been compiled from Lesher (1989), Lesher and Stone (1996), Lesher et al. (2001), Lesher and Keays (2002), and this study:

Province Selection

1) "Continental" tectonic settings (e.g., intra-continental rifts, rifted continental margins, rifted arcs) containing sialic basement (normally inferred from the presence of inherited zircons and/or Sm-Nd isotopic characteristics) appear to be more favourable than non-continental tectonic settings (e.g., mid-oceanic ridges, back-arc basins). Although assimilation of sialic crust alone does not appear to be an effective mechanism of inducing sulfide saturation and the segregation of economic abundances of sulfides (Lesher and Arndt, 1995; Lesher and Stone, 1996), it may provide an environment in which S-rich rocks may accumulate.

2) Large igneous provinces of any age that contain lava channels or magma conduits and potential sulfur sources (sulfidic sedimentary rocks, sulfidic volcanic rocks, VMS mineralization) are favourable, although younger Archean (~2.7 Ga) greenstone belts and lower Proterozoic (~1.9 Ga) volcanic belts, which appear to have been characterized by more voluminous eruption of komatiitic lavas, appear to be most favourable.

3) Regions underlain by older, cooler, denser lithosphere (e.g., Yilgarn Craton, Western Australia) may be more favorable than regions underlain by younger, hotter, less dense lithosphere (e.g., Superior Province), as this may influence the rate at which komatiites are erupted and therefore their potential to become channelized.

4) Rift-phase greenstones, which are characterized by elongate granitoid domes, linear tectonic patterns, complex volcanic stratigraphy, more abundant komatiitic rocks, especially komatiitic peridotites and komatiitic dunites, and more abundant sulfidic shales and/or cherts, appear to be more prospective than platform-phase greenstones, which are characterized by equi-spaced granitoid batholiths with intervening stellate greenstone belts, a more coherent volcanic stratigraphy, more abundant komatiitic basalts, and shallow water volcaniclastic rocks or oxide facies iron-formation (Groves and Batt, 1984). The former are interpreted to have formed in deeper water under conditions of greater crustal extension, whereas the latter are interpreted to have formed in relatively deep water under conditions of high crustal extension and appear to be superimposed on older platform-phase greenstones (Groves and Batt, 1984; Ludden et al., 1986).

5) Provinces where mafic-ultramafic magmas (komatiites, komatiitic basalts, picrites, ferropicrites, high-Mg basalts) have been generated by high degree partial melting of the mantle. The type of magma (i.e., Al-depleted, Al-undepleted, Ti-enriched, ferropicritic) and therefore the composition and depth of the source, does not appear to be important.

Area Selection

1) Areas that contain thicker, more magnesian units and are more "disordered" (e.g., poor lateral continuity of highly-magnesian flow units, locally absent interflow metasediments) than those in adjacent sequences in the same province or region and which may represent areas of higher flow rates and channelized flow.
2) Areas where *most* of the lavas and/or intrusions are *not* contaminated or depleted in PGE, indicating a fertile magma.
3) Areas containing S-rich metasedimentary rocks (e.g., sulfide-facies iron formations, sulfidic cherts, sulfidic argillites) are more favourable than sequences containing oxide-facies iron formations or other non-sulfide-bearing sedimentary rocks.
4) Areas that contain Zn-rich chromites may be favourable if attributable to incorporation of Zn-rich sediments, but is not critical and may be modified during metamorphism.
5) Areas exposed around structural highs are more accessible, but not critical.

Unit Selection

1) Units enriched in olivine with mesocumulate to adcumulate textures. Komatiitic dunites will be characterized by olivine ± chromite ± sulfide primary assemblages, whereas komatiitic peridotites will be characterized by olivine ± chromite ± pyroxene ± sulfide primary assemblages. Serpentinized units will contain abundant magnetite and will exhibit high magnetic susceptibilities, whereas talc-carbonated units will not.
2) Units with poor across-plunge continuity, but good down-plunge continuity, although establishing this will depend on physical volcanology (e.g., lava channel vs. channelized sheet flow), orientation, and deformation.
3) Units that appear to have thermomechanically-eroded footwall rocks and/or contain xenoliths or xenomelts, particularly those that appear to transgress sulfidic sediments.
4) Units that are *locally* contaminated, normally indicated by enrichment in HILE relative to MILE with negative Nb-Ta-(Ti) anomalies (see discussion by Lesher et al., 2001).
5) Units that are *locally* depleted/enriched in chalcophile elements (CE) relative to associated units, depending on the physical volcanology (see discussion by Lesher and Arndt, 1995; Lesher and Stone, 1996; Lesher et al., 2001).

8.2.2 Type III PGE–(Cu)-(Ni) Mineralization

Some of the province- and area-scale exploration criteria for PGE-(Cu)-(Ni) mineralization in komatiitic rocks are similar to those for Ni-Cu-(PGE) mineralization, particularly the criteria related to the generation of a sulfide-undersaturated magma, however, many of the other criteria are not relevant. In particular, the criteria related to lava channelization, thermomechanical erosion, and incorporation of S are not important. Instead, the following unit selection criteria appear to be more important:

1) Units that have differentiated to the point at which sulfide reaches the liquidus, which is normally near the point at which plagioclase reaches the liquidus (see discussion by Lesher and Stone, 1996). Such units are characterized by peridotitic (olivine ± pyroxene) lower cumulate zones and gabbroic (pyroxene-plagioclase) upper differentiated zones, with or without the presence of spinifex-textured rocks.

2) Very thick (>1 km) units, especially those exhibiting evidence for magma replenishment (e.g., geochemical reversals) to increase the mass of magma from which PGEs may be extracted, are more favourable than thinner units.

3) Units containing thin sulfide-bearing horizons, which are thin and readily oxidized and weathered relative to adjacent sulfide-poor lithologies.

4) Units that contain evidence of *local* depletion of CEs (PGE >>> Cu > Ni: see discussion by Lesher and Stone, 1996).

8.3 KOMATIITE-ASSOCIATED NI-CU-(PGE) DEPOSITS IN THE ABITIBI GREENSTONE BELT

Naldrett and Gasparini (1971), Coad (1979), Green and Naldrett (1981), and Davis (1999) have reviewed the occurrences of komatiite-associated Ni-Cu-(PGE) deposits in the Abitibi greenstone belt. Duke (1986), Barnes and Naldrett (1987), Brügmann et al. (1987), Davis (1997), and Houlé et al. (2002) conducted work on specific Ni-Cu-(PGE) deposits in the Abitibi greenstone belt. The following discussions are based on those reviews and our studies of the deposits.

8.3.1 Type I Mineralization in the AGB

Type I stratiform basal Ni-Cu-(PGE) mineralization has thus far only been identified in the Tisdale assemblage (e.g., Hart, Langmuir, McWatters, and Redstone deposits in the Shaw Dome; Texmont deposit in the Bartlett Done; Sothman deposit in the Halliday dome) and Kidd-Munro assemblage (e.g., Mickel showing in southern Munro Township; Alexo mine and Dundonald deposit in Dundonald Township; Marbridge deposit in the stratigraphically-equivalent Malartic Group).

The host rocks in these localities are all AUK, similar to most (e.g., Kambalda, Damba-Silwane, Perseverance), but not all (e.g., Boa Vista, Forrestania, Ruth Well) mineralized komatiites world-wide (Lesher, 1989; Lesher and Stone, 1996; Ferreira-Filho et al., submitted). However, as the physical volcanology of the lavas is the most important factor in the development of komatiite-associated Ni-Cu-(PGE) deposits (Lesher et al., 1984; Lesher, 1989; Barnes et al., 1999; Lesher and Keays, 2002), this may simply reflect greater degrees of lava channelization within those assemblages compared to other komatiite-bearing assemblages (Houlé et al., 2001). Thick, olivine mesocumulate and adcumulate units, most likely representing lava channels, magma conduits, or the channel-flow facies of channelized sheet flows/sills, have been identified thus far only in the Kidd-Munro and Tisdale assemblages (Houlé et al., 2001), supporting the importance of volcanic facies in localizing Ni-Cu-(PGE) mineralization in komatiites.

Some, but not all, of the komatiites in these areas also show evidence of *local* crustal contamination (Section 3.8.3). Although felsification may reduce the solubility of sulfide in a magma (see review by Naldrett, 1989), it is not a very efficient ore-forming process in komatiites (which are strongly undersaturated in sulfide) and even very strongly contaminated komatiitic magmas do not normally reach sulfide saturation (Lesher and Arndt, 1996; Lesher and Stone, 1996). The presence of *local* rather than *wholesale* contamination is consistent with incorporation of S from associated sedimentary and/or volcanic rocks during emplacement, rather than by incorporation of S from crustal rocks during ascent (see discussion by Lesher et al., 2001). Thus, the local abundance of S-rich iron-formations in the Tisdale assemblage and S-rich graphitic sediments in the Kidd-Munro assemblage may be another reason why Ni-Cu-(PGE) mineralization is localized in the Tisdale and Kidd-Munro assemblages (Houlé et al., 2001). Neither the Pacaud nor the Stoughton-Roquemaure assemblages contain S-rich iron formations.

8.3.1.1 AREAS RECOMMENDED FOR FURTHER EXPLORATION

The following areas in the Abitibi greenstone belt satisfy the exploration criteria for Type I Ni-Cu-(PGE) mineralization:

- Dundonald Township
- Deloro, Shaw, Carman, Langmuir, Eldorado, and Adams Townships (Shaw Dome)
- Geike, Zavitz, Price, and McArthur Townships (Bartlett Dome)
- Bannockburn, Hutt, and Semple Townships (Halliday Dome)
- Holloway Township (Lightening Mountains Section, Lake Abitibi area)
- Natal Township (Shining Tree area)
- Garrison Township (Porcupine-Destor Fault Zone)
- Keith and Kenogaming Townships (Swayze Belt)

8.3.2 Type II Mineralization in the AGB

Type IIb strata-bound internal disseminated Ni-Cu-(PGE) mineralization has thus far only been identified in the Tisdale assemblage (e.g., Bannockburn) and Kidd-Munro (= Malartic Group) assemblage (e.g., Dumont) and both areas are sub-economic. The host rocks in these areas also appear to be AUK. Although the grades in deposits of this type are much lower than in Type I deposits, the total masses of sulfide are as high or higher and, as discussed by Lesher and Keays (2002), the amount of S is greater than could have dissolved in the host rock. As such, an external S source also appears to be necessary in Type II deposits.

8.3.2.1 AREAS RECOMMENDED FOR FURTHER EXPLORATION

The following areas in the Abitibi greenstone belt satisfy the exploration criteria for Type II Ni-Cu-(PGE) mineralization:

- Deloro, Shaw, Carman, Langmuir, Eldorado, and Adams Townships (Shaw Dome)
- Geike, Zavitz, Price, and McArthur Townships (Bartlett Dome)
- Bannockburn, Hutt, and Semple Townships (Halliday Dome)
- Holloway Township (Lightening Mountains Section, Lake Abitibi area)
- Garrison Township (Porcupine-Destor Fault Zone)

8.3.3 Type III Mineralization in the AGB

Type III stratiform "reef-style" PGE-(Cu)-(Ni) mineralization has been identified in thick, differentiated komatiitic units in the Kidd-Munro assemblage (e.g., Fred's Flow: Crocket and MacRae, 1986), in thick, differentiated tholeiitic units in the Kidd-Munro assemblage (e.g., Centre Hill Complex: Vaillancourt et al., 2003), and in thick, differentiated ferropicritic units in the Stoughton-Roquemaure assemblage (e.g., Boston Creek Sill: Stone et al., 1993, 1996). Although the magma types are very different, all were initially undersaturated in sulfide and appear to have fractionated to the point where plagioclase and sulfide appeared as liquidus phases, further supporting the points made above that the composition of the magma is not particularly important.

8.3.3.1 AREAS RECOMMENDED FOR FURTHER EXPLORATION

The following areas in the Abitibi greenstone belt satisfy the exploration criteria for Type III PGE-(Cu)-(Ni) mineralization:

- Lincoln-Nippising Peridotite in Skead and McElroy Townships
- LUH (lower ultramafic horizon) in the Shaw Dome in Eldorado, Langmuir, and Deloro Townships

8.3.4 Type IV Mineralization in the AGB

Type IVa Ni-enriched metasediment mineralization has thus far been identified only in the Tisdale assemblage (e.g., Langmuir and Redstone). Green and Naldrett (1981) interpreted the metasediment-hosted Ni-Cu-(PGE) mineralization in the Langmuir mine to be of magmatic origin (Type I) followed by remobilisation of Ni-mineralization via metamorphism and/or deformation, whereas Robinson and Hutchinson (1982) interpreted the metasediment-hosted Ni-Cu-(PGE) mineralization in the Redstone mine to be of volcanic-exhalative origin. Although the Type IVa ores at Langmuir are slightly depleted in Rh and strongly depleted in Rh and Ir relative to elements of similar compatibility, suggesting that they formed via a non-magmatic process (Lesher and Keays, 2002), it is not clear whether this process involved metamorphic fluids or was controlled by differences in solid-state diffusion rates for the different metals. For reasons discussed by Groves et al. (1979), Keays et al. (1982) and Lesher and Keays (2002), a volcanic-exhalative origin is not favoured.

No Type IVb hydrothermal vein mineralization has been identified in the Abitibi greenstone belt.

8.3.5 Type V Mineralization in the AGB

Type V (tectonic offset) Ni-Cu-(PGE) mineralization is abundant in the Redstone deposit and is locally abundant in most of the other Ni-Cu-(PGE) deposits in the Abitibi greenstone belt (e.g., Naldrett and Gasparini, 1971; Coad, 1979; Green and Naldrett, 1981; Robinson and Hutchinson, 1982).

At present, mobilization or remobilization of PGE by faulting, metasomatism, or alteration is not in itself responsible for formation of PGE, but can be responsible for concentrating or upgrading PGE-mineralization.

8.4 CHALCOPHILE ELEMENT GEOCHEMISTRY OF KOMATIITES IN THE ABITIBI GREENSTONE BELT

The CE geochemistry of komatiites in the Abitibi greenstone belt is summarized in Figures 3.8-3.9 (Section 3). The most important observations are:

1) Fractional crystallization (FC) of olivine explains the majority of the geochemical variations in Ni and Co for non-mineralized samples with <35 wt.% MgO.
2) Accumulation of olivine ± chromite explains the majority of the geochemical variations in Ni and Co for non-mineralized samples with >35 wt.% MgO.
3) Cu abundances lie broadly between the abundances predicted by AFC and FC models, but have been extensively mobilized during alteration and/or metamorphism.

Some samples in the Tisdale and Kidd-Munro assemblages (e.g., parts of the LKH in Deloro and Langmuir Townships in the Shaw Dome, parts of the komatiite sequences in the Dundonald Beach area in Dundonald Township) are *locally* depleted in Ni and Co relative to normal fractionation trends, which may be attributed to fractional segregation of olivine + sulfide or to crystallization of olivine followed by batch equilibration with sulfide. PGE data allow discrimination between these processes.

Mineralized samples in the Kidd-Munro and Tisdale assemblages are enriched in Ni and Co relative to normal fractionation trends. Small numbers of samples in the Stoughton-Roquemaure assemblage in the Lake Abitibi region and the Tisdale assemblage in the Porcupine-Destor Fault Zone appear to be strongly enriched in Ni. S analyses are not available and the samples are not described as mineralized, thus the data, which were obtained by AAS in 1973, are likely erroneous.

PGE analyses provide more insights into the sulfide saturation history of the lavas. Most have PGE abundances similar to those predicted by FC of olivine (Figure 3.14) with Ni/Pd, Pd/Ir, and Pd/Cr ratios indicating that they were undersaturated in sulfide (Figures 8.2 and 8.3). However, mineralized komatiites at the Dundonald, Texmont, and Hart deposits lie closer to the AFC trend (Figure 8.1). Samples in the upper parts of the Boston Creek Sill also appear to have attained sulfide-saturation, as marked by lower Pd/Cu ratios (Figure 8.3).

There are minor differences between mantle-normalized CE diagrams for mineralized and non-mineralized komatiites (Figure 8.4) reflecting minor fractionation of Cu-PPGE and Ni-Co-IPGE during sulfide segregation (Barnes et al., 1988). Non-mineralized komatiites in the Pacaud, Kidd-Munro, and Tisdale assemblages have relatively flat CE patterns, typical of S-undersaturated high-degree partial melts. Non-mineralized parts of the Boston Creek sill (i.e., peridotite and clinopyroxenite zones) in the Stoughton-Roquemaure assemblage also exhibit flat CE patterns. Importantly, non-mineralized TDKB, AUK, and ADK–TEK have similar PGE patterns. Thus, regardless of the depth of the composition of the source (and depth of partial melting), all were undersaturated in sulfide, formed by high degree partial melting, and are fertile host magmas.

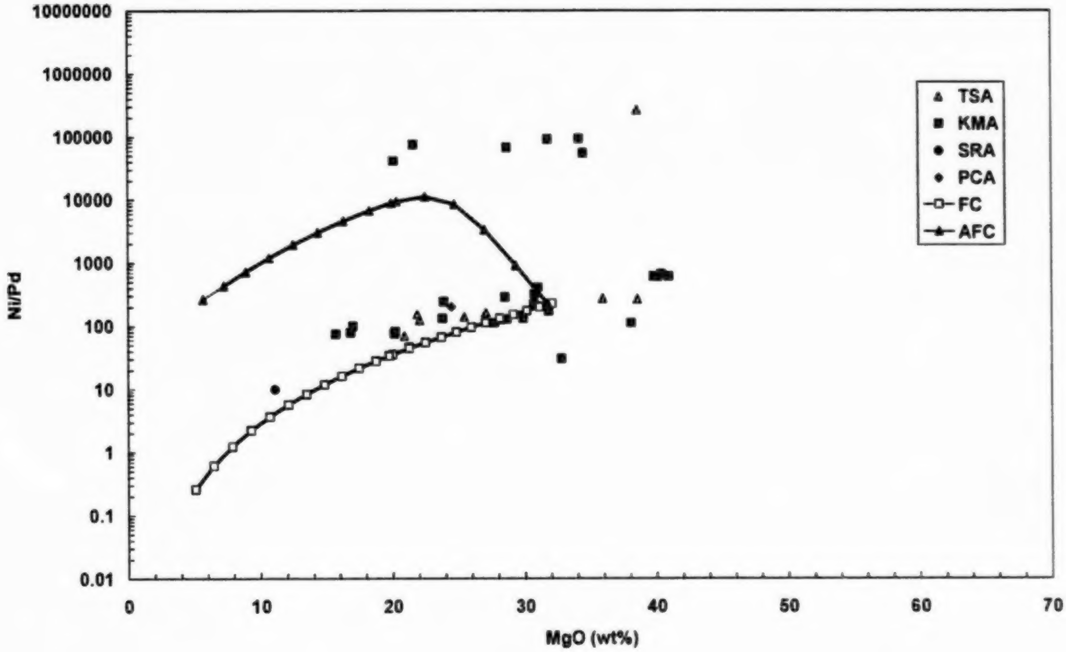

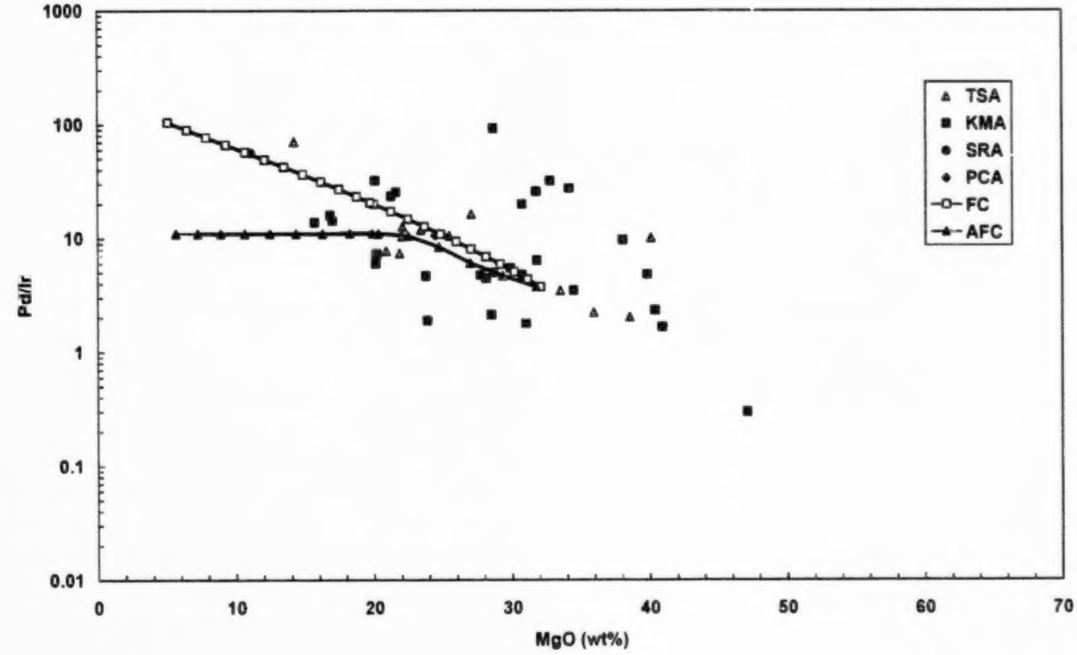

Figure 8.1. Ni/Pd and Pd/Ir vs. MgO (wt.% volatile-free) for komatiites in the Abitibi greenstone belt.

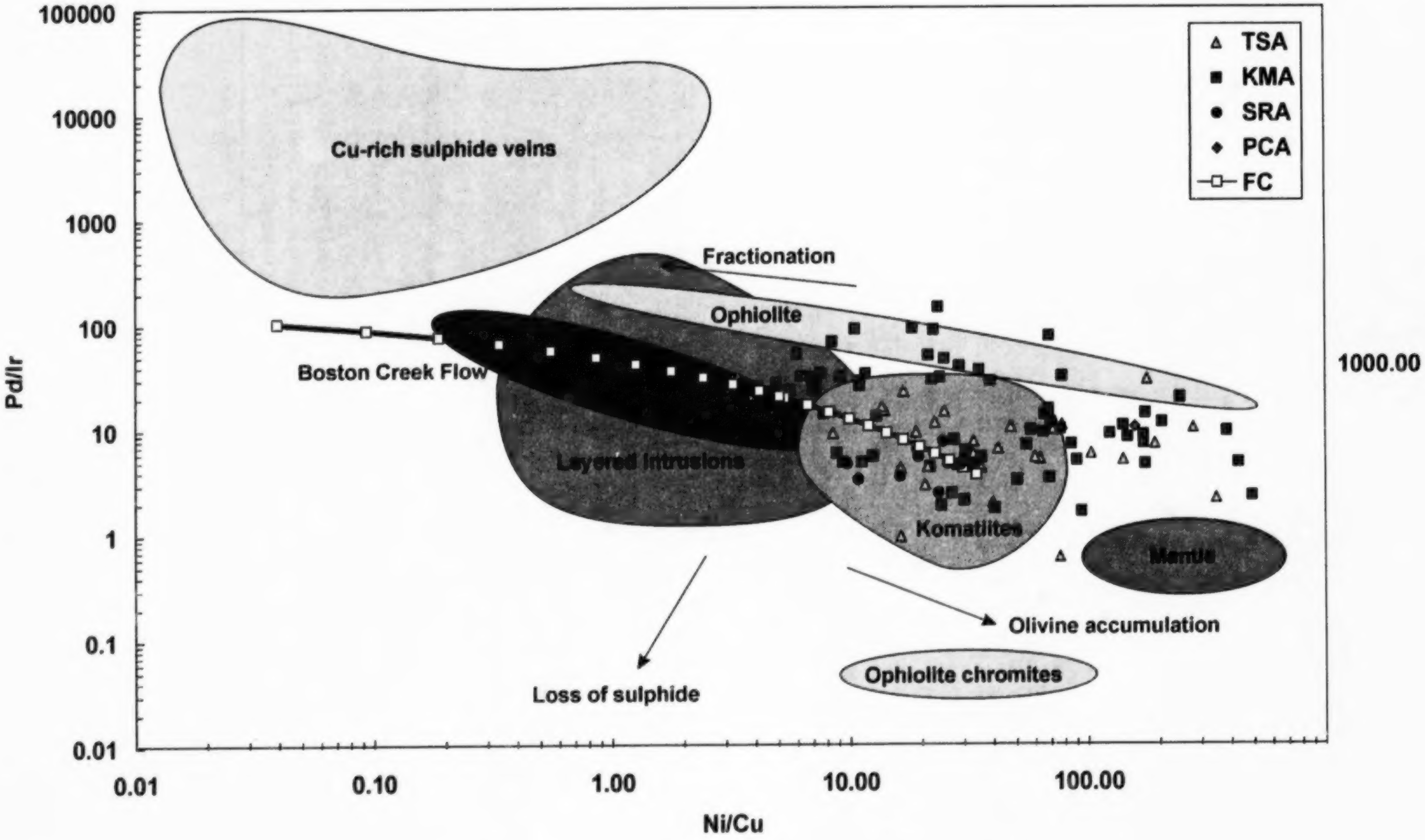

Figure 8.2. Pd/Ir vs. Ni/Cu for komatiites in the Abitibi greenstone belt. Fields for mafic and ultramafic rocks from Barnes et al. (1988).

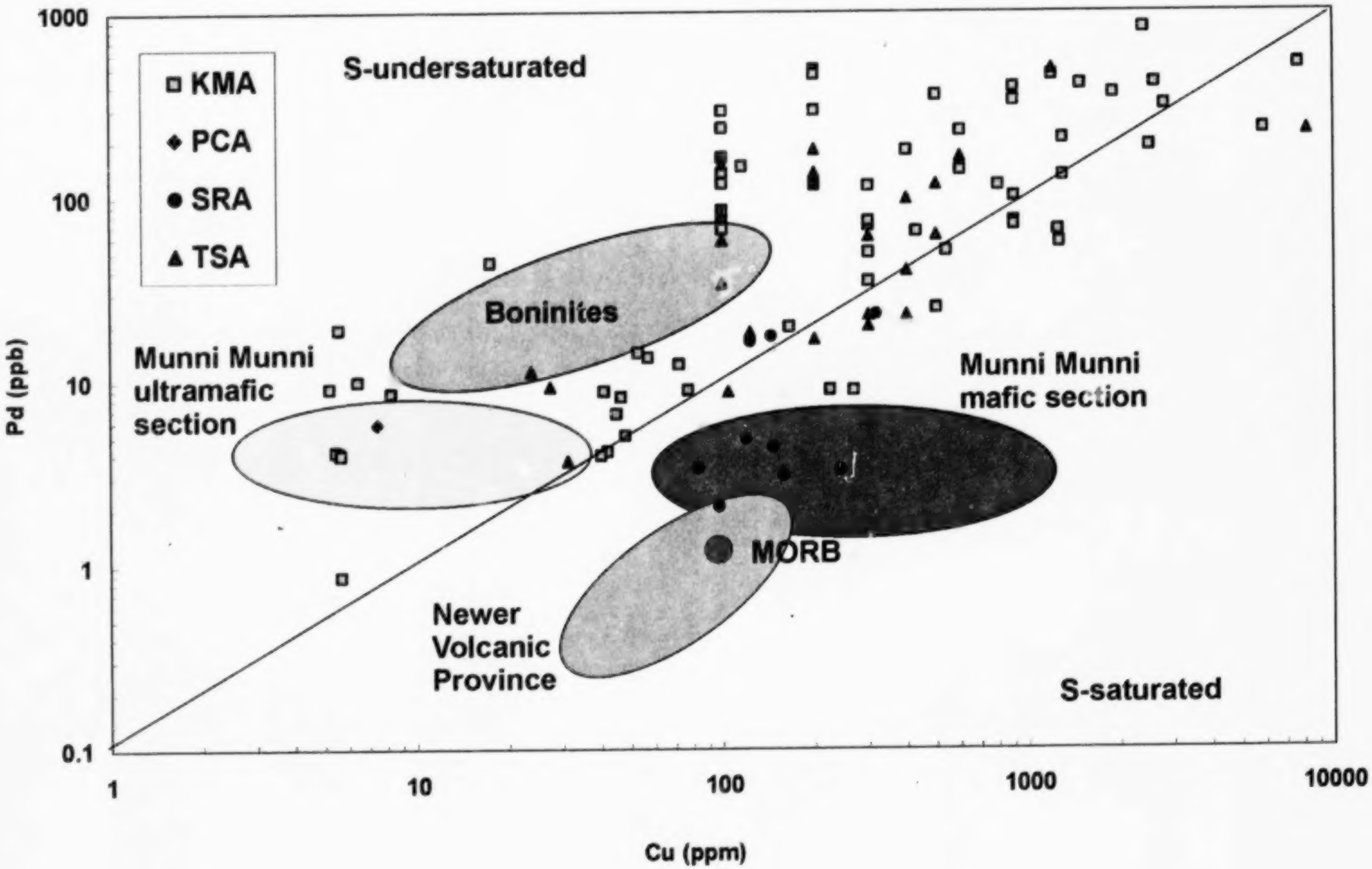

Figure 8.3. Pd (ppb) vs. Cu (ppm) for komatiites in the Abitibi greenstone belt.

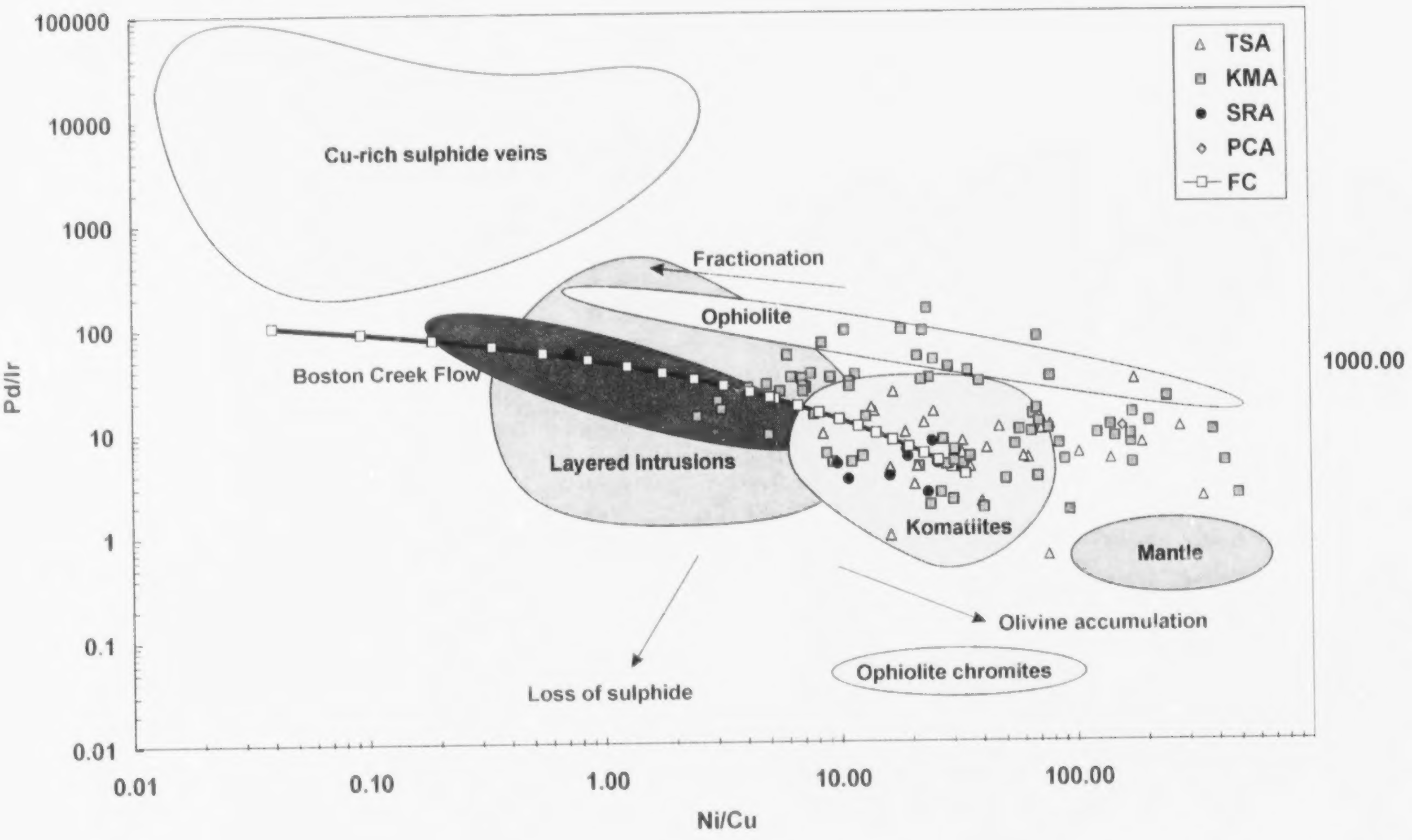

Figure 8.2. Pd/Ir vs. Ni/Cu for komatiites in the Abitibi greenstone belt. Fields for mafic and ultramafic rocks from Barnes et al. (1988).

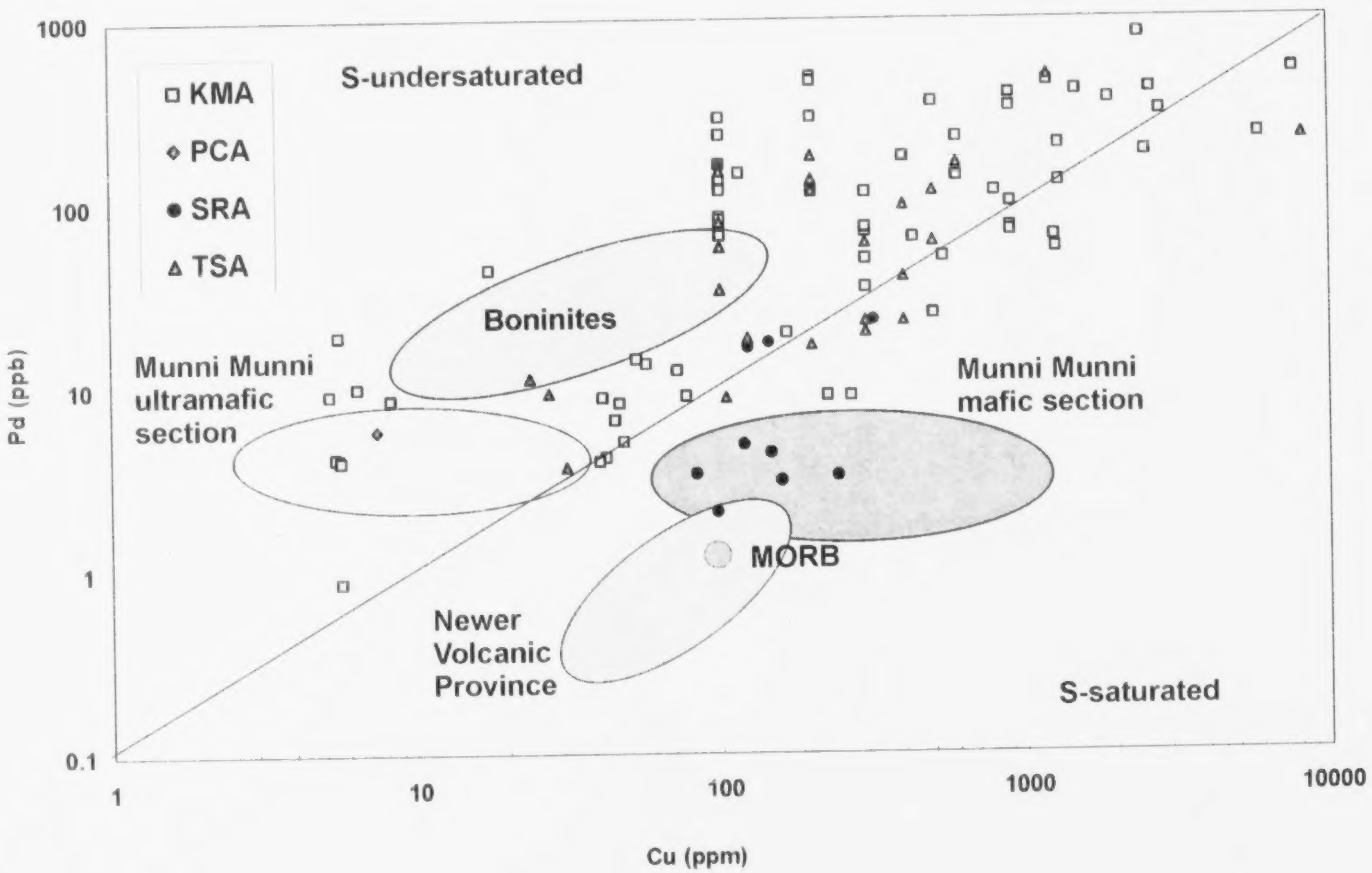

Figure 8.3. Pd (ppb) vs. Cu (ppm) for komatiites in the Abitibi greenstone belt.

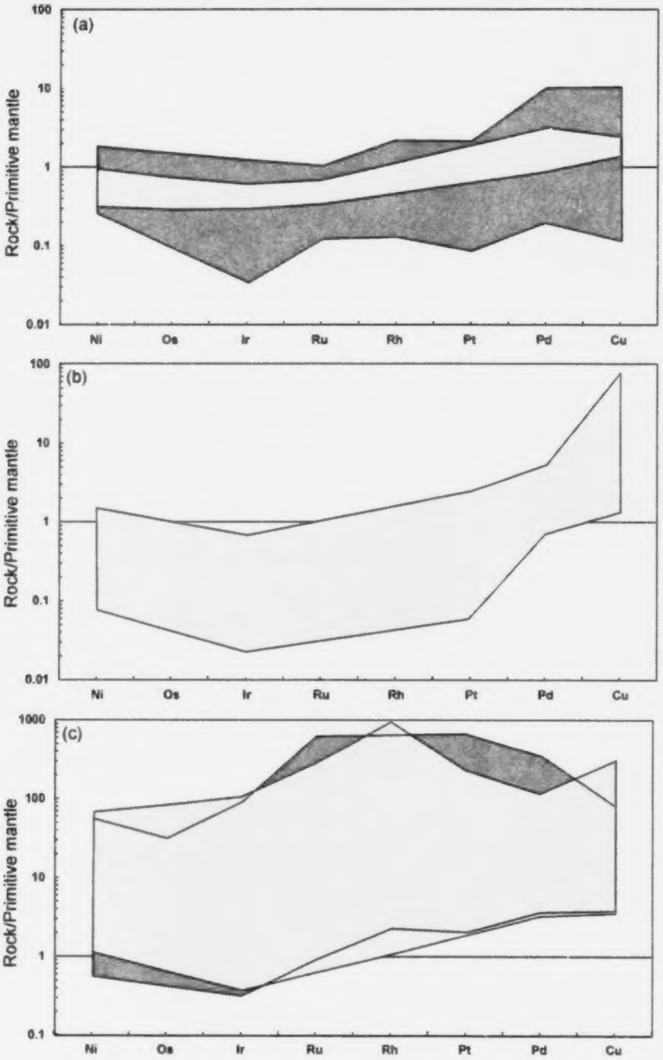

Figure 8.4. Mantle-normalized PGE diagrams for komatiites in the Abitibi greenstone belt, including (a) non-mineralized komatiites from Brügmann et al., (1987: light grey) and this study (dark grey); (b) mineralized ferropicrites from the Boston Creek sill (Stone et al., 1993, 1996); and (c) massive sulfides (light grey) and net-textured and disseminated sulfides (dark grey) from Alexo (Barnes and Naldrett, 1987).

The mineralized komatiites in the database are from the following localities and assemblages, which contain both Type I (stratiform contact) Ni-Cu-(PGE) and Type III (stratiform internal "reef style") PGE-(Cu)-(Ni) mineralization:

1) Alexo mine in Dundonald Township (Kidd-Munro belt, Kidd-Munro assemblage): Type I mineralization
2) Dundeal prospect in Dundonald Township (Kidd-Munro belt, Kidd-Munro assemblage): Type I mineralization
3) Hart deposit in Eldorado Township (Shaw Dome, Tisdale assemblage): Type I mineralization
4) Texmont deposit in Geikie Township (Bartlett Dome, Tisdale assemblage): Type I mineralization
5) Boston Creek sill in Boston Township (Round Lake Dome, Stoughton-Roquemaure assemblage): Type III mineralization
6) Fred's Flow in Munro Township (Kidd-Munro belt, Kidd-Munro assemblage): Type III mineralization

Mineralized komatiites have significantly higher abundances of PGE, Ni, and Cu than non-mineralized komatiites. Massive ores (e.g., Barnes and Naldrett, 1987; Barnes, 1985) have relatively flat mantle-normalized CE patterns (e.g., elevated Pt/Ni, Pd/Ni, Pt/Ir, or Pd/Ir ratios: Figure 8.4), consistent with equilibration at relatively low R factors (<100-300, where R = mass ratio of silicate liquid to sulfide liquid: Campbell and Naldrett, 1979: Table 8.1) and therefore a relatively non-turbulent environment (see discussion by Lesher and Campbell, 1993). Net-textured ores (e.g., Alexo) and komatiites containing disseminated sulfides (e.g., Barnes and Naldrett, 1986) have slightly more arch-shaped mantle-normalized CE patterns (Barnes et al., 1987), consistent with equilibration at slightly higher R factors (400-1200) and therefore slightly more turbulent conditions (Table 8.1).

Table 8.1. Calculated R-factors for Abitibi greenstone belt Ni-Cu-PGE deposits/showings.

Showing/Deposit	R-factor range	Av. R-factor	N	Reference
Alexo	20 - 408	149	33	Barnes and Naldrett (1987); Barnes (1985)
Dumont	60 - 1371	545	48	Duke (1986)
Dundonald	153 – 978	721	20	Barnes (1985)
Hart	15 – 1197	473	9	Barnes (1985)
Langmuir	13 – 285	145	14	Green and Naldrett (1981)
Texmont	216 - 915	460	17	Barnes (1985)
Kambalda*	100 - 500			
Katinniq*	300 – 1100			

The R-factor is calculated using equations from Campbell and Naldrett (1979), and the average of R-factor estimates based on Pd, Pt, Rh, Ru and Ir calculated.
Initial liquid composition is derived from sample 23355 (Pyke Hill fine-grained random spinifex) with Pd = 8.25 ppb, Pt = 7.52 ppb, Rh = 1.03 ppb, Ru = 1.62 ppb and Ir = 1.29 ppb.
D_{Pd} = 35 000; D_{Pt} = 35 000; D_{Rh} = 20 000; D_{Ru} = 15 000; D_{Ir} = 15 000.
* Calculated also Ni and Cu data

Type I (stratiform contact) Ni-Cu-(PGE) mineralization in the Abitibi greenstone belt occurs only in the Kidd-Munro and Tisdale assemblages. Most komatiite-hosted Ni-Cu-(PGE) mineralization is hosted by AUK (e.g., Kambalda, Raglan), but some are hosted in ADK (e.g., Boa Vista: Ferreira-Filho et al., submitted; Forrestania: Perring et al., 1996; Ruth Well: Nisbet and Chinner, 1981). Thus, the depth of partial melting in not an important parameter in the genesis of magmatic Ni-Cu-(PGE) deposits (Lesher and Stone, 1996). Instead, the most important control appears to be the physical volcanology and the nature of the underlying lithologies: mineralized komatiites worldwide are typically associated with lava channels and channelized sheet flows where komatiites have melted associated S-rich country rocks (Lesher, 1989). This is supported in the Abitibi greenstone belt by geochemical evidence of crustal interaction and, more importantly, greater degrees of lava channelization within the Kidd-Munro and Tisdale assemblages. Importantly, the sulfide-facies iron formations and graphitic sediments that appear to represent the predominant S sources for this deposit type, are only present in the Kidd-Munro and Tisdale assemblages. Thus, the Kidd-Munro and Tisdale assemblages are the most prospective assemblages for Type I Ni-Cu-(PGE) mineralization in the Abitibi greenstone belt.

The younger assemblages (Kidd-Munro and Tisdale) contain larger volumes of komatiites and larger amounts of thick, highly magnesian cumulate flows than the older assemblages (Pacaud and Stoughton-Roquemaure). Because the thicker, more magnesian cumulate flows are interpreted to represent channelized flows and channelized sheet flows that formed under higher discharge rates (Lesher et al., 1984), this suggests that komatiite discharge rates increased with time. This may be the result of the plume source being closer to the lithosphere (shallower depth of partial melting), allowing for higher degrees of partial melting, larger volumes of magma, and lower magma viscosities. This trend toward higher eruption rates is similar to the trends within some individual sequences (e.g., Dundonald), in which the lower units are less magnesian, but the reverse of the trends in other sequences (e.g., Alexo), in which the lower units are more magnesian. The significance of these differences is presently being studied by M.G. Houlé as part of a PhD dissertation at Laurentian University and the University of Ottawa.

9 Future Work

- Extension of the spatial and temporal geochemical and petrogenetic analyses into equivalent lithologies in the Québec part of the Abitibi greenstone belt.
- Interpretation of the geochemical data and petrogenetic interpretations within the context of the volcanic architecture.
- Os and Hf isotopic analysis of komatiites in each of the komatiite-bearing assemblages to track possible differences and/or changes in their source regions.
- More detailed geological, stratigraphic, volcanological, and geochemical studies of areas where ADK–TEK and AUK are intercalated (e.g., Newton Township, Round Lake Dome) to establish the stratigraphic and volcanological relationships between these two komatiite types in order to provide additional constraints on their petrogenesis and tectonic setting.
- More detailed interpretation of the geochemistry and petrogenesis of the ferropicrites in the Abitibi greenstone belt, including their source(s) and petrogenetic relationships to the komatiites.
- An evaluation of the basaltic rocks associated with the komatiites, including their source(s), petrogenetic relationships to the komatiites, and presence (if any) of temporal variations similar to the komatiites.

Acknowledgments

This work has been supported at various stages by grants from Outokumpu Ltd., the U.S. National Science Foundation (EAR-9405994), the Ontario Geological Survey (99-020), and the Natural Sciences and Engineering Research Council of Canada (IRC 663-001/97 and OG 203171/98). The samples for the Outokumpu project were collected in collaboration with P.C. Davis, W.E. Stone, M.S. (Larson) Stone, and A.M. Baird, with assistance from T. Schuster and M. Mainville. We are very grateful to them and to many other colleagues who provided geological/geochemical data or helpful information, including N.T. Arndt, S.-J. Barnes, C.T. Barrie, J. Bédard, B. Berger, O.M. Burnham, I.H. Campbell, A. Fowler, A. Fyon, H.L. Gibson, D. Gamble, J. Goutier, C.T. Herzberg, M.G. Houlé, G. Johns, R. Kerrich, P. Pilote, I. Puchtel, K.Y. Tomlinson, N. Trowell, and W. Mueller. The work by Tucker Barrie on the Kidd-Munro Extension project and by Rob Kerrich and colleagues on CAMIRO project 93-E06 was particularly helpful in this project. The majority of the high-quality trace element data used in this study were generated in the Ontario Geosciences Laboratories in the Willet Green Miller Mines and Minerals Research Centre in Sudbury.

Appendix A. Sample Preparation and Analytical Methods

PREPARATION METHODS

All samples analyzed in the Outokumpu study and this study were taken from well-characterized outcrops and diamond drill cores. Weathered surfaces and veins were removed with a diamond rock saw, all surfaces were ground on a diamond-bonded steel lap to remove saw marks, cleaned in water, and air-dried. The blocks were then crushed in a steel jaw crusher with removable plates that were cleaned with a steel wire brush, compressed air, and a methanol-soaked KimWipe® between samples. The samples analyzed in the Outokumpu study were pulverized in an agate shatterbox at the University of Western Ontario, under the supervision of Dr. C. Wu whereas the samples analyzed in this study were pulverized in a mild steel shatterbox at the Ontario Geoscience Laboratories, which was cleaned with Killarney quartzite, compressed air, and a methanol-soaked KimWipe® between samples. No systematic difference in geochemical composition resulting from the different preparation methods is evident in the database (Appendix B (MRD 120), available separately from this report).

ANALYTICAL METHODS

Major and Minor Elements

The major element data generated for the Outokumpu study and this study were obtained by wavelength-dispersive X-Ray fluorescence spectrometry (WD-XRFS) on fused glass disks at the University of Western Ontario (Dr. C. Wu, analyst), the Laurentian University Central Analytical Facility (Dr. J. Huang, analyst), or the Ontario Geoscience Laboratories (Dr. R. Bowins, Chief Scientist) in Sudbury. Ni, Cu, Co, Cr, V and Zn data were obtained in the same laboratories by either WD-XRF of pressed powders or, more rarely, atomic absorption spectrophotometry (AAS) following a mixed-acid digestion.

Replicate analyses of internal standards and reference materials over the duration of the project indicate that major elements (>1 wt.%) are generally accurate to within 2% of the amount present and that minor elements (1-0.1%) are accurate to within 5% of the amount present.

Trace Elements

Trace elements were determined by a combination of WD-XRFS of pressed powder pellets, inductively coupled plasma mass spectrometry (ICP-MS), and, more rarely, atomic absorption spectrophotometry (AAS).

Samples for ICP-MS analysis were prepared using a 10-day closed-beaker mixed-acid digestion method (Tomlinson et al., 1999c) to ensure complete digestion of refractory phases and analyzed as solutions on a Perkin-Elmer Elan 5000 ICP-MS at the Ontario Geoscience Laboratories. Comparisons of Zr abundances determined by this method and by the non-destructive WD-XRFS method indicates that most/all of the zircon was digested in most/all samples.

One international standard reference material (SRM) was analyzed in each batch of 25 samples, one internal SRM was analyzed in each batch of 10 samples, and a solution duplicate was analyzed in each batch of 10 samples. Analytical data for three international SRMs (BIR-1: Icelandic basalt, JB-3:

Japansese basalt, MRG-1: Mount Royal gabbro) and four internal SRMs (51-97-011: Winnipegosis peridotite, 94-077: Alexo komatiite, UMPL-1: Photo Lake pyroxenite, WA37916: William Lake dunite) utilized in this study are given in Tables A.1 and A.2. The trace element analyses appear to be accurate to within 10% and precise to within 5% of the amounts present, provided that the abundances are not too close to the detection limits.

Volatile-Free Recalculation

Because the samples in the database (Appendix B, MRD 120) have experienced different degrees of post-emplacement hydration, carbonatization, sulfidation, and/or oxidation, all of the data have been recalculated to 100% volatile free with total Fe as FeO and have been corrected for FeS measured as FeO (i.e., $O \equiv S$) using the following factor:

$$\text{VF Factor} = 100/(\Sigma \text{ major and minor elements} - 0.5\ S)$$

Data Filtering

We have attempted to include only high quality data from well-established laboratories in the database. However, trace element data obtained by ICP-MS before ca., 1995 often exhibit negative Zr-Hf anomalies suggesting incomplete digestion of such as zircon and other refractory minerals. Such data have not been included in the subset of data used in the geochemical interpretations, but have been included in the database for completeness.

Some of the HFSE data reported by Barrie (1999) were only reported to 1 and rarely 2 significant digits, and as a consequence are very quantitized, so they have been excluded from the interpretations.

Although several (in some times many) years elapsed between sampling, analysis, and publication, the year of publication of the data or the prefix on the sample number (e.g., 73J454: indicating field work done in, 1973) provide an indication of the time that the chemical analyses were completed. Many of the samples in the Outokumpu project that had been previously analyzed using incomplete dissolution methods were reanalyzed as part of this study, as indicated in the database.

Table A.1. Comparison of reference values for international standard reference materials and values measured in the Ontario Geoscience Laboratories *as unknowns* during the course of this study.

	BIR-1			JB-3			RGM-1			MRG-1		
	RV	**AV**	**CV**	**RV**	**AV**	**CV**	**RV**	**AV**	**CV**	**RV**	**AV**	**CV**
Cs	0.005	0.006	-20.0	1.1	0.948	13.8	9.6	10.2	-6.25	0.57	0.6	-5.26
Rb	0.25	0.216	13.6	13	14.8	-13.9	149	154	-3.36	8.05	7.49	6.96
Sr	108	119	-10.2	395	434	-9.87	108	111	-2.78	266	291	-9.40
Nb	0.6	0.541	9.83	2.3	1.93	16.1	8.9	9	-1.12	20	20.6	-3.00
La	0.62	0.676	-9.03	8.89	8.36	5.96	24	24	0.00	9.8	9.57	2.35
Ce	1.95	1.98	-1.54	21.5	20.5	4.65	47	45.9	2.34	26	27.2	-4.62
Pr	0.38	0.403	-6.05	3.39	3.2	5.60	4.7	5.48	-16.6	3.4	4.03	-18.5
Nd	2.5	2.51	-0.40	15.4	15.7	-1.95	19	20	-5.26	19.2	19.1	0.52
Sm	1.1	1.15	-4.55	4.27	4.18	2.11	4.3	3.96	7.91	4.5	4.62	-2.67
Eu	0.54	0.545	-0.93	1.31	1.27	3.05	0.66	0.6	9.09	1.39	1.46	-5.04
Gd	1.85	1.82	1.62	4.47	4.38	2.01	3.7	3.6	2.70	4	4.09	-2.25
Tb	0.36	0.363	-0.83	0.75	0.70	7.33	0.66	0.56	15.2	0.51	0.56	-9.80
Dy	2.5	2.42	3.20	4.55	4.37	3.96	4.08	3.66	10.3	2.9	2.98	-2.76
Ho	0.57	0.59	-3.51	0.79	0.96	-21.5	0.95	0.76	20.0	0.49	0.53	-8.16
Er	1.7	1.69	0.59	2.61	2.67	-2.30	2.6	2.29	11.9	1.12	1.22	-8.93
Tm	0.26	0.262	-0.77	0.41	0.396	3.41	0.37	0.35	5.41	0.11	0.15	-36.4
Yb	1.65	1.7	-3.03	2.62	2.47	5.73	2.6	2.46	5.38	0.6	0.86	-43.3
Lu	0.26	0.272	-4.62	0.39	0.399	-2.31	0.41	0.4	2.44	0.12	0.11	8.33
Hf	0.6	0.604	-0.67	2.68	2.8	-4.48	6.2	6.22	-0.32	3.76	3.9	-3.72
Ta	0.04	0.04	0.00	0.15	0.122	18.7	0.95	0.88	7.37	0.8	0.87	-8.75
Th	0.03	0.032	-6.67	1.3	1.34	-3.08	15.1	15	0.66	0.93	0.7	24.7
U	0.01	0.011	-10.0	0.46	0.48	-4.35	5.8	5.85	-0.86	0.24	0.25	-4.17
Y	16	15.9	0.62	27	26	3.70	25	22.8	8.80	14	13.2	5.71
Zr	15.5	13.2	14.8	98.3	82.8	15.8	219	198	9.59		93.5	
RMSD			7.50			9.34			8.38			14.2
N		2			1			1			1	

RV = recommended values from Govindaraju (1994), AV = analyzed values from Ontario Geoscience Laboratories, CV = coefficient of variation = 100*(RV-AV)/RV, RMSD = root mean square of deviations

Table A.2. Reproducibility of trace element data for in-house standard reference materials analysed by ICP-MS during the course of this study.

		51-97-011			94-077			UMPL-1			WA37916		
Sample	**DL**	**Mean**	**SD**	**CV**	**Mean**	**SD**	**CV**	**Mean**	**SD**	**CV**	**Mean**	**SD**	**CV**
Cs (ppm)	0.01	0.113	0.004	3.54	1.38	0.09	6.52	0.13	0.01	7.69	0.250	0.008	3.20
Rb	0.2	0.73	0.04	5.48	8.9	0.6	6.74	4.7	0.5	10.64	1.94	0.04	2.06
Sr	2.0	7	2	28.6	31.6	0.9	2.85	329	6	1.82	0.3	0.3	100
La	0.2	3.0	0.1	3.33	0.65	0.01	1.54	9.4	0.3	3.19	0.08	0.01	12.5
Ce	0.3	7.1	0.3	4.23	1.79	0.05	2.79	29.7	0.8	2.69	0.17	0.02	11.8
Pr	0.03	1.07	0.05	4.67	0.32	0.01	3.13	5.4	0.3	5.56	0.027	0.005	18.5
Nd	0.2	4.9	0.3	6.12	1.76	0.08	4.55	26	1	3.85	0.123	0.009	7.32
Sm	0.03	1.48	0.04	2.70	0.67	0.01	1.49	6.4	0.3	4.69	0.04	0.01	25.0
Eu	0.004	0.72	0.03	4.17	0.26	0.02	7.69	1.65	0.05	3.03	0.007	0.005	71.4
Gd	0.03	1.71	0.05	2.92	0.96	0.03	3.13	5.8	0.3	5.17	0.057	0.005	8.77
Tb	0.001	0.30	0.02	6.67	0.17	0.04	23.5	0.84	0.06	7.14	0.003	0.005	166
Dy	0.01	2.03	0.07	3.45	1.21	0.07	5.79	4.9	0.1	2.04	0.07	0.01	14.3
Ho	0.002	0.455	0.009	1.98	0.27	0.03	11.1	1.00	0.06	6.00	0.013	0.005	38.5
Er	0.006	1.32	0.04	3.03	0.81	0.05	6.17	2.71	0.07	2.58	0.053	0.005	9.43
Tm	0.004	0.19	0.01	5.26	0.12	0.01	8.33	0.39	0.02	5.13	0.003	0.005	166
Yb	0.01	1.25	0.04	3.20	0.80	0.06	7.50	2.32	0.05	2.16	0.070	0.008	11.4
Lu	0.001	0.198	0.004	2.02	0.12	0.02	16.7	0.37	0.03	8.11	0.003	0.005	166
Y	0.2	12.7	0.5	3.94	7.8	0.7	8.97	27.2	0.7	2.57	0.57	0.02	3.51
Zr	6.0	31	2	6.45	15	1	6.67	38	5	13.2	1.6	0.3	18.8
Nb	0.08	1.69	0.03	1.78	0.50	0.04	8.00	4.3	0.1	2.33			
Hf	0.01	1.07	0.06	5.61	0.54	0.06	11.1	1.55	0.10	6.45	0.050	0.008	16.00
Ta	0.3	0.110	0.007	6.36	0.03	0.03	100	0.20	0.03	15.0			
U	0.01	0.27	0.01	3.70				0.15	0.02	13.3			
Th	0.05	0.90	0.04	4.44	0.04	0.02	50	0.24	0.04	16.7			
n		4			6			9			4		
Average				5.15			13.2			6.29			43.6

DL = detection limit, Mean = average of n samples, SD = standard deviation about mean, CV = coefficient of variation = 100*SD/Mean

Bibliography and References

Abbott, D.H., Burgess. L., Longhi, J., and Smith, W.H.F., 1994. An empirical thermal history of the Earth's upper mantle, Journal of Geophysical Research, v. 99, 13,835-13,850.

Allègre, C.J., 1982. Genesis of Archaean komatiites in a wet ultramafic subducted plate. *In*: Arndt, N.T. and Nisbet, E.G. (Editors), Komatiites. Unwin and Allen, London, p. 495-500.

Anderson, D.L., 1994. Komatiites and picrites: evidence that the "plume" source is depleted. Earth and Planetary Science Letters, v. 128, p. 303-311.

Arndt, N.T., 1975. Ultramafic rocks of Munro Township and their volcanic setting. Unpublished PhD thesis. University of Toronto, 192 pp.

Arndt, N.T., 1976. Melting relations of ultramafic lavas (komatiites) at 1 atm and high pressure. Carnegie Institution of Washington Year Book, v. 75, p. 555-562.

Arndt, N.T., 1986. Differentiation of komatiite flows. Journal of Petrology, v. 27, p. 279-301.

Arndt, N.T., 1994. Archean komatiites; *in* Archean Crustal Evolution, edited by K.C. Condie, p. 11-40.

Arndt, N.T., Albarede, F., and Nisbet, E.G., 1997a. Mafic and ultramafic magmatism; *in* Greenstone Belts, edited by L. Ashwal and M.J. de Wit, Oxford Monographs on Geology and Geophysics, v. 35, p. 233-254.

Arndt, N.T., and Jenner, G.A., 1986. Crustally contaminated komatiites and basalts from Kambalda, Western Australia. Chemical Geology, v. 56, p. 229-255.

Arndt, N.T., and Lesher, C.M., 1992. Fractionation of REE by olivine and the origin of Kambalda komatiites. Geochimica et Cosmochimica Acta, v. 56, p. 4191-4204.

Arndt, N.T., and Nesbitt, R.W., 1982. Geochemistry of Munro Township basalts; *in* Komatiites, edited by N.T. Arndt, and Nisbet, E., p. 309-329.

Arndt, N.T., and Nisbet, E.G., 1982. What is a komatiite? *in* Komatiites, edited by N.T. Arndt, and Nisbet, E., p. 19-27.

Arndt, N.T., Kerr, A.C., and Tarney, J., 1997b. Dynamic melting in plume heads: the formation of Gorgona komatiites and basalts. Earth and Planetary Science Letters, v. 146, p. 289-301.

Arndt, N.T., Naldrett, A.J., and Pyke, D.R., 1977. Komatiitic and iron-rich tholeiitic lavas of Munro Township, northeast Ontario. Journal of Petrology, v. 18, p. 319-369.

Arndt, N.T., Teixeria, N.A., and White, W.M., 1989. Bizarre geochemistry of komatiites from the Crixás greenstone belt, Brazil. Contributions to Mineralogy and Petrology, v. 101, p. 187-197.

Arth, J.G., 1976. Behaviour of trace elements during magmatic processes – a summary of theoretical models and their applications. Journal of Research, United States Geological Survey, 4, p. 41-47.

Attoh, K., and Ekwueme, B.N., 1997. The West African Shield; *in* Greenstone Belts, edited by L. Ashwal and M.J. de Wit, Oxford Monographs on Geology and Geophysics, v. 35, p. 517-528.

Ayer, J.A. 1995. Precambrian geology, northern Swayze greenstone belt. Ontario Geological Survey, Report 297, 57 pp.

Ayer, J.A., Amelin, Y., Corfu, F., Ketchum, J., Kwok, K., and Trowell, N.F., 2002. Evolution of the southern Abitibi greenstone belt based on U-Pb geochronology: autochthonous volcanic construction followed by plutonism, regional deformation and sedimentation. Precambrian Research, v. 115, p. 63-95.

Ayer, J.A., Trowell, N.F., Amelin, Y., and Corfu, F., 1998. Project Unit 95-24. Geological compilation of the Abitibi greenstone belt in Ontario: toward a revised stratigraphy based on compilation and new geochronology results; *in* Summary of Field Work and Other Activities 1998, Ontario Geological Survey, Miscellaneous Paper 169, p. 14-24.

Ayer, J.A., Trowell, N.F., Madon, Z., Kamo, S., Kwok, Y.Y., and Amelin, Y., 1999. Compilation of the Abitibi greenstone belt in the Timmins-Kirkland Lake area: revisions to stratigraphy and new geochronology results; *in* Summary of Field Work and Other Activities 1999, Ontario Geological Survey, Open File Report 6000, p. 4-1 to 4-14.

Baars, F.J., 1997. The Sao Francisco Craton; *in* Greenstone Belts, edited by L. Ashwal and M.J. de Wit, Oxford Monographs on Geology and Geophysics, v. 35, p. 529-557.

Baird, A.M., 1999. Geochemistry of Chromites in Intrusive and Extrusive Komatiites in the Abitibi greenstone belt, Ontario; unpublished MSc thesis, University of Alabama, 189 pp.

Barley, M.E., 1997. The Pilbara Craton; *in* Greenstone Belts, edited by L. Ashwal and M.J. de Wit, Oxford Monographs on Geology and Geophysics, v. 35, p. 657-664.

Barling, J., and Goldstein, S.L., 1990. Extreme isotopic variations in Heard Island lavas and the nature of mantle reservoirs. Nature, v. 348, p. 59-62.

Barnes, S.-J., Gorton, M.P. and Naldrett, A.J., 1981. Grant 17; Platinum group elements in Abitibi komatites associated with Ni-sulphide deposits; *in* Geoscience Research Grant Program, Summary of Research 1980-1981, Ontario Geological Survey, Miscellaneous Paper 98, p. 1-11.

Barnes, S.-J., Naldrett, A.J., and Gorton, M.P., 1985. The origin of the fractionation of platinum-group elements in terrestrial magmas. Chemical Geology, v. 53, p.303-323.

Barnes, S.J., and Brand, N.W., 1999. The distribution Cr, Ni, and chromite in komatiites, and application to exploration for komatiite-hosted nickel sulphide deposits. Economic Geology, v. 94, p. 129-132.

Barnes, S.J., Hill, R.E.T., Perring, C.S., and Dowling, S.E., 1999. Komatiite flow fields and associated Ni-sulphide mineralization with examples from the Yilgarn Block, Western Australia. *In* Dynamic Processes in Magmatic Ore Deposits and their Application in Mineral Exploration, Geological Association of Canada, Short Course Volume 13, p. 159-194.

Barnes, S.-J., 1985. The petrography and geochemistry of komatiite flows from the Abitibi greenstone belt and a model for their formation. Lithos, v. 18, p. 241-270.

Barnes, S-J., and Naldrett, A.J., 1987. Fractionation of the platinum-group elements and gold in some komatiites of the Abitibi greenstone belt, northern Ontario. Economic Geology, v. 82, p. 165-183.

Barnes, S.-J., and Often, M., 1990. Ti-rich komatiites from northern Norway. Contributions to Mineralogy and Petrology, v. 105, p. 42-54.

Barnes, S.-J., Boyd, R., Korneliussen, A., Nilsson, L-P., Often, M., Pederson, R.B., and Robins, B., 1988. The use of mantle normalisation and metal ratios in discriminating between the effects of partial melting, crystal fractionation and sulphide segregation on platinum-group elements, Gold, Nickel and Copper: Examples from Norway. *in* Geoplatinum 87, edited by H.M. Pritchard, P.J. Potts, J.F.W Bowles, and S. Cribb, Elsevier, p. 113-143.

Barnes, S-J., Gorton, M.P., and Naldrett, A.J., 1983. A comparative study of olivine and clinopyroxene flows from Alexo, Abitibi greenstone belt, Ontario, Canada. Contributions to Mineralogy and Petrology, v. 83, p. 293-308.

Barrie, C.T., 1999. The Kidd-Munro Extension project. Year 3 Report. Unpublished report, 263 pp.

Barrie, C.T., 1999. Komatiite flows of the Kidd Creek footwall, Abitibi subprovince, Canada; *in* The Giant Kidd Creek Volcanogenic Massive Sulfide Deposit, Western Abitibi Subprovince, Canada, edited by M.D. Hannington and C.T. Barrie, Economic Geology Monograph 10, p. 143-161.

Barrie, C.T. and Corfu, F., 1999. The Kidd-Munro extension project: results of U-Pb geochronology for year 1. *In*: Summary of Field Work and Other Activities 1998, Ontario Geological Survey, Miscellaneous Paper 169, p. 74-81.

Barrie, C.T., Corfu, F., Davis, P.C., Coutts, A.C., and MacEachern, D., 1999. Geochemistry of the Dundonald komatiite-basalt suite and genesis of Dundeal Ni deposit, Abitibi Subprovince, Canada. Economic Geology, v. 94, p. 845-866.

Beattie, P., Ford, C., and Russell, D., 1991. Partition coefficients for olivine-melt and orthopyroxene-melt systems. Contributions to Mineralogy and Petrology, v. 109, p. 212-224.

Beattie, P., Ford, C., and Russell, D., 1993. Partition coefficients for olivine-melt and orthopyroxene-melt systems: Erratum. Contributions to Mineralogy and Petrology, v. 114, p. 288.

Beresford, S.W. and Cas, R.A.F, 2001. Komatiitic invasive lava flows, Kambalda, Western Australia. Canadian Mineralogist, v. 39, p. 525-536.

Beresford, S.W., Cas, R.A.F., Lambert, D.D., and Stone, W.E., 2000. Vesicles in thick komatiite lava flows, Kambalda, Western Australia. Journal Geological Society of London, v. 157, p. 11-14.

Beswick, A.E., 1982. Some geochemical aspects of alteration and genetic relations in komatiitic suites; *in* Komatiites, edited by N.T. Arndt, and Nisbet, E.G, p. 283-308.

Bickle, M. J., 1978a. Melting experiments on peridotitic komatiites. Progress in Experimental Petrology, NERC Progress Report 4, Series D, v. 11, p. 187-195.

Bickle, M.J., 1978b. Heat loss from the Earth: a constraint on Archean tectonics from the relation between geothermal gradients and the rate of plate production. Earth and Planetary Science Letters, v. 40, p. 301-315.

Bickle, M.J., 1982. The magnesium contents of komatiitic liquids; *in* Komatiites, edited by N.T. Arndt and E.G. Nisbet, George Allen and Unwin, London, p. 479-493.

Blenkinsop, T.G., Martin, A., Jelsma, H.A., and Vinyu, M.L., 1997. The Zimbabwe Craton; *in* Greenstone Belts, edited by L. Ashwal and M.J. de Wit, Oxford Monographs on Geology and Geophysics, v. 35, p. 567-580.

Blichert-Toft, J., and Arndt, N.T., 1999. Hf isotope compositions of komatiites. Earth and Planetary Science Letters, v. 171, p. 439-451.

Boehler, R., Chopelas, A., and Zerr, A., 1995. Temperature and chemistry of the core-mantle boundary. Chemical Geology, v. 120, p. 199-205.

Borg, G., and Shackleton, R.M., 1997. The Tanzania and NE-Zaire cratons; *in* Greenstone Belts, edited by L. Ashwal and M.J. de Wit, Oxford Monographs on Geology and Geophysics, v. 35, p. 608-619.

Brandt, G., and de Wit, M.J., 1997. The Kaapvaal Craton, South Africa; *in* Greenstone Belts, edited by L. Ashwal and M.J. de Wit, Oxford Monographs on Geology and Geophysics, v. 35, p. 581-607.

Brügmann, G.E., Arndt, N.T., Hofmann, A.W., and Tobschall, H.J., 1987. Noble metal abundances in komatiite suites from Alexo, Ontario and Gorgona Island, Columbia. Geochimica et Cosmochimica acta, v. 51, p. 2159-2169.

Brügmann, G.E., Naldrett, A.J., and Duke, J.M., 2000. The platinum-group element distribution in the Dumont Sill, Québec: Implications for the formation of Ni-sulfide mineralization. Mineralogy and Petrology, v. 42, p. 97-119.

Byerley, G.R., 1999. Komatiites of the Mendon Formation: Late-stage ultramafic volcanism in the Barberton Greenstone Belt. *in* Geologic Evolution of the Barberton Greenstone Belt, South Africa, edited by D.R. Lowe and G.R. Byerley, Geological Society of America, Special Paper, v. 329, p. 189-212.

Campbell, I.H., 2000. The mantle's chemical structure; in The Earth's Mantle: Composition, Structure, and Evolution, edited by I. Jackson, Cambridge University Press, p. 259-305.

Campbell, I.H., and Naldrett, A.J., 1979. The influence of silicate:sulphide ratios on the geochemistry of magmatic sulphides. Economic Geology, v. 74, p. 1503-1505.

Campbell, I.H., and Griffiths, R.W., 1990. Implications of mantle plume structure for the evolution of flood basalts. Earth and Planetary Science Letters, v. 99, p. 79-93.

Campbell, I.H., Griffiths, R.W., and Hill, R.I., 1989. Melting in an Archaean mantle plume: heads it's basalts and tails it's komatiites. Nature, v. 339, p. 697-699.

Campbell, I.H., Lesher, C.M., Coad, P., Franklin, J.M., Gorton, M.P., and Thurston, P.C., 1984. Rare earth element mobility in alteration pipes below massive Cu-Zn sulphide deposits. Chemical Geology, v. 45, p. 181-202.

Campbell, I.H., Naldrett, A.J., and Barnes, S.J., 1983. A model for the origin of the platinum-rich sulfide horizons in the Bushveld and Stillwater complexes. Journal of Petrology, v. 24, p.133-165.

Carlson, R.W., 1991. Physical and chemical evidence on the cause and characteristics of flood basalt volcanism. Australian Journal of Earth Sciences, v. 38, p. 525-544.

Cattell, A., and Arndt, N., 1987. Low- and high-alumina komatiites from a Late Archean sequence, Newton Township, Ontario. Contributions to Mineralogy and Petrology, v. 97, p. 218-227.

Chauvel, C., Dupre, B., and Jenner, G.A., 1985. The Sm-Nd age of Kambalda volcanics is 500 Ma too old! Earth and Planetary Science Letters, v. 74, p. p.315-324.

Coad, P.R., 1979. Nickel sulphide deposits associated with ultramafic rocks of the Abitibi Belt and economic potential of mafic-ultramafic intrusions; Ontario Geological Survey, Study 20, 84 pp.

Coffin, M.F., and Eldholm, O., 1994. Large igneous provinces: crustal structure, dimensions, and external consequences. Reviews of Geophysics, v. 32, p. 1-36.

Condie, K.C., 1992. Chemical composition and evolution of the upper continental crust: contrasting results from surface samples and shales. Chemical Geology, v. 104, p. 1-37.

Corfu, F., and Noble, S.R., 1992. Genesis of the southern Abitibi greenstone belt, Superior Province, Canada: Evidence from zircon Hf isotope analyses using a single filament technique. Geochimica et Cosmochimica Acta, v. 56, p., 2081-2097.

Crocket, J.H., and MacRae, W.E., 1986. Platinum-group element distribution in komatiitic and tholeiitic volcanic rocks from Munro Township, Ontario. Economic Geology, v. 81, p. 1242-1251.

Dann, J.C., 2001. Vesicular komatiites, 3.5-Ga Komati Formation, Barberton Greenstone Belt, South Africa: inflation of submarine lavas and origin of spinifex zones. Bulletin of Volcanology, v. 63, p. 462-481.

Davies, G.F., 1999. Dynamic Earth: Plates, Plumes and Mantle Convection, Cambridge University Press, 464 pp.

Davis, P.C., 1997. Volcanic Stratigraphy in the Abitibi greenstone belt, Dundonald and Munro Townships, Ontario. Unpublished MSc thesis, University of Alabama, 201 pp.

Davis, P.C. (Editor), 1999. Classic komatiite localities and magmatic Fe-Ni-Cu-(PGE) sulphide deposits of the Abitibi Greenstone Belt, Ontario-Québec. International Geology Correlation Program, Project 427, Dynamic processes in ore-forming magmatic systems, Mineral Exploration Research Centre Guidebook 1, 70 pp.

Dalziel, I.W.D., Lawver, L.A., and Murphy, J.B., 2001. Plumes, orogenesis and supercontinental fragmentation. Earth and Planetary Science Letters, v. 178, p. 1-11.

Deer, W.A., Howie, R.A., and Zussman, J., 1992. An introduction to the rock-forming minerals. Longman Scientific Technical, London, 696 pp.

Dickin, A.P., 1995. Radiogenic Isotope Geology, Cambridge University Press, Cambridge, 490 pp.

Dimroth, E., Imreh, L., Rocheleau, M. and Goulet, M., 1982. Evolution of the south-central segment of the Archean Abitibi belt, Quebec. Part 1: stratigraphy and paleogeographic model. Canadian Journal of Earth Sciences, v. 19, p. 1729-1758.

Donaldson, C.H., 1982. Spinifex-textured komatiites: a review of textures, mineral compositions and layering; *in* Komatiites, Allen and Unwin, edited by N.T. Arndt and E. Nisbet, p. 213-245.

Donaldson, C.H., 1984. Pyroxene accumulation in spinifex-textured rocks. Geological Magazine, v. 121, p. 650.

Donaldson, M.J., Lesher, C.M., Groves, D.I., and Gresham, J.J., 1986. Comparison of Archean dunites and komatiites associated with nickel mineralisation in Western Australia: implications for dunite genesis. Mineralium Deposita, v. 21, p. 296-305.

Dostal, J., and Mueller, W.U., 1997. Komatiitic flooding of a rifted Archean rhyolitic arc complex: geochemical signatures and tectonic significance of the Stoughton-Roquemaure Group, Abitibi greenstone belt, Canada. The Journal of Geology, v. 105, p. 545-563.

Duke, J.M., 1979. Computer simulation of the fractionation of olivine sulfide from mafic ultramafic magmas. Canadian Mineralogist, v. 17, p. 507-514.

Duke, J.M., 1986. Petrology and Economic Geology of the Dumont Sill: An Archean Intrusion of Komatiitic Affinity in Northwestern Quebec. Economic Geology Report 35, Geological Survey of Canada, Ottawa, 56 pp.

Duke, J.M., and Naldrett, A.J., 1978. A numerical model of the fractionation of olivine molten sulfide from komatiite magma. Earth and Planetary Science Letters, v. 39, p. 255-266.

Eakins, P.R., 1972. Canton de Roquemaure, Comte d'Abitibi-Ouest. Quebec Department Mines, Geology Report, P.R.150, 72 pp.

Echeverria, L.M., 1982. Komatiites from Gorgona Island, Colombia; *in* Komatiites, edited by N.T. Arndt, and Nisbet, E., p. 199-209.

Echeverria, L.M., and Aitken, B.G., 1986. Pyroclastic rocks: another manifestation of ultramafic volcanism on Gorgona Island, Colombia. Contributions to Mineralogy and Petrology, v. 92, p. 428-436.

Eckstrand, O.R, and Williamson, B.L., 1985. Vesicles in the Dundonald komatiites; Geological Association of Canada – Mineralogical Association of Canada Annual Meeting, Program and Abstracts, v. 10, p. A-16.

Fan, J., and Kerrich, R., 1997. Geochemical characteristics of aluminum depleted and undepleted komatiites and HREE-enriched low-Ti tholeiites, western Abitibi greenstone belt: A heterogeneous mantle plume-convergent margin environment. Geochimica et Cosmochimica Acta, v. 61, p. 4723-4744.

Faure, G., 1986. Principles of Isotope Geology, New York, J. Wiley & Sons, 589 pp.

Feng, R., Kerrich, R., and Maas, R., 1993. Geochemical, oxygen, and neodymium isotope compositions of metasediments from the Abitibi greenstone belt and Pontiac Subprovince, Canada: evidence for ancient crust and Archean terrane juxtaposition. Geochimica et Cosmochimica Acta, v. 57, p. 641-658.

Ferreira-Filho, C.F., Lesher, C.M., and Araujo, S.M., submitted, Geochemistry of the komatiite-associated Boa Vista nickel sulphide deposit, Crixás, central Brazil. Economic Geology.

Fleet, M.E., and Macrae, N.D., 1975. A spinifex textured rock from Munro Township. Canadian Journal of Earth Sciences, v. 12 , p. 928-939.

Francis, D., Ludden, J., Johnstone, R., and Davis, W., 1999. Picrite evidence for more Fe in Archean mantle reservoirs. Earth and Planetary Science Letters, v. 167, p. 197-213.

Fujimaki, H., Tatsumoto, M., and Aoki, K., 1984. Partition coefficients of Hf, Zr and REE between phenocrysts and groundmass. Journal of Geophysical Research, p. B662-B672.

Gelinas, L., Lajoie, J., and Brooks, C., 1977. The origin and significance of Archean ultramafic volcaniclastics from Spinifex Ridge, La Motte Township. Geological Association of Canada, Special Paper 16, p. 297-309.

Ghomshei, M.M., Arkani-Hamed, J., Strangway, D.W., and Russel, R.D., 1990. Underplating of oceanic lithosphere in the Archean: a possible mechanism for the formation of Archean komatiites. Tectonophysics, v. 172, p. 291-302.

Gibson, S.A., Thompson, R.N., and Dickin, A.P., 2000. Ferropicrites: geochemical evidence for Fe-rich streaks in upwelling mantle plumes. Earth and Planetary Science Letters, v. 174, p. 355-374.

Govindaraju, K., 1994. Compilation of working values and sample description for 383 geostandards. Geostandards Newsletter, v. 18, 158 p.

Green, A.H., and Naldrett, A.J., 1981. Langmuir volcanic peridotite-associated nickel deposits, Canadian equivalents of the Western Australian occurrences. Economic Geology, v. 76, p. 1503-1523.

Green, D.H., 1975. Genesis of Archean peridotitic magmas and constraints on Archean thermal gradients and tectonics. Geology, v. 3, p. 15-18.

Gresham, J.J., and Loftus-Hills, G.D., 1981. The geology of the Kambalda nickel field, Western Australia. Economic Geology, v. 76, p. 1373-1416.

Grove, T.L., de Wit, M.J., and Dann, J.C., 1997. Komatiites from the Komati type section, Barberton, South Africa; *in* Precambrian Greenstone Belts, edited by L. Ashwal and M.J. de Wit, Oxford Monographs on Geology and Geophysics, v. 35, p. 438-453.

Groves, D.I., and Batt, W.D., 1984. Spatial and temporal variations of Archaean metallogenic associations in terms of evolution of granitoid- greenstone terrains with particular emphasis on the Western Australian Shield; *in* Archean Geochemistry, edited by Kroner, A., Hanson, G.N., and Goodwin, A.M., Springer-Verlag, Berlin, p. 73-98.

Groves, D.I., Barrett, F.M., and McQueen, K., 1979. The relative roles of magmatic segregation, volcanic exhalation, and regional metamorphism in the generation of volcanic-associated nickel ores of Western Australia. Canadian Mineralogist, v. 17, p. 319-336.

Gruau, G., Tourpin, S., Fourcade, S., and Blais, S., 1992. Loss of isotopic (Nd, O) and chemical (REE) memory during metamorphism of komatiites: new evidence from eastern Finland. Contributions to Mineralogy and Petrology, v. 112, p. 66-82.

Hamilton, W.B., 1998. Archean tectonics and magmatism. International Geology Reviews, v. 40, p. 1-39.

Hanksi, E., Huhma, H., Rastas, P., and Kamenetsky, V.S., 2001. The Palaeoproterozoic komatiite-picrite association of Finnish Lapland. Journal of Petrology, v. 42, p. 855-876.

Hanski, E.J., 1992. Petrology of the Pechenga ferropicrites and cogenetic, Ni-bearing gabbro-wehrlite intrusions, Kola Peninsula, Russia. Geological Survey Finland, Bulletin 367, 192 pp.

Heather, K.B., 1998. New insights on the stratigraphy and structural geology of the southwestern Abitibi greenstone belt: Implications for the tectonic evolution and setting of mineral deposits in the Superior Province; *in* The first age of giant ore formation: stratigraphy, tectonics and mineralization in the Late Archean and Early Proterozoic, Papers presented at the Prospectors and Developers Association of Canada Annual Convention, Toronto, p. 63-101.

Heather, K.B. and Shore, G.T., 1999. Geology Swayze Greenstone Belt, Ontario. Geological Survey of Canada, Open File 3384a (Sheet 1). Scale 1: 50 000.

Herzberg, C.T., and O'Hara, M.J., 1985. Origin of mantle peridotite and komatiite by partial melting. Geophysical Research Letters, v. 12, p. 541-544.

Herzberg, C.T., and O'Hara, M.J., 1998. Phase equilibrium constraints of the origin of basalts, picrites and komatiites. Earth Science Reviews, v. 44, p. 39-79.

Herzberg, C.T., Fyfe, W.S., and Carr, M.J., 1983. Density constraints on the formation of the continental Moho and crust. Contributions to Mineralogy and Petrology, v. 84, p. 1-5.

Hill, R.E.T., Barnes, S. J., Gole, M. J., and Dowling, S.E., 1990. Physical volcanology of komatiites: a field guide to the komatiites of Norseman-Wiluna Greenstone Belt, Eastern Goldfields Province, Yilgarn Block, Western Australia; Excursion Guide Book - Geological Society of Australia, v. 1, 100 pp.

Hill, R.E.T., Barnes, S.J., Gole, M.J., and Dowling, S.E., 1995. The volcanology of komatiites as deduced from field relationships in the Norseman-Wiluna greenstone belt, Western Australia. Lithos, v. 34, p. 159-188.

Hill, R.I., 1993. Mantle plumes and continental tectonics. Lithos, v. 30, p. 193-206.

Hollings, P., and Kerrich, R., 1999. Trace element systematics of ultramafic and mafic volcanic rocks from the 3 Ga North Caribou greenstone belt, northwestern Superior Province. Precambrian Research, v. 93, p. 257-279.

Hollings, P., Wyman, D., and Kerrich, R., 1999. Komatiite-basalt-rhyolite volcanic associations in northern Superior Province greenstone belts: significance of plume-arc interaction in the generation of the proto continental Superior Province. Lithos, v. 46, p. 137-161.

Hollings, P., 2002. Archean Nb-enriched basalts in the northern Superior Province. Lithos, v. 64, p. 1-14.

Hollings, P., and Wyman, D., 1999. Trace element and Sm-Nd systematics of volcanic and intrusive rocks from the 3 Ga Lumby Lake greenstone belt, Superior Province; evidence for Archean plume-arc interaction. Lithos, v. 46, p. 189-213.

Hollings, R., and Kerrich, R., 2000. An Archean arc basalt-Nb-enriched basalt-adakite association; the 2.7 Ga Confederation assemblage of the Birch-Uchi greenstone belt, Superior Province. Contributions to Mineralogy and Petrology, v. 139, p. 208-226.

Houlé, M.G., Lesher, C.M., Gibson, H.L., and Sproule, R.A., 2002. Project Unit 99-021. Recent advances in komatiites volcanology in the Abitibi greenstone belt. Ontario Geological Survey, Open File Report 6100, p. 7-1 to 7-19.

Houlé, M., Lesher, C.M., Gibson, H.L., Fowler, A.D., and Sproule, R.A., 2001. Project Unit 99-021. Physical volcanology of komatiites in the Abitibi greenstone belt. Ontario Geological Survey, Open File Report 6070, p. 13-1 to 13-17.

Houlé, M., Lesher, C.M., Fowler, A.D., Gibson, H.L., Sproule, R.A., Ayer J.A., and Thurston, P.C., 2000. Project Unit 99-021. Physical volcanology and metallogenesis of komatiites in the Abitibi greenstone belt, Superior Province, Canada. Ontario Geological Survey, Open File Report 6032, p. 11-1 to 11-8.

Howe, J.M., Easton, R.M., Grunsky, E.C., Jensen, L.S., and Thurston, P.C., 1987. Komatiite database, Parts I and II; Ontario Geological Survey, Open File Report 5677.

Huppert, H.E., and Sparks, R.S.J., 1985. Komatiites I: eruption and flow. Journal of Petrology, v. 26, p. 694-725.

Huppert, H.E., and Sparks, R.S.J., 1984b. Cooling and contamination of mafic and ultramafic magmas during ascent through continental crust. Earth and Planetary Science Letters, v. 74, p. 371-386.

Huppert, H.E., Sparks, R.S.J., Turner, J.S., and Arndt, N.T., 1984. Emplacement and cooling of komatiitic lavas. Nature, v. 309, p. 19-22.

Imreh, L., 1974. Utilization of ultrabasic extrusions in mining research; structural outline and lithostratigraphy of La Motte, eastern Abitibi, Quebec, Canada. Bulletin Volcanology, v. 38, p. 291-314.

Inoue, T., 1994. Effect of water on melting phase relations and melt composition in the system Mg_2SiO_4-$MgSiO_3$-H_2O up to 15 GPa. Physics of the Earth and Planetary Interiors, v. 85, p. 237-263.

Isley, A.E., and Abbott, D.H., 1999. Plume-related volcanism and deposition of banded iron formation. Journal of Geophysical Research, B 104, 461-477.

Jackson, S.L., and Fyon, A.J., 1991. The western Abitibi subprovince in Ontario; *in* Geology of Ontario, edited by P.C. Thurston, H.R. Williams, R.H. Sutcliffe and G.M. Stott, Ontario Geological Survey, Special Volume 4, p. 405-482.

Jackson, S.L., and Sutcliffe, R.H., 1990. Central Superior Province geology: evidence for an allochthonous, ensimatic, southern Abitibi greenstone belt. Canadian Journal of Earth Sciences, v. 27, p. 582-589.

Jackson, S.L., Fyon, A.J., and Corfu, F., 1994. Review of Archean supracrustal assemblages of the southern Abitibi greenstone belt in Ontario, Canada: products of microplate interaction within large-scale plate-tectonic setting. Precambrian Research, v. 65, p. 183-205.

Jahn, B-M., Gruau, G., and Glikson, A.Y., 1982. Komatiites of the Onverwacht Group, S. Africa: REE geochemistry, Sm/Nd age and mantle evolution. Contributions to Mineralogy and Petrology, v. 80, p. 25-40.

Jensen, L.S., 1976. Regional stratigraphy and structure of the Timmins-Kirkland Lake area, districts of Cochrane and Timiskaming, and Kirkland Lake area, District of Timiskaming. Ontario Geological Survey, Miscellaneous Paper no.67, p. 87-95.

Jensen, L.S., 1981. A petrogenetic model for the Archaean Abitibi Belt in the Kirkland Lake area, Ontario. Unpublished PhD thesis, University of Saskatchewan, 520 pp.

Jensen, L.S., 1985. Stratigraphy and petrogenesis of Archean metavolcanic sequences, southwestern Abitibi Subprovince, Ontario; *in* Evolution of Archean Supracrustal Sequences, edited by L. D. Ayres, P. C. Thurston, K. D. Card and W. Weber, Geological Society of Canada, Special Paper 28, p. 65-87.

Jensen, L.S., 1992. Geology of McNeil and Robertson Townships, Ontario Geological Survey, Miscellaneous Paper 160, p. 53-59.

Jensen, L.S., 1993. Project Unit 93-06: Geology of Cleaver and Hincks Townships. Ontario Geological Survey, Miscellaneous Paper 162, p. 41-45.

Jensen, L.S., and Langford, F.F., 1985. Geology and petrogenesis of the Archean Abitibi belt in the Kirkland Lake area, Ontario. Ontario Geological Survey, Miscellaneous Paper 123, 130 pp.

Jochum, K.P., Arndt, N.T., and Hofmann, A.W., 1991. Nb-Th-La in komatiites: constraints on komatiite petrogenesis mantle evolution. Earth and Planetary Science Letters, v. 107, p. 272-289.

Johnstone, R., 1987. Geology of the Stoughton-Roquemaure Group, Beatty and Munro Townships, Northeastern Ontario; unpublished M.Sc. Thesis, Carleton University, 325 pp.

Keays, R.R., Nickel, E.H., Groves, D.I. and McGoldrick, P.J., 1982. Iridium and palladium as discriminants of volcanic exhalative, hydrothermal and magmatic nickel sulfide mineralization. Economic Geology, v. 77, p. 1535-1547.

Kerrich, R., and Xie, Q., 2002. Composition recycling structure of an Archean super-plume; Nb-Th-U-LREE systematics of Archean komatiites and basalts revisited. Contributions to Mineralogy and Petrology, v, 142, p. 476-484.

Kerrich, R., Polat, A., Wyman, D., and Hollings, P., 1999a. Trace element systematics of Mg-, to Fe-tholeiitic basalt suites of the Superior Province; implications for Archean mantle reservoirs and greenstone belt genesis. Lithos, v. 46, p. 163-187.

Kerrich, R., Wyman, D., Hollings, P., and Polat, A., 1999b. Variability of Nb/U and Th/La in 3.0 to 2.7 Ga Superior Province ocean plateau basalts; implications for the timing of continental growth and lithosphere recycling. Earth and Planetary Science Letters, v. 168, p. 101-115.

Kinzler, R. J., and Grove, T. L., 1985. Crystallization and differentiation of Archean komatiite lavas from northeast Ontario: phase equilibrium and kinetic studies. American Mineralogist, v. 70, p. 40-51.

Krapez, B., and Eisenlohr, B., 1998. Tectonic settings of Archaean (3325-2775 Ma) crustal-supracrustal belts in the West Pilbara Block. Precambrian Research, v. 88, p. 173-205.

Kushev, V.G., 1997. The Inari-Kola Craton; *in* Greenstone Belts, edited by L. Ashwal and M.J. de Wit, Oxford Monographs on Geology and Geophysics, v. 35, p. 707-709.

Kushev, V.G., and Kornilov, M.F., 1997. The Ukranian Shield; *in* Greenstone Belts, edited by L. Ashwal and M.J. de Wit, Oxford Monographs on Geology and Geophysics, v. 35, p. 726-729.

Lafrance, I., 2001. Caractérisation des minéralisations nickélifères associées aux komatiites de la ceinture archéenne de Vénus, Noveau-Québec. Mémoire de maîtrise, Université du Québec à Montréal, Canada, 185 pp.

Lahaye, Y., and Arndt, N.T., 1996. Alteration of a komatiite flow from Alexo, Ontario, Canada. Chemical Geology, v. 126, p. 1448-1458.

Lahaye, Y., Arndt, N.T., Byerley, G., Chauvel, C., Fourcade, S., and Gruau, G., 1995. The influence of alteration on the trace-element and Nd isotopic compositions of komatiites. Chemical Geology, v. 126, p. 43-64.

Lahaye, Y., Barnes, S-J., Frick, L.R., and Lambert, D.D., 2001. Re-Os isotopic study of komatiitic volcanism and magmatic sulphide formation in the southern Abitibi greenstone belt, Ontario, Canada. The Canadian Mineralogist, v. 39, p. 473-490.

Larsen, L.M., and Pedersen, A.K, 2000. Processes in high-Mg, high-Ti magmas: evidence from olivine, chromite, and glass in Palaeogene picrites from West Greenland. Journal of Petrology, v. 41, p. 1071-1098.

Larson, M.S., 1996. Physical volcanology and petrogenesis of intrusive and extrusive komatiites in the Shaw Dome area, Abitibi greenstone belt, Ontario, Canada; MSc thesis, University of Alabama, Tuscaloosa, United States, 259 pp.

Lesher, C.M., 1989. Komatiite-associated nickel sulphide deposits. Reviews in Economic Geology, v. 4, p. 44-101.

Lesher, C.M., and Burnham, O.M., 1999. Mass balance and mixing in dynamic ore-forming magmatic systems; *in* Keays, R.R., Lesher, C.M., Lightfoot, P.C., and Farrow, C.E.G. (Editors), Dynamic Processes in Magmatic Ore Deposits and their Application to Mineral Exploration, Geological Association of Canada Short Course, v. 13, p. 413-449.

Lesher, C.M., and Burnham, O.M., 2001. Multicomponent elemental and isotopic mixing in Ni-Cu-(PGE) ores at Kambalda, Western Australia. Canadian Mineralogist, v. 39, p. 421-446.

Lesher, C.M., and Groves, D.I., 1984. Geochemical and mineralogical criteria for the identification of mineralized komatiites in Archaean greenstone belts of Australia; *in* Petrology: Igneous and Metamorphic Rocks, Proceedings of the 27th International Geological Congress, Volume 9, VNU Science Press, Utrecht, p. 283-302.

Lesher, C.M., and Keays, R.R., 2002. Komatiite-Associated Ni-Cu-(PGE) Deposits: Mineralogy, Geochemistry, and Genesis; *in* L.J. Cabri (Editor), The Geology, Geochemistry, Mineralogy, and Mineral Beneficiation of the Platinum-Group Elements, Canadian Institute of Mining, Metallurgy and Petroleum, Special Volume 54, p. 579-617.

Lesher, C.M., and Stone, W.E., 1996. Exploration geochemistry of komatiites; *in* Igneous Trace Element Geochemistry: Applications for Massive Sulphide Exploration, Geological Association of Canada, Short Course v. 12, p. 153-204.

Lesher, C.M., Arndt, N.T., and Groves, D.I., 1984. Genesis of komatiite-hosted nickel-sulphide deposits at Kambalda, Western Australia: a distal volcanic model; *in* Buchanan, D.J., and Jones, M.J. (Editors), Sulphides in Mafic and Ultramafic Rocks, Institution of Mining and Metallurgy, London, p. 70-80.

Lesher, C.M., Burnham, O.M., Keays, R.R., and Hulbert, L., 1999. Geochemical discrimination of barren and mineralized komatiites in dynamic ore-forming magmatic systems; *in* Keays, R.R., Lesher, C.M., Lightfoot, P.C., and Farrow, C.E.G. (Editors), Dynamic Processes in Magmatic Ore Deposits and their Application to Mineral Exploration, Geological Association of Canada Short Course, v.13, p. 451-477.

Lesher, C.M., Burnham, O.M., Keays, R.R., Barnes, S.J., and Hulbert, L., 2001. Geochemical discrimination of barren and mineralized komatiites associated with magmatic Ni-Cu-(PGE) sulphide deposits. Canadian Mineralogist, v. 39, p. 673-696.

Lesher, C.M., Stone, W.E., and Arndt, N.T., 1997. Nd isotope geochemistry of komatiites in the Abitibi-Pontiac greenstone belt. Geological Association of Canada-Mineralogical Association of Canada Annual Meeting, Ottawa, Program with Abstracts, v. 22, p. A88.

Lesher, C.M. and Campbell, I.H., 1993. Geochemical and fluid dynamic modelling of compositional variations in Archean komatiite-hosted nickel sulfide ores in Western Australia. Economic Geology, v. 88, p.804-816.

Lesher, C.M., 1983. Localization and genesis of komatiite-hosted Fe-Ni-Cu sulphide mineralization at Kambalda, Western Australia. Unpublished PhD thesis, University of Western Australia, 319pp.

Lesher, C.M., and Arndt, N.T., 1995. REE and Nd isotope geochemistry, petrogenesis and volcanic evolution of contaminated komatiites at Kambalda, Western Australia. Lithos, v.34, p.127-157.

Lesher, C.M., Lee, R.F., Groves, D.I., Bickle, M.J., and Donaldson, M.J., 1981. Geochemistry of komatiites from Kambalda, Western Australia: I. Chalcophile element depletion – a consequence of sulfide liquid separation from komatiitic magmas. Economic Geology, v.76, p. 1714-11728.

Lewis, J.D., and Williams, I.R., 1973. The petrology of an ultramafic lava near Murphy Well, Eastern Goldfields, Western Australia. Annual Report - Western Australia, Geological Survey, v. 73, pp.60-68.

Lowe, D.R., 2000. Petrology and sedimentology of cherts and related silicified sedimentary rocks in the Swaziland Supergroup. Special Paper - Geological Society of America, v. 329, p. 83-114.

Ludden, J.N., and Gélinas, L., 1982. Trace element characteristics of komatiites and komatiitic basalts from the Abitibi metavolcanic belt of Quebec; *in* Arndt, N. T., and Nisbet, E. G., eds., Komatiites: London, Allen & Unwin, p. 331-346.

Ludden, J., Hubert, C., and Gariépy, C., 1986. The tectonic evolution of the Abitibi greenstone belt of Canada. Geological Magazine, v. 123, p. 153-166.

Machado, N., Brooks, C., and Hart, S.R., 1986. Determination of initial $^{87}Sr/^{86}Sr$ and $^{143}Nd/^{144}Nd$ in primary minerals from mafic and ultramafic rocks: experimental procedure and implications for the isotopic characteristics of the Archean mantle under the Abitibi greenstone belt. Geochimica et Cosmochimica Acta, v. 50, p. 2335-2348.

Madore, L. and Larbi, Y., 2000. Géologie de la région de la rivière Arnaud (SNRC 25D) et des régions littorales adjacentes (SNRC 25C, 25E et 25F). Ministère des Ressources naturelles, Québec; RG 2000-05, 37 pages.

Mathez, E.A., 1999. Factors controlling the concentrations of platinum-group elements in layered intrusions and chromitites; *in* Keays, R.R., Lesher, C.M., Lightfoot, P.C., and Farrow, C.E.G. (Editors), Dynamic Processes in Magmatic Ore Deposits and their Application to Mineral Exploration, GAC Short Course Notes, v. 13, p. 251-286.

Maurice, C., and Francis, D., 2000. Archean volcanism in the NE Superior Province; Géologie Québec, Geological Research Information Seminar, Program with Abstracts, p. 14.

McCulloch, M.T., and Bennett, V. C., 2000. Early differentiation of the Earth: An isotopic perspective; *in* The Earth's Mantle: Composition, Structure, and Evolution, edited by I. Jackson, Cambridge University Press, p. 127-158.

McDonough, W.F., and Sun, S-S., 1995. The composition of the earth. Chemical Geology, v. 120, p. 223-253.

Meijer, A., Tsung-Tak, K., and Tilton, G.R., 1990. U-Th-Pb partitioning behavior during partial melting in the upper mantle: implications for the origin of high mu components and the "Pb paradox". Journal of Geophysical Research, v. 95, p. 433-448.

Mueller, W.U., Pilote, P., and Daigneault, R., 1999. Évolution et contexte géodynamique du bloc de Malartic, zone volcanique sud, sous-province de l'Abitibi. *In*: Séminaire d'information sur la recherche géologique, Programme et Résumés, MRN, DV-99-03, 20.

Muir, J.E., and Comba, C.D.A., 1979. The Dundonald deposit: an example of volcanic-type nickel-sulphide mineralization. The Canadian Mineralogist, v. 17, p. 351-359.

Muir, T.L., 1979. Discrimination between extrusive and intrusive Archean ultramafic rocks in the Shaw Dome area using selected major and trace elements. Canadian Journal of Earth Sciences, v. 16, p.80-90.

Murck, B.W., and Campbell, I.H., 1986. The effects of temperature, oxygen fugacity and melt composition on the behaviour of chromium in basic and ultrabasic melts. Geochimica et Cosmochimica Acta, vl.50, p. 1871-1887.

Myers, J.S., and Swager, C., 1997. The Yilgarn Craton, Australia; *in* Greenstone Belts, edited by L. Ashwal and M.J. de Wit, Oxford Monographs on Geology and Geophysics, v. 35, p. 640-656.

Naldrett, A.J., and Gasparini, E.L., 1971. Archaean nickel sulphide deposits in Canada: Their classification, geological setting and genesis with some suggestions as to exploration; *in* The Archaean Rocks, edited by Glover, J.E., Proceedings of the First Symposium on Archaean Rocks, Special Publication 3, Geological Society of Australia, Adelaide, p. 331-347.

Naldrett, A.J., and Turner, A.R., 1977. The geology and petrogenesis of a greenstone belt and related nickel sulphide mineralization at Yakabindie, Western Australia. Precambrian Research, v. 5, p. 43-103.

Naldrett, A. J., 1989. Magmatic sulfide deposits; Oxford Monographs on Geology and Geophysics, v.14, 186p.

Naldrett, A.J., and Barnes, S.J., 1986. The behavior of platinum group elements during fractional crystallization and partial melting with special reference to the composition of magmatic sulfide ores. Fortschritte der Mineralogie, v. 64, p. 113-133.

Nesbitt, R.W., and Sun, S.S., 1976. Geochemistry of Archean spinifex textured peridotites and magnesian and low magnesian tholeiites. Earth and Planetary Science Letters, v. 31, p. 433-453.

Nesbitt, R.W., Sun, S-S., and Purvis, A.C., 1979. Komatiites: geochemistry and genesis. Canadian Mineralogist, v. 17, p. 165-186.

Nisbet, E.G., 1982. The tectonic setting and petrogenesis of komatiites; *in* Komatiites, edited by N.T. Arndt, and Nisbet, E., p. 501-526.

Nisbet, E.G., and Chinner, G.A., 1981. Controls on the eruption of mafic and ultramafic lavas, Ruth Well Ni-Cu prospect, West Pilbara. Economic Geology, v. 76, p. 1729-1735.

Nisbet, E.G., Cheadle, M.J., Arndt, N.T., and Bickle, M.J., 1993. Constraining the potential temperature of the Archean mantle: a review of evidence from komatiites. Lithos, v. 30, p. 291-307.

O'Hanley, D.S., 1997. Serpentinites and rodingites as records of metasomatism and fluid history. Oxford Monographs on Geology and Geophysics, v. 35, p. 164-175.

Ohmoto, H., 1986. Stable isotope geochemistry of ore deposits; *in* J.W. Valley, H.P. Taylor, and J.R. O'Neil (Editors), Stable Isotopes in High Temperature Geological Processes, Reviews in Mineralogy, v. 16, Mineralogical Society of America, p. 491-559.

Ohtani, E., 1990. Majorite fractionation and the genesis of komatiites in the deep mantle. Precambrian Research, v. 48, p., 195-202.

Oliver, H.S., Hughes, D.J., Hall, R.P., and Johns, G.W., 2000. Project Unit 98-15: lithogeochemistry of the Shining Tree area. Ontario Geological Survey, Open File Report 6032, p. 6.1-6.14.

Oliver, H.S., Hughes, D.J., Hall, R.P., Thurston, P.C., and Johns, G.W., 1999. The mafic and ultramafic volcanic rocks of the Shining Tree greenstone belt, northeastern Ontario, Canada. Ontario Geological Survey, Open File Report 6000, p. 11.1-11.12.

Ontario Geological Survey, 2001. Whole rock lithogeochemical data of prospective versus barren volcanic belts for volcanogenic massive sulphide (VMS) deposits, Superior Province, Ontario: Operation Treasure Hunt. Ontario Geological Survey, Miscellaneous Release-Data 85.

Parman, S.W., Dann, J.C., Grove, T.L., and deWit, M.J., 1997. Emplacement conditions of komatiite magmas from the 3.49 Ga Komati Formation, Barberton greenstone belt, South Africa. Earth and Planetary Science Letters, v. 150, p. 303-323.

Peach, C. L., Mathez, E. A., and Keays, R. R., 1990. Sulphide melt-silicate melt distribution coefficients for noble metals and other chalcophile elements as deduced from MORB: implications for partial melting. Geochimica et Cosmochimica Acta, v. 54, p. 3379-3389.

Perring, C.S., Barnes, S.J., and Hill, R.E.T., 1995. The physical volcanology of Archaean komatiite sequences from Forrestania, Southern Cross Province, Western Australia. Lithos, v. 34, p. 189-207.

Perring, C.S., Barnes, S.J., and Hill, R.E.T., 1996. Geochemistry of komatiites from Forrestania, Southern Cross Province, Western Australia: Evidence for crustal contamination. Lithos, v. 37, p. 181-197.

Polat, A., and Kerrich, R., 2000. Archean greenstone belt magmatism and the continental growth-mantle evolution connection: constraints from Th-U-Nb-LREE systematics of the 2.7 Ga Wawa Subprovince, Superior Province, Canada. Earth and Planetary Science Letters, v. 175, p. 41-54.

Polat, A., and Kerrich, R., 2001. Geodynamic processes, continental growth, and mantle evolution recorded in late Archean greenstone belts of the southern Superior Province, Canada. Precambrian Research, v. 112, p. 5-25.

Polat, A., Kerrich, R., and Wyman, D.A., 1999. Geochemical diversity in oceanic komatiites and basalts from the late Archean Wawa greenstone belts, Superior Province, Canada: trace element and Nd isotope evidence for a heterogeneous mantle. Precambrian Research, v. 94, p. 139-173.

Puchtel, I.S., Shchipansky, A.A., Samsonov, A.V., and Zhuravlev, D.Z., 1997. The Karelian granite-greenstone terrain in Russia; *in* Greenstone Belts, edited by L. Ashwal and M.J. de Wit, Oxford Monographs on Geology and Geophysics, v. 35, p. 699-706.

Puchtel, I.S., Hofmann, A.W., Mezger, K., Jochum, K.P., Shchipansky, A.A., and Samsonov, A.V., 1998. Oceanic plateau model for continental crustal growth in the Archaean; a case study from the Kostomuksha greenstone belt, NW Baltic Shield. Earth and Planetary Science Letters, v. 155, p. 57-74.

Pyke, D. R., 1973. Archean Ultramafic Flows in Munro Township, Ontario. Geological Society of America Bulletin, v. 84, p.955-977.

Pyke, D.R., 1978. Geology of the Peterlong Lake area, districts of Timiskaming and Sudbury. Ontario Geological Survey, Report 171, 53 pp.

Richards, M.A., Duncan, R.A., and Courtillot, V. E., 1989. Flood basalts and hot-spot tracks: plume heads and tails. Science, v. 246, p. 103-107.

Robinson, D.J., and Hutchinson, R.W., 1982. Evidence for a volcanogenic-exhalative origin of a massive nickel sulfide deposit at Redstone, Timmins, Ontario; *in* Hutchinson, R.W., Spence, C.D., and Franklin, J.M. (Editors), Precambrian Sulfide Deposits, Special Paper 25, Geological Association of Canada, Waterloo, p. 211-254.

Rogers, J.J.W., and Giral, R.A., 1997. The Indian Shield; *in* Greenstone Belts, edited by L. Ashwal and M.J. de Wit, Oxford Monographs on Geology and Geophysics, v. 35, p. 620-635.

Rollinson, H., 1993. Using geochemical data. Longman Scientific, 352 pp.

Rudnick, R.L., Barth, M.G., McDonough, W.F., and Horn, I., 1998. Rutiles in eclogites: a missing Earth reservoir found? Geological Society of America, Program with Abstracts, v. 30(7), p. A207.

Sasseville, C., and Tomlinson, K.Y., 2000. Structure, stratigraphy, and geochemistry of the Mesoarchean Wallace Lake greenstone belt, southeastern Manitoba. Current Research - Geological Survey of Canada, Report 2000-C14, 9 pp.

Saunders, A.D., and Tarney, J., 1984. Geochemical characteristics and tectonic significance of back-arc basins; *in* Marginal Basin Geology, edited by B.P. Kokelaar and M.F. Howells, Special Publication of the Geological Society of London, v. 16, p. 59-76.

Saverikko, M., 1983. Explosive komatiitic volcanism in Finnish Lapland. Geologi, v. 35, p. 21-23.

Saverikko, M., 1985. Komatiitic explosive volcanism and its tectonic setting in Finland, the Fennoscandian (Baltic) Shield. Bulletin of the Geological Society of Finland, v. 62, p. 3-38.

Shirey, S.B., and Walker, R.J., 1995. Carius tube digestions for low blank rhenium-osmium analysis. Analytical Chemistry, v. 67, p. 2136-2141.

Shore, M., and Fowler, A.D., 1999. The origin of spinifex texture in komatiites. Nature, v. 397, p. 691-693.

Sproule, R.A., Lesher, C.M., Ayer, J., Thurston, P.C., and Herzberg, C.T., 2002. Spatial and Temporal Variations in the Geochemistry of Komatiitic Rocks in the Abitibi Greenstone Belt. Precambrian Research, v. 115, p. 153-186.

Stamatelopopoulou-Seymour, K., and Francis, D., 1988. Magmatic interaction between mantle and crust during the evolution of the Archean Lac Guyer greenstone belt, New Quebec. Canadian Journal of Earth Sciences, v. 25, p. 691-700.

Stamatelopoulou-Seymour, K., Francis, D., and Ludden, J., 1983. The petrogenesis of Lac Guyer komatiites and basalts and the nature of the komatiite-komatiitic basalt compositional gap. Contributions to Mineralogy and Petrology, v. 84, p. 6-14.

Stanton, R.L., 1972. Ore Petrology. McGraw-Hill, 713 pp.

Stone, M.S., and Stone, W.E., 2000. A crustally contaminated komatiitic dyke-sill-lava complex, Abitibi greenstone belt, Ontario. Precambrian Research, v. 102, p. 21-46.

Stone, W.E., and Lesher, C.M., 1995. Geochemistry and petrogenesis of Archean high MgO lavas in the Abitibi-Pontiac region, Ontario and Quebec: implications for magmatism and tectonism. Precambrian '95 (Montreal), Abstract Volume, p. 28.

Stone, W.E., Crocket, J.H., and Fleet, M.E., 1993. Sulphide-poor platinum-group mineralization in komatiitic systems: Boston Creek flow, layered basaltic komatiite, Abitibi Belt, Ontario. Economic Geology, v. 88, p. 817-836.

Stone, W.E., Lesher, C.M., and Arndt, N.T., 1997. Nd isotope geochemistry of komatiites in the Abitibi-Pontiac greenstone belt. GAC-MAC annual meeting, Ottawa, A88.

Stone, W.E., Crocket, J.H., Dickin, A.P., and Fleet, M.E., 1995. Origin of Archean ferropicrites: geochemical constraints from the Boston Creek flow, Abitibi greenstone belt, Ontario, Canada. Chemical Geology, v. 121, p. 51-71.

Stone, W.E., Crocket, J.H., Fleet, M.E., and Larson, M.S., 1996. PGE mineralization in Archean volcanic systems: geochemical evidence from thick, differentiated mafic-ultramafic flows, Abitibi greenstone belt, Ontario, and implications for exploration. Journal of Geochemical Exploration, v. 56, p. 237-264.

Stone, W.E., Deloulé, E., Larson, M.S., and Lesher, C.M., 1997. Evidence for hydrous high MgO melts in the Precambrian. Geology, v. 25, p. 143-146.

Stone, W.E., Jensen, L.S., and Church, W.R., 1987. Petrography and geochemistry of an unusual Fe-rich basaltic komatiite from Boston Township, northeastern Ontario. Canadian Journal of Earth Sciences, v. 24, p. 2537-2550.

Storey, M., Mahoney, J.J., Kroenke, L.W., and Saunders, A.D., 1991. Are oceanic plateaus sites of komatiite formation? Geology, v., 19, p. 376-379.

Storey, M., Mahoney, J., and Saunders, A., 1997. Cretaceous basalts in Madagascar and the transition between plume and continental lithosphere mantle sources. Geophysical Monograph, American Geophysical Union, Vol. 100, pp. 95-122.

Stott, G.M., 1997. The Superior Province, Canada; *in* Greenstone Belts, edited by L. Ashwal and M.J. de Wit, Oxford Monographs on Geology and Geophysics, v. 35, p. 480-507.

Sun, S.S., 1980. Lead isotopic studies of young volcanic rocks from mid-ocean ridges, ocean islands and island arcs. Philosophical Transactions of the Royal Society, A297, p. 409-445.

Sun, S.S., and Nesbitt, R.W., 1978. Petrogenesis of Archean ultrabasic and basic volcanics: evidence from rare earth elements. Contributions to Mineralogy and Petrology, v. 65, p.301-325.

Tabatabai, M. 1979. Petrography and geochemistry of the McArthur Township area, Ontario. Unpublished MSc. thesis, Brock University.

Tassinari, C.C.G., 1997. The Amazonian Craton; *in* Greenstone Belts, edited by L. Ashwal and M.J. de Wit, Oxford Monographs on Geology and Geophysics, v. 35, p. 558-566.

Taylor, S.R., and McLennan, S.M., 1995. The geochemical evolution of the continental crust. Reviews in Geophysics, v. 33, p. 241-265.

Thompson, R.N., and Gibson, S.A., 2000. Transient high temperatures in mantle plume heads inferred from magnesian olivines in Phanerozoic picrites. Nature, v. 407, p. 502-506.

Thurston, P.C., 1991. Archean geology of Ontario: introduction; *in* Geology of Ontario, edited by P.C. Thurston, H.R. Williams, R.H. Sutcliffe and G.M. Stott, Ontario Geological Survey, Special Volume 4, p. 73-78.

Thurston, P.C., 1994. Archean volcanic patterns; *in* Archean Crustal Evolution, edited by K.D. Condie, Elsevier, New York, p. 45-84.

Tomlinson, K.Y., and Condie, K.C., 2001. Archean mantle plumes: evidence from greenstone belt geochemistry. Special Paper - Geological Society of America, v. 352, p. 341-357.

Tomlinson, K.Y., Hughes, D.J., Thurston, P.C., and Hall, R.P., 1999a. Plume magmatism and crustal growth at 2.9 to 3.0 Ga in the Steep Rock and Lumby Lake area, Western Superior Province. Lithos, v. 46, p. 103-136.

Tomlinson, K.Y., and Sasseville, C., 2000. Geochemistry and Nd isotopes of the Wallace Lake greenstone belt and implications for correlations between the North Caribou Terrane and the central Wabigoon Subprovince. Lithoprobe Western Superior Transect, sixth annual workshop, Lithoprobe Report, v. 77, p. 127-136.

Tomlinson, K.Y., Davis, D.W., Thurston, P.C., Hughes, D.J., and Sasseville, C. 1999b. Geochemistry, Nd isotopes and geochronology from the central Wabigoon Subprovince and North Caribou Terrane; regional correlations leading towards a Mesoarchean reconstruction. Lithoprobe Western Superior Transect, Lithoprobe Report, p. 136-146.

Tomlinson, K.Y., Bowins, R., and Hechler, J. 1999c. Refinement of hafnium (Hf) and zirconium (Zr) ICP-MS analysis by improvement in the sample digestion procedure; *in* Summary of Field Work and Other Activities 1998, Ontario Geological Survey, Miscellaneous Paper 169, p. 189-192.

Tourpin, S., Gruau, G., Blais, S., and Fourcade, S., 1991. Resetting of REE and Nd and Sr isotopes during carbonization of a komatiite flow from Finland. Chemical Geology, v. 90, p. 15-29.

Vaillancourt, C., Sproule, R.A., Macdonald, C.-A., Takats, P., and Lesher, C.M., 2003. Classification of mafic-ultramafic intrusions in Ontario and implications for Ni-Cu-PGE exploration. Ontario Geological Survey, Open File Report 6102, 335p.

Viljoen, M.J. and Viljoen, R.P., 1969. The geology and geochemistry of the lower ultramafic unit of the Onverwacht Group and a proposed new igneous rock. Special Publication of the Geological Society of South Africa, v. 2., p.221-244.

Walker, R.J., Shirey, S.B., and Stecher, O., 1988. Comparative Re-Os, Sm-Nd and Rb-Sr isotope and trace element systematics for Archean komatiite flows from Munro Township, Abitibi Belt, Ontario. Earth and Planetary Science Letters, v. 87, p. 1-12.

Weaver, B.L., and Tarney, J., 1981. The Scourie dyke suite: Petrogenesis and geochemical nature of the Proterozoic sub-continental mantle. Contributions to Mineralogy and Petrology, v. 78, p. 175-188.

Wederpohl, H., 1995. The composition of the continental crust. Geochimica et Cosmochimica Acta, v. 59, p. 1217-1239.

White, R., and McKenzie, D., 1989. Magmatism at rift zones; the generation of volcanic continental margins and flood basalts. Journal of Geophysical Research, B, Solid Earth and Planets, v. 94, p. 7685-7729.

Williams, D.A., Kerr, R.C., and Lesher, C.M., 1998. Emplacement and erosion by Archean komatiite lava flows: Revisited. Journal of Geophysical Research, v. 103, no. B11 (10 November, 1998), p. 27533-27549.

Williams, D.A., Kerr, R.C., and Lesher, C.M., 1999. Thermal and fluid dynamics of komatiitic lavas associated with magmatic Ni-Cu-(PGE) sulphide deposits; *in* Keays, R.R., Lesher, C.M., Lightfoot, P.C., and Farrow, C.E.G. (Editors), Dynamic Processes in Magmatic Ore Deposits and their Application to Mineral Exploration, Geological Association of Canada Short Course, v. 13, p. 367-412.

Woodall, R., and Travis, G.A., 1969. Proceedings - Commonwealth Mining and Metallurgical Congress, v. 2, p. 517-533.

Wyman, D. A., Ayer, J. A., and Devaney, J. R., 2000. Niobium-enriched basalts from the Wabigoon Subprovince, Canada; evidence for adakitic metasomatism above an Archean subduction zone. Earth and Planetary Science Letters, v. 179, p. 21-30

Wyman, D. A., Kerrich, R., and Polat, A., 2002. Assembly of Archean cratonic mantle lithosphere and crust: plume-arc interaction in the Abitibi-Wawa subduction-accretion complex. Precambrian Research, v. 115, p. 37-62.

Wyman, D.A., 1999. A 2.7 Ga depleted tholeiite suite: evidence of plume-arc interaction in the Abitibi greenstone belt, Canada. Precambrian Research, v. 97, p. 27-42.

Wyman, D.A., and Hollings, P., 1998. Long-lived mantle-plume influence on an Archean protocontinent; geochemical evidence from the 3 Ga Lumby Lake greenstone belt, Ontario, Canada. Geology, v. 26, p.719-722.

Wyman, D.A., Bleeker, W., and Kerrich, R., 1999a. A 2.7 Ga komatiite, low Ti tholeiite, arc tholeiite transition, and inferred proto-arc geodynamic setting of the Kidd Creek Deposit; evidence from precise trace element data. Economic Geology Monographs, 1999, v. 10, p. 511-528.

Wyman, D.A., Kerrich, R., and Groves, D.I., 1999b. Lode gold deposits and Archean mantle plume-island arc interaction, Abitibi Subprovince, Canada. Journal of Geology, Vol. 107, 6, pp. 715-725.

Xie, Q., 1996. Trace element systematics of mafic-ultramafic volcanic rocks from the Archean Abitibi greenstone belt, Canada: Implications for chemical evolution of the mantle and Archean greenstone belt development. Unpublished PhD thesis, University of Saskatchewan, 222p.

Xie, Q., McCauig, T.C., and Kerrich, R., 1993. Secular trends in the melting depths of mantle plumes: evidence from HFSE/REE systematics of Archean high-Mg lavas and modern oceanic basalts. Geochimica et Cosmochimica Acta, v. 57, p. 4111-4118.

Metric Conversion Table

Conversion from SI to Imperial			Conversion from Imperial to SI		
SI Unit	*Multiplied by*	*Gives*	*Imperial Unit*	*Multiplied by*	*Gives*
			LENGTH		
1 mm	0.039 37	inches	1 inch	**25.4**	mm
1 cm	0.393 70	inches	1 inch	**2.54**	cm
1 m	3.280 84	feet	1 foot	**0.304 8**	m
1 m	0.049 709	chains	1 chain	20.116 8	m
1 km	0.621 371	miles (statute)	1 mile (statute)	**1.609 344**	km
			AREA		
1 cm^2	0.155 0	square inches	1 square inch	**6.451 6**	cm^2
1 m^2	10.763 9	square feet	1 square foot	**0.092 903 04**	m^2
1 km^2	0.386 10	square miles	1 square mile	2.589 988	km^2
1 ha	2.471 054	acres	1 acre	0.404 685 6	ha
			VOLUME		
1 cm^3	0.061 023	cubic inches	1 cubic inch	**16.387 064**	cm^3
1 m^3	35.314 7	cubic feet	1 cubic foot	0.028 316 85	m^3
1 m^3	1.307 951	cubic yards	1 cubic yard	0.764 554 86	m^3
			CAPACITY		
1 L	1.759 755	pints	1 pint	0.568 261	L
1 L	0.879 877	quarts	1 quart	1.136 522	L
1 L	0.219 969	gallons	1 gallon	**4.546 090**	L
			MASS		
1 g	0.035 273 962	ounces (avdp)	1 ounce (avdp)	28.349 523	g
1 g	0.032 150 747	ounces (troy)	1 ounce (troy)	**31.103 476 8**	g
1 kg	2.204 622 6	pounds (avdp)	1 pound (avdp)	**0.453 592 37**	kg
1 kg	0.001 102 3	tons (short)	1 ton (short)	**907.184 74**	kg
1 t	1.102 311 3	tons (short)	1 ton (short)	**0.907 184 74**	t
1 kg	0.000 984 21	tons (long)	1 ton (long)	**1016.046 908 8**	kg
1 t	0.984 206 5	tons (long)	1 ton (long)	**1.016 046 90**	t
			CONCENTRATION		
1 g/t	0.029 166 6	ounce (troy)/ ton (short)	1 ounce (troy)/ ton (short)	34.285 714 2	g/t
1 g/t	0.583 333 33	pennyweights/ ton (short)	1 pennyweight/ ton (short)	1.714 285 7	g/t

OTHER USEFUL CONVERSION FACTORS

	Multiplied by	
1 ounce (troy) per ton (short)	31.103 477	grams per ton (short)
1 gram per ton (short)	0.032 151	ounces (troy) per ton (short)
1 ounce (troy) per ton (short)	20.0	pennyweights per ton (short)
1 pennyweight per ton (short)	0.05	ounces (troy) per ton (short)

Note: Conversion factors which are in bold type are exact. The conversion factors have been taken from or have been derived from factors given in the Metric Practice Guide for the Canadian Mining and Metallurgical Industries, published by the Mining Association of Canada in co-operation with the Coal Association of Canada.

ISSN 0826-9580
ISBN 0-7794-4456-6